Investigating the effect of linear velocity in reciprocating contacts

by

Christo Kleynhans

A dissertation submitted in partial fulfilment
of the requirements for the degree

Master of Engineering (Chemical Engineering)

in the

Department of Chemical Engineering

Faculty of Engineering, the Built Environment and Information
Technology

University of Pretoria
Pretoria

08 February 2021

Contents

List of Figures

List of tables

List of equations

Synopsis

In Tribology, the well-known Stribeck curve is often used to relate friction behaviour to the properties of a system. Richard Stribeck, (Jacobson, 2003), (Stribeck, 1902) developed these curves while researching various bearings and found that the Stribeck curve can be generated for all tribological contacts of the Hertzian type. These curves give a relation between the coefficient of friction and the Sommerfeld number for a lubricant and given surfaces. All his test work was done on contacts that move in a single direction, unidirectional motion. This leaves the question, could Stribeck curves be applied to reciprocating contacts and how does linear velocity affect wear in these contacts?

This research project is aimed to further the knowledge on how linear velocity affects reciprocating contacts with a focus on Stribeck curves and lubricity. Tests were conducted on two reciprocating instruments using ball and disk configurations. Two parameters were varied to change the linear velocity, namely oscillating frequency, and stroke length. To shift focus away from viscosity, n-Hexadecane was used as the base fluid due to its lack of lubrication properties. To improve the base fluid lubricity 3 carboxylic acids with 3 different chain lengths were used as additives.

Nomenclature

Nomenclature	Description
Hersey number	The Hersey number is a value calculated using $\frac{\mu v}{P}$. Where μ is the viscosity, v the linear velocity and P the applied load
Sommerfeld number	The Sommerfeld no expands on the Hersey number by taking some properties of bearings into account. It can be calculated by using $(\frac{r^2}{c})(\frac{\mu N}{P})$. Where μ is the viscosity, N the speed of the rotating shaft, P the applied load, r the shaft radius and c the shaft clearance.
Coefficient of friction	A relation defined as $\mu = F/W$. This factor gives the relation between the size of the frictional forces F experienced compared to the applied normal force W.
Base fluid/liquid	The bulk compound used in a lubricant.
Additive	A compound added to a lubricant at low concentrations.
Endpoint	Refers to the end of a stroke on a reciprocating test instrument.
FS Test	Frequency Scan test. A test where the oscillating frequency is changed during the test while other parameters are kept constant.

Abbreviations

Abbreviation	Description
HL regime	Hydrodynamic lubrication regime
EHL regime	Electrohydrodynamic lubrication regime
ML regime	Mixed lubrication regime
BL Regime	Boundary lubrication regime
HFRR	High Frequency Reciprocating Rig
WSD	WSD- wear scar diameter.
SRV	Schwingung (Oscillating), Reibung (Friction), Verschleiss (Wear)

The experimental run naming system

Each test was named in the following format X000_YY_111N_22c_33RH_runZ. The following tables explain each element of the naming system.

Abbreviation	Description
X	The first letter refers to the additive used during the test. M- Myristic (C-14), P- Palmitic (C-16), S- Stearic acid (C-18) and
000	The first set of numbers refers to the concentration of the additive in ppm.
Y	The following two letters describe the test type. FS- Frequency scan and FW- Friction and wear.
111N	Refers to the applied load during the test in Newtons.
22c	Refers to the test chamber temperature in Celsius.
33RH	Refers to the test chamber relative humidity at the chamber temperature.
2mm	Runs using a 2 mm stroke have an added phrase, 2mm, before the last phrase.
runZ	Refers to the run. When runs are combined this phrase can be replaced with a Long- Full (Raw) data set, or short (averaged at each point) data set.

1. Introduction

In tribology, the well-known Stribeck curve is often used to relate friction behaviour to the properties of a system. Richard Stribeck, (Jacobson, 2003), (Stribeck, 1902) developed these curves while researching various bearings and found that the Stribeck curve can be generated for all tribological contacts of the Hertzian type. These curves give a relation between the coefficient of friction and the Sommerfeld number for a lubricant and given surfaces. All his test work was done on contacts that move in a single direction, unidirectional motion. This leaves the question, could Stribeck curves be applied to reciprocating contacts and how does linear velocity affect wear in these contacts?

This project aims to further the understanding of Stribeck curves with a focus on the role of linear velocity in reciprocating contacts. Two reciprocating instruments, each using a ball and disk configuration were used for testing. Two parameters were varied to change the linear velocity, namely oscillating frequency, and stroke length. To shift focus away from viscosity, n-Hexadecane was used as the base fluid because of its low viscosity and no inherent lubricity. To improve the lubricity of the base fluid, three carboxylic acids were used as anti-wear additives: myristic-, palmitic- and stearic-acid.

To understand the role linear velocity plays in reciprocating contacts several factors need to be investigated. The most obvious factor is the linear velocity itself. Stribeck curves give a strong indication of how friction and wear will be affected but Stribeck curves were generated on non-reciprocating contacts. Because of the oscillatory nature of the contact in this study, time-based factors are also important. Consider a ball on disk instrument where the ball oscillates across a disk. As the oscillating frequency of a ball is increased, the time that the ball specimen takes to reach the same spot on the disk again is drastically reduced. The same could be said of unidirectional surfaces. Depending on the surfaces involved, as the speed of one surface is increased it will reach the same point on the other surface again at some point. Consider a pin on disk instrument. The pin will reach the same start point on the disk and if the velocity has

increased the pin will reach that point faster. Where the difference comes in is that a bi-directional instrument's velocity is dependent on its position on the disk while a unidirectional instrument has a constant velocity.

From these factors, the following questions were raised to achieve the objectives of this study.

- Can a Stribeck curve be generated using reciprocating contacts?
- Will changes in the linear velocity follow trends established by Stribeck curves?
- Will the size of a molecule affect the relation between linear velocity and the lubrication regime?

The following were also investigated to support results:

- Effect of sample volume
    - The time between when a lubricant sample is placed onto the test specimen and the start of the test averaged 30 minutes in this study. From the literature reviewed around diffusion rates of fatty acids, there is more than enough time for the bulk of the additives to move to the lubricant-metal and lubricant-air interfaces. This will be discussed further in the literature study.
    - Can different volumes achieve different wear results because of surface concentration compared to bulk concentration?
- Surface lubricant starvation.
    - As the top specimen moves across the bottom specimen, the lubricant is moved out of the way. In situations where the lubricant cannot flow back into the wear scar before the ball comes back to that position severe wear occurs. This situation is referred to as lubricant starvation, (Cann, 1996).
    - Is the oscillating frequency used in this experiment high enough to cause lubricant starvation? Increasing the stroke length while

maintaining the oscillating frequency also increases the chance that lubricant starvation will take place.

- Repeatability and resolution of tests with changes in the oscillating frequency
    - The SRV takes an analogue signal and produces a digital data set.
    - How will a fixed data acquisition rate affect the repeatability and resolution of test results?

The following chapters, in order, will be

- A literature review that focuses on Stribeck curves, boundary lubrication and additive layers.
- A chapter on the instruments and compounds used in the experiments.
- This chapter contains all the planning for initial experiments. Because of the exploratory nature of this study, it was necessary to run a set of tests to understand how our instruments would react with the test methods used.
- A results chapter for all the initial test work that was conducted.
- Planning and results of all the test work conducted to investigate:
    - Can Stribeck curves be applied to reciprocating contacts?
    - How changes in linear velocity affect reciprocating contacts.
- Conclusions on results
- Recommendations for projects to follow this study.

2. Literature

The literature chapter discusses the basic theorems of tribology with a strong focus on Stribeck curves, boundary lubrication and additive layers.

Tribology is the field of study that focuses on lubricants and materials for surfaces in relative motion. Knowledge generated in this field is used to understand how lubricants and contact surface properties affect friction and wear. One interesting example is brake pads. In brake pads, the friction needs to be as high as possible without excessive wear rates to give good performance and a reasonable life span. Tribology can be applied in the manufacturing, automotive, aquatic and military sectors to name but a few (Batchelor & Stachowiak, 2003, p. 2), (Bhushan B. , 2001, p. 9).

The performance required from a lubricant is dependent on the application. A metalworking fluid needs to lubricate, clean, remove heat, protect the work surface from tarnishing and not cause any harm to users or machines. Gear oils, on the other hand, need good cold start properties, high shear stability, and have good extreme pressure properties. This shows how broad the word performance is in the lubrication industry. For this study, good performance refers specifically to low friction and low wear. There are 2 things to consider when talking about friction and wear:

- The viscosity of the lubricant.
- The lubricity of the lubricant.

Higher viscosity lubricants tend to give better wear protection, but it is not always possible to use a high viscosity product and high viscosity also means more energy losses. This is where lubricity comes in. Lubricity is defined as a qualitative measurement of a lubricant's performance independent of bulk fluid viscosity (Appeldoorn & Dukek, 1966).

4

2.1.   Friction and Wear

The term coefficient of friction is one of the easiest ways to describe what is happening in a tribo-system. The coefficient of friction (μ) gives indications on:

- The resistance to motion.
- The level of energy losses.
- Type of wear that occurs.
- The lubrication regime.

To calculate the coefficient of friction in a system the ratio of the normal force (W) and the frictional force (F), equation 2-1, is required (Batchelor & Stachowiak, 2003, p. 357).

$$\mu = \frac{F}{W}$$

2-1

Higher coefficient of friction indicates more frictional forces. While we measure a single frictional force, it is comprised of several forces, (Bhushan B. , 2002).

- The force required to shear the lubricant (viscosity related).
- The force required to shear or deform the surfaces in a tribo-system (relates to wear).
- The force required to shear boundary films.

One way to visualize how this occurs is thinking of the liquid between two surfaces as several solid layers on top of each other. The first layer next to the moving surfaces can be seen as sticking to the surface, the non-slip boundary condition typically used in fluid dynamics. The following layer is then sheared to move with the first layer as shown in Figure 2-1. The size of the shear force required to move each layer is dependent on the viscosity of the liquid.
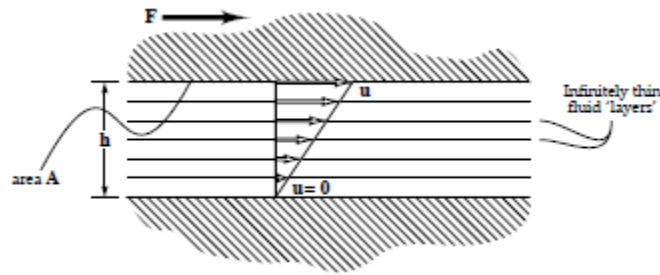
Figure 2-1: Visual representation of liquid layers between two surfaces, (Batchelor & Stachowiak, 2003, p. 12).

Wear can be defined as the material loss over time between surfaces in relative motion. Generally, a higher coefficient of friction indicates higher wear rates. There are many types of wear and can be grouped into severe, mild, and minor wear. The different wear types are shown in Table 2-1 within their respective groups. Severe wear usually occurs when there is no lubricant present or under a load above the load-carrying capacity of the lubricant, implying no lubricating film.

Table 2-1: Different wear types (Batchelor & Stachowiak, 2003, pp. 2-5).

Wear type	Description	Reference page (Batchelor & Stachowiak, 2003) unless otherwise stated.
Severe		
Adhesive	Adhesion between asperities.	533 – 550
Mild		
Abrasive	Particle or fluid abrasion.	483 – 509
Erosive	Impacting particles.	509 – 521
Cavitation	Fast-flowing fluids causing implosions.	524 – 525
Corrosive	Chemical attack.	553 – 567
Oxidative	Oxygen as the corrosive agent.	560 – 556
Fatigue	Repetitive stresses causing fatigue.	571 – 589
Minor		
Fretting	Trapped fluid causing wear.	593 – 603
Impact	Repeated surface impacts.	603 – 609
Melting	Surfaces melt due to flash temperatures.	609 – 611
Diffusive	High temperatures causing diffusion of surface material.	612 – 613

6

The following chapters discuss the wear mechanisms that are expected to play a role during tests in this study.

2.1.1. Adhesive Wear

During adhesive wear there is metal to metal contact that can cause cold welding, resulting in severe deformation and high coefficient of friction. When a hard material cold welds to a softer material the hard material will pull some of the softer material from its surface (material pull-out). This process causes significant deformations in the softer material and very high wear.

The brittleness of material used also has a significant effect on adhesive wear. Brittle materials tend to show little deformation and the result is a clean break during material pull-out, reducing the number of wear particles that are formed (Batchelor & Stachowiak, 2003, p. 543).

The adhesive wear mechanism is shown in Figure 2-2. After the initial adhesion (a) shear bands start to form (b). At some point, a crack will start to form (c) and initiating the formation of a new shear band. As the shear bands grow the crack grows and new bands are formed until it reaches (f) where the hard material pulls the softer material apart.
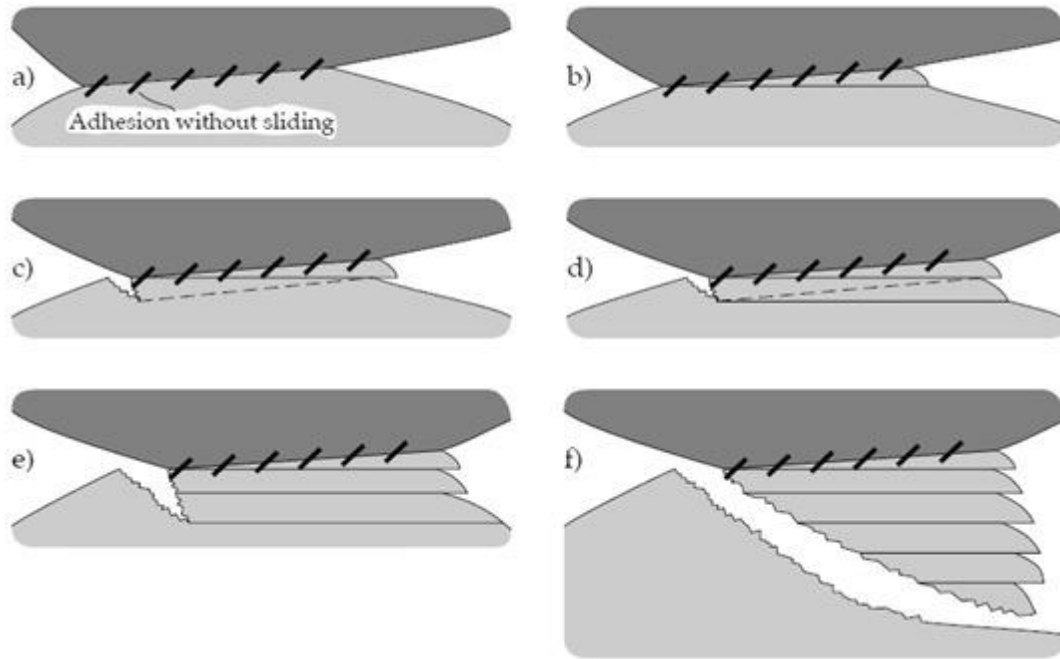
Figure 2-2: Adhesive wear (Batchelor & Stachowiak, 2003). Dark colour, hard materials, light colour is the softer material.

Two things can happen to the soft material that is attached to the harder material. The material can be sheared off generating a wear particle or stay attached, creating a transfer film that will be flattened up to the point of adhesive failure of the components.

The wear particles generated in this process will generally be harder than the remaining surface. Most manufactured parts undergo surface treatment to case harden the part. For example, the rollers for tube roller mills are case hardened to make them resistant to wear. The inner ductile metal allows the part to handle high pressures because of the ductility without shattering. If wear particles are formed from a hardened surface layer, wear can increase drastically (Gohar & Rahnejat, 2012, p. 66).

The transfer film creates an area that will carry most of the load applied to the surfaces. This can drastically decrease the surface area causing adhesive failure much earlier than expected. A transfer film is shown in an SEM-image, Figure 2-3.
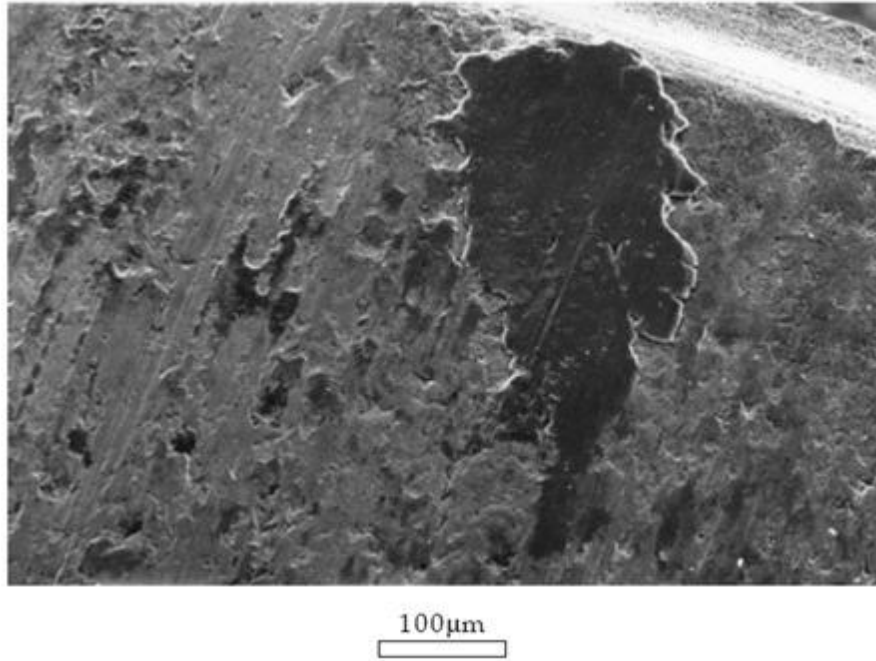
Figure 2-3: Transfer film on a metal surface (Langenhoven, 2012). The darker surfaces are indications of transfer films.

Adhesive wear is expected to occur at low velocities with weak additive layers or a high load above the load-carrying capacity of the lubricant.

2.1.2. Corrosive wear

Corrosive wear can be detrimental or helpful in a system. In corrosive wear, a chemical reacts with the metal surface forming a new surface layer. This layer's properties differ from the metal and can give a surface film with low shear strength. A low shear strength layer can reduce the coefficient of friction observed and protect the surface by preventing adhesive wear between asperities. Problems start to occur when the new layer is broken away by friction. When the layer is broken away the corrosive molecule will quickly react with the nascent material generating a new layer. Corrosive wear becomes detrimental when this cyclical process is too rapid resulting in rapid material loss. The following are possible scenarios that can occur during corrosive wear (Rengstorff, Miyoshi, & Buckley, 1986), (Batchelor & Stachowiak, 2003, p. 554):

- Durable film formation providing a low coefficient of friction, Figure 2-4.1.
- Weak film formation, rapid wear due to the cyclic formation and destruction of the film, Figure 2-4.2.
- Rapid corrosion due to galvanic coupling between the new layers and metal. Only applicable for highly corrosive substances, Figure 2-4.3.
- Uncontrolled adhesive wear with poor lubricity followed by corrosion of the nascent metal, Figure 2-4.4.
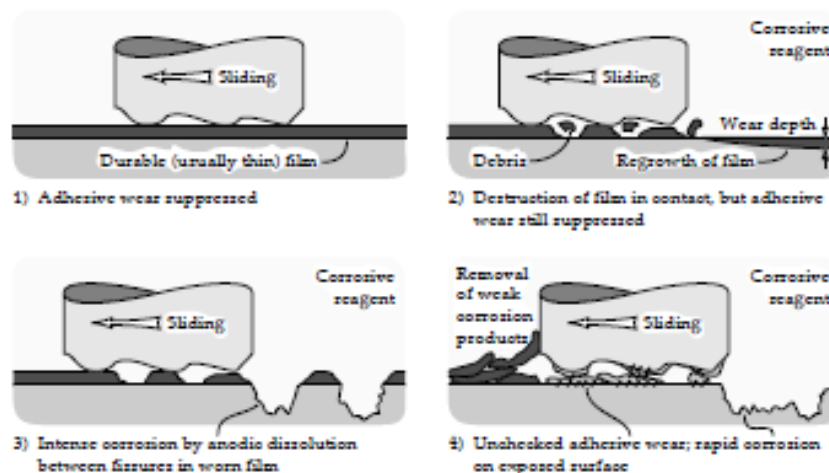
Figure 2-4: Different possible scenarios during corrosive wear (Batchelor & Stachowiak, 2003, p. 554)

There are mass transfer limitations that limit the thickness of the corroded layer. As the layer grows the chemistry causing the corrosive wear must travel further through the corroded layer to reach unreacted metal. Normally the corroded layer grows up to the mass transfer limitation. Because of the poor mechanical properties of some corroded layers, the film never grows to this thickness. One such property is that the corroded layer has a lower shear strength compared to the metal surface.

Water content in the lubricant and temperature also play a significant role in corrosive wear. Higher temperatures increase the corrosion reaction rate and gives the energy to overcome the activation energy of the reaction. For acids and alcohols, higher water content also gives higher wear rates.

Corrosion is not necessarily caused by contaminants. The lubricant itself can also be corrosive. For example, neat cutting oil often uses chlorinated paraffin for their extreme pressure properties. During operation, these chemistries can corrode metal surfaces if sufficient anti-rust additives are not added. The activity of a lubricant determines how corrosive the lubricant will be, but the activity also affects lubricity performance. If the activity is too high the lubricant will cause corrosive wear. If the activity is too low the lubricant provides less protection and severe adhesive wear may occur. This implies that there is an optimum lubricant activity for a load and temperature that will minimize the wear rate (Batchelor & Stachowiak, 2003).
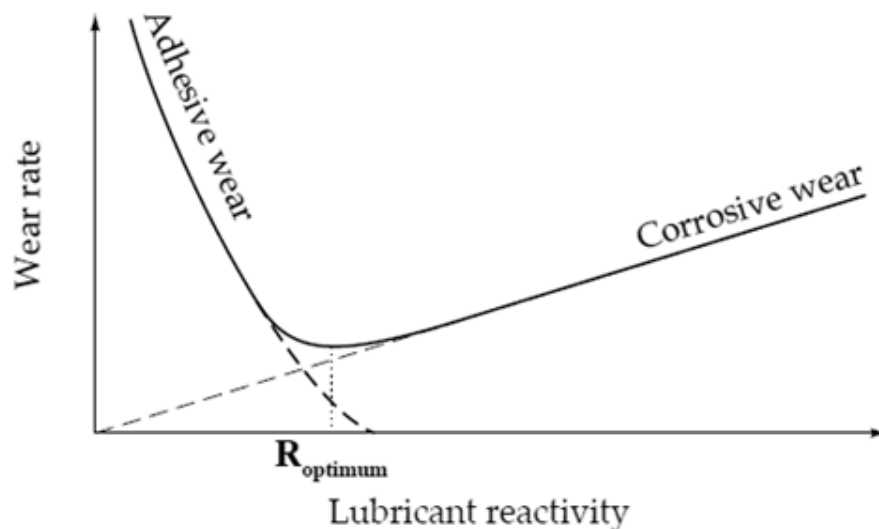
Figure 2-5: Optimum lubricant activity to minimise the sum of adhesive and corrosive wear (Batchelor & Stachowiak, 2003).

Corrosive wear becomes more rapid when there are wear particles present. The abrasive wear caused by the particles breaks down the corroded layer leaving a new metal surface. The new surface is rapidly corroded forming a new corrosion layer with weaker shear strength than the metal that can then easily be removed by the abrasive particles. This can result in rapid material loss.

2.2. Stribeck curves

We know that for a liquid lubricant between two surfaces in motion that the viscosity and its lubricity play a major role in its performance. A Stribeck curve gives the relation between the coefficient of friction and a set of parameters called the Hersey number.

A Stribeck curve consists of four lubricating regimes that describe the lubricating film and the severity of wear that will generally take place. The 4 lubricating regimes are hydrodynamic lubrication (HL), elastohydrodynamic- (EHL), mixed- (ML) and boundary- (BL). Each regime is shown on a general Stribeck curve in Figure 2-6 below.
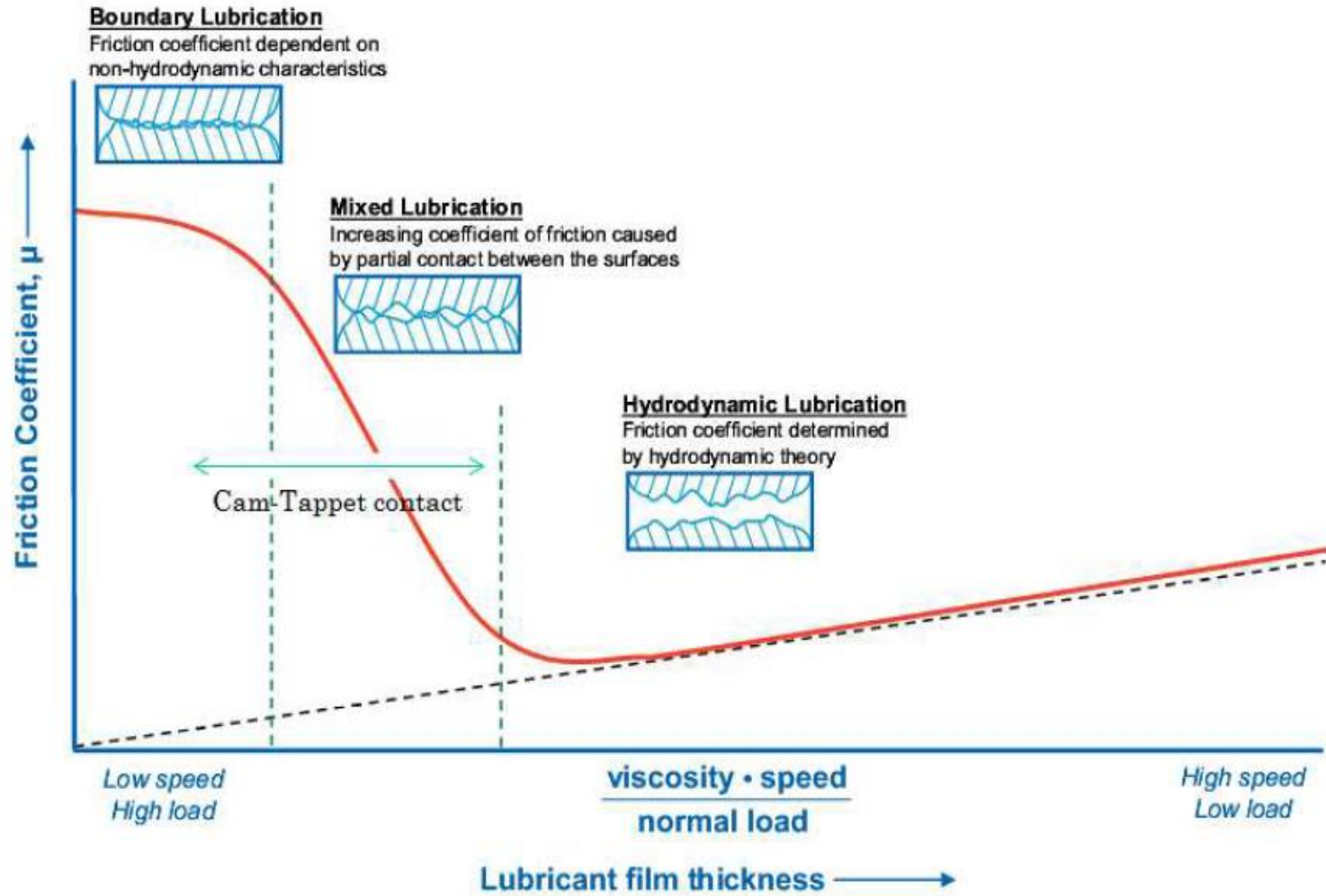
Figure 2-6: Stribeck curve with lubrication regimes adapted from (Hutchings, 1992).

13

2.2.1. Hydrodynamic lubrication regime

In the hydrodynamic lubrication regime, the theoretical values for the coefficient of friction for lubricants with low shear strength are in the order of 0.001 (Bhushan B. , 2002), (Roberts, 1990) with film thicknesses ranging from 5 to 500 µm under applied loads of 1 – 2 kPa (Batchelor & Stachowiak, 2003, p. 282). In this regime, the load-carrying capacity of the lubricant ensures a separation distance between surfaces thicker than the surface roughness. This is the ideal regime giving the best possible lubrication but in practice, it is very difficult to maintain. Theoretically, there is no wear in this regime because the two surfaces never touch or get deformed. A hydrodynamic film can be maintained under the following conditions (Batchelor & Stachowiak, 2003):

- A sliding velocity high enough to develop the required hydrodynamic pressure (giving the lubricant sufficient load-carrying capacity) to maintain a lubricant film thicker than the height of the asperities of the two surfaces combined. The hydrodynamic pressure is also affected by the viscosity of the lubricant.
- A pressure field that can be attained by having the two surfaces at an angle, or using stepped surfaces to ensure that there is an in- and outflow (pressure gradient in the lubricant).

2.2.2. Elastohydrodynamic Lubrication regime

In this regime, the lubricant is subjected to pressures of up to 5 GPa. Under these high pressures, the surfaces deform elastically (Bhushan B. , 2002) but, the two surfaces still do not come into contact with each other. The elastic deformation allows situations where the film thickness between two surfaces are smaller than the average surface roughness (Ratoi, Angel, Bovington, & Spikes, 2000). With EHL the lubricant film drastically decreases from the thickness seen in the hydrodynamic regime to values between 0.5 and 5 µm, (Batchelor & Stachowiak, 2003, p. 282).

2.2.3. Mixed lubrication regime

The ML regime is the regime that most industrial and commercial tribo-systems operate in. ML regime is Elastohydrodynamic over the largest part of the contact area but, at the asperities there is penetration of the EHL layer, illustrated in Figure 2-7 below. Between the asperities EHL films persist, the film thickness in mixed lubrication ranges from 0.01 – 1 µm at the asperities, (Hamrock, Jacobson, & Schmid, 2005).
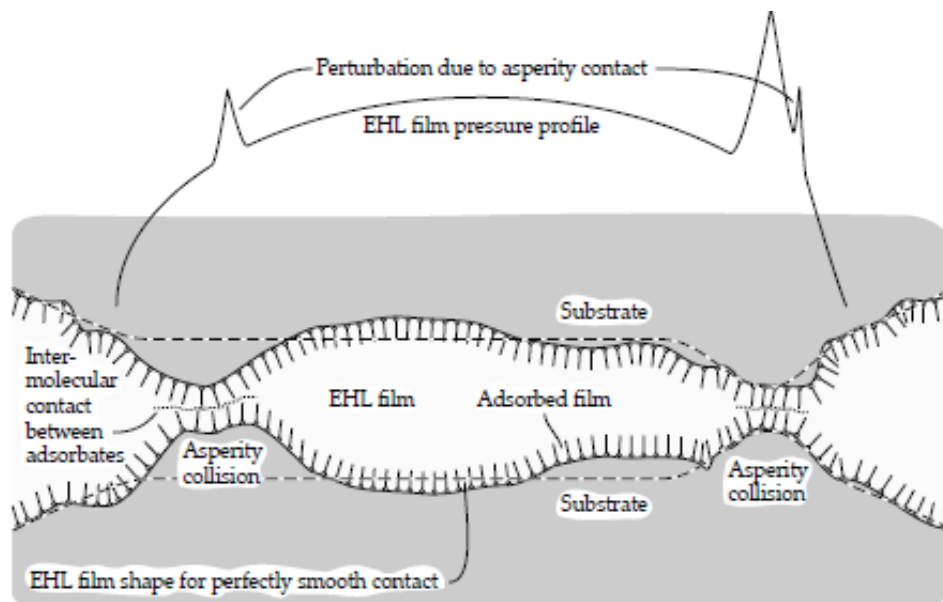
Figure 2-7: Mixed lubrication model, (Batchelor & Stachowiak, 2003, p. 198).

2.2.4. Boundary layer lubrication regime

In the BL regime, the layer that protects the two surfaces can be a single molecular layer (thin film boundary lubrication) or multiple molecular lengths (thick film boundary lubrication) (Anghel, Bovington, & Spikes, 1999). To protect surfaces in the BL regime surfactant-like molecules can be added to the lubricant to generate stronger boundary layers. The commonly used functional groups of

these molecules are fatty acids, alcohols, or esters. The polar head of these additives attaches to the metal surface by adsorption or chemisorption and the tail interacts with the main bulk of the lubricant, as illustrated in Figure 2-8 below (Batchelor & Stachowiak, 2003).
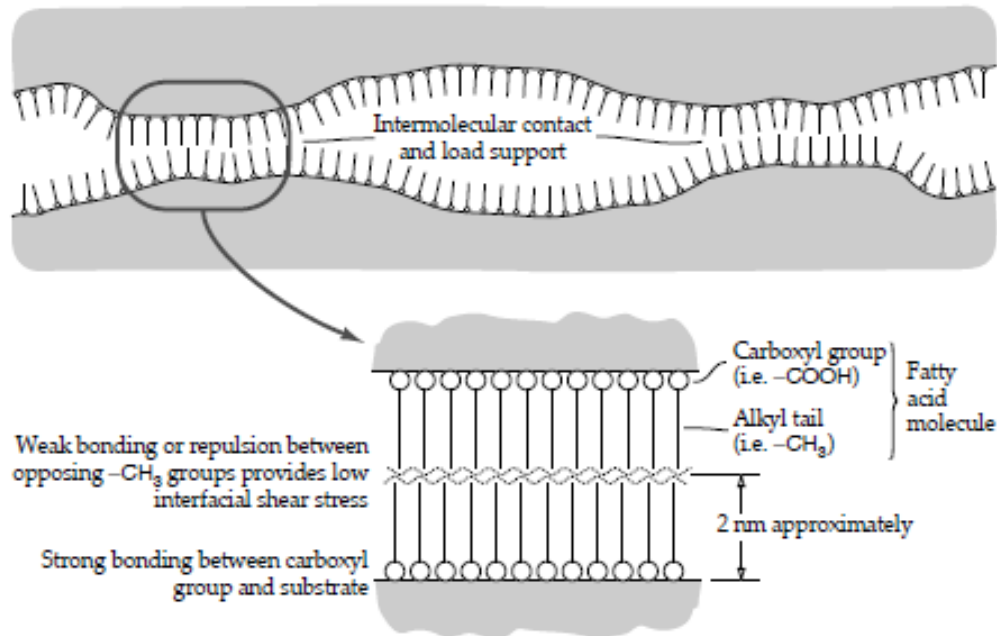
Figure 2-8: Boundary lubrication model (Batchelor & Stachowiak, 2003, p. 387)

2.3. The role of temperature in lubrication

Litzow and Jess (Litzow, Jess, Matzke, Caprotti, & Balfour, 2009) performed experiments on additised low sulfur diesel on the HFRR and HiTOM (Figure 2-9 and Figure 2-10). The effect of temperature on the load-carrying capacity and the wear scar was tested. The wear scar diameter shows a maximum, but for tests above 90 °C, some of the lubricant would evaporate. Testing the composition of the residue from runs above 90 °C Litzow and Jess found that the residue had a higher concentration of polar compounds. Increased temperatures tended to increase load-carrying capacities while increasing wear scars.
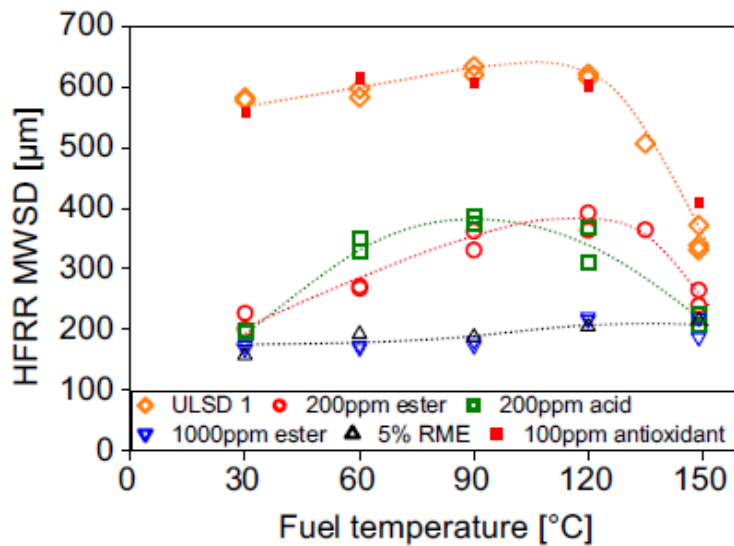
Figure 2-9: Effect of temperature on the wear scar diameter for additised low sulphur diesel (Litzow, Jess, Matzke, Caprotti, & Balfour, 2009).
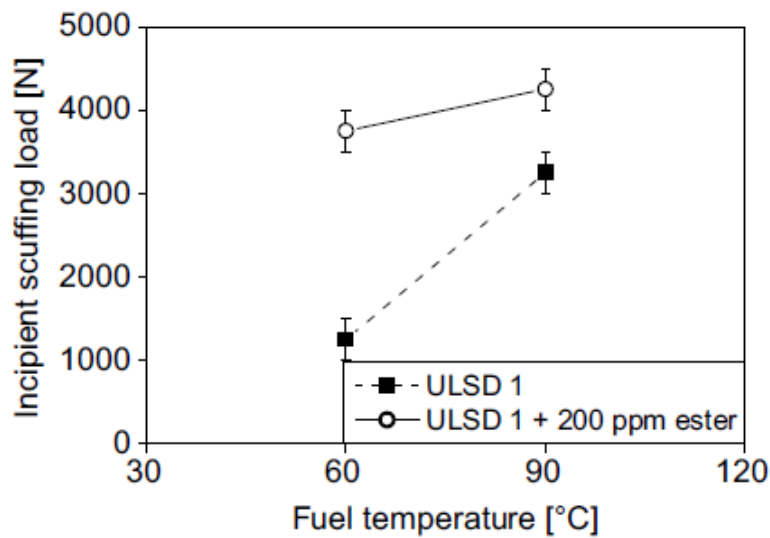
Figure 2-10: Effect of temperature on the load-carrying capacity for additised low sulphur diesel (Litzow, Jess, Matzke, Caprotti, & Balfour, 2009).

It is also important to note that lubricants with a high lubricity showed much less of an effect due to temperature changes. In Figure 2-9 comparing the 1000 ppm ester sample to the 200 ppm ester sample, it is clear that the sample with higher

17

lubricity was much less affected by temperature changes. This same fact can be seen in Figure 2-10 with a small increase in the load-carrying capacity for the additised sample compared to the larger increase in the unadditised sample's load-carrying capacity.

Tests done by (Lacey, Gunsel, DeLa Cruz, & Whalen, 2001) with a modified HFRR gave similar results to the results in Figure 2-9. They are given in Figure 2-11.
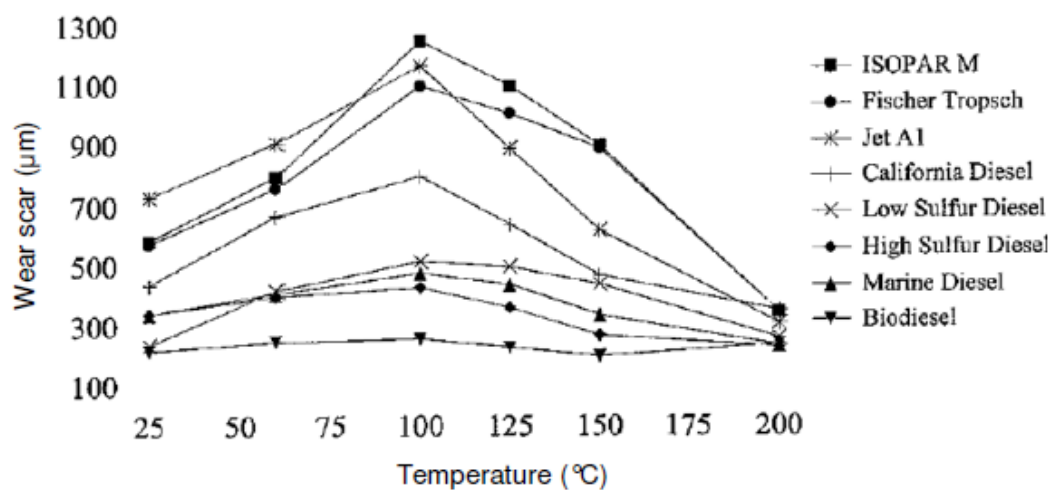
Figure 2-11: Wear test with an HPHFRR (High-pressure HFRR), (Lacey, Gunsel, DeLa Cruz, & Whalen, 2001).

2.4.   Additives

In general lubricant with no additives will not react chemically with a lubricated surface to protect or lubricate said surface. The role additives play in lubrication is to reduce the effect surface contact has on friction and/or wear (Roberts, 1990). Two different types of additives can be used to achieve this. Friction modifiers adsorb onto a lubricated surface to form a low shear layer. They can be oil-soluble polar compounds or insoluble solids. Anti-wear/extreme pressure additives chemically bond with a lubricated surface. Anti-wear additives reduce wear rates while extreme pressure additives increase the load-carrying capacity of the lubricant (Papay, 1983). These additives work in the boundary and mixed

18

lubrication regimes. The difference between the two is in the mechanical properties of the boundary films that the additives produce (Papay, 1983). Friction modifiers attach to surfaces and form a film that has low shear strength. This low shear strength film reduces the coefficient of friction because the top layers of the orderly packed film can be sheared easily. These types of lubricant additives also reduce wear but, under extreme conditions, the film becomes so thin that the additive molecules that are adsorbed are rubbed off. The anti-wear additives form high shear strength films that physically protect a surface by forming a sacrificial film. These films can handle harsher conditions, higher loads, and machining speeds.

Most additives that are added for lubricity improvements have the same functional groups (Litzow, Jess, *et al*, 2009). These functional groups are carboxylic acids, esters, and amides.

2.4.1. Molecular Shape

The shape of an additive molecule has a large effect on the effectiveness and properties of the boundary layer formed. Because linear molecules can be closely packed next to one another the van der Waals forces between the molecules are strong and keep the molecules together to form a durable layer. Branched molecules cannot be packed as closely and have weaker van der Waals forces between the alkyl groups. The effect that the branched structure has on lubricity is shown in Figure 2-12.
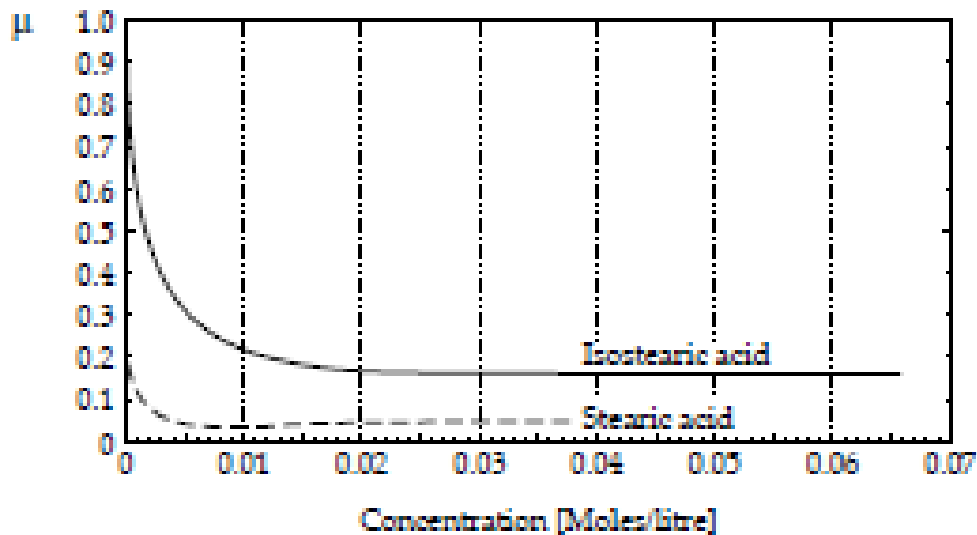
Figure 2-12: Coefficient of friction comparison between branched and unbranched molecules with the same number of carbons and functional group (Batchelor & Stachowiak, 2003, p. 365).

The branched iso-stearic acid does not lower the coefficient of friction as much as stearic acid. The additives have similar chain lengths but the branched isosteric tail results in a weaker boundary film. Figure 2-12 also shows that the effect the additive has on the coefficient of friction becomes less as the concentration is increased and will reach a plateau.

Another problem that may occur with branched additives is the formation of deep interactive zones. The branched parts can cause areas of the additive layer on the surface to group together producing a roughness in the film structure, illustrated in Figure 2-13. The large and deep interaction zones mean that additives from the other surface can enter in between the additives from the other layer increasing the coefficient of friction observed (Batchelor & Stachowiak, 2003, p. 365).
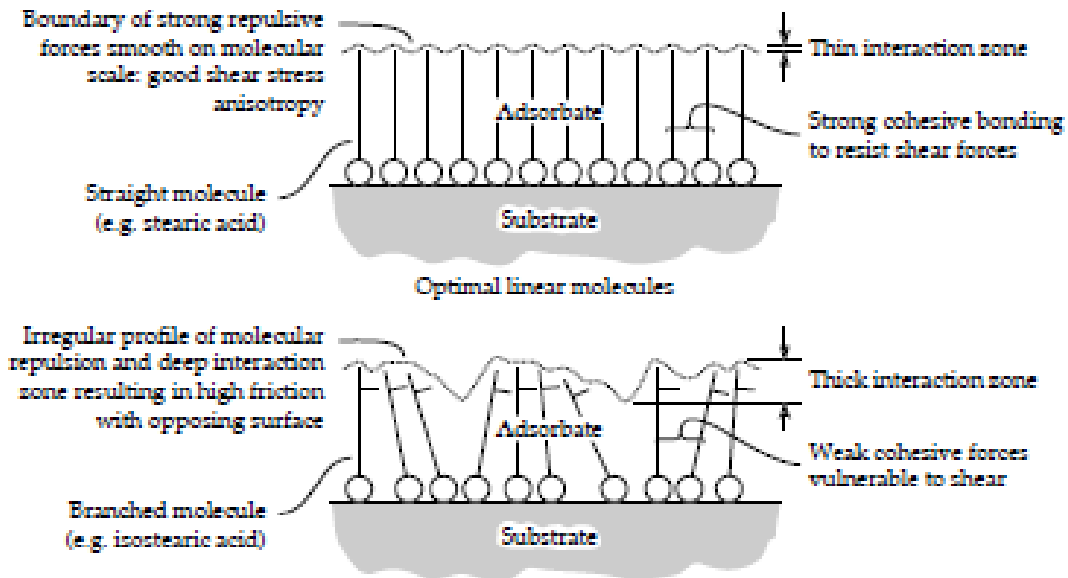
Figure 2-13: Film structure disruption due to branched additive structure (Batchelor & Stachowiak, 2003, p. 365).

2.4.2. Chain length

The chain length of the additive affects the boundary layer strength and the solubility in the base fluid. The critical chain length is 12 carbons (Batchelor & Stachowiak, 2003). An alcohol molecule containing 18 carbons provides a lower coefficient of friction than a fatty acid with 12 carbons. This is unexpected since the fatty acid is more polar, but the longer chain length creates a film with lower shear strength (Ratoi, Angel, Bovington, & Spikes, 2000).

2.4.3. Effect of additive concentration

The effect of bulk concentration on diffusion and absorption rates is well known in the engineering field. Higher bulk concentration of a species gives higher absorption and higher diffusion rates. This implies that there is a critical concentration at which an additive can reproduce a film at a specific sliding velocity. In Figure 2-14 this critical concentration is the inflection point in each graph.
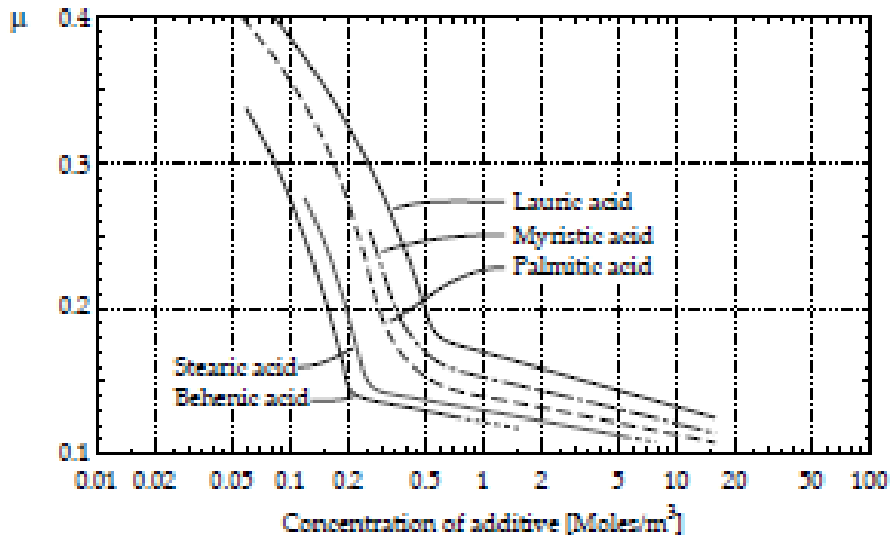
Figure 2-14: Effect of fatty acid concentration on the coefficient of friction
(Batchelor & Stachowiak, 2003, p. 372)

There is also a point where adding more additive will have very little effect on lubricity and is dependent on the total surface area on the surfaces used.

An interesting phenomenon to notice is that as the chain length increases the critical concentration decreases, in Figure 2-14. There is also a bigger jump in the critical concentration at the 18-carbon chain length discussed previously. Behenic acid which has 22 carbons has a much lower critical concentration than lauric acid which is a 12-carbon molecule. This implies that the strength of the film formed plays a role in the inflection point.

2.4.4. Summary on additives

The following summary gives general indications of trends that have been found concerning lubricity and additives.

- General
  - In general, an additive with a higher molecular mass has better lubricity properties compared to a molecule with lower molecular mass with the same functional group.

22

- Functional groups play a significant role in the lubricity of an additive.
  - Liquids with higher lubricity are less affected when other factors are changed.

- Diesters (Anastopoulos, E, Zannikos, Kalligeros, & Teas, 2001)
  - For the same di-carboxylic acid used to produce the diester:
    - Longer alcohol length increases lubricity
    - For the same alcohol length, increasing the di-carboxylic length does not give any significant lubricity improvements.

- Fatty acid esters (Anastopoulos, E, Karonis, Zannikos, & Kalligeros, 2001)
  - Higher kinematic viscosity of the fatty acid gives better lubricity

- Mono-carboxylic esters (Anastopoulos G. , Lois, Zannikos, Kalligeros, & Teas, 2002)
  - Esters with the oxygen group in the middle of the molecule gives better lubricity compared to a similar ester with the same molecular mass where the molecule is less symmetrical.

- Ethers (Anastopoulos G. , Lois, Zannikos, Kalligeros, & Teas, 2002)
  - Marginally better lubricity when the molecule is more symmetrical

- Alcohols (Anastopoulos G. , Lois, Zannikos, Kalligeros, & Teas, 2002)
  - Better lubricity additive compared to a similar ether, possibly due to the higher polarity of the alcohol

2.5.   Surface tribo-chemistry

With reactive nascent metals, some interesting reaction products can be formed during the wear process. The products can include:

- Soap layers
- Amorphous layers
- Oxide layers
- Decomposition products

- Polymerization

2.5.1. Soap layers

Soap layers are thick layers of metal fatty acids. There are generally two reactions that form soaps (Batchelor & Stachowiak, 2003, p. 384). Soap layers will normally be formed via reaction 2-2. The metal oxides are much less reactive than the metal hydroxides; this implies that reaction 2-3 will only happen under favourable conditions.

$$Fatty\ acid + metal\ hydroxide\ \rightarrow Soap + Water \qquad\qquad 2\text{-}2$$

$$Fatty\ acid + metal\ oxide\ \rightarrow Iron\ soap \qquad\qquad 2\text{-}3$$
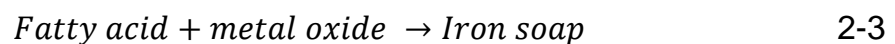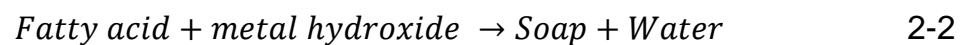
The thick soap layer can act as a protective film for the metal surface. Soap formation is dependent on water content.

2.5.2. Amorphous layers

As wear takes place oxide layers are rubbed off the metal surface to form particles. If these particles are worn down to a fine powder the powder can form an amorphous layer on the metal surfaces that can act as a protective film (Batchelor & Stachowiak, 2003, p. 388). Films like these are often used in dry lubrication where liquid are unusable due to operating or atmospheric conditions.

2.5.3. Oxidation of base fluids

Oxidation of the base fluid can give better lubricity under certain conditions. When the base fluid is oxidized it can cause an increase in its viscosity and acidity (activity). The increase in viscosity can reduce wear but increase energy usage while the increase in activity implies that more corrosive wear could occur.

The extent of base fluid oxidation depends on the following (Batchelor & Stachowiak, 2003, pp. 86 - 88):

- Temperature. An increase in temperature increases the rate of oxidation.
- The material of the surfaces. Some metals tend to act as a catalyst for oxidation, like iron, while metals like copper can inhibit oxidation.
- The contact area of metal and lubricant interface.
- The water content of the base fluid (higher water content increases oxidation).
- Base fluid composition. Unsaturated compounds tend to be oxidised at higher rates. Also implies that lower temperatures are required to oxidise unsaturated compounds.

Figure 2-15 below shows the effect that oxidation can have on the lubricity of base fluids.
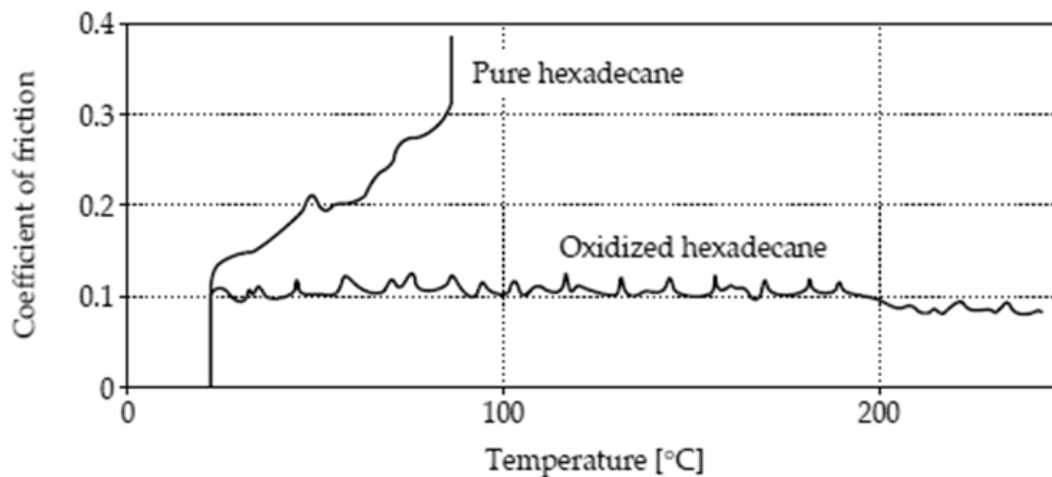
Figure 2-15: Friction comparison between pure hexadecane and oxidized hexadecane (Batchelor & Stachowiak, 2003, p. 88)

2.6.   Film formation

2.6.1. Physisorption

Physisorption is dependent on van der Waals forces; the stronger these forces are between the surface and the additive, the stronger the adsorbed additive layer will be. This process is reversible and is an exothermic process. Increasing temperature will increase the speed of the absorption process but will move the equilibrium (Batchelor & Stachowiak, 2003, p. 362)

Consider stearic acid (C-18) (Figure 2-16). The polar end has an affinity for polar materials, like metals and metal oxides. The non-polar end has an affinity towards non-polar substances implying that the molecule will arrange itself to have its tail in the non-polar lubricant and the head on the metal, Figure 2-17.
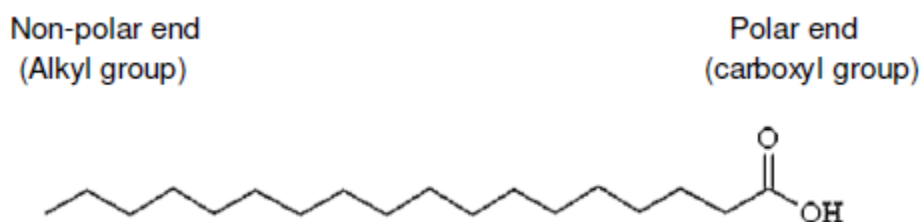
Figure 2-16: Stearic acid (C-18), an 18-carbon molecule with a polar carboxyl group.
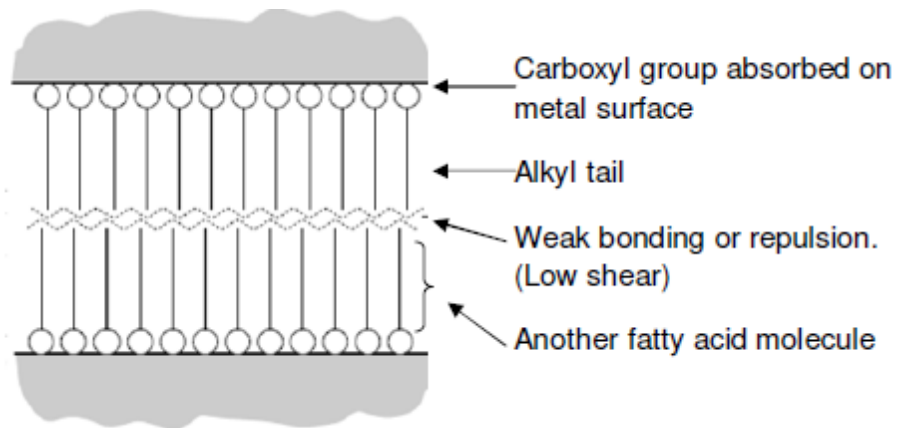
Figure 2-17: Single molecular layer separation with adsorbed lubricants
(Batchelor & Stachowiak, 2003, p. 362).

How molecules arrange themselves onto a surface is extremely important. When a fatty acid is absorbed onto a metal surface the layer that is formed can be described in one of 3 ways. Solid-like, liquid-like or gas-like, Figure 2-18.
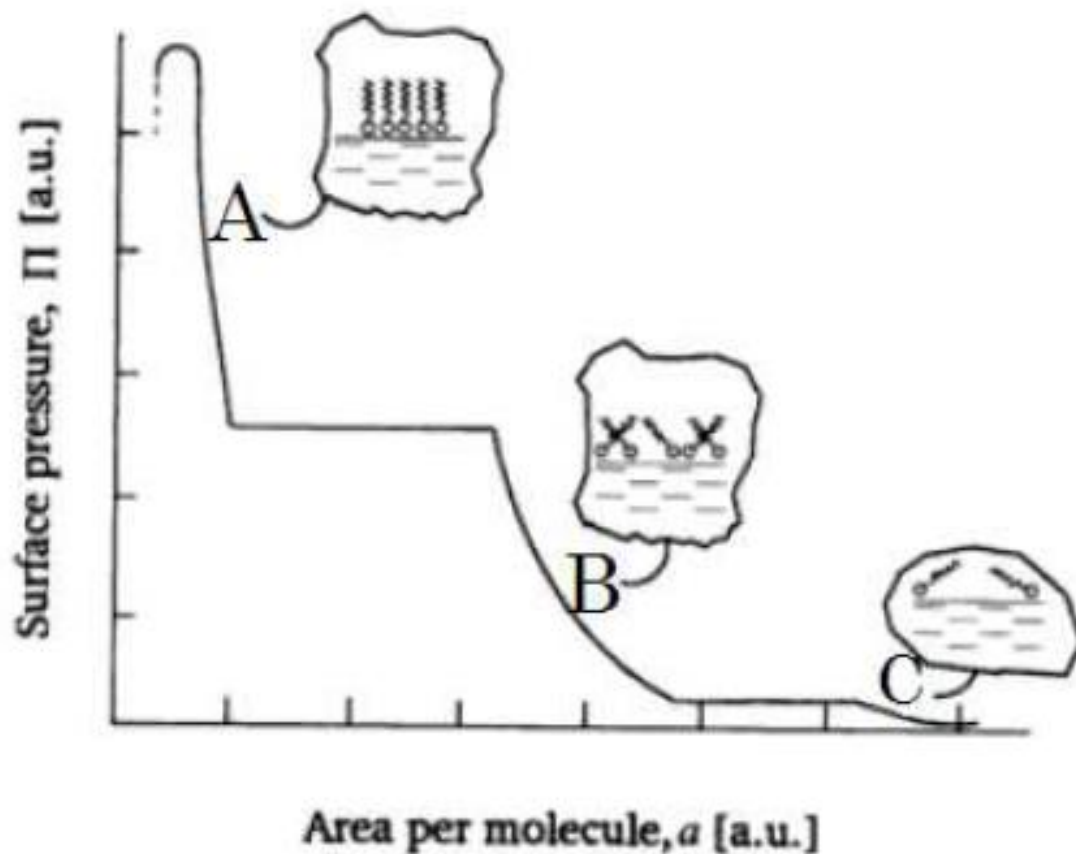
Figure 2-18: Surface pressure versus area per molecule for a long chain organic compound. A- solid-like film, B- liquid-like film, C-gas like film, (Petty, 1996).

The solid-like film gives better protection and higher load-carrying capacity to the surface film.

2.6.2. Chemisorption

Chemisorption is a more permanent exothermic bond. The additive is changed in the process and the heat of chemisorption is much higher than for physisorption implying that a chemisorbed layer will be much stronger than a physisorbed layer.

2.6.3. Temperature dependence of films

As stated, earlier physisorption and chemisorption are dependent on temperature. When the critical temperature for desorption is reached the film will become unstable. This destroys the orderly packed film that is formed and immediately increases the coefficient of friction. The desorption temperature is also pressure dependent. At higher pressures, the desorption temperature will increase (Batchelor & Stachowiak, 2003, pp. 376 - 377).

2.7.   Diffusion

Absorption and diffusion rates are very important factors when considering surface-active additives. According to Okabe, Masuko and Sakurai (Batchelor & Stachowiak, 2003, p. 373), there is a concentration, Figure 2-14, called the friction transition concentration where the concentration is high enough to repair a damaged boundary layer in oscillatory motion. During oscillatory motion, the additive has a limited time to repair any damage caused by friction to the protective surface. The rate-limiting factor for boundary layer repair is believed to be the re-adsorption rate of additive onto the wear surface after a stroke (Batchelor & Stachowiak, 2003, p. 373). The rate of re-adsorption is affected by the diffusion rate of the additive in the bulk to the surface and the rate of absorption. Diffusion rates depend on the additive used (smaller diffuses faster) and the concentration while the absorption rate depends on the surface reactivity, competition for the surface, additive species used and temperature.

2.8.   Concluding remarks

The lubricity of a lubricant is affected by the following:

- Temperatures of both the atmosphere and the contacts
- Atmospheric composition
- The water content of the liquid
- Atmospheric humidity

- Additive functional group, molecular size, and stearic interference in the boundary layer

Other factors which are important to keep track of are:

- Surface properties of contact
- Material properties of materials in contact
- Test method used
- Surface configuration
- Presence of oxygen

3. Equipment and materials

The equipment that was used to conduct the experiments is the High-Frequency Reciprocating Rig (HFRR) and the SRV (Schwingung (Oscillating), Reibung (Friction), Verschleiss (Wear)) machine. In addition, the following equipment was used to supplement results from the HFRR and SRV:

- Nanovea optical profilometer.
- Carl Zeis Microscope with x5, x10 lenses and a Canon EOS 300D digital camera.
- Stabinger viscometer, SVM 3000 Anton Paar

To maintain the partial pressure of water in the SRV and HFRR test chamber a custom humidifier was used, shown in Figure 3-1 below. To allow for constant monitoring and control, a Simulink control interface, shown in Figure 3-2, was programmed and connected to the flow controllers. This set-up allowed constant monitoring and control of the water vapour partial pressure in the control chamber. Control was possible within 0.1% relative humidity of the set point.
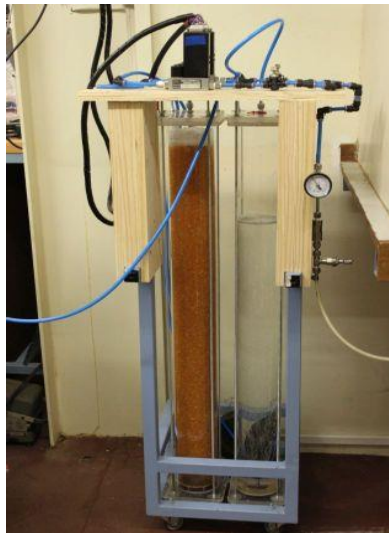
Figure 3-1: The humidifier.
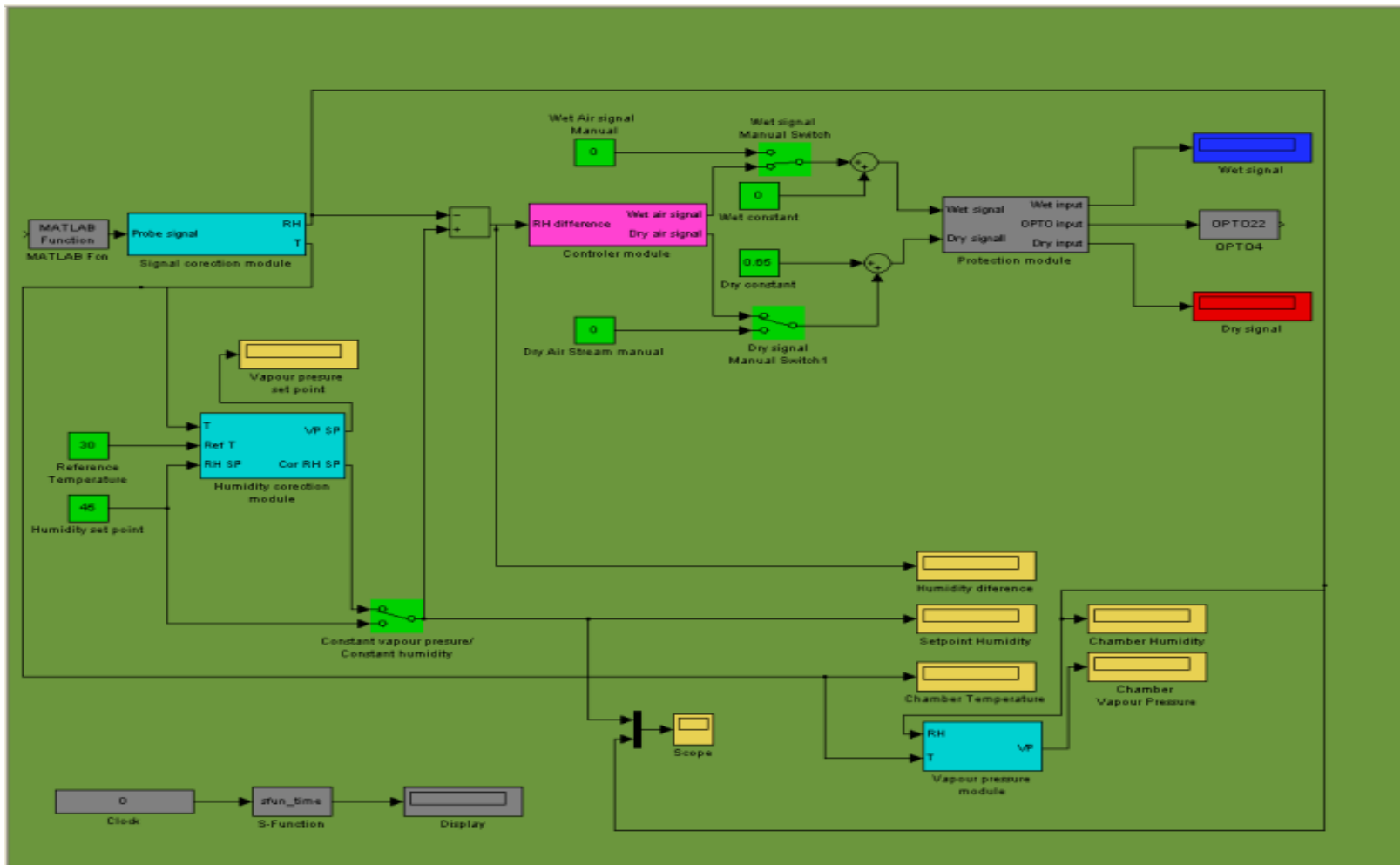
Figure 3-2: Humidifier Simulink control interface.

3.1. HFRR

The HFRR, shown in Figure 3-3, is a reciprocating device that oscillates a top specimen (ball) across a fixed bottom specimen (disc) which is held within a 2 mL bath. The bath temperature can be controlled using an electric heater onto which the bottom specimen holder is fastened. Measurements made by the machine include the bath temperature, coefficient of friction and electrical contact resistance (ECR). The ECR is given as a film % and is an indication of how thick the layer between the ball and disk specimen's metal surfaces is (typically metal oxides). A Perspex box was built to create a chamber to isolate the HFRR from the atmosphere. The Perspex box allowed the humidity of the environment to be controlled with the humidifier.
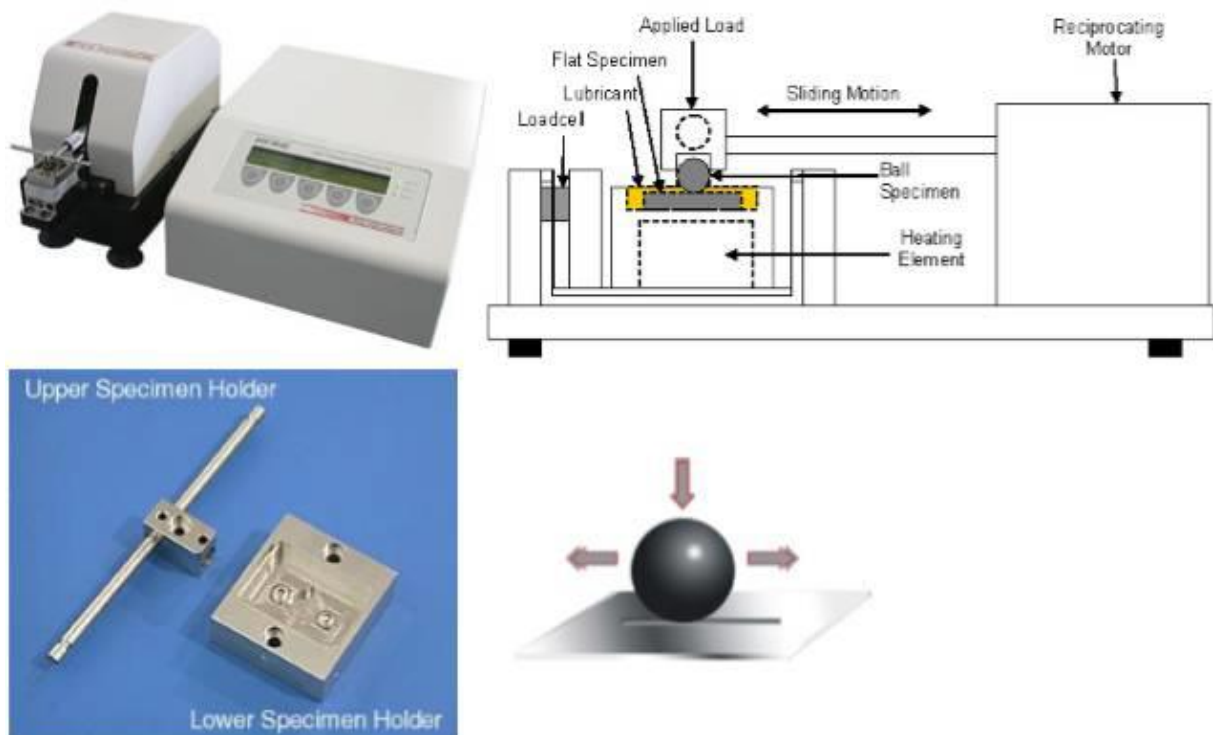
Figure 3-3: Pictures and diagrams of the HFRR (PCS Instruments, 2005).

The upper and lower specimens conform to the ISO 12156 standard, details are given in Table 3-1.

Table 3-1: HFRR specimen standards.

Test Ball (top specimen)	
Material	AISI E52100 steel
Hardness	Rockwell: 58 – 66
Surface Finish	Ra <0.05 μm
Diameter	6 mm
Test Disk (bottom specimen)	
Material	AISI E52100 steel
Hardness	Rockwell: 58 – 66
Surface Finish	Ra <0.05 μm
Diameter	10 mm

The following list summarizes the various standards applicable to the HFRR-apparatus:

- ASTM D6079, Evaluating lubricity of diesel fuels.
- ASTM D7688, Standard test methods for evaluating lubricity of diesel fuels.
- ISO 12156, Diesel fuel- Assessment of lubricity.
- IP 450, Diesel fuel – Assessment of lubricity.

For this project, ISO 12156 was used as the base for all tests. Details of this method are given in Table 3-2.

Table 3-2: ISO 12156 test details.

Parameter	Condition
Movement	Oscillatory
Applied load	2 N
Stroke length	1 mm
Frequency of oscillation	50 Hz
Test duration	75 min
Block temperature	60 °C
Fluid volume	2 mL

3.2.   SRV

The SRV, shown in Figure 3-4, is a very versatile machine with several different specimens and movement configurations. For this project, the ball and disk with reciprocating movement were used, the same configuration as for the HFRR.

What makes the SRV special is the ability to control the heating block temperature, oscillating frequency, stroke length and the applied load via a spring-loaded shaft. All these parameters can be pre-programmed to change during a test using steps or a gradient giving the SRV much more versatility compared to the HFRR.
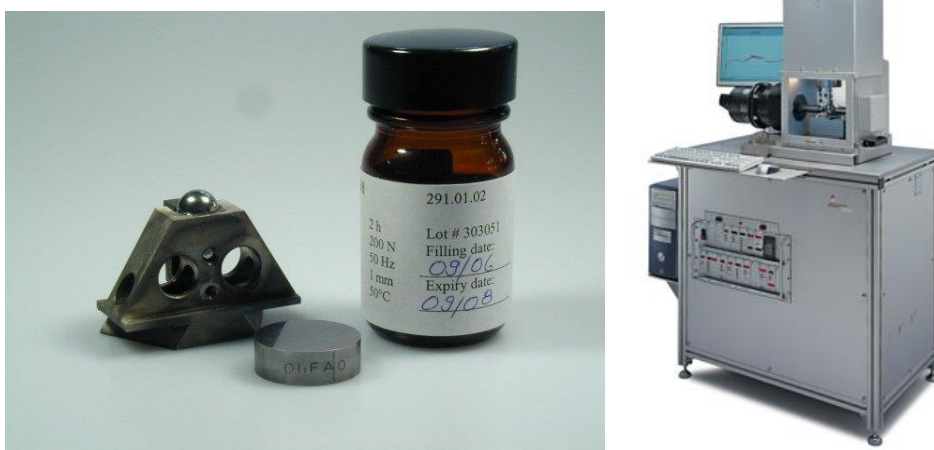
Figure 3-4: On the left: SRV specimens. On the right: Optimol SRV 4 machine.

Details on the test specimens and SRV are given in Table 3-3.

Table 3-3: SRV 4 test specifications.

SRV specifications	
Surface configuration	
Ball	10mm Diameter AISI -52100
Disk	24mm Diameter AISI -52100, 7.8mm thick
Ra	Ra=0.047 microns, 0.003 deviation
Test condition ranges, (for this set of experiments).	
Applied load	30 - 2000N
Oscillating frequency	2 - 500 Hz
Stroke length	1 – 3 mm
Temperature range	Temperature of the disk and the heating block: Room – 200 ºC
Test time	Varies.
Test standards	DIN 51834, ASTM D6425, ASTM D5707, ASTM D5706, EN31, DIN100C6

3.3.   Microscope

To gather information on the wear damage that occurred on the specimens, a microscope with a digital camera was used to take pictures at 5- and 10-times magnification. The pictures are then manually measured using software called Axiovision to find the wear track and wear scar lengths. The microscope details are given in Table 3-4.

Table 3-4: Microscope specifications.

Microscope specifications	
Microscope	Zeiss
-Model	Scope A1
-Magnification	5x/0.13HD
	10x/0.2HD
	20x/0.4HD
Digital camera	
-Model	AxioCam ERC 5s
-Software, pc	Axiovision Rel. 4.8.2

3.4. Profilometer

The Nanovea profilometer is also an optical device used to look at a surface but where the microscope uses light to take an image the profilometer uses a laser to measure intensity and distance. The measurements are placed into a matrix that can be used to build a 3-D image of the surface. The average height, surface roughness, deepest point (valley), the highest point (peak) and the volume of valleys or peaks can be calculated using the gathered information. All these values can then be used to describe the wear track and scar more accurately.

3.5.   Materials

The following table gives information on the chemicals used during experiments.

Table 3-5: Materials used during experiments.

Chemical	Use	Notes
n-Hexadecane	Used as the base fluid for most experiments.	
Industrial gear oil	Used in initial experiments to protect the SRV and investigate lubricant starvation.	Iso 460 oil. 460 viscosity grade oil.
Lubricity additives	Used to give n-hexadecane some lubricity. Carboxylic acids used: • C-14, Myristic acid (C-14)- $CH_3(CH_2)_{12}COOH$ • C-16, Palmitic acid (C-16)- $CH_3(CH_2)_{14}COOH$ • C-18, Stearic acid (C-18)- $CH_3(CH_2)_{16}COOH$	All the lubricity additives used are irritants to the skin and eyes.
n-Hexane	The non-polar solvent used to clean specimens.	• Volatile • Flammable • Irritant
Acetone	The polar solvent used to clean specimens.	• Volatile • Flammable • Irritant
Toluene	Solvent used that can clean both polar and non-polar residues on specimens.	• Volatile • Flammable • Irritant • Carcinogenic

3.5.1. n-Hexadecane

n-Hexadecane was chosen as the base fluid for the experiments. This decision was made because of the large amount of experimental data available in literature and within our tribology laboratory using n-hexadecane as the base fluid. It has also been shown that n-hexadecane has very low lubricity and reacts like a Newtonian fluid (Ratoi, Angel, Bovington, & Spikes, 2000), making it a perfect candidate for experimental work investigating additives. Using a base fluid

with a single compound also ensured that the base fluid composition remained constant between tests. N-hexadecane is a liquid at room temperature with a freezing point of 18 °C with a boiling point (287 °C) in the boiling point range of diesel (180 – 360 °C). n-hexadecane or cetane has been given the cetane number of 100 and is used to determine the cetane rating of diesel fuels.

4. Initial experiments

Standards like ASTM D5706 and D7421 are typically used in industry to determine the load-carrying capacity of a lubricant. By determining the load-carrying capacity a part of the Stribeck curve for that lubricant is generated. Before this project, limited experience was available on changing the oscillating frequency for an SRV test. Several experiments were conducted before delving into how linear velocity affects wear.

During these tests, the following was investigated.

- Generating a Stribeck curve by
    - Changing the applied load
    - Changing sliding speed
- The volume of lubricant used
- Effect of the oscillating frequency
- SRV data acquisition frequency

4.1. Generating Stribeck curves

With two ways to generate Stribeck curves on the SRV, it was important to know if the two methods would give different results. The two different methods are:

- Constant load while varying the oscillating frequency.
- Constant oscillating frequency while varying the load.

In addition, the following was also investigated during these tests

- Lubricant starvation
- The effect of the sampling rate of the SRV
- Oscillating frequency range

Lubricant starvation was investigated by using a high viscosity lubricant. A high-performance commercial ISO 460 gear oil was used as the high viscosity

lubricant. The product's high lubricity would help to protect the SRV from damage while the limits of the machine are tested. The following tests were conducted:

- Gear oil load-carrying capacity tests
    - Test started with a 50 N run in for 1 minute
    - Oscillating frequency 25, 50,75 and 100 Hz.
    - Temperature 50°C.
    - Relative Humidity 50 %.
    - The applied load was increased in 50 N steps over 30 seconds and then held constant for 30 seconds after each 50 N increase.
- Constant Load tests
    - Test started with a 50 Hz running-in period of 5 minutes
    - Run the test at a constant load
    - Change the oscillating frequency in 25 Hz step increase/decrease
    - After 100 Hz decrease the oscillating frequency back down to 25 Hz in 25 Hz steps waiting 5 min after each step.
    - Temperature 50 °C
    - Relative Humidity 50 %

4.1.1. Generating Stribeck curves by changing the load

To test whether the SRV could handle the required frequencies with ease an open gear lubricant with good lubricating properties was used to run load-carrying capacity tests at 25 Hz, 50 Hz, 75 Hz and 100 Hz. The results obtained with the open gear lubricant are given in Figure 4-1 to Figure 4-4. During the start of each run increases in load reduces the coefficient of friction corresponding to movement on the Stribeck curve from EHL to the mixed lubrication regimes. As the load increases further, the coefficient of friction starts to increase indicating movement into the boundary lubrication regime on the Stribeck curve.
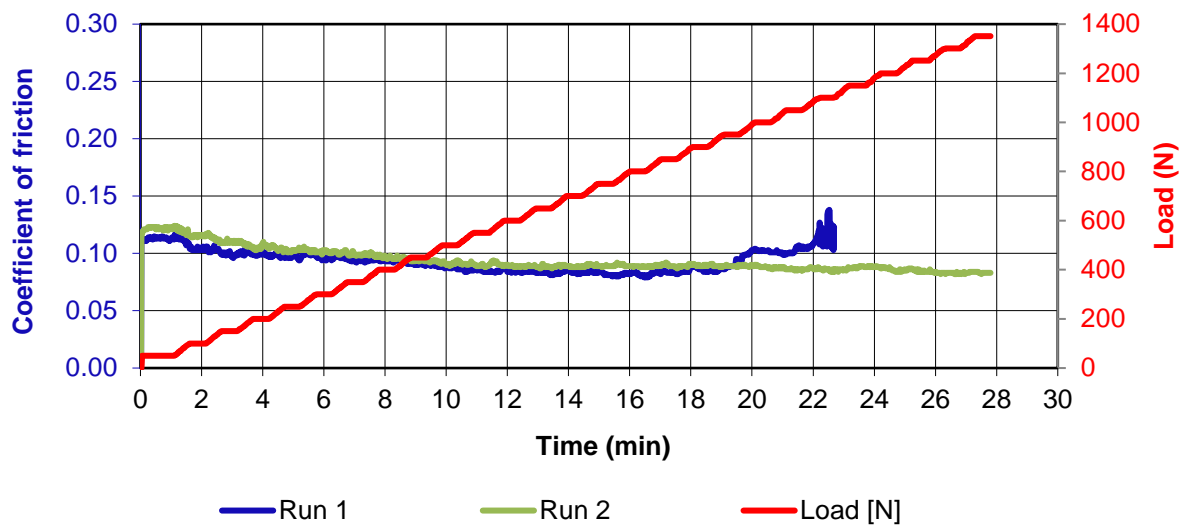
Figure 4-1: Open gear lubricant test at 25 Hz, 50°C,1 mm stroke and 50% relative humidity.
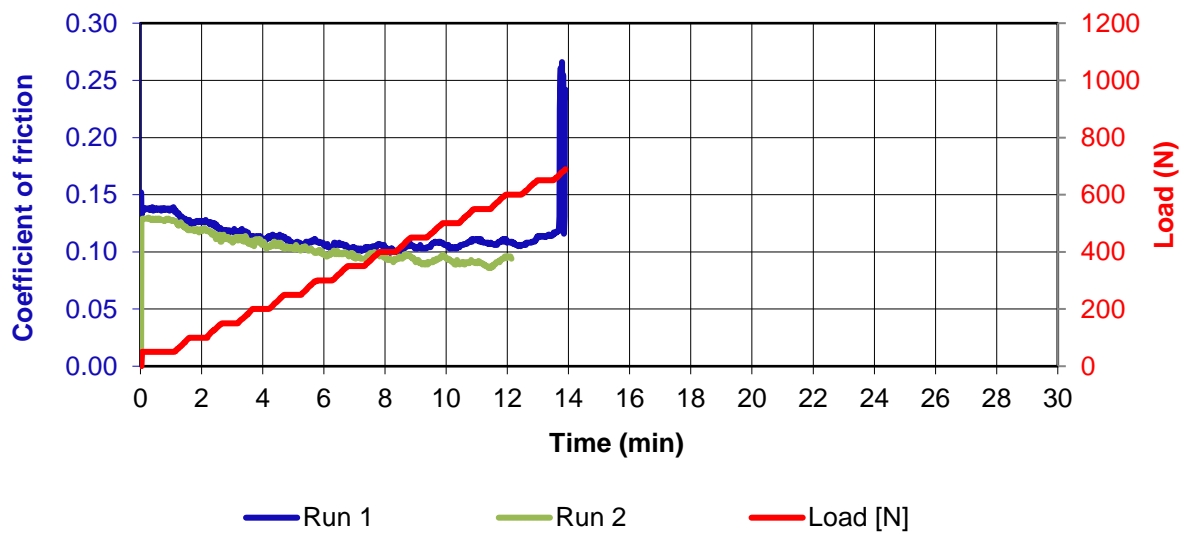
Figure 4-2: Open gear lubricant test at 50 Hz, 50°C,1 mm stroke and 50% relative humidity.
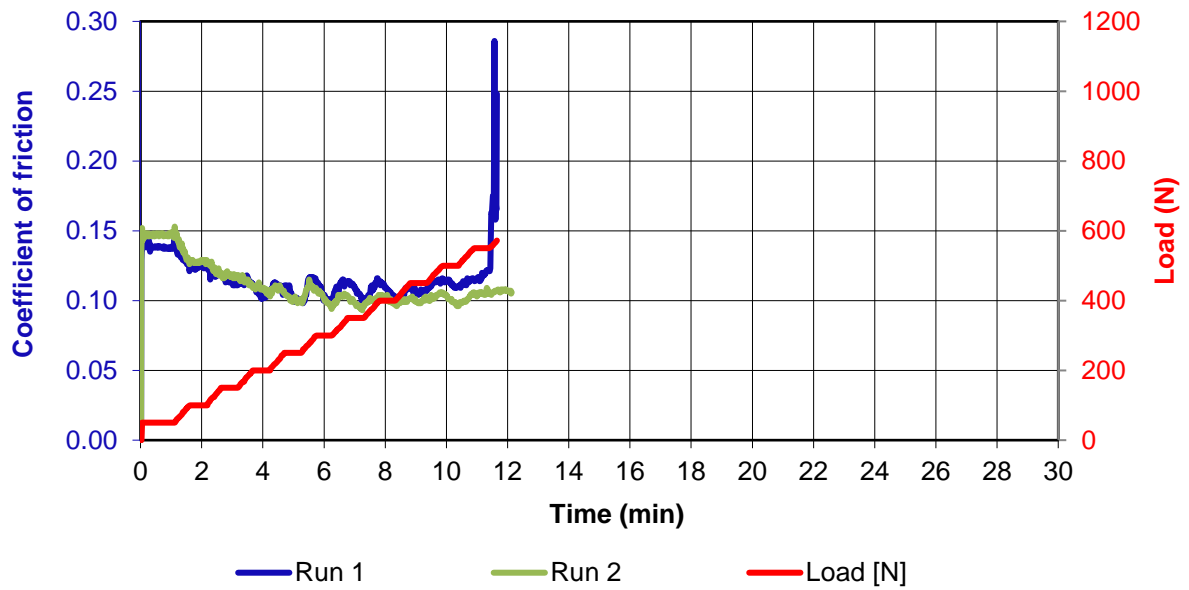
Figure 4-3: Open gear lubricant test at 75 Hz, 50°C,1 mm stroke and 50% relative humidity.
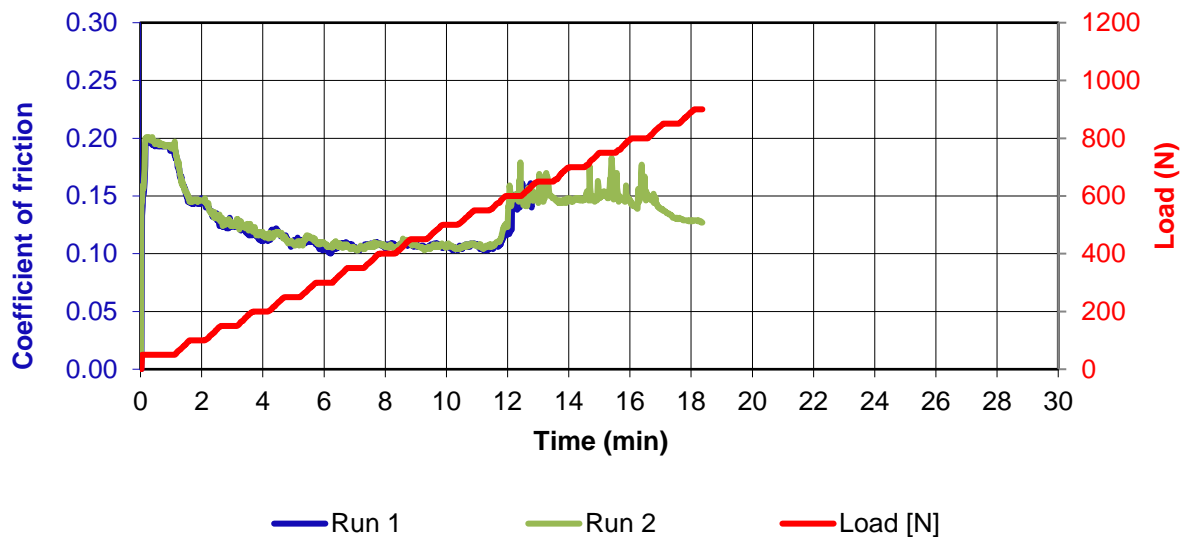
Figure 4-4: Open gear lubricant test at 100 Hz, 50°C,1 mm stroke and 50% relative humidity.

Each load increase happened gradually over 30 s. Something to notice is that each time the increase happens there is an increase in the coefficient of friction which is followed by a decrease to a new stable coefficient of friction. This behaviour is most pronounced during the 75 Hz run, Figure 4-7. Deformations in the wear surfaces can explain this behaviour. Increased load causes more deformations in the two surfaces increasing the real contact area, reducing the pressure which leads to the decreased coefficient of friction. During the initial deformations, a higher coefficient of friction is observed corresponding to the energy required to cause the deformations. As the surfaces conform towards each other during the constant load stage the coefficient of friction start to drop again with the increased surface area. The SRV can measure the wear depth to some extent. While the test is running there is a sensor that measures how far the top specimen has moved from a zero point up- or downwards. Because this measurement is taken under load it is important to remember that any deformations in the specimen or any material being loaded will be included in the wear depth measurement. The wear depth measurement from the SRV supports the idea of increased coefficient of friction due to more deformations during the load increases, Figure 4-5 to Figure 4-8. Before the SRV start oscillation, the load is applied. The deformations in the driveshaft, disk, ball specimen and the heating block are shown at the start of the wear depth graphs. When oscillation starts a new zero is set to ensure that all these initial deformations are not measured. All the results show a steep increase in the wear depth (deformations) during load increases followed by a gradual increase (wear) at constant load. For LCC test these jumps will always be observed as more deformation take place with a load increase than material wear. Unfortunately, the SRV stops recording wear depth when breakthrough occurs.
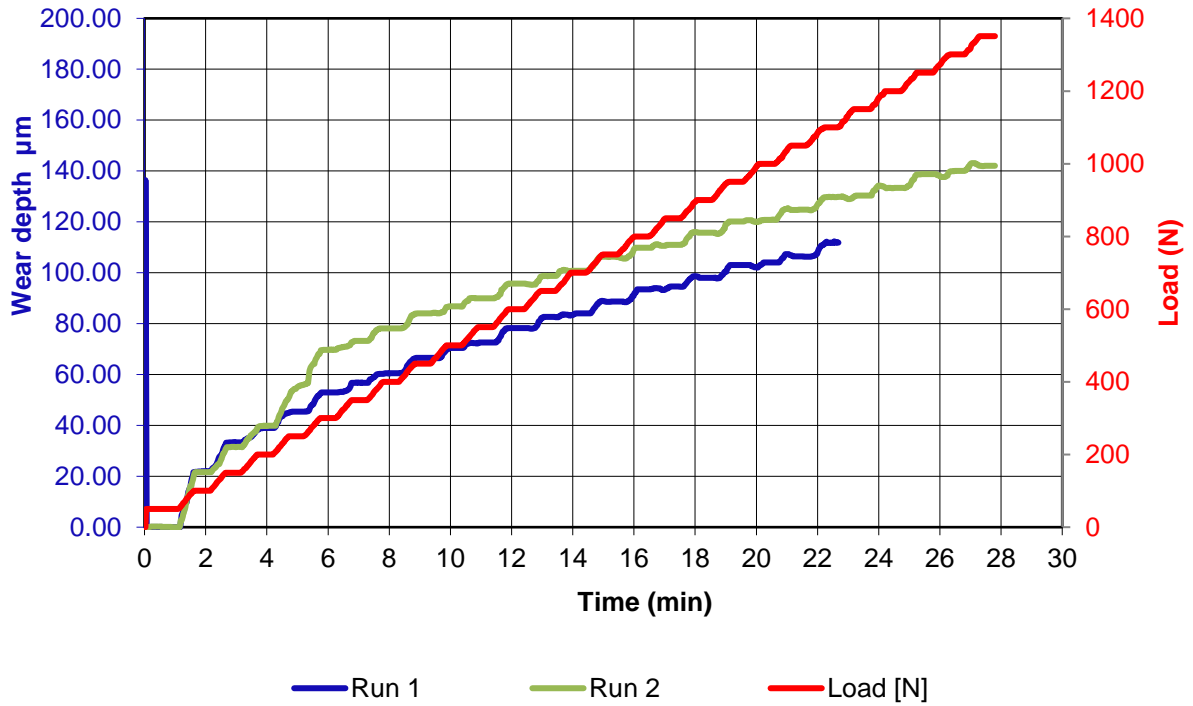
Figure 4-5: Wear results for open gear lubricant tests at 25 Hz.
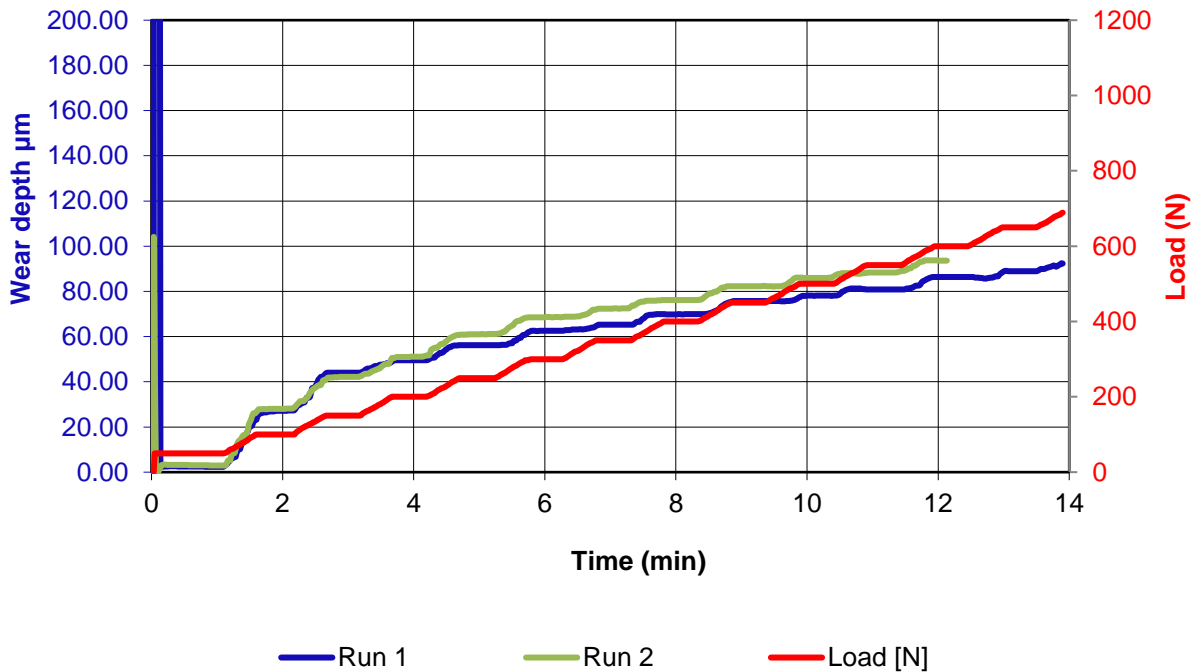
Figure 4-6: Wear results for open gear lubricant tests at 50 Hz.
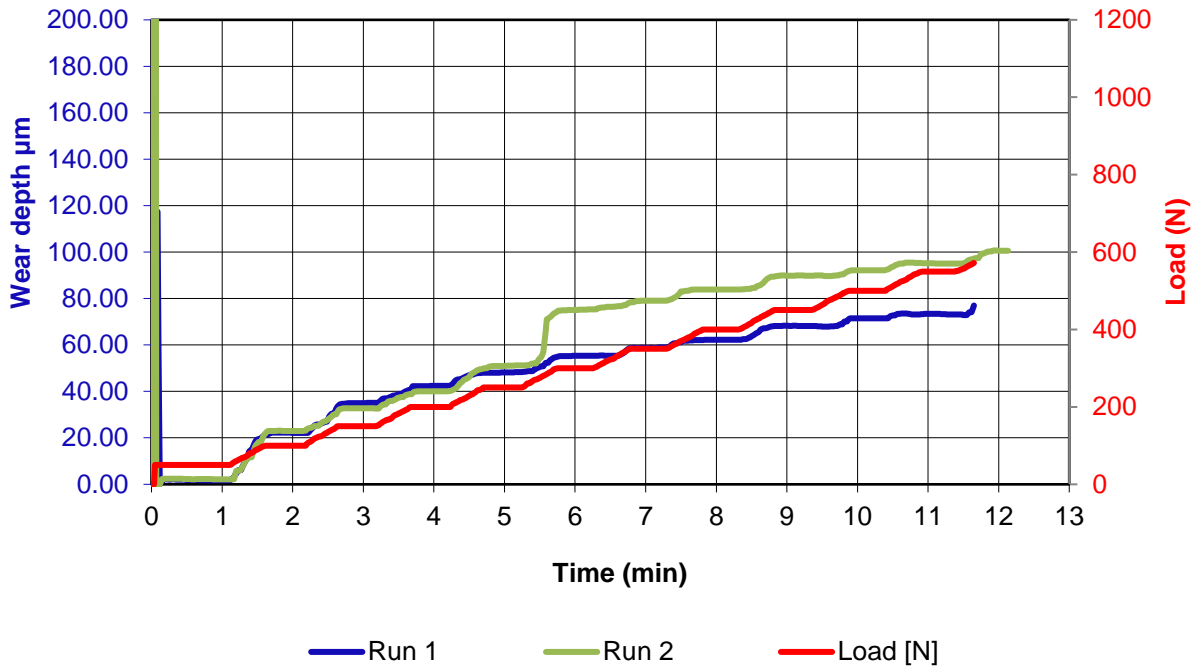
Figure 4-7: Wear results for open gear lubricant tests at 75 Hz.
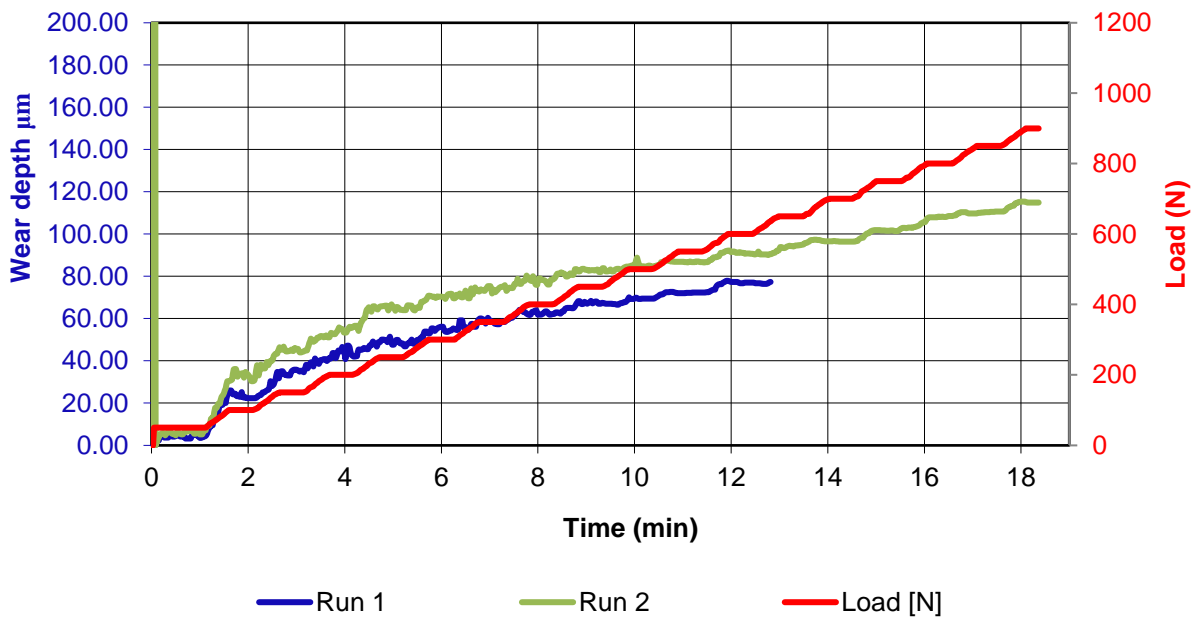
Figure 4-8: Wear results for open gear lubricant tests at 100 Hz

Figure 4-4 and Figure 4-8 require special consideration. As the oscillating frequency is increased results for the coefficient of friction and wear depth both become more erratic. With the top specimen moving so fast it is possible that the

measuring probes cannot keep up, because the measuring frequency is too low. To investigate the effect frequency has on the coefficient of friction the average coefficient of friction was calculated at every constant 30 s load stage to produce Figure 4-9 - Figure 4-12.

The 3-dimensional graph, Figure 4-9, shows the complexity of changing load and frequency. Generally, changes in load will reduce the coefficient of friction up to the mixed lubrication regime and then start to increase the coefficient of friction. The oscillating frequency has the opposite trend according to the Stribeck curve. Increasing the oscillating frequency will move the system out of the mixed lubrication regime, lowering the coefficient of friction, followed by increases in the coefficient of friction as the system enters the elastro-hydrodynamic regime. Increases in oscillating frequency will increase the coefficient of friction due to more hydrodynamic drag in the fluid. Very low oscillating frequencies will lower the hydrodynamic pressure to such an extent that the liquid can no longer sustain a load.
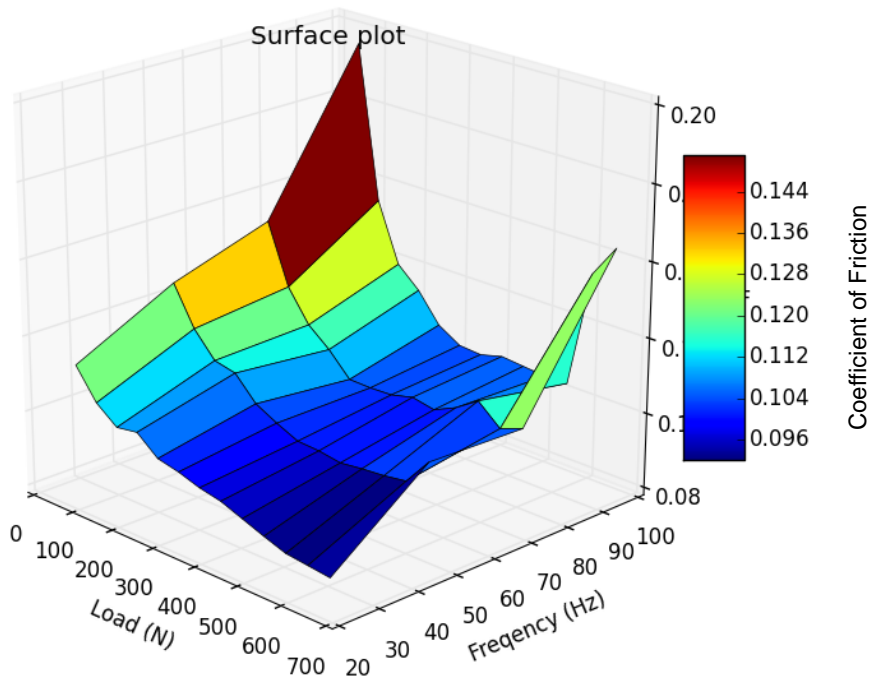
Figure 4-9: 3-D plot of the average coefficient of friction (on the y-axis with a colour scale for visualisation) at each constant load section for all the open gear lubricant load-carrying capacity runs at different oscillating frequencies.
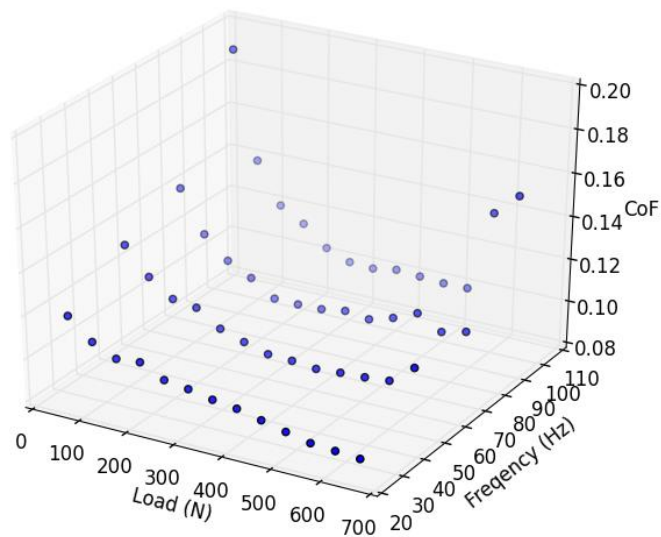
Figure 4-10: Separate data points without surfaces included for Figure 4-9.

Two 2-dimensional plots (Figure 4-11 and Figure 4-12) of Figure 4-9 were made to give more detail on the general trends observed. From Figure 4-11 the effect of load can be seen. At lower loads increases in the load decreases the coefficient of friction. At higher load, close to the load-carrying capacity, increases in the load increase coefficient of friction. This trend corresponds with a Stribeck curve. The general trend for the oscillating frequency can also be seen. Lower oscillating frequencies resulted in a lower coefficient of friction, less liquid shearing.
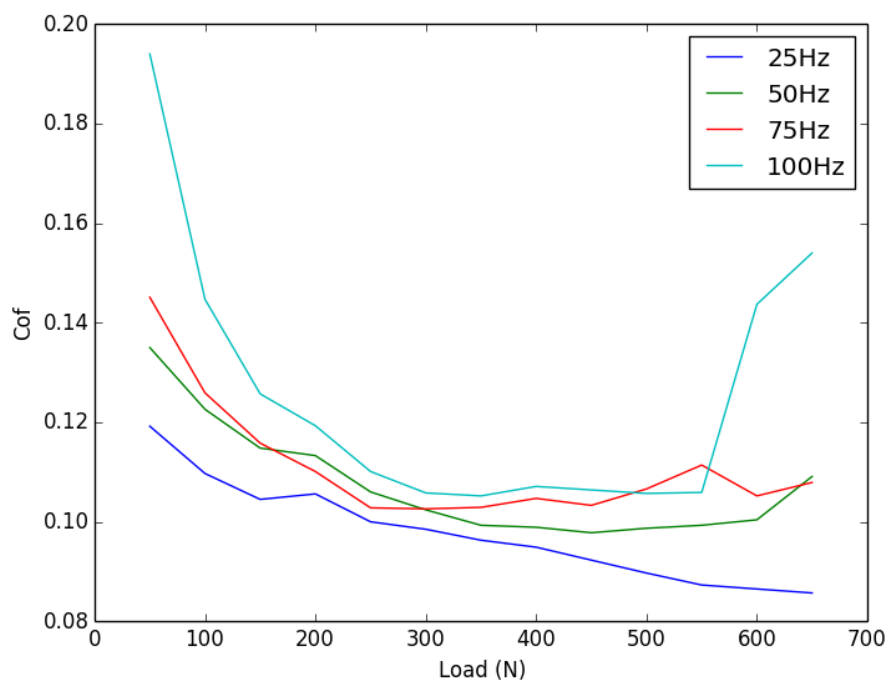
Figure 4-11: 2-D plot of the average coefficient of friction data against the applied load.

The graph still does not explain why the load-carrying capacity of the oil decreased at higher oscillating frequencies. The load-carrying capacity for all the tests is shown in Table 4-1. According to literature increases in the linear velocity of two sliding contacts will increase the hydrodynamic pressure, increasing the boundary layer thickness, (Ratoi et al, 2000). The hydrodynamic pressure

becomes even more important if a higher viscosity fluid is used. Higher velocities increase the pressure in the liquid which in turn increases the viscosity of the liquid. This is why gear oils traditionally have higher viscosities to make full use of hydrodynamic pressure to protect the gears from wear (Roberts, 1990) With oscillating systems, the hydrodynamic pressure to keep surfaces apart is lost at the endpoint where the velocity returns to zero for a moment.

Table 4-1: Load-carrying capacity results for the open gear lubricant tests.

Oscillating Frequency (Hz)	Load-carrying capacity Run 1	Load-carrying capacity Run 2
25	1100 (Stroke)	1351 (Stopped due to high load)
50	689	733
75	572	600
100	637	900 (Initial: 637)
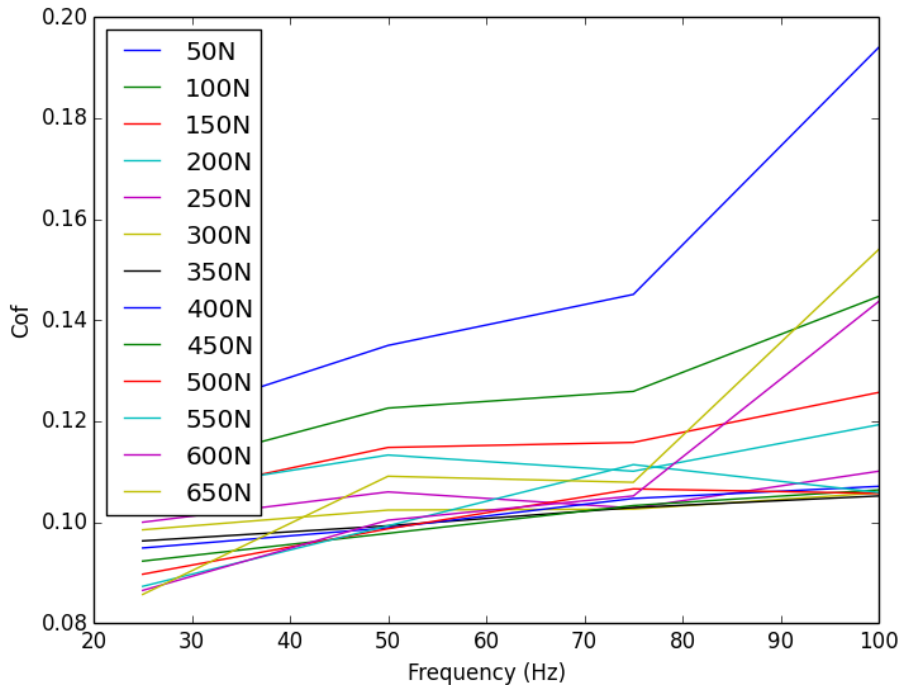
Figure 4-12: 2-D plot of the average coefficient of friction data against oscillating frequency.

The expectation for the load-carrying capacity was that higher hydrodynamic pressure at high oscillating frequencies would increase the load-carrying capacity. From the results in Table 4-1, this expectation was wrong. The results at 25 Hz where much higher compared to results at other frequencies and how breakthrough occurred was also different. Some of the tests were stopped due to measurements other than a coefficient of friction above 0.3 or a coefficient of friction above 2.7 for more than 20 s.

Run 1 at 25 Hz was stopped due to the irregular stroke length while run 2 was stopped after the applied load surpassed 1350, Figure 4-13. The second run was stopped to reduce the risk of damaging the SRV. Both runs at 25 Hz reached a coefficient of friction of 0.3 but both runs started to stick and slip at higher loads. Both tests at 100 Hz failed but the SRV did not stop the runs when the coefficient of friction went above 0.3. Run 2 was left to continue to see if catastrophic breakthrough would occur at higher loads, the value in the parentheses.
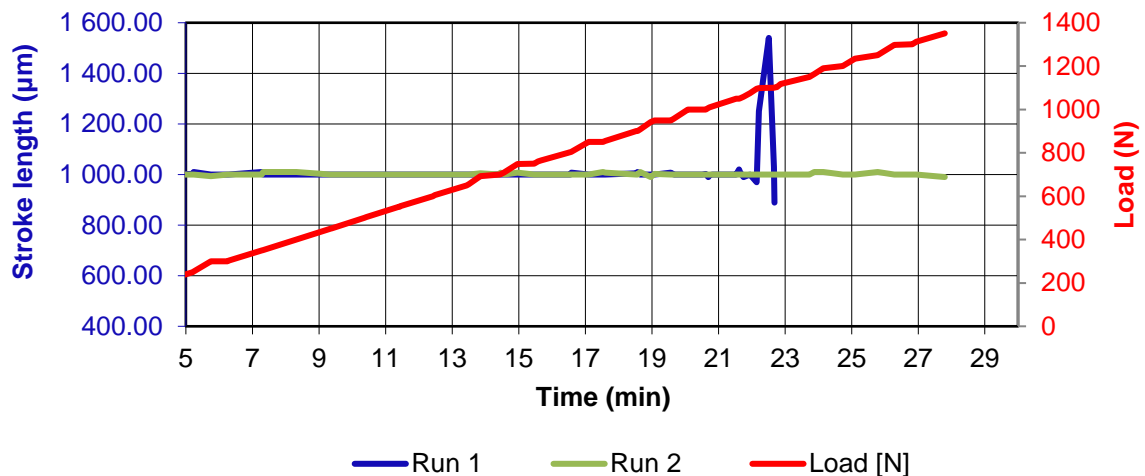
Figure 4-13: Stroke length for tests at 25 Hz.

The following are possible explanations for this observation.

Lubricant starvation at higher frequencies

The viscosity of a fluid is a measurement of its resistance to deformation. Fluids with high viscosities are more difficult to deform and deform slower under the same stresses compared to fluids with lower viscosities. Lubricants with very high viscosity, like greases, have been seen to have a load-carrying capacity as low as 200 N, while the expected results are above 1000 N. While running a friction and wear test, a grease will sustain a load for a time and then fail suddenly. When the same grease is tested at a higher temperature where the grease can flow back into the wear scar the results change drastically, (Cann, 1996). Visual observation during and after tests did not show signs of lubricant starvation using the gear oil. It is safe to assume that using the less viscous n-hexadecane at high oscillating frequencies will not result in lubricant starvation and that lubricant starvation was not the cause of unexpected results at higher oscillating frequencies.

The sensitivity of additives to the oscillating frequency

Every molecule in a fluid has a certain diffusion rate that is affected by the concentration gradient of the molecule in the fluid, its shape, the molecular weight, and the size of the molecule. If the diffusion and absorption rate is slower than the rate at which the adsorbed layer is removed, an increase in wear will be observed, (Batchelor & Stachowiak, 2003). At higher frequencies and loads the rate at which the additive film layer is removed increases. This suggests that there is a band of frequencies under which an additive can operate under a load. This will be investigated in later chapters by running tests with additives that have different chain lengths. The atmosphere also plays a significant role in a surface-active additive's performance. Oxygen and water have been shown to compete with fatty acids for surface area (Langenhoven, 2014). Running tests with different chain length fatty acids can be used to investigate if the diffusion rates play a role. The atmospheric composition should be kept constant during these tests to avoid different adsorption rates due to competition.

Contact temperatures

Increases in the oscillating frequency can result in higher contact temperatures. The higher temperatures could, in turn, affect the composition of the lubricant. Higher temperatures could also lead to more chemical wear (Batchelor & Stachowiak, 2003, pp. 86 - 88), (Kaline, 2004).

As the friction between two contacting surfaces increases, more energy is absorbed into the surfaces as heat. At higher frequencies, the rate of heat generation on the two surfaces increases resulting in higher contact temperatures.

An increase in the block temperature was observed in runs at an oscillating frequency of a 100 Hz, Figure 4-14. Other runs maintained stable block temperatures of 50 °C. The SRV is designed to maintain the block temperature but for these tests, the block's temperature increased by 5 degrees. The block temperature increased at the load where an increase in the coefficient of friction was observed in Figure 4-4.
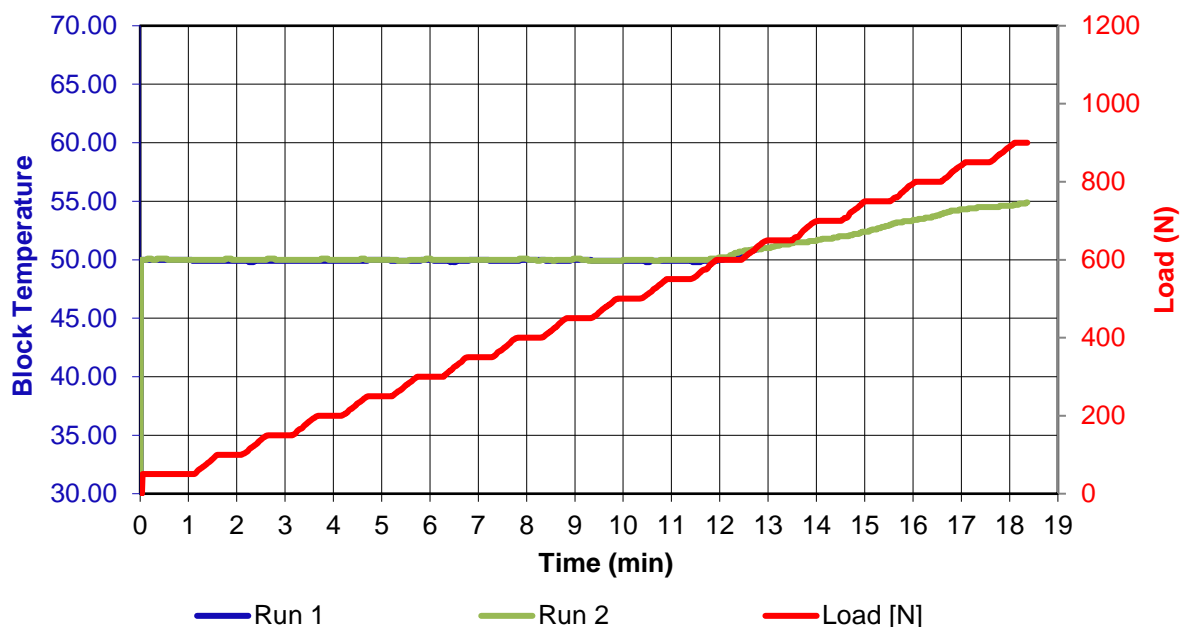
Figure 4-14: Block temperature data for the open gear lubricant test at 100 Hz.

Increases in contact temperatures will also change the physical properties of the specimens, making them softer, resulting in more elastic deformations. This is important to consider. As the oscillating frequency was increased the load-carrying capacity decreased but, there was an increase in the load-carrying capacity for the 100 Hz runs compared with the 75 Hz runs. The 75 Hz run did not show any block temperature increases. With the increased temperature and more deformations taking place, the real contact surface area increases reducing the pressure resulting in a higher than expected load-carrying capacity.

Motor power output

When the oscillating frequency is increased the power output of the motor driving the oscillatory motion increases. The higher power output to achieve the higher oscillating frequencies results in more force being used to move the top specimen.

According to equation 4-1 if an object needs to be accelerated faster more force must be applied to the object.

$$F = Ma \qquad\qquad 4\text{-}1$$

This is important to consider when changing the oscillating frequency. The top specimen needs to be accelerated (a) from a standstill and then decelerated to stop at the end of its stroke. This implies that the top specimen is not moving at a constant velocity as in unidirectional tribosystems. The higher the desired oscillating frequency is, the faster the acceleration must be to achieve the necessary speed. To achieve a higher acceleration, more force is required (F). This means that when operating under high frequencies the motor applies more force to the top specimen. The force exerted by the motor on the top specimen is the maximum force that can be measured as the frictional force. This can explain what happened at 25 Hz runs.

Tests at 25 Hz had strange behaviour in the stroke length data. At all the other test frequencies the stroke length remained stable up to the load-carrying

capacity of the lubricant. Looking at Figure 4-15, the stroke length for run 1 changes drastically at 22 minutes indicating seizure between the two specimens but the corresponding coefficient of friction at this point was below 0.15. This is a situation where there is simply not enough force put in to move the top specimen to result in a coefficient of friction above 0.3 at the required acceleration.
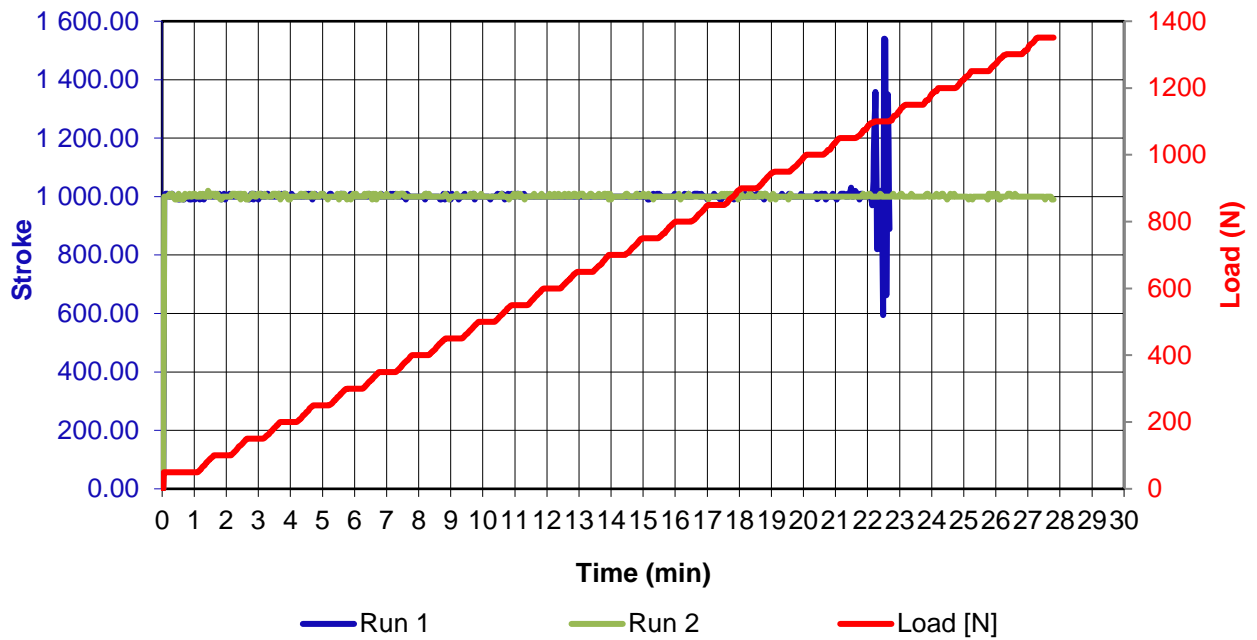
Figure 4-15: Stroke length data of open gear lubricant tests at 25 Hz.

Figure 4-16 shows the stroke length of a test at 50 Hz. The sudden change in the stroke length of run 1 corresponds to the point where the coefficient of friction went above 0.3.
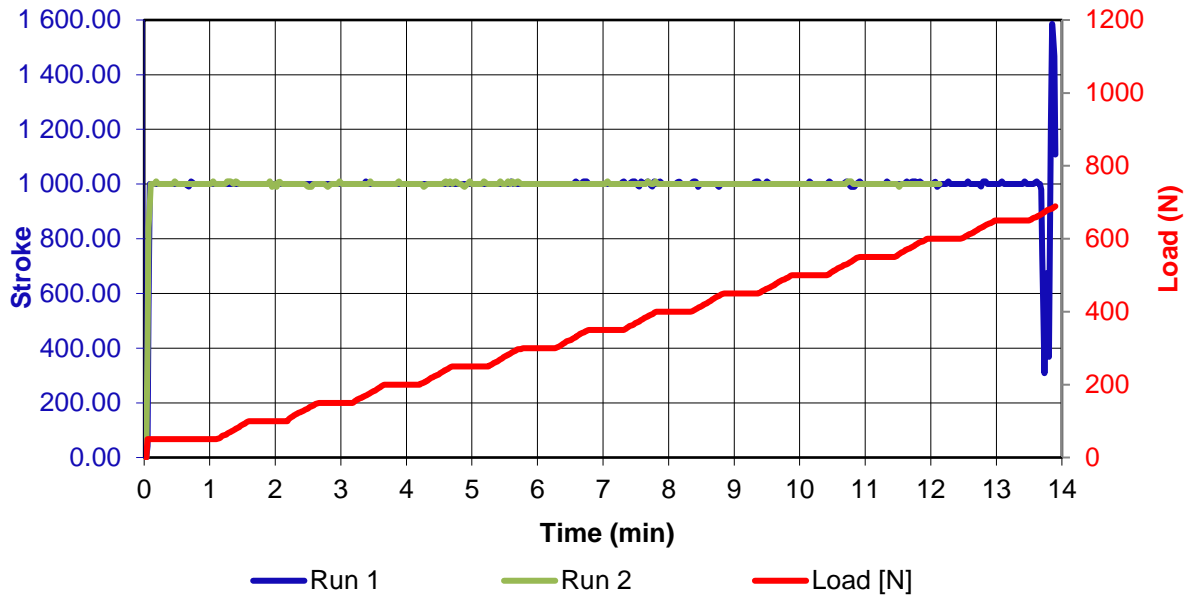
Figure 4-16: Stroke length data of open gear lubricant tests at 50 Hz.

The runs at 25 Hz never failed because of the high coefficient of friction but there was contact between the surfaces. The force the motor exerts on the top specimen explains the behaviour. If the force the motor exerts is lower than the force required to break any contact points the top specimen will start to stick and then overshoot as the force ramps up to get the ball moving again, explaining the irregular stroke length. The low coefficient of friction observed is also due to the limiting force of the motor. If the force the motor applies is lower than the frictional force required to give a coefficient of friction above 0.3 then we will never see a coefficient of friction this high for these runs.

Static and kinetic coefficient of friction

Due to the oscillatory movement of the top specimen in the SRV, there are moments at the end of each stroke where the top specimen stops. This implies that both the static and kinetic coefficient of friction plays a role in the coefficient of friction observed during a test.

The SRV gives the coefficient of friction data in one-second intervals (an average of several readings depending on the sample rate used in the SRV's software). If

the average includes the static coefficient of friction it stands to reason that higher oscillating frequencies (more static coefficient of friction data points) would result in a higher average coefficient of friction simply due to how an average would be calculated in such a situation. As we increase the oscillating frequency the coefficient of friction will also increase due to higher liquid shear.

A question that came up at this point is why we do not see the change in lubricating regime during a stroke in the coefficient of friction results. To investigate this raw data was taken from a test. The results are given in Figure 4-17. The results are similar to those shown in Figure 5-1 to Figure 5-3, as will be shown later, but in this case, all the measured points are shown, instead of an average over every 1 s interval, the standard reporting method for the SRV. The raw data suggests that the SRV takes 62.5 coefficient of friction measurements per second. Sample rate was set to 64 Hz. This implies that some data points are missing.
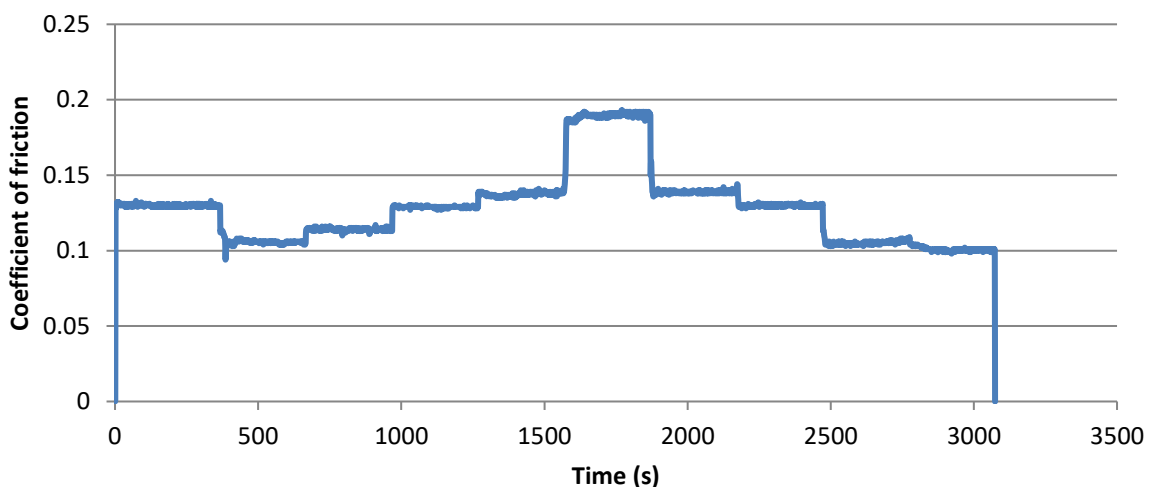
Figure 4-17: Raw coefficient of friction data collected for an FS (frequency scan) rest at 50 N using M500.

Using at smaller sections of the data, Figure 4-18 to Figure 4-20 provides very important insight into what data the SRV captures. Note that there is a constant difference of 0.00062 between all recorded values of the coefficient of friction.

This shows with the bit resolution used on the SRV that the SRV cannot distinguish between values with a smaller difference than 0.00062. This value tells us what we can consider as being a different value when comparing results. If two results do not differ by 2 times 0.00062 (0.00124) or more, we cannot say that there is a difference between the two results at all.
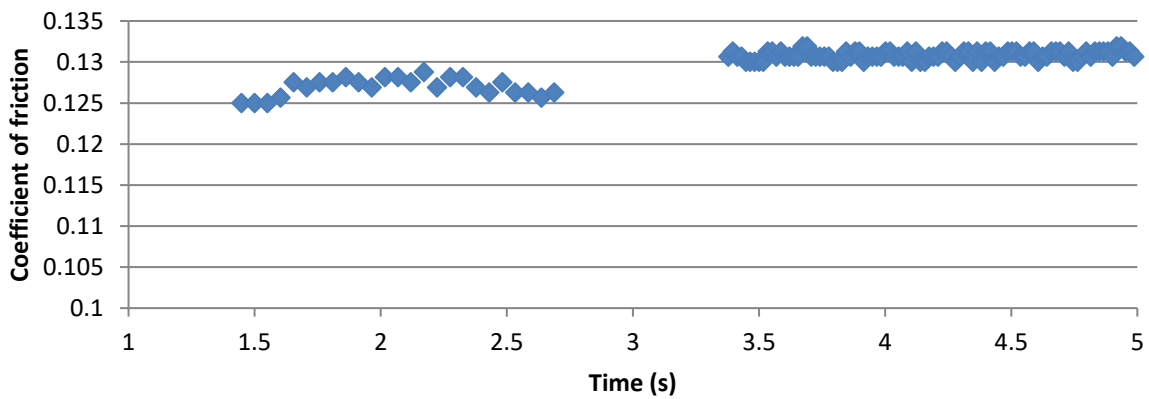
Figure 4-18: Raw data from Figure 4-17 for 1 – 5 seconds, 50 Hz.
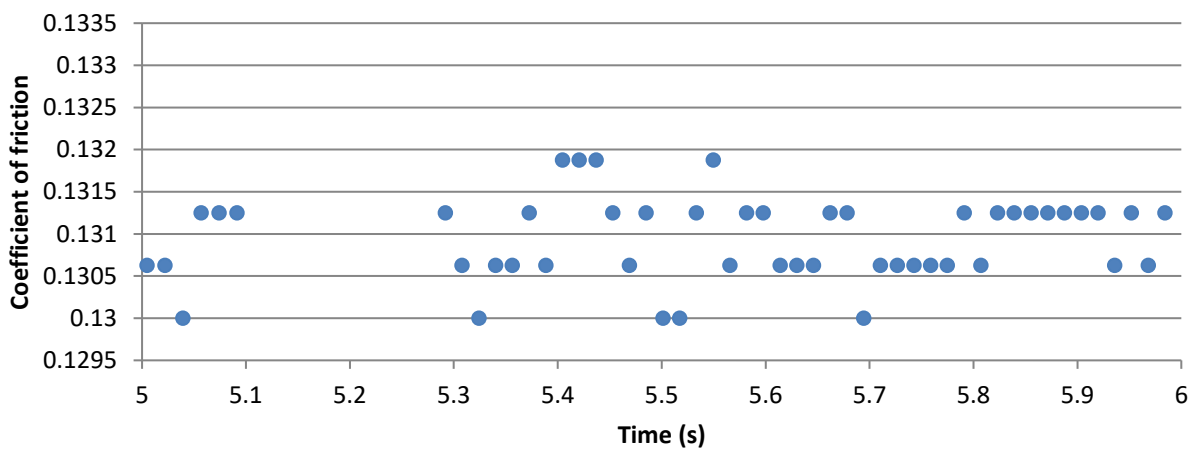
Figure 4-19: Raw data from Figure 4-17 for 5 – 6 seconds, 50 Hz.
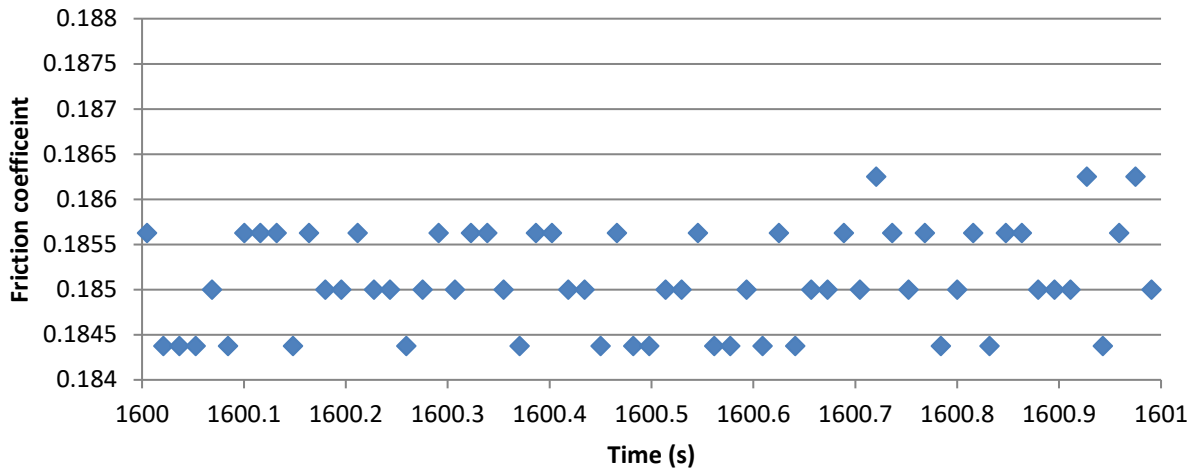
Figure 4-20: Raw data from Figure 4-17 for 1600 – 1601 seconds, 100 Hz.

Secondly, focusing on Figure 4-18 the gaps in data points are the missing data points. A gap of missing data is also observed in Figure 4-19 around 5.2 seconds. From the data, it is apparent that the SRV does not record all the coefficient of friction values. This explains why a full Stribeck curve is not generated with each stroke on the SRV. At the endpoints of a stroke where the top specimen stops and changes direction, we can expect a higher coefficient of friction. From this info, we can conclude that static coefficient of friction is never measured on the SRV and that this is due to a filtering mechanism added to the machine's software that cuts out measurements taken at the endpoints. This limits the machine's ability to detect that the film is being removed at the endpoints and only shows this failure if there is material pull-out at the endpoint resulting in severe wear. If it is the endpoints of a stroke that results in lower than expected load-carrying capacity the effect of the endpoints will have to be minimised. One way to do this would be to increase the stroke length while reducing the oscillating frequency. By doing this the test operates in the same lubrication regime but, the number of times an endpoint is reached during the test is reduced.

4.1.2. Generating Stribeck curves by changing the oscillating frequency

To compare the two methods that can be used to generate a Stribeck curve, the gear oil was tested on the SRV in runs where the load was kept constant while the oscillating frequency was changed. The average for the runs is shown in Figure 4-21.
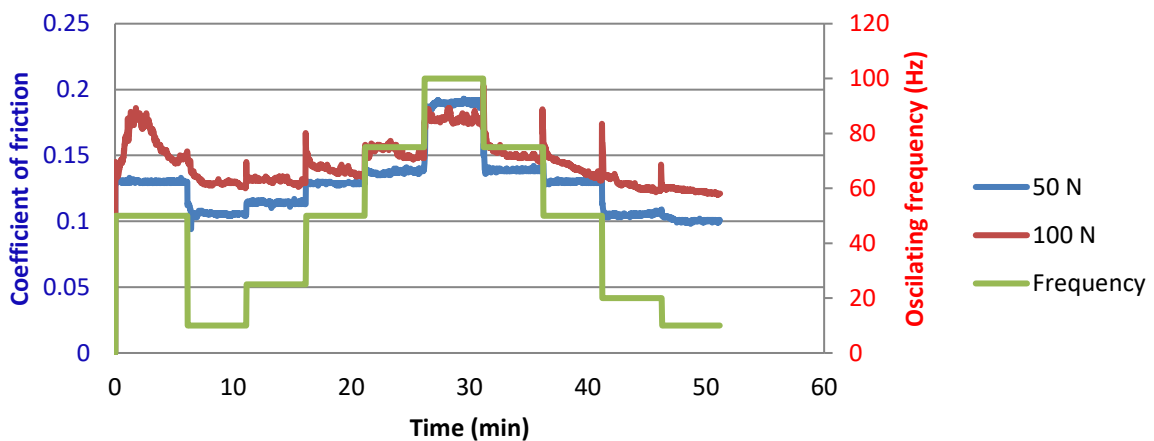
Figure 4-21: Results for runs using a gear oil while changing the oscillating frequency.

Comparing the results from these tests with the results of section 4.1.1 gave Figure 4-22.
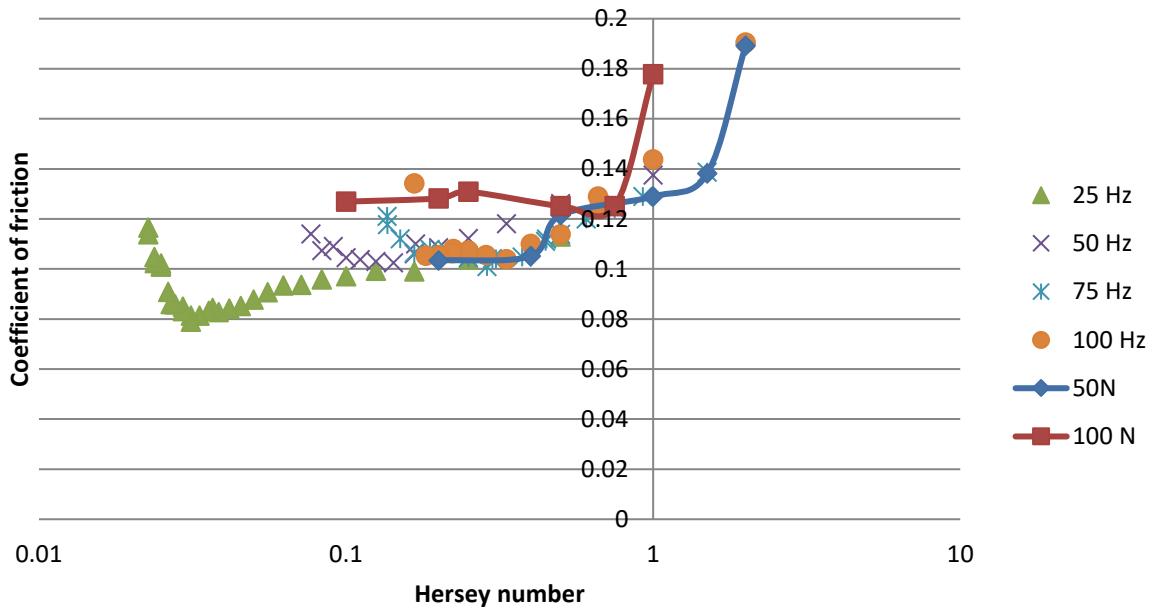
Figure 4-22: Comparison between runs where the oscillating frequency is changed versus the applied load.

Both methods generated Stribeck curves and at some Hersey numbers, the different methods also gave a similar coefficient of friction. As the load is increased a reduction in the Hersey number takes place and we find that results for all the constant frequency runs are similar up to the point where we enter boundary layer lubrication. Lower oscillating frequencies resulted in a shift in the curve to the left.

The constant frequency runs gave more consistent results and more defined Stribeck curves. It is better to use constant frequency and change the load to produce a Stribeck curve. To investigate why the constant load runs gave odd results further testing was done and will be discussed in section 5.

4.2.   HFRR performance baseline

Because the HFRR is a common industry quality control instrument it was chosen to establish the baseline performance of all three additives, myristic (C-14), palmitic (C-16) and stearic acid (C-18) in an n-hexadecane base. ISO 12156 conditions were used for tests. Each test was repeated once. This gave an

61

independent measure of performance making it possible to notice any deviations from the norm.

During these runs, Myristic (C-14), palmitic (C-16) and stearic acid (C-18) were added to n-hexadecane as surface-active additives at 250, 500 and 1000 ppm. These will be the same additives and concentrations used on the SRV for further work.

4.2.1. Results

To determine a performance baseline for the additives several tests were conducted on the HFRR according to ISO 12156-1, results given in Figure 4-23.
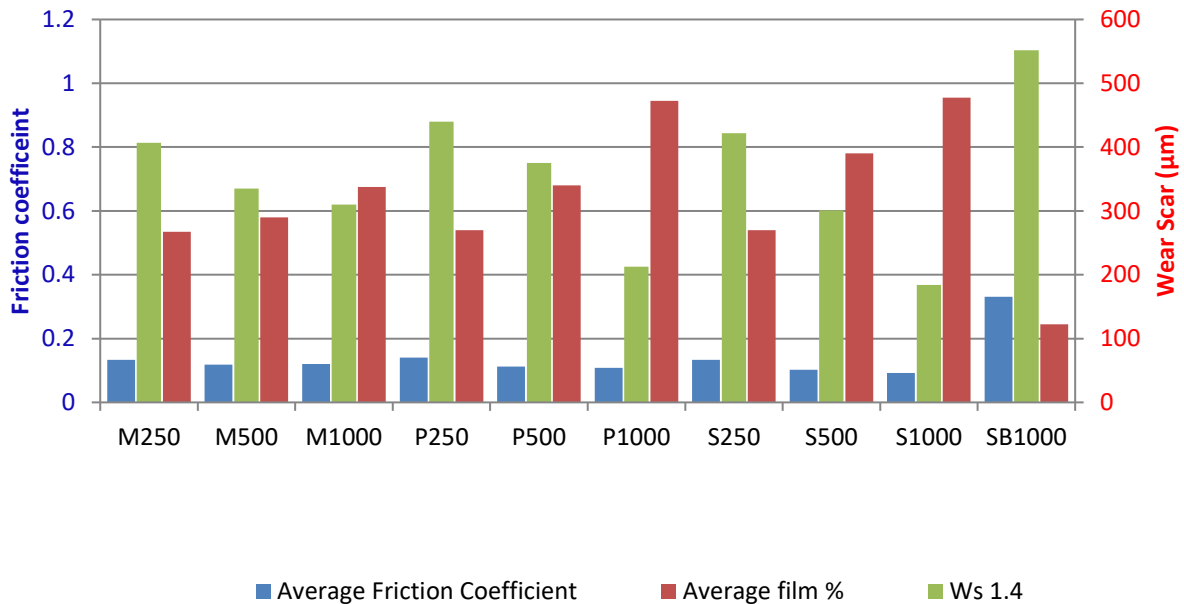
Figure 4-23: Data from HFRR.

For Figure 4-24 as the additive concentration is increased the performance of the lubricant increases (reduces the coefficient of friction). Myristic acid (C-14), according to theory as discussed under heading 2.4.2, should be the additive with the lowest performance among all the acids used, however, at 250 ppm the Myristic run had a lower coefficient of friction compared to palmitic and stearic

acid (C-18). The small difference implies similar performance at this additive level. At higher concentrations palmitic and stearic acid (C-18) start to outperform the myristic acid (C-14) as expected.
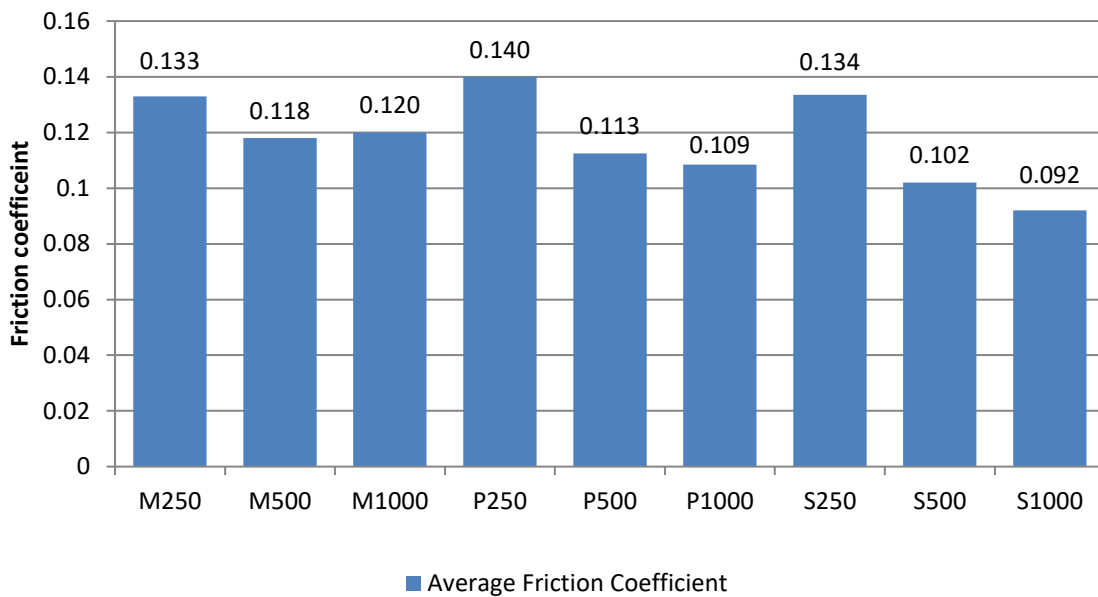
Figure 4-24: Coefficient of friction data from HFRR.

Using the coefficient of friction to calculate the percentage change in recorded values between concentration steps, Figure 4-25 shows how adding more stearic (C-18) or palmitic acid (C-16) has a higher impact on coefficient of friction compared to adding more myristic acid (C-14). We know that stearic (C-18) and palmitic acid (C-16) will form a stronger boundary layer due to the longer carbon chain compared to myristic acid (C-14), (Ratoi, Angel, Bovington, & Spikes, 2000). A longer carbon chain implies stronger inter-molecular forces, and this explains why the stearic and palmitic acid (C-16) give a higher percentage increase compared to myristic acid. A good question will be why does myristic acid give simar performance compared to the other two additives at 250 ppm. Longer additive chain of the C16 and C18 fatty acids will only give a stronger layer if other molecules absorb next to it. If there are no chains close enough to

take advantage of the stronger van der Waals forces between longer chains the performance difference between longer and shorter chains will decrease. This explains why we see similar results at 250 ppm for all 3 additives. The only difference is the chain length and if there is not enough additive on the metal surfaces to take advantage of the chain length you will not see the performance benefits. As the concentration is increased, more of the surface area can be covered resulting in a boundary film that has densely packed molecules increasing the molecular forces between molecules.
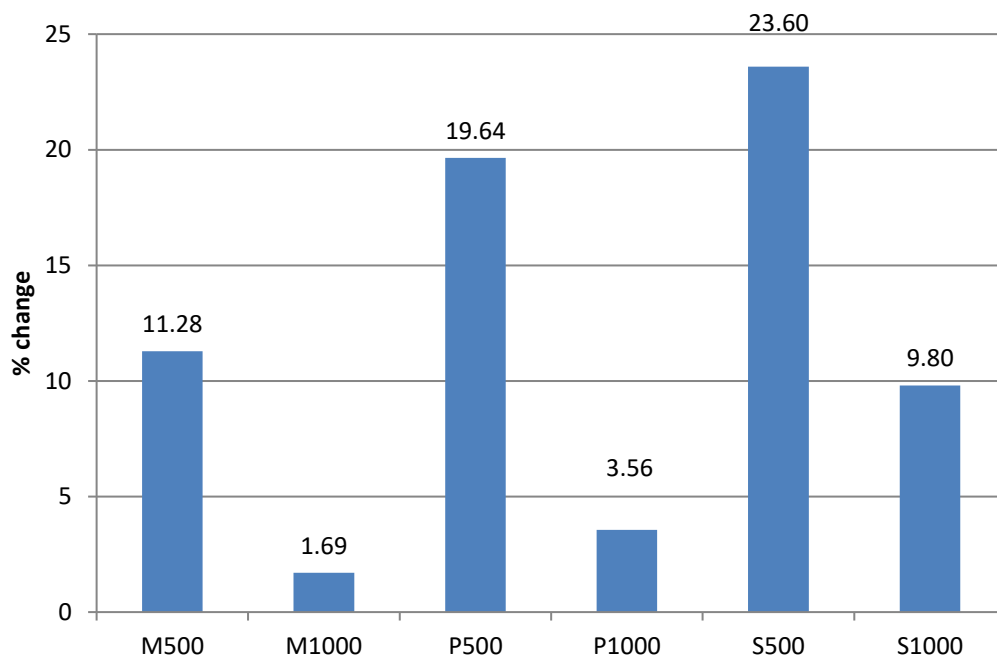
Figure 4-25: Percentage change in the recorded coefficient of friction based on successive concentration steps.

The smaller change in the coefficient of friction from 500 ppm to 1000 ppm is due to the surface becoming saturated with additive. Adding more additive increases the bulk fluid's additive concentration, but at higher concentrations, the surface is already covered in additives. If the wear surface becomes saturated with additive, more additive in the bulk fluid will not increase the amount of additive on the surface because there is no open surface area. Work done by Marais, (2009, p. 72) has shown that increasing additive concentration above 1000 ppm with these acids had almost no effect on the coefficient of friction.

The %film-reading from the HFRR, Figure 4-26, shows a similar performance pattern. As with the coefficient of friction, myristic acid (C-14) gives a comparable performance at 250 ppm but falls far behind at higher concentrations. Figure 4-27 shows the same difference in film strength between the additives with stearic acid (C-18) giving the strongest film followed by palmitic (C-16) and myristic acid (C-14).
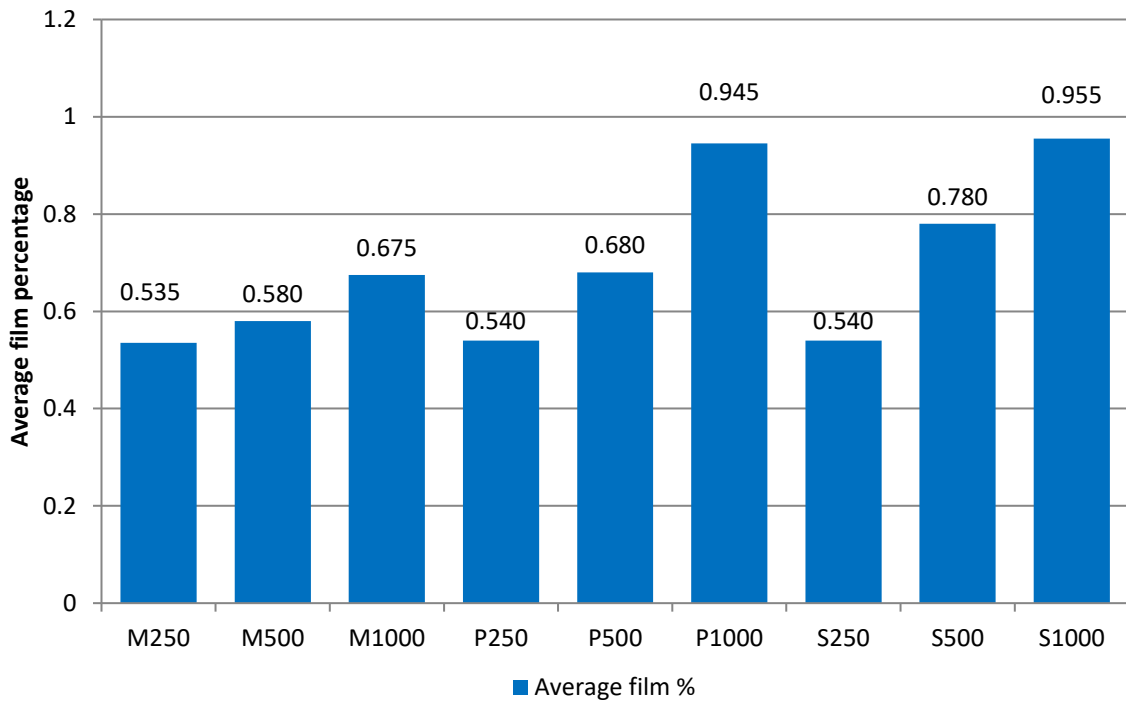
Figure 4-26: Film percentage data from HFRR.

What is also interesting is the reduction in percentage change from 500 to 1000 ppm for stearic acid (C-18). The other two additives both show that the film thickness is still changing rapidly from 500 ppm upwards. The reason for this is likely layer strength. Stearic acid (C-18) forms the strongest protective layer and the thickest layer of the additives. This shows that if the boundary layer is strong enough, adding what is considered to give full surface area coverage does not give you the improvements that would be expected. The performance for layer thickness will level off sooner as the layer becomes more effective at handling the applied load.
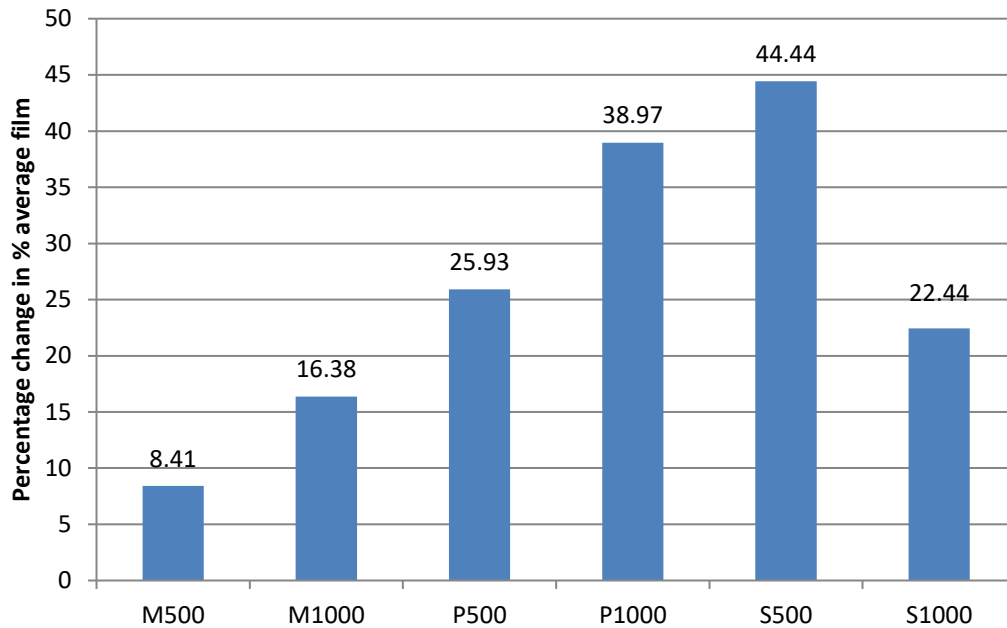
Figure 4-27: Percentage changes in average film percentage for runs on the HFRR.

Figure 4-28 shows that the wear on the ball specimen followed the same pattern with myristic acid (C-14) doing slightly better at 250 ppm and being the weakest additive at higher concentrations. The decrease in $WS_{1.4}$ for palmitic and stearic is also much higher compared to myristic acid (C-14) as the concentration is increased.
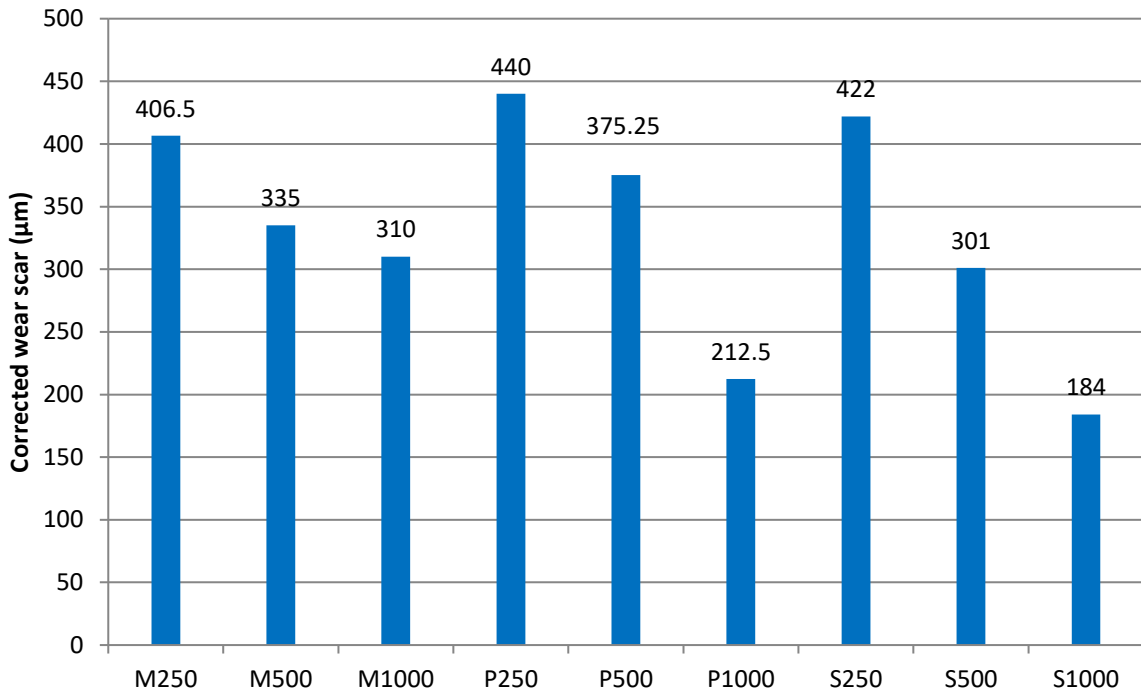
Figure 4-28: WS$_{1.4}$ data from HFRR, obtained using an optical microscope after test completion.

Figure 4-29 has a strange trend where the percentage change becomes higher for the 500 to 1000 ppm change for palmitic and stearic acid (C-18). For myristic acid, the percentage change decreases with the change from 500 to 1000 ppm. This solidifies the idea that myristic acid (C-14) does not have the protective strength to take full advantage of the increased concentration.
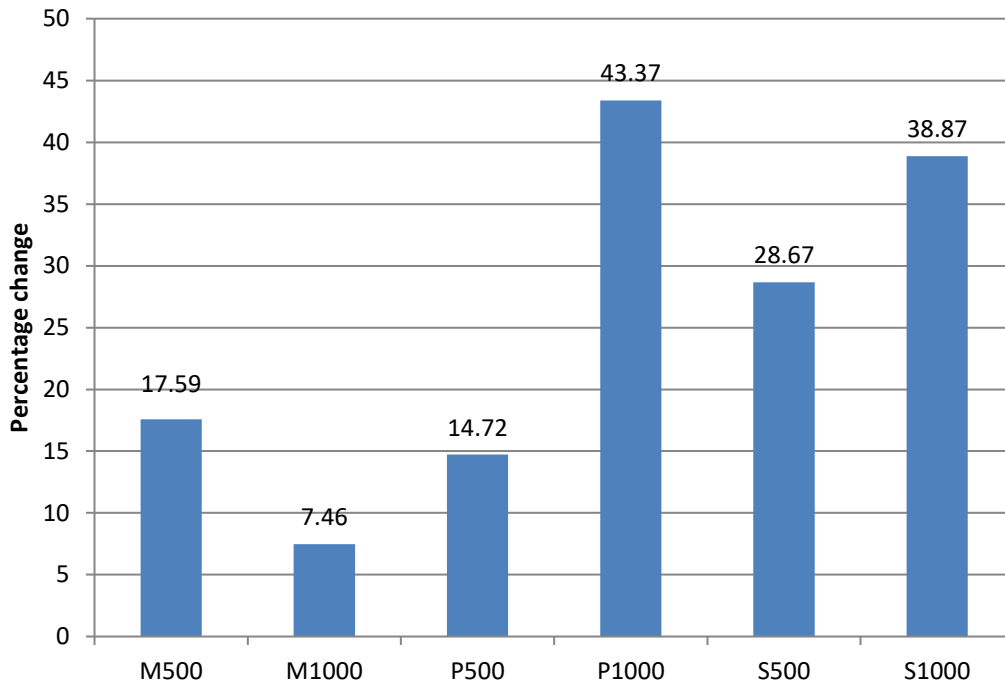
Figure 4-29: Percentage change in $WS_{1.4}$ between concentration steps.

Performance ranking

From the HFRR results, the following conclusions can be made on the performance of similar fatty acids as additives. Longer chain additives have better performance due to a stronger film. The van der Waals forces that play a role in making the additive film stronger is only utilised fully if there is a densely packed additive layer. At low concentrations, similar wear results can be expected.

Profile Wear data

The surfaces for all runs were scanned using a profilometer. The small size of the wear scar made it very difficult to accurately calculate wear volume. For this reason, only the wear data from wear tracks were used. Figure 4-30 and Figure 4-31 give the wear volume and wear area averages for all the HFRR runs. As with the wear scar diameters, the wear track, (Figure 4-30) area shows that myristic acid (C-14) gives better performance at low additive concentrations but wear volume tells a different story, see Figure 4-31.

Figure 4-30: The surface area of the wear track for HFRR tests

Figure 4-31: Average wear volume for HFRR runs of the wear track.

The wear volume gives a very strange picture. Wear scar measurements (2-D) showed that myristic acid (C-14) did have similar or better performance to the other additives but profile a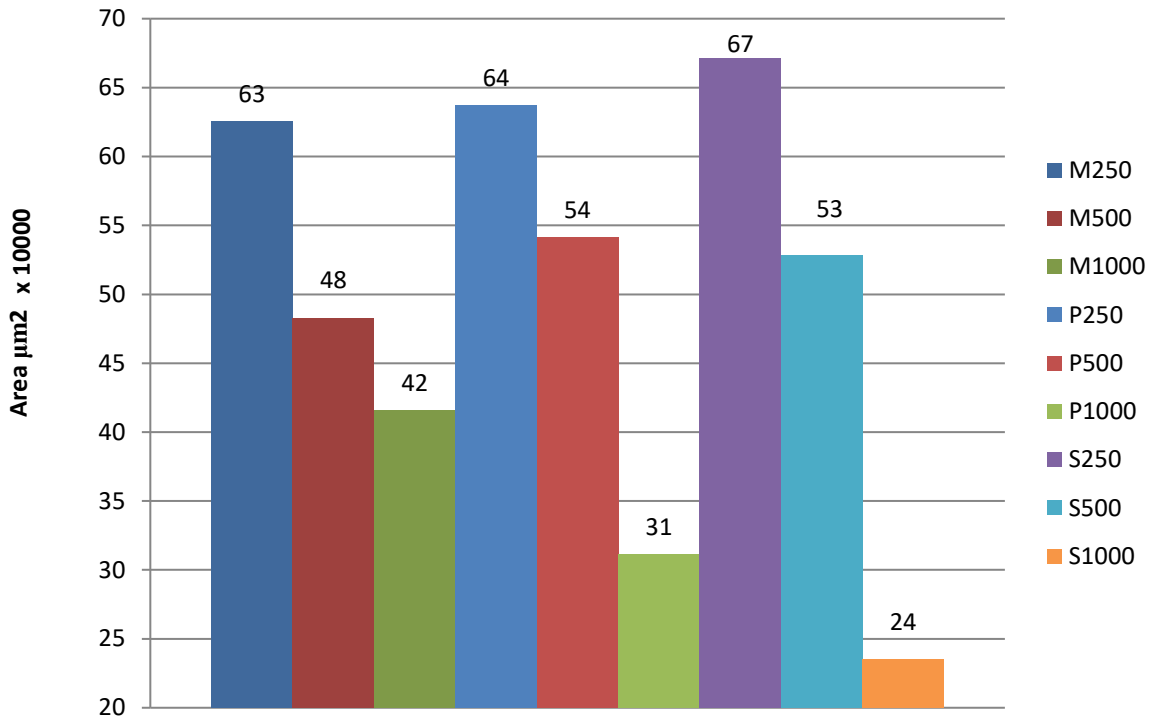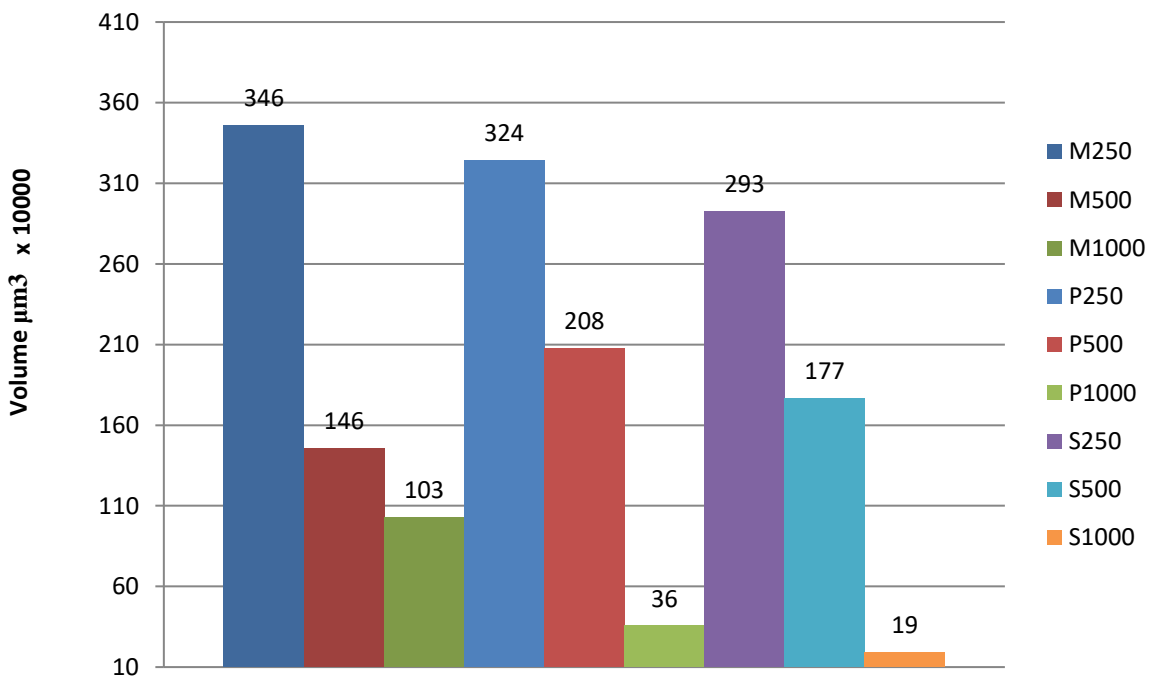nalysis (3-D) shows that myristic acid (C-14) still offered the least amount of surface protection regarding wear volume. This shows that at concentrations of 250 and 500 ppm there is a difference in 3-dimensional wear on the ball and disk. Myristic acid (C-14) showed less wear on the ball producing a sharper ball scar that produced a deep wear track with a small area. For palmitic (C-16) and stearic acid (C-18) the wear track was wider but not as deep corresponding to a flatter and wider ball wear scar. The ball wear scar was flat producing a wider wear area but not a deep wear track. Work done by (Litzow, Jess, Matzke, Caprotti, & Balfour, 2009) found similar results using additive and unadditised diesel. This shows that wear scar measurements and the coefficient of friction could be insufficient to get a full image of how each additive performs. This shows that only looking at 2-dimensional wear measurements is not sufficient. Coefficient of friction and wear volume correlation is not as simple as more friction more wear.

4.3.   Test fluid volume

As discussed in chapter 2 fatty acid additives behave like surfactants due to their polar nature. This implies that they will gather at interfaces between polar and non-polar substances. The base fluid, n-hexadecane, is strictly non-polar which implies that a polar additive will move towards the liquid-metal and liquid-atmosphere interfaces where their polar heads can interact with polar surfaces and the non-polar tail with the bulk non-polar fluid.

Because of the surfactant like nature of the fatty acids used we can expect different test results for different volumes of liquid when operating in mixed- and boundary lubrication regime. Tests were conducted on the SRV and HFRR. Table 4-2 below gives the parameters used for the fluid volume experiments.

Table 4-2: Conditions for experiments using different test fluid volumes.

	HFRR	SRV
Test fluid volume	1, 2 mL	0.3, 0.8 mL
Test temperature	60 °C	50 °C
Base fluid	n- hexadecane	n- hexadecane
Additive	Palmitic acid (C-16)	Palmitic acid (C-16)
Relative humidity of the test chamber	50 %	50 %

4.3.1. Results

Tests on the SRV

Under standard testing conditions, the SRV's bottom specimen can take 0.3 mL (1 – 2 drops) of test fluid. To increase the volume a copper ring was manufactured to fit onto the disk allowing for larger volumes and continuous feeds if required. With the ring, the maximum volume is 1 mL. Filling to 1 mL does cause some spillages when the test starts. Testing showed that tests could be conducted suing 0.8 mL without loss of test sample from the ring. The first sets of tests using 0.3 mL of lubricant had a coefficient of friction above 0.6 for longer than 30 s at the very start of each test. Runs using 0.8 mL of lubricant did not show a high coefficient of friction at the start of a test. The results are shown in Figure 4-32 to Figure 4-34. Each test was duplicated, and results averaged.

The second run for 0.8 mL given in Figure 4-32 showed signs of failure at 100 N load but the SRV did not stop the test. Looking at the difference in the running in period between 0.8 mL and 0.3 mL it seems as if more lubricant results in a shortened run in time and a lower coefficient of friction during the running-in period. For 0.8 mL runs the measured coefficient of friction, during the running-in period, were more repeatable compared to the 0.3 mL runs. This effect could be attributed to the following:

71

- Because the additive used is surfactant-like they prefer surfaces to being in the bulk liquid. Larger volumes of sample imply that there is more additive available and if the surfaces were not saturated during the 0.3 mL runs the surface concentration of additive for the 0.8 mL runs will be higher.
- Flow effect. With more lubricant, the flow back into the wear track after the top specimen starts moving away from a point on the track should be faster. The test results with the high viscosity gear oil and visual inspection suggest that this is not the case.
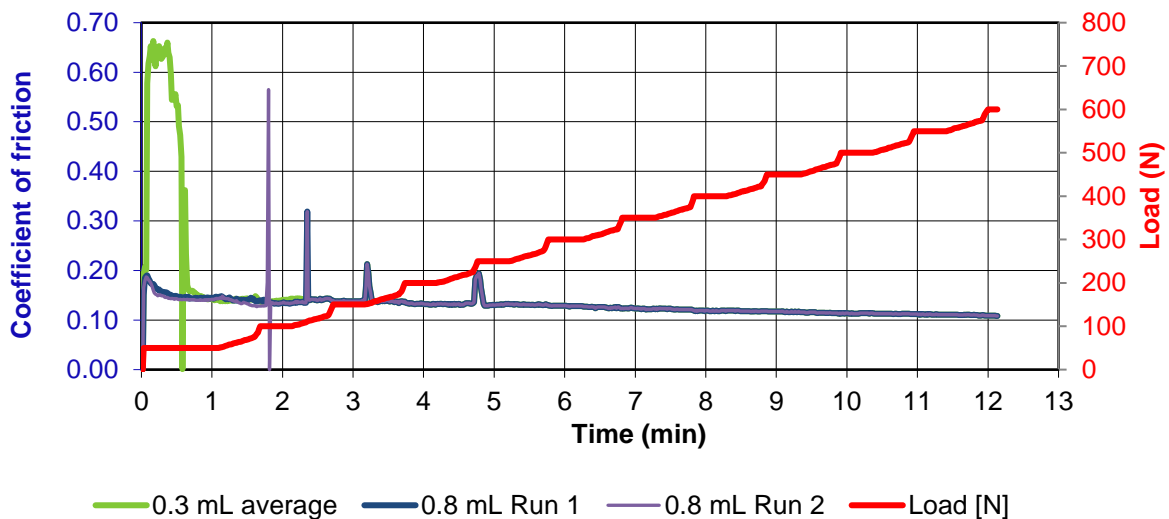

Figure 4-32: 250 ppm palmitic acid (C-16) in n-hexadecane, Run 1 and run 2 for 0.8mL coefficient of friction was very close. The two lines lie on top of each other excluding the first 2 1/2 minutes.
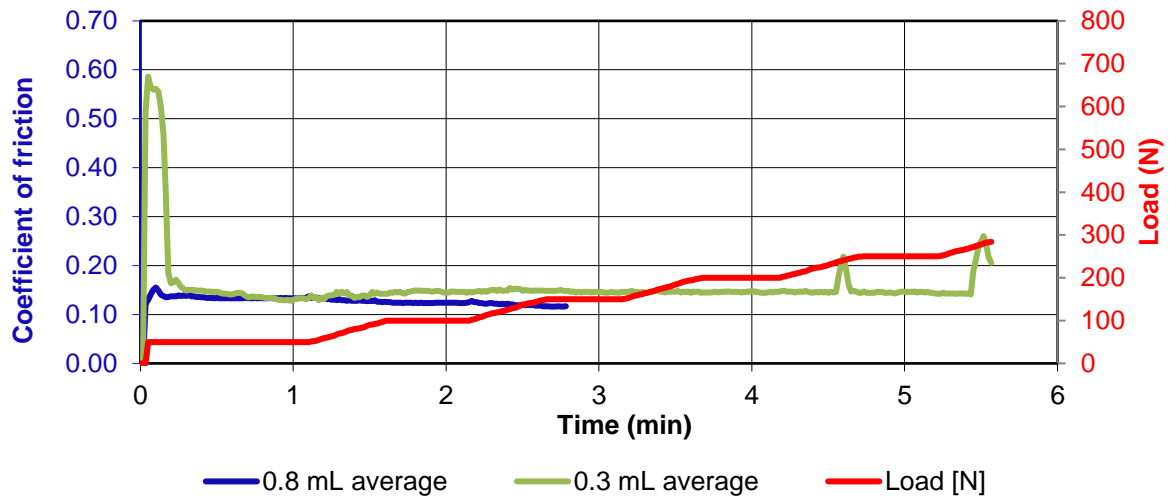
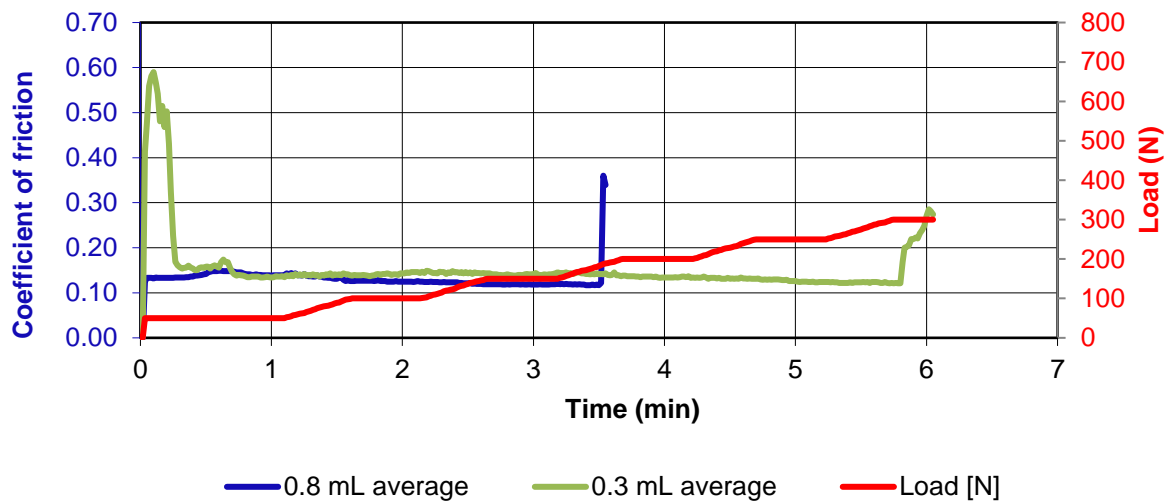Figure 4-33: 500 ppm palmitic acid (C-16) in n-hexadecane.

Figure 4-34: 1000 ppm palmitic acid (C-16) in n-hexadecane.

At 250 ppm palmitic acid (C-16) coefficient of friction after the running in time were the same for 0.3- and 0.8-mL lubricant. At higher concentrations, 0.8 mL had a lower average coefficient of friction after the 100 N load increase.

The load-carrying capacity results for the figures above are shown in Table 4-3. The first thing to notice is that the runs at 250 ppm with 0.3 mL lubricant had a higher load-carrying capacity compared to other results. Looking at Figure 4-32 during the running in time and shortly thereafter there where spikes in the coefficient of friction. At this concentration, the initial protective film could not maintain the applied load resulting in wear that increased the surface area that the load is applied to. For runs where the starting coefficient of friction was lower, less wear took place, implying that after the running-in period that the surface area for the 250 ppm runs was larger than for the other runs. This is the reason why the 0.3 mL had a higher load-carrying capacity compared to 0.8 mL runs.

The results obtained during these tests were compared with results obtained by other researchers from the University of Pretoria, (Moller, 2012) (Langenhoven, 2014). This was done to see how temperature affects results. Langenhoven used batch tests with 1 mL of liquid at 80 °C and Möllerconducted continuous flow tests at 110 °C. Parts of Möller'sand Langenhoven's results are tabulated in Table 4-3.

Table 4-3: Palmitic acid (C-16) in n-hexadecane load-carrying capacity results at 50 Hz, ranges are used for Langenhoven's and Möller'sresults to show the range of results they got during tests.

Test no	Load-carrying capacity (N)	Langenhoven results @ 80 °C	Möller results @110 °C
250 ppm 0.3 mL	600	100 – 300	400 – 600
250 ppm 0.8 mL	100	100 – 300	400 – 600
500 ppm 0.3 mL	284	200 – 300	600 – 800
500 ppm 0.8 mL	150	200 – 300	600 – 800
1000 ppm 0.3 mL	300		600 – 800
1000 ppm 0.8 mL	190		600 – 800

As expected, (Litzow, et al, 2009), at a lower temperature, 50 °C, lower load-carrying capacities are achieved, Figure 2-10. Möller'sresults are considerably higher to what was achieved in this study. The higher temperature used in his

study would result in more chemical bonding and a constant feed of lubricant would increase the surface concentration on the wear surfaces over time. Both factors will increase the load-carrying capacity. Results using 0.8 mL of test fluid were like Langenhoven's results but none of the results was close to Möller'sat 110 °C. From these results, the decision was made to use 1 mL of lubricant for all experiments on the SRV. Results between 0.8 mL and 1 mL will not differ much according to Langenhoven's results. To push the lubrication into the boundary regime the decision was also made to use a low temperature at first with loads between 30 N (lowest load the SRV can supply with accuracy) and 100 N (the load-carrying capacity of palmitic acid (C-16) at 250 ppm).

Tests on the HFRR

Testing the effect of lubricant volume was also done on the HFRR to support results on the SRV. The large bath size on the HFRR also allows us to test a larger difference in volumes. The standard volume of 2 mL and half of that (1mL) were used. The average coefficient of friction given in Table 4-4 shows that at lower additive concentrations the 1 mL runs had a higher coefficient of friction. At higher concentrations of the additive similar coefficient of friction is observed for both volumes. This shows that if the surface becomes saturated, increasing the volume will have little to no effect and that if the surface is not saturated with additive, that adding more additive, by increasing the liquid volume, will result in a lower coefficient of friction.

Table 4-4: Average coefficient of friction for myristic acid (C-14) runs on the HFRR.

M250_2mL	M250_1mL	M500_2mL	M500_2mL	M1000_2mL	M1000_2mL
0.138	0.152	0.118	0.113	0.120	0.118

Looking at the average coefficient of friction during HFRR runs, Figure 4-35 – Figure 4-37 a clear difference can be seen in the coefficient of friction of the M250_1mL runs compared to the 2 mL runs. The runs at higher concentrations

look similar and gave similar averages while at M250 coefficient of friction were more erratic for the 1 mL runs. Erratic coefficient of friction generally indicates that the lubrication film is not handling the load effectively.

The average coefficient of friction for 1 mL runs was slightly lower at 500 and a 1000 ppm myristic acid (C-14) compared to the 2 mL runs. This could be a viscosity related effect. Because the 2 mL runs had more liquid to shear than the 1 mL runs.
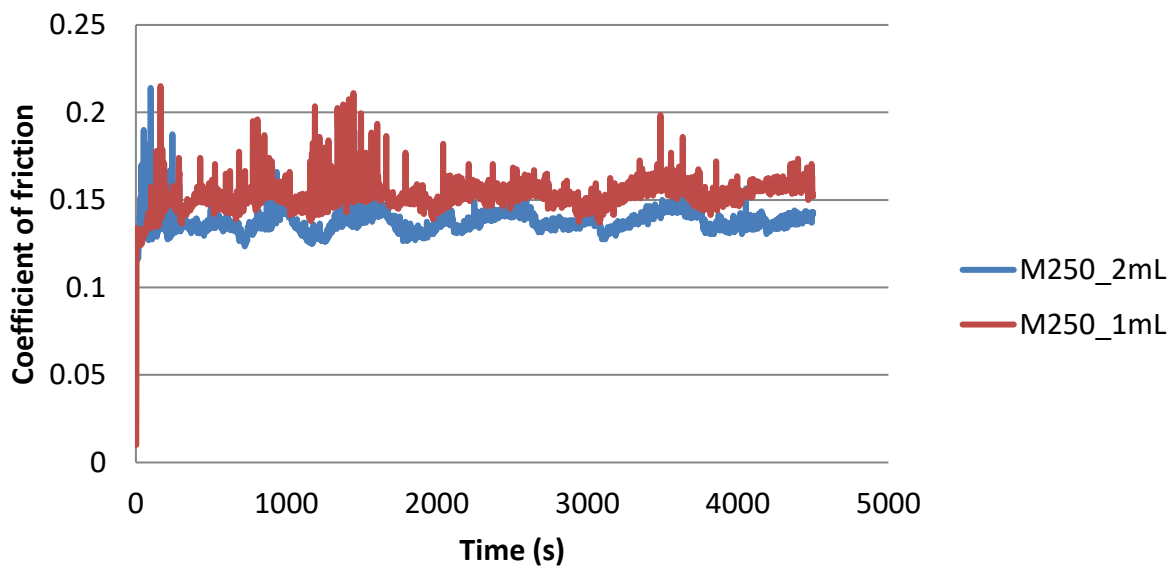

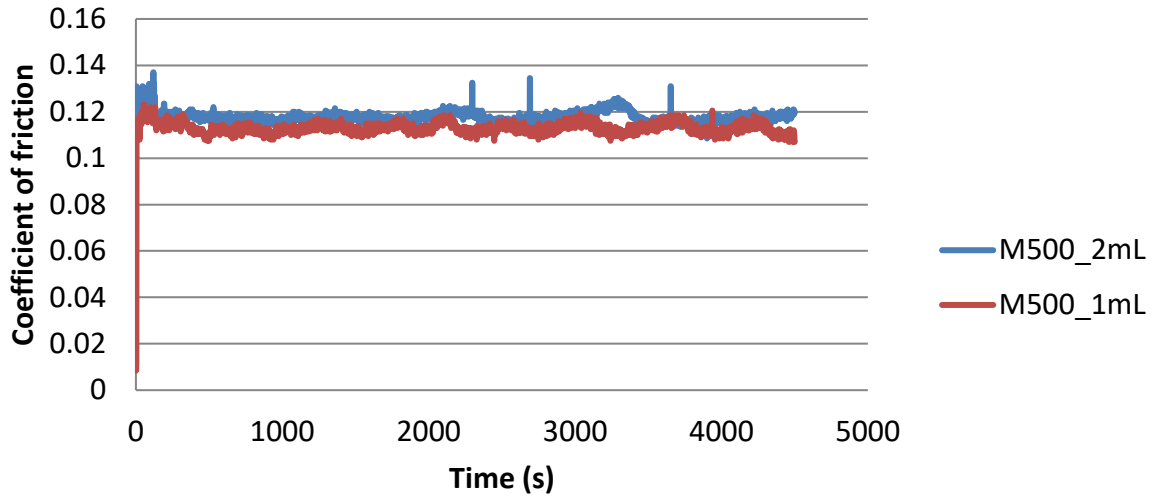Figure 4-35: Average coefficient of friction for runs with 250 ppm myristic acid (C- 14), on the HFRR

Figure 4-36: Average coefficient of friction for runs with 500 ppm myristic acid (C-14), on the HFRR.
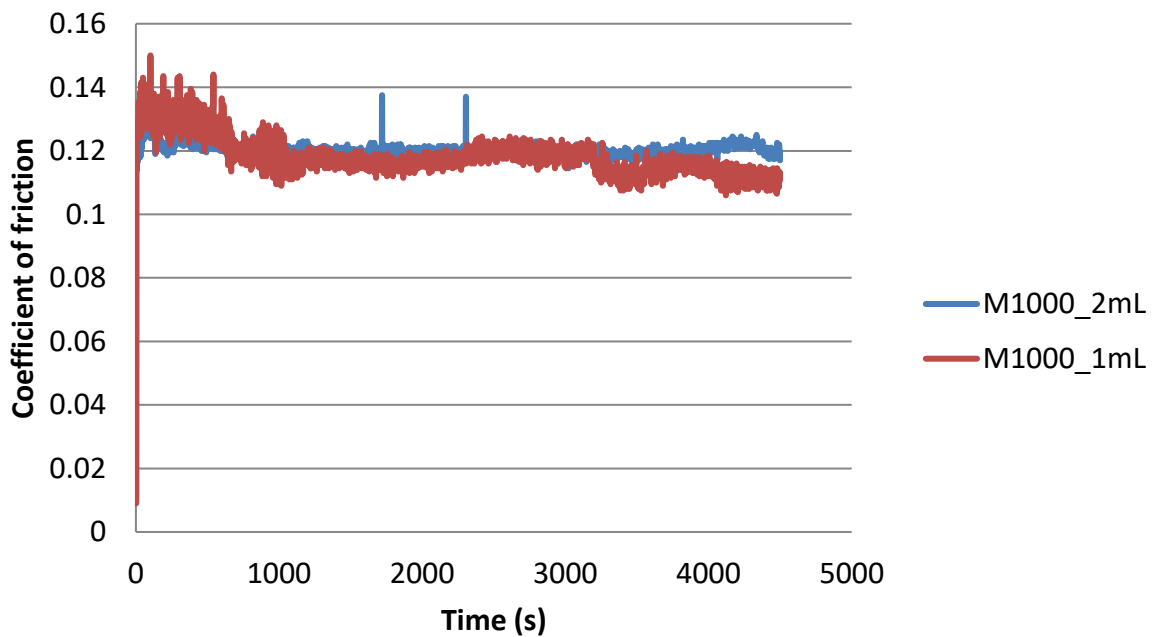

Figure 4-37: Average coefficient of friction for runs with 1000 ppm myristic acid (C-14), on the HFRR.

The results on the HFRR correspond well with results on the SRV. These results show that the highest amount of liquid possible should be used for the tests to avoid differences caused by liquid volume.

4.4.   Summary of what was learned from the initial experiments.

Everything that was learned from the initial experiments was used to investigate how changing the linear velocity affects friction and wear in reciprocating systems.

Generating a Stribeck curve

- Showed that changing the load with constant linear velocity gives better Stribeck curves compared to using a constant load and changing the linear velocity by changing the oscillating frequency.
- In reciprocating contacts, higher linear velocities can lead to failure of the lubrication film while Stribeck curves suggest that higher velocities should not result in failure.
- The SRV has physical limitations when it comes to operating at low linear velocity and loads.
- The SRV does not record all measured coefficient of friction data. We expect to observe higher and lower coefficient of friction in a single stroke corresponding to the kinetic and static friction during a stroke, but this is not the case.
- Operating at an oscillating frequency of 100 Hz is not high enough to cause lubricant starvation.

HFRR Performance baseline

- Additive different chain lengths but similar structures have a similar coefficient of friction and 2-dimensional wear performance at low additive treat rates.

- Higher treat rates of additives with longer chain lengths give better performance.
- Longer chain length additives have better returns on concentration increases. Need less additive to give more performance.

Test fluid volume

- The amount of test fluid affects the observed coefficient of friction but also affects the load-carrying capacity of test fluid.
- More test fluid increases the coefficient of friction, due to more liquid being sheared.
- More test fluid increases the surface additive concentration leading to a more densely packed additive layer and higher load carrying capacities.

5. Results & discussion

This chapter contains the results focused on investigating the effect of linear velocity in reciprocating contacts.

Frequency scans (FS)

These tests were designed to delve deeper into the effect that changing the oscillating frequency has on friction and wear. The tests were conducted as follows:

- Frequency scan (FS) test.
    - The oscillating frequency is changed during the test from 5 Hz to 100 Hz at 1 mm stroke and back to 5 Hz. Changing back to 5 Hz allows us to compare the coefficient of friction during the first half and the second half of the test.
    - Tests will be conducted at 30 °C and 80 °C to determine temperature dependencies. As discussed in Chapter 2 temperature plays a major role in the effectiveness of additives.
    - 2 mm stroke will also be used with frequency changes between 2 Hz and 50 Hz to maintain the same linear speed compared to the 1 mm stroke to investigate the validity of Stribeck curves generated.

5.1. Frequency scans at 30 °C

5.1.1. M250

To show what the raw data looked like and give a better idea of how tests were performed all the tests done for M250 at 30 °C, 30 RH, and 1 mm stroke is shown in Figure 5-1 to Figure 5-3. Only summaries or results of special cases will be shown and discussed under subsequent headings. As expected, increases in the load resulted in a decrease in the coefficient of friction as seen in chapter 4, up to the point where the load becomes too high for the lubricant to sustain. Depending on where the system is on the Stribeck curve an increase in linear velocity will

decrease or increase the coefficient of friction and push the lubricating regime from boundary to mixed and further on into the hydrodynamic regimes. This indicates that increases in linear velocity should not result in lubrication failure or breakthrough. Figure 5-1 and Figure 5-2 follow the expected trends but in Figure 5-3 where the load was increased to 100 N breakthrough occurs. This test is in contradiction to the generic Stribeck curve discussed in Chapter 2. If the load cannot be carried by the lubricant, breakthrough should occur at lower oscillating frequencies, not higher. The increased hydrodynamic pressure as the oscillating frequency is increased should have increased the load-carrying capacity, not decreased it. Chapter 4's test work showed similar results with a high viscosity fluid so we can conclude that this behaviour is not due to a lubricant's viscosity. Lubricant starvation or channelling is not a problem when using liquid lubricants under these test conditions.
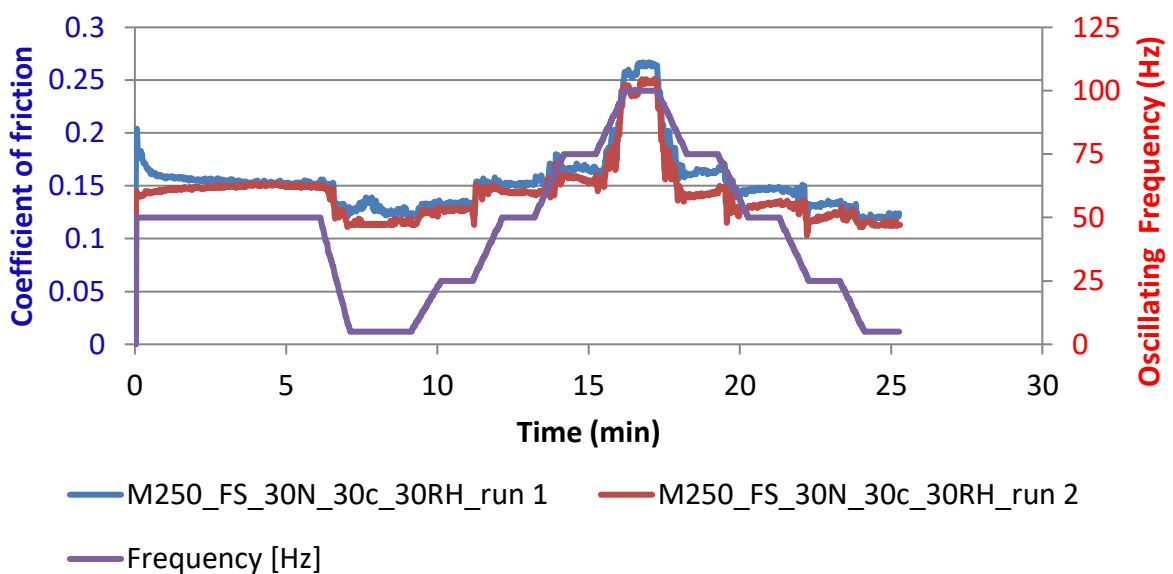
Figure 5-1: M250 at 30 °C, 30 % relative humidity and 1 mm stroke under a load of 30 N.
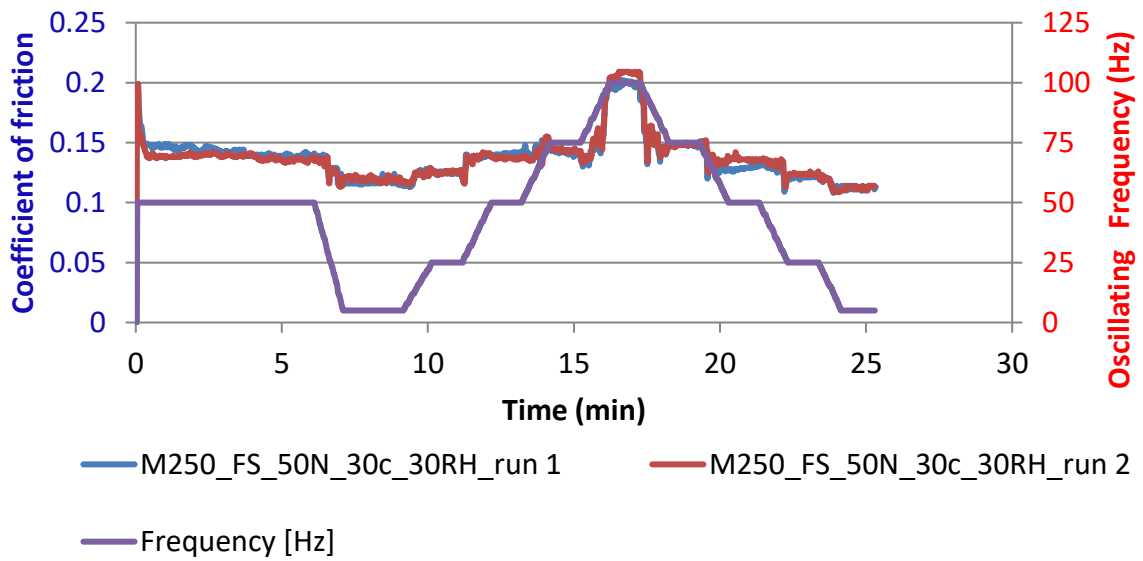
Figure 5-2: M250 at 30 °C, 30 % relative humidity and 1 mm stroke under a load of 50 N.
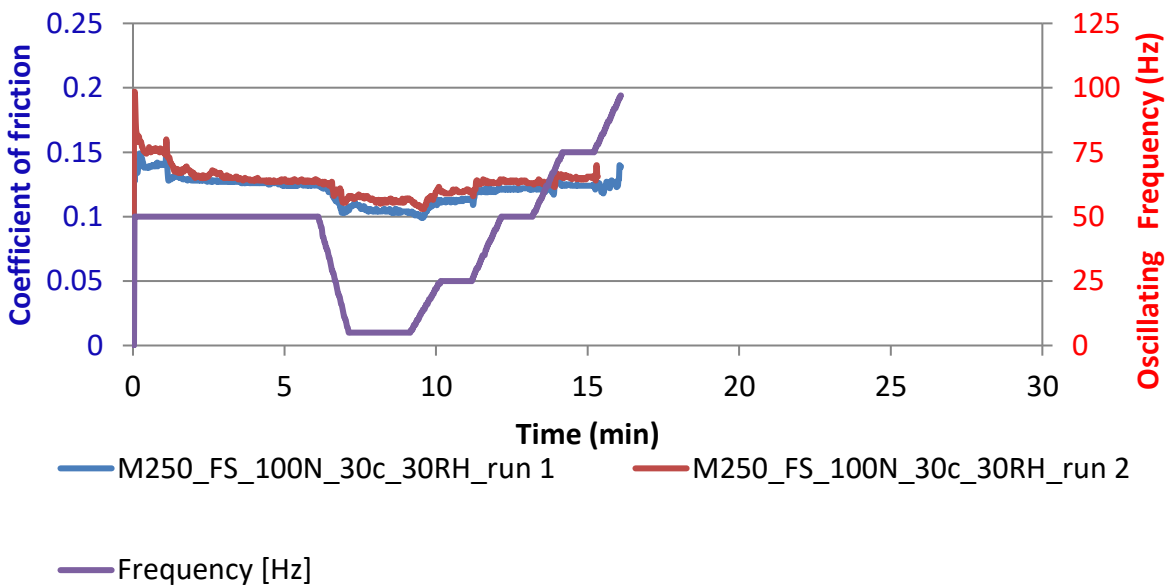
Figure 5-3: M250 at 30 °C, 30 % relative humidity and 1 mm stroke under a load of 100 N.

This behaviour was not exclusive to runs with myristic acid (C-14) at 250 ppm.

M500 data is shown in Figure 5-4. The same behaviour is observed where failure occurred as the oscillating frequency was increased. This behaviour was not seen in the test using the commercially available gear oil. The failures at increased oscillating frequencies can be explained by looking at the origin of the Stribeck curve. This curve was generated using unidirectional motion, but these test results were generated using a bidirectional device. Bidirectional devices change the speed of the moving specimen as it moves across the stationary specimen to change direction. This implies that every stroke can generate a full Stribeck curve on its own.
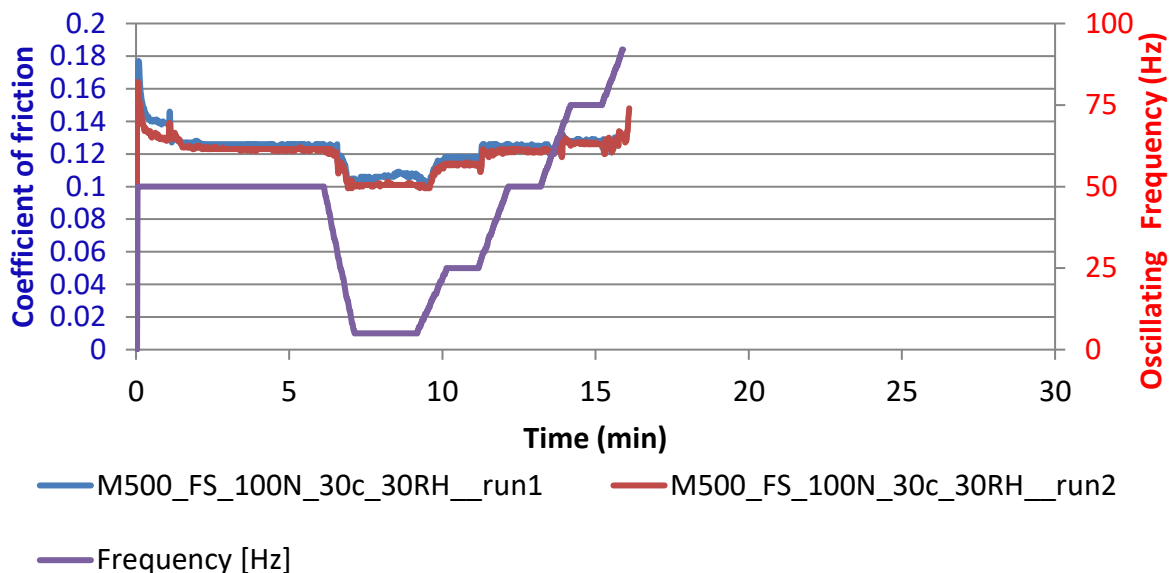
Figure 5-4: FS runs for M500 at 30 °C, 30 % relative humidity and 1 mm stroke under a load of 100 N.

Results from (Ratoi, et al., 2000) show that boundary layer additives that have not been chemically absorbed onto a surface do not survive static contact like the contact observed at the end of a stroke where the velocity is 0 for a moment. In Figure 5-5 material pull-out occurred at the endpoint. Endpoint refers to the two endpoints of a stroke. This behaviour was observed on several other tests where severe damage occurred at the endpoint indicating where the initial fusion

between the ball and disk specimens occurred. This explains why breakthrough occurred with increased oscillating frequency. The point of failure was at the end where the additive layer is removed during the momentary static contact. The only concern now is why breakthrough did not occur sooner during runs at lower oscillating frequencies?

As the frequency is increased, the time that a surface layer has to regenerate before the top specimen returns to the specified area is reduced. Under the high frequency, the surface layer is degraded faster than it is regenerated at the endpoints, resulting in failure.
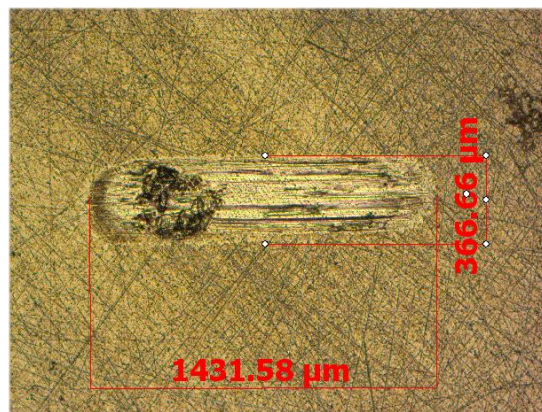
Figure 5-5: Microscope image of wear track for M500 at 100 N load and 30 °C

Figure 5-6 and Figure 5-7 show coefficient of friction averages for every test with M250 at 30 °C and 30 % RH. In Figure 5-6 at lower frequencies (left-hand side of the graph) the coefficient of friction between tests, at the same Hersey number are relatively close but as the oscillating frequency is increased (higher Hersey number) the difference in recorded coefficient of friction increases. This shows that at some point the effect on the endpoints in the stroke starts to play a role on the coefficient of friction recorded resulting in a different coefficient of friction for different Hersey numbers. We know that the endpoints are not measured due to machine limitations. The erratic nature of the coefficient of friction at 100 N indicates that there is some sticking taking place but the failure at the endpoints is not catastrophic up to an oscillating frequency of 75 Hz.
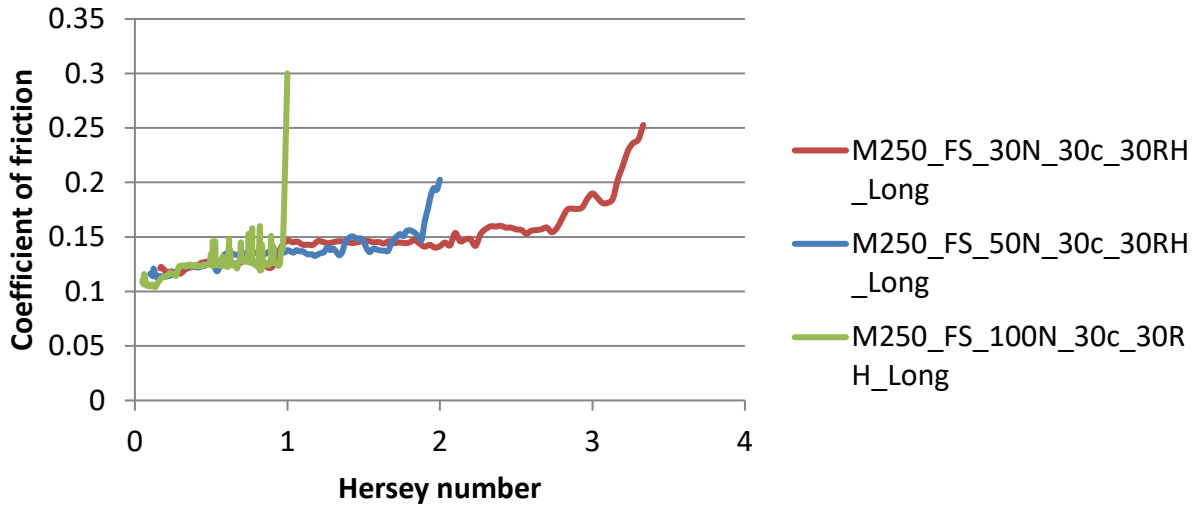
Figure 5-6: Combined results for tests with M250 at 30 °C and 30 % RH using Hersey number as the x-axis.

Figure 5-7 gives the same data as Figure 5-6 but plotting the data with oscillating frequency on the x-axis does give some insight that the graph above does not. There is a pattern observable in every single data set generated. There is a dip in the coefficient of friction between 25 and 50 Hz and a sudden increase followed by a decrease in the coefficient of friction between 50 and 75 Hz. This strange behaviour is also seen between 75 and 100 Hz. At all these points the SRV vibrates and makes a different noise. These deviations seem to be due to natural oscillating frequencies of some of the materials in the SRV and affect the recorded coefficient of friction or an inherent weakness of the motor used. This makes values around those frequencies unreliable.
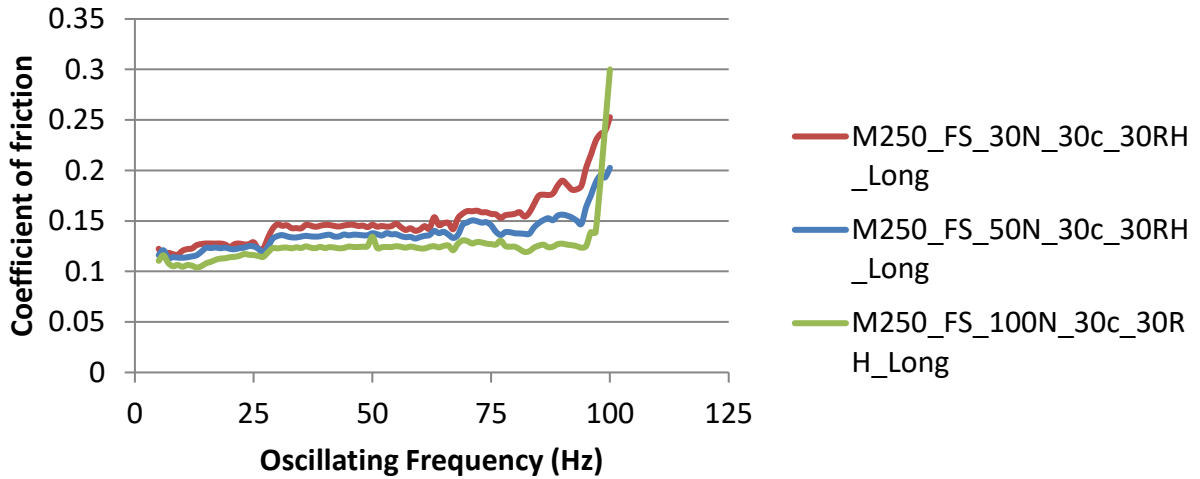
Figure 5-7: Combined results for tests with M250 at 30 °C and 30 % RH using oscillating frequency as the x-axis.

5.1.2. M500

Looking at all the results for runs with M500, Figure 5-8 gives the same trends as M250. Lower coefficient of friction as the load is increased and results for the same Hersey number differ more and more between tests as the oscillating frequency is increased. For the run at 100 N the coefficient of friction are stable at higher oscillating frequencies. This shows that the effect the endpoints have on the system can be reduced by increasing the concentration of the additive. As discussed in Chapter 2 increasing a lubricant's lubricity lessens the severity of parameters that increase wear, like temperature.
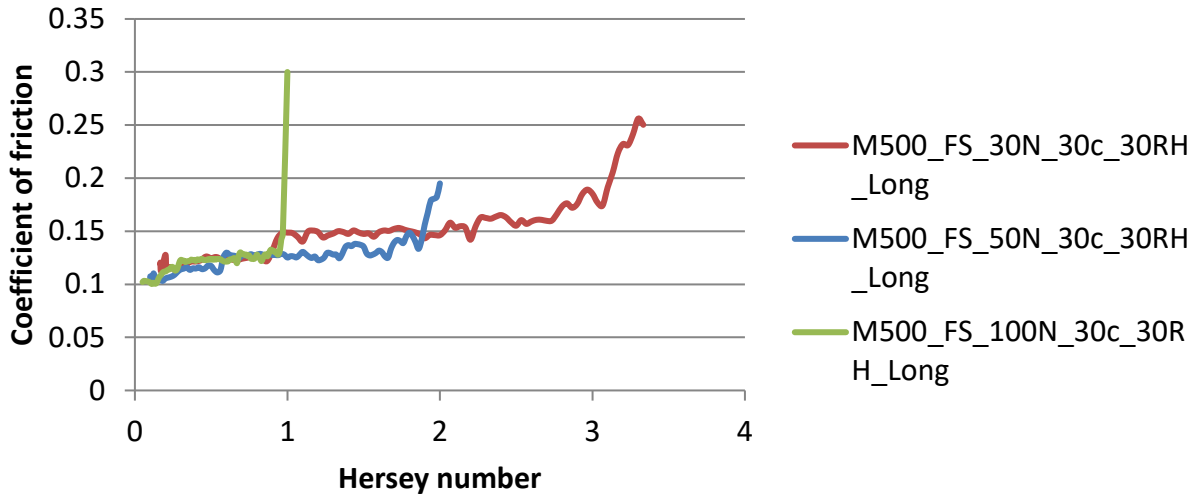
Figure 5-8: Combined results for tests with M500 at 30 °C and 30 % RH using Hersey number as the x-axis.

5.1.3. M1000

As expected, increasing the additive concentration led to an improvement in the strength and recovery rate of the additive layer. Runs with 1000 ppm of myristic acid (C-14), Figure 5-9, showed the same trend as lower concentrations but no breakthroughs occurred. What this indicates is that there is more additive available to ensure that breakthrough does not occur at the endpoints. The higher bulk fluid concentration is allowing the additive layer at the endpoints to recover in time or the additive layer is strong enough to survive the static contact at the endpoints. This indicates that when damage occurs in oscillating contacts wear can be reduced by using more surface-active additives. This does not solve the problem of how to generate a Stribeck curve by changing the oscillating frequency on the SRV. The end-points are an inherent property of any oscillating test.
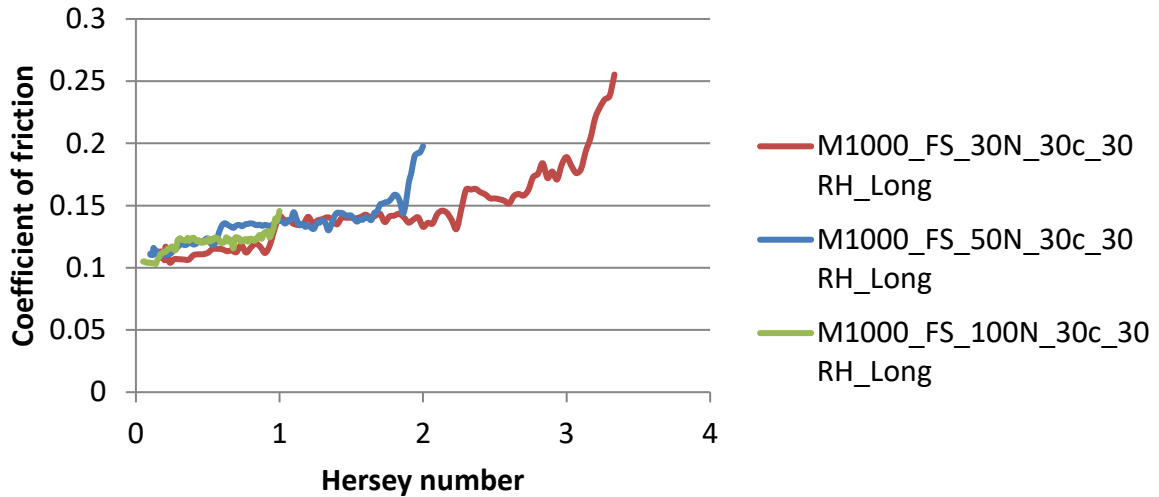
Figure 5-9: Combined results for tests with M1000 at 30 °C and 30 % RH using Hersey number as the x-axis.

5.1.4. P250

For runs using 250 ppm palmitic acid (C-16), P250, at a 100 N load things were more complicated compared to the M250 runs, data is shown in Figure 5-10. Comparing run 1 and run 2 it is important to notice the differences during the running-in time. It is possible that the high coefficient of friction during the run-in for run 2 resulted in the test failing much later than run 1.
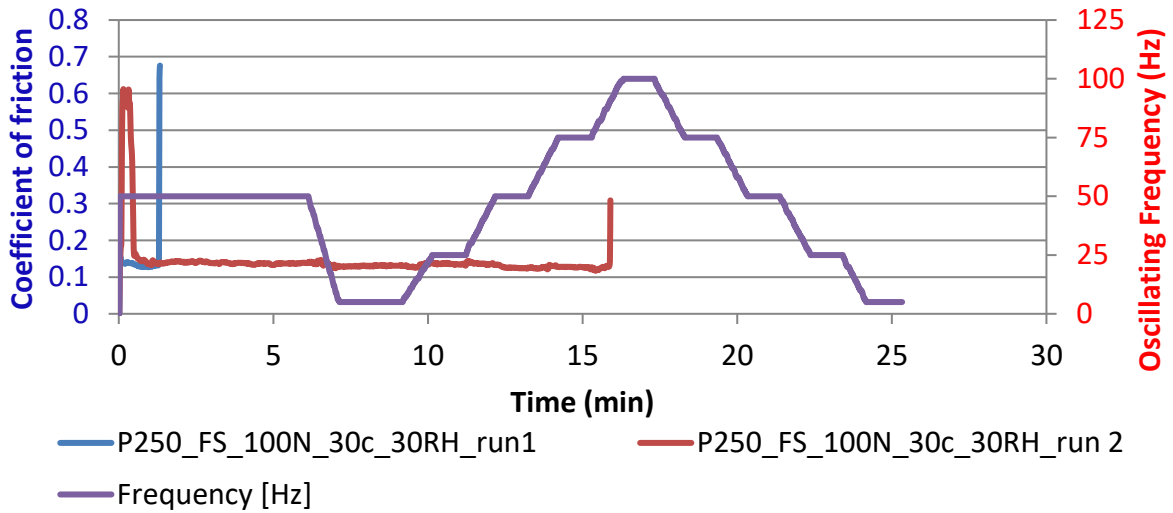
Figure 5-10: FS runs for P250 at 30 °C, 30 % relative humidity and 1 mm stroke under a load of 100 N.

This behaviour shows how big an effect the running in time can have on results and should be kept in mind when analysing results. All the other tests were completed without any breakthroughs. Averages for all the P250 tests are given in Figure 5-11. Looking at these graphs compared to M250 there is a clear difference in trends for the 100 N runs. For the 100 N runs the coefficient of friction was higher at low frequencies compared to runs at lower loads indicating a difference in how palmitic acid (C-16) works compared to myristic acid (C-14) at low frequencies.
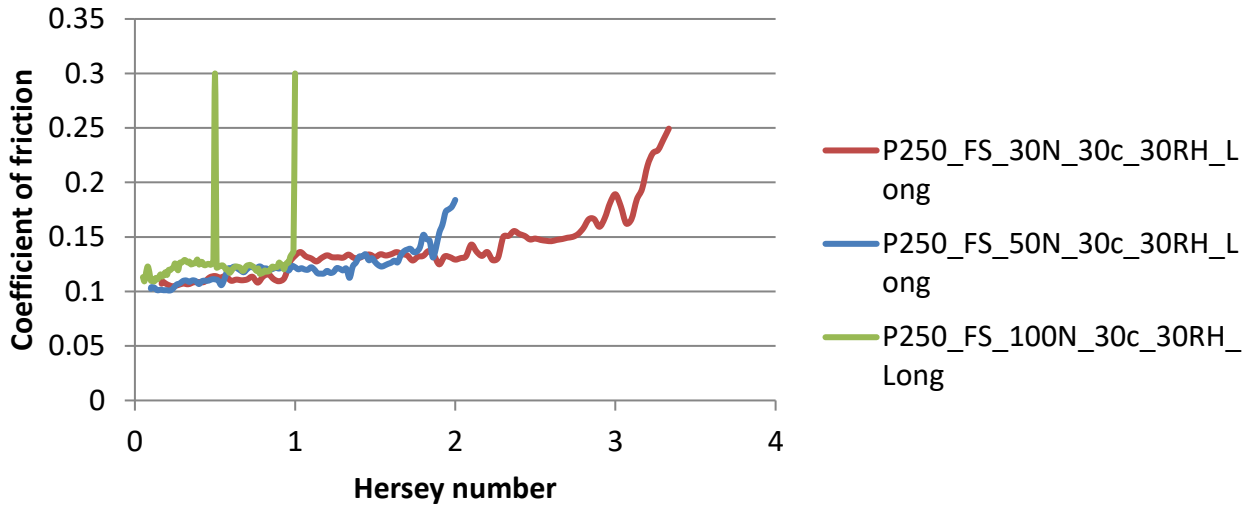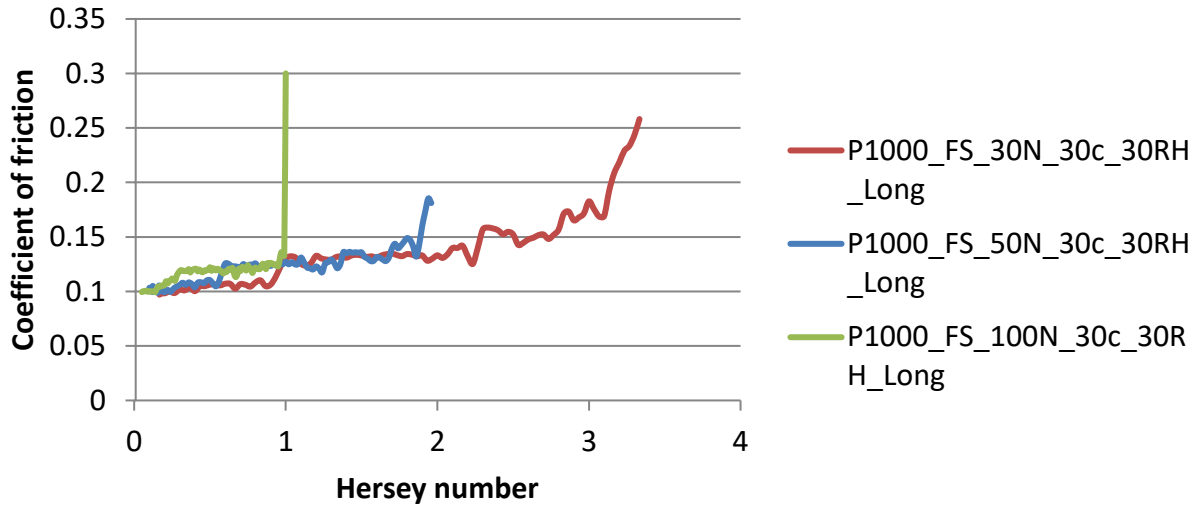
Figure 5-11: Combined results for tests with P250 at 30 °C and 30 % RH using Hersey number as the x-axis.

5.1.5. P500

As with P 250, runs at a 100 N did not complete the test, Figure 5-12. In this case, the data is clearer. 2 Repeats failed during the 100 Hz step increase while run 1 showed a large coefficient of friction at the start of the test. The high coefficient of friction observed during the run-in time, for run 1, implies that the contact area was bigger which explains why run 1 was able to complete the test where the other 2 runs did not. This shows the inherent problem with running a test with consecutive conditions. The surface history plays a significant role, especially at lower concentrations. What is very important to note is that at 30 N and 50 N applied loads the coefficient of friction in the first half and in the second half compared well. **This indicates that the run-in period is the most important part to achieve repeatable results.**
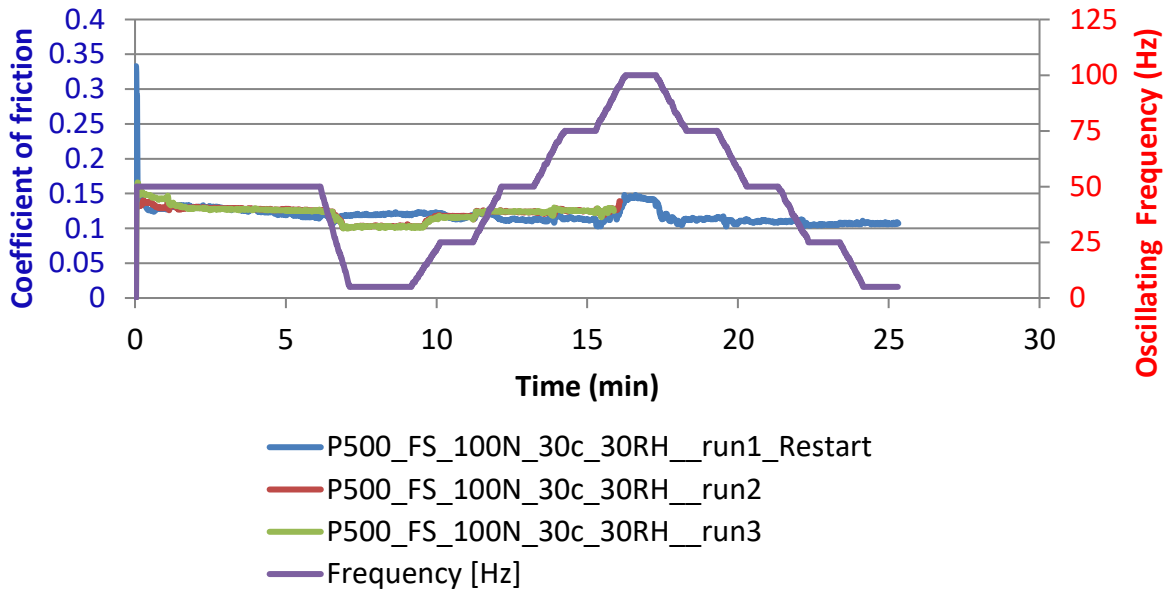
Figure 5-12: P500 test results at 100 N load.

5.1.6. P1000

P1000 at a 100 N, Figure 5-13 also had tests that failed and tests that finished the entire run with good coefficient of friction repeatability. There is however no indication to why 1 of the 3 runs was able to complete the run. What has been made clear at this point is that there are differences in the running-in period with all the tests. Differences in the run-in time can result in different results because the tests have a surface history. Load-carrying capacity tests with a high coefficient of friction at the start have been seen to reach much higher loads than they should. This can be attributed to the larger surface area after a high coefficient of friction resulting in larger surface areas.
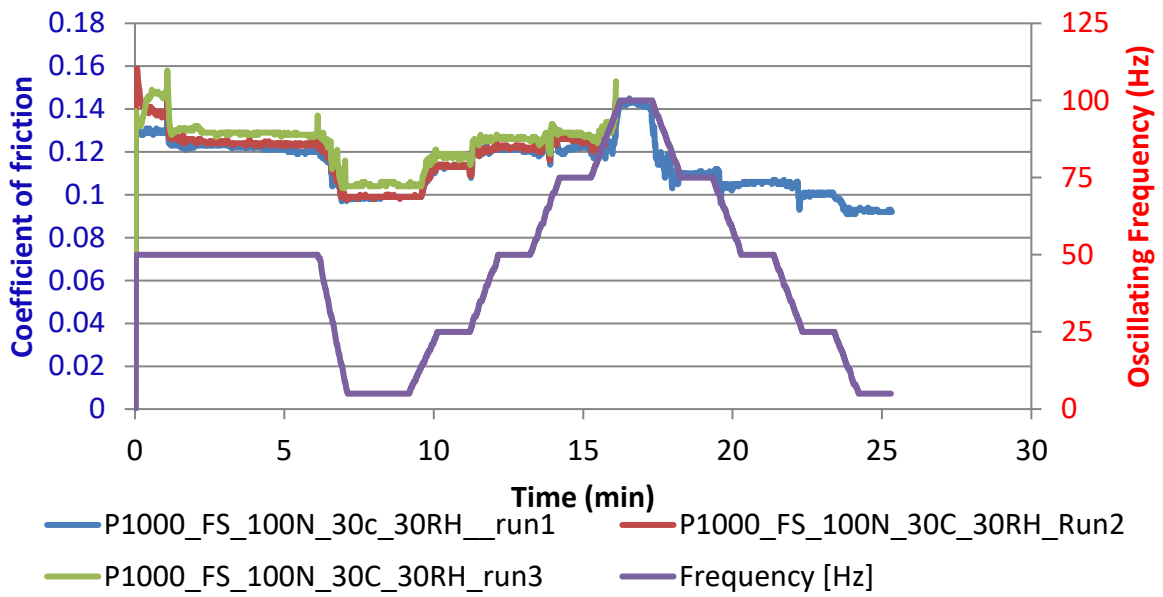
Figure 5-13: Runs for P1000 at 30 °C and 30 % RH and a load of 100 N.

The combined results for P1000, Figure 5-14 gave the same trends as observed previously. One change to observe is that the coefficient of friction did not differ much at low oscillating frequencies between the different load runs. This indicates that at 250 and 500 ppm additive concentrations the higher coefficient of friction observed for low oscillating frequencies during the 100 N runs could be due to additive layer strength.
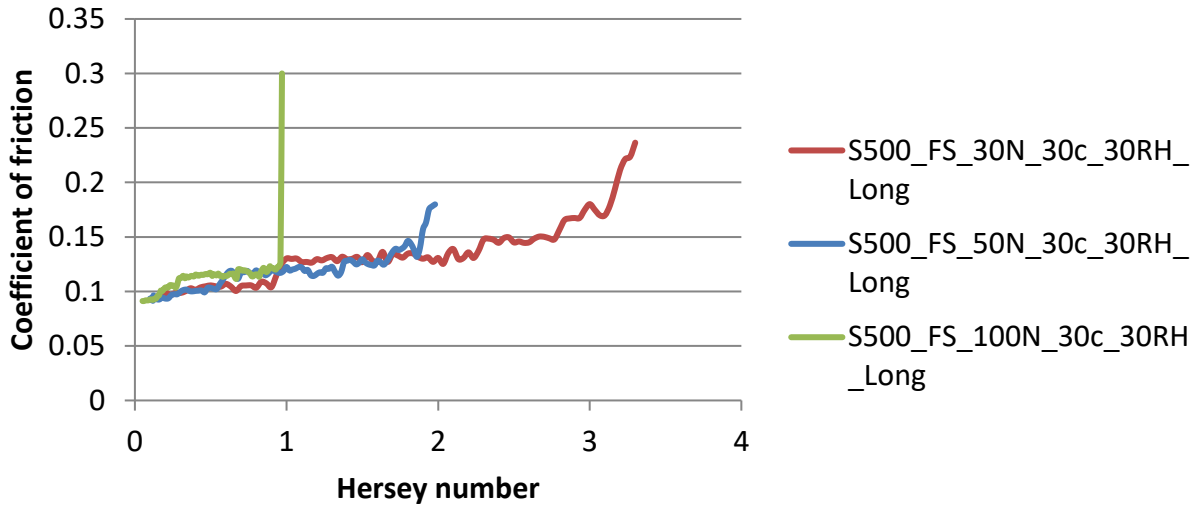
Figure 5-14: Combined results for tests with P1000 at 30 °C and 30 % RH using Hersey number as the x-axis.

5.1.7. S250

Runs with S250 at a 100 N load, Figure 5-15, both had a high coefficient of friction during the running-in period and finished the tests without breakthrough elsewhere.
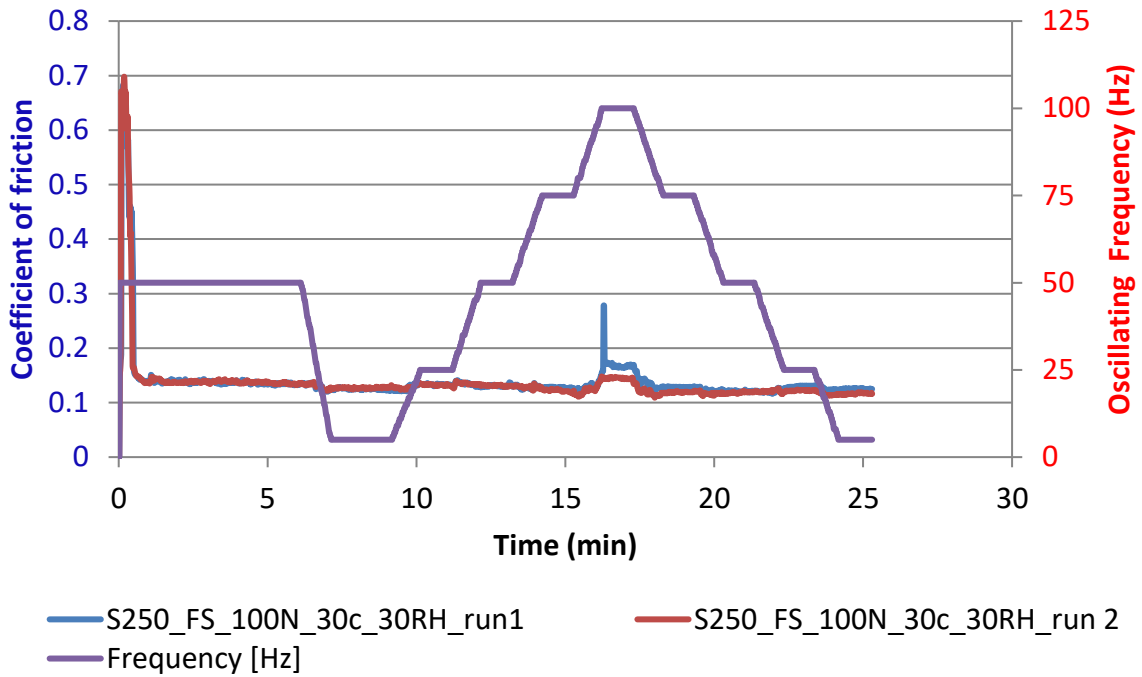
Figure 5-15: Runs for S250 at 30 °C and 30 % RH and a load of 100 N.

Combining all the results for S250, Figure 5-16, shows the same trend observed for palmitic acid (C-16) where the coefficient of friction for runs with 100 N at low oscillating frequencies was higher compared to other, indicating that the runs are closer to failure.
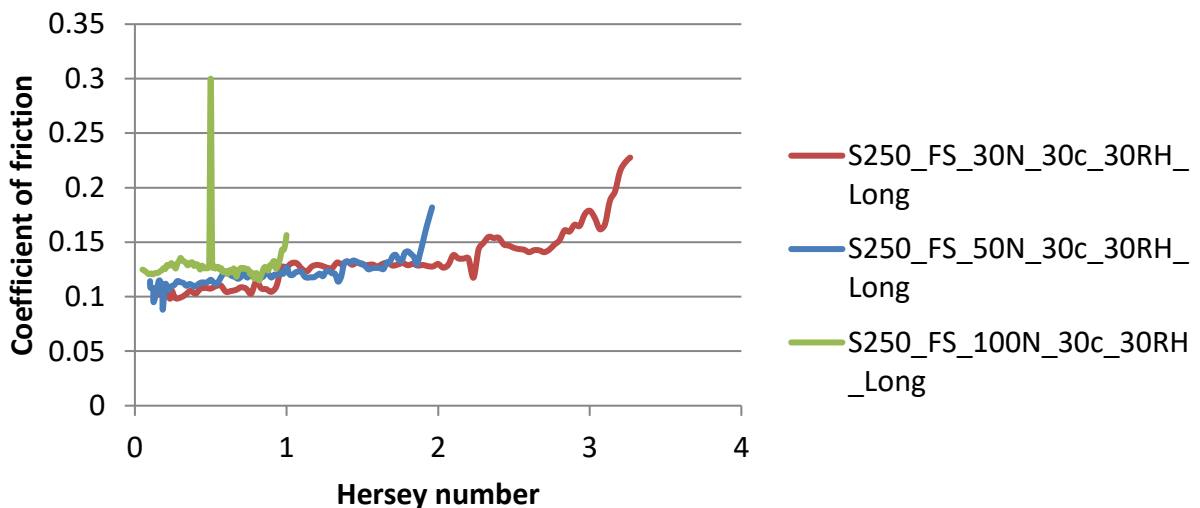
Figure 5-16: Combined results for tests with S250 at 30 °C and 30 % RH using Hersey number as the x-axis.

94

5.1.8. S500

Runs with S500, Figure 5-17, both failed during the step to 100 Hz. This shows that the runs using 250 ppm should also have failed at the 100 Hz step increase or at a lower frequency because of the lower additive concentration used. Runs using 250 ppm stearic acid (C-18) completed the tests because of the high coefficient of friction at the start of the run increasing the surface area.
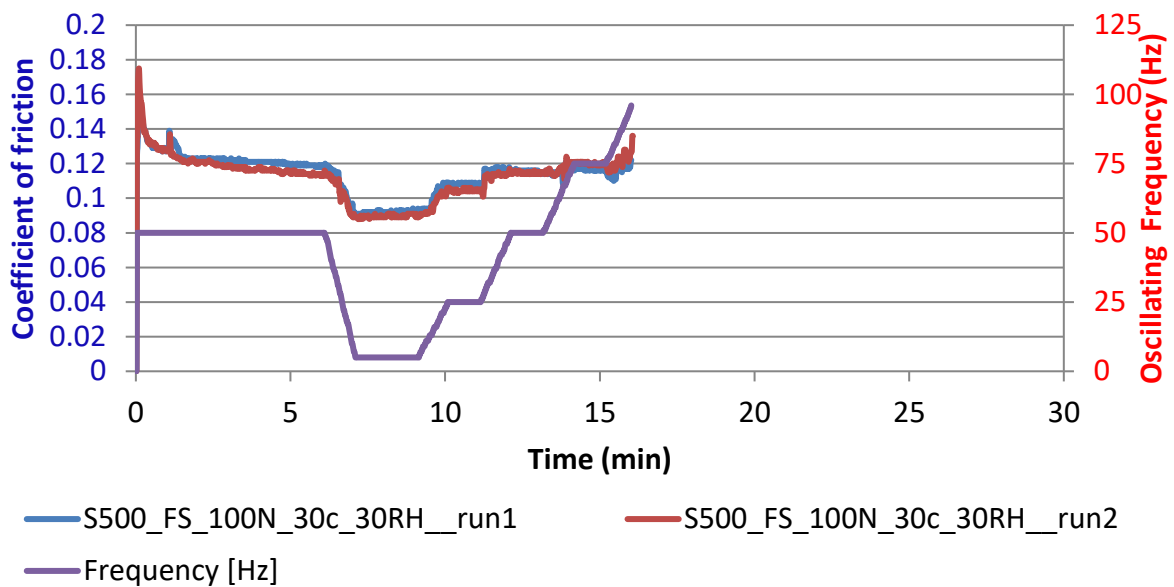
Figure 5-17: Runs for S500 at 30 °C and 30 % RH and a load of 100 N.

Looking at the combined results, Figure 5-18 for all runs with 500 ppm stearic acid (C-18) shows the coefficient of friction, at 100 N load, below the runs at other loads at low oscillating frequencies.

Figure 5-18: Combined results for tests with S500 at 30 °C and 30 % RH using Hersey number as the x-axis.

5.1.9. S1000

Runs with S1000 at a 100 N were problematic, Figure 5-19. Runs were completed with high repeatability based on the coefficient of friction but 2 out of 3 tests failed during the increase to 100 Hz. Run 1 also had a spike in the coefficient of friction during the increase but the coefficient of friction stayed below 0.3. The combined results, Figure 5-20 solidifies the idea that the deviations observed in the coefficient of friction are affected by the additive concentration with the results following the expected trend for 1000 ppm additive concentration but not for lower concentrations. The coefficient of friction was also similar for the same Hersey number between different runs with deviation at high oscillating frequencies and where a change in vibrational tone occurred on the SRV. When comparing the coefficient of friction, Figure 5-20 before any jump has occurred, all 3 runs have a similar coefficient of friction up to the point where the first jump in the coefficient of friction occurs. Each of the increases on Figure 5-20 corresponds to the increase in the coefficient of friction observed in Figure 5-21 between 25 and 50 Hz.
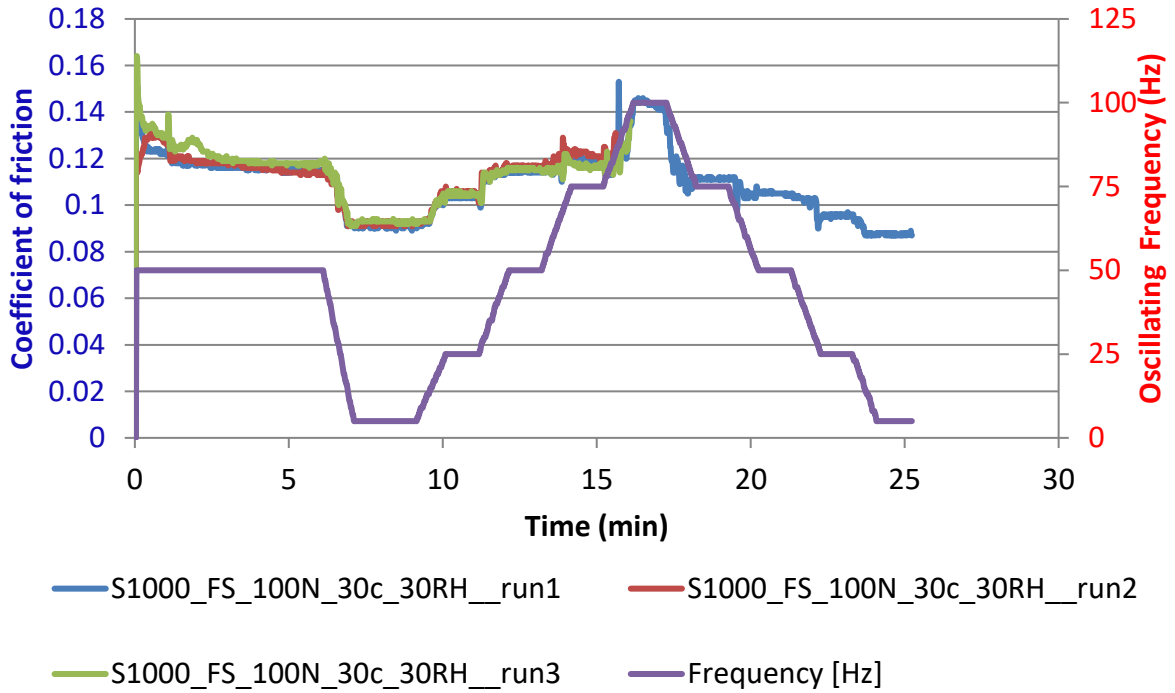
Figure 5-19: Runs for S1000 at 30 °C and 30 % RH and a load of 100 N.
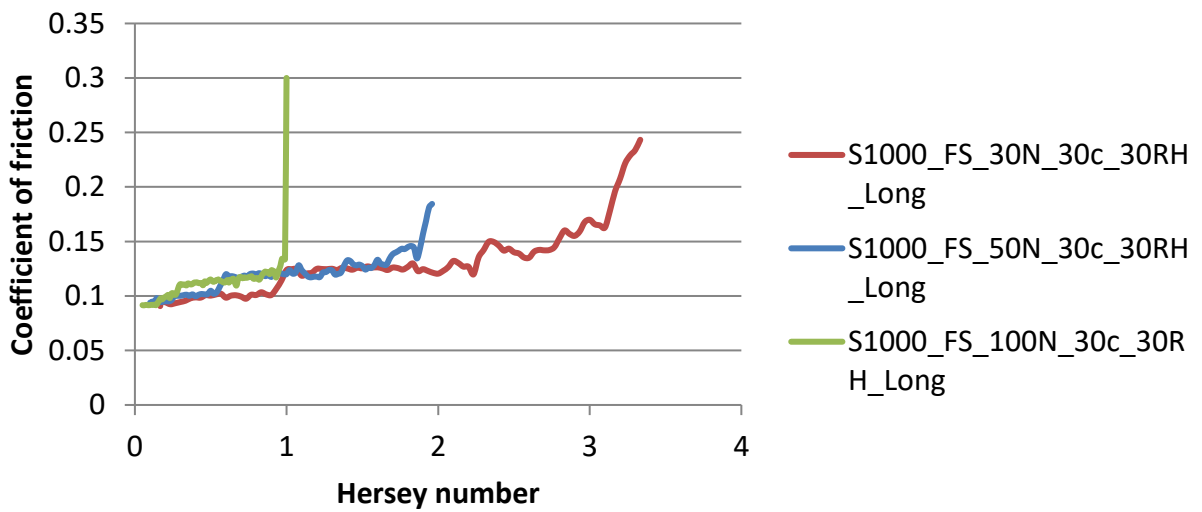
Figure 5-20: Combined results for tests with S1000 at 30 °C and 30 % RH using Hersey number as the x-axis.
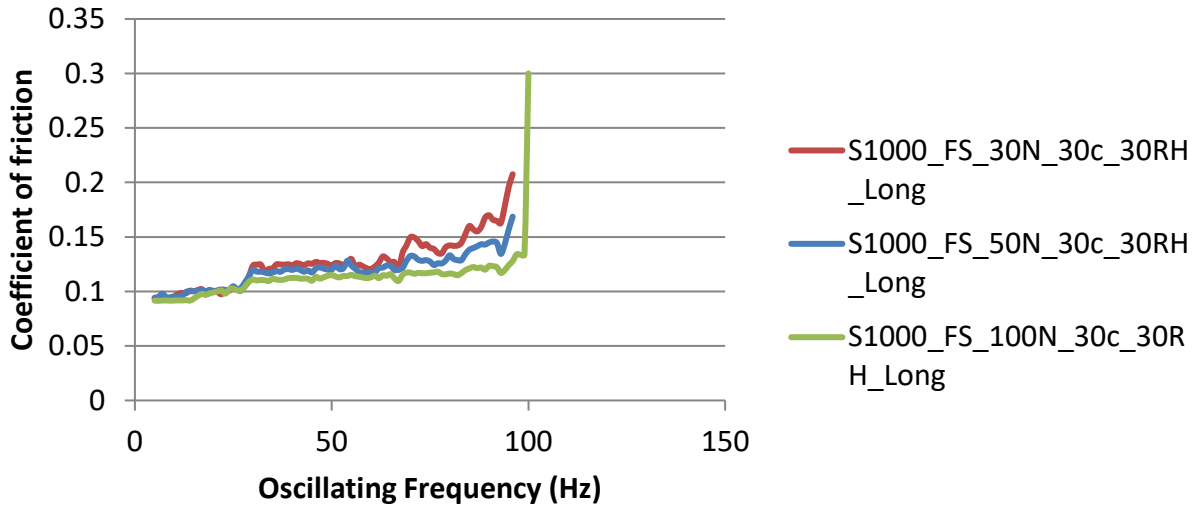
Figure 5-21: Combined results for tests with S1000 at 30 °C and 30 % RH using oscillating frequency as the x-axis.

The 100 N coefficient of friction is higher compared to the other runs until the 50 N run reaches the 25 to 50 Hz increase. From here on the 30 N run has a lower coefficient of friction compared to the similar values of the 50 and 100 N runs. When the 30 N runs reaches the 25 to 50 Hz increase, all three runs have a similar coefficient of friction again.

5.1.10. The average coefficient of friction of different additives

Using all the coefficient of friction data collected during the different oscillating frequency steps the following graphs were generated using a 95% confidence interval with a P-test to generate the error bars. Figure 5-22 makes it clear that increases in the concentration of the additive decrease the coefficient of friction. As discussed in Chapter 4.2 with the HFRR more additive gives a stronger protective layer reducing contact between the wear surface, reducing the coefficient of friction. However, there are diminishing returns on the extra protection more additive will give due to limited surface area. The confidence interval for every section is also small compared to the differences between different tests indicating that there is a significant difference between results. If results are absent from a graph, a breakthrough occurred at the specific or a

lower frequency. The same trends were observed for palmitic acid (C-16), Figure 5-23, and stearic acid (C-18), Figure 5-24.
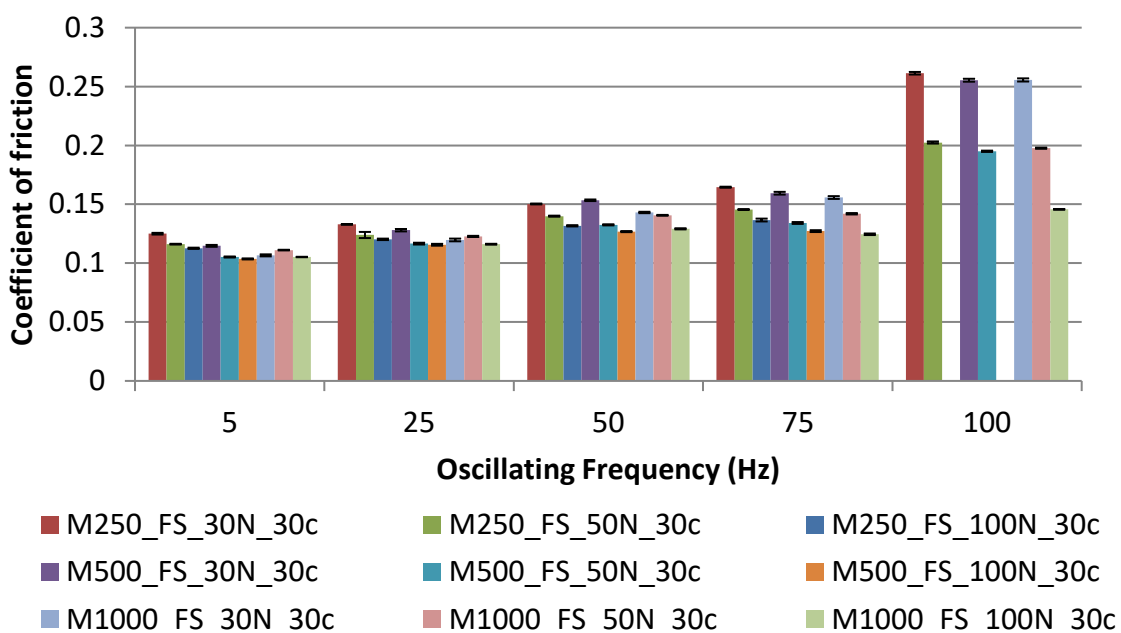
Figure 5-22: Statistical information for runs with myristic acid (C-14) at 30 °C.
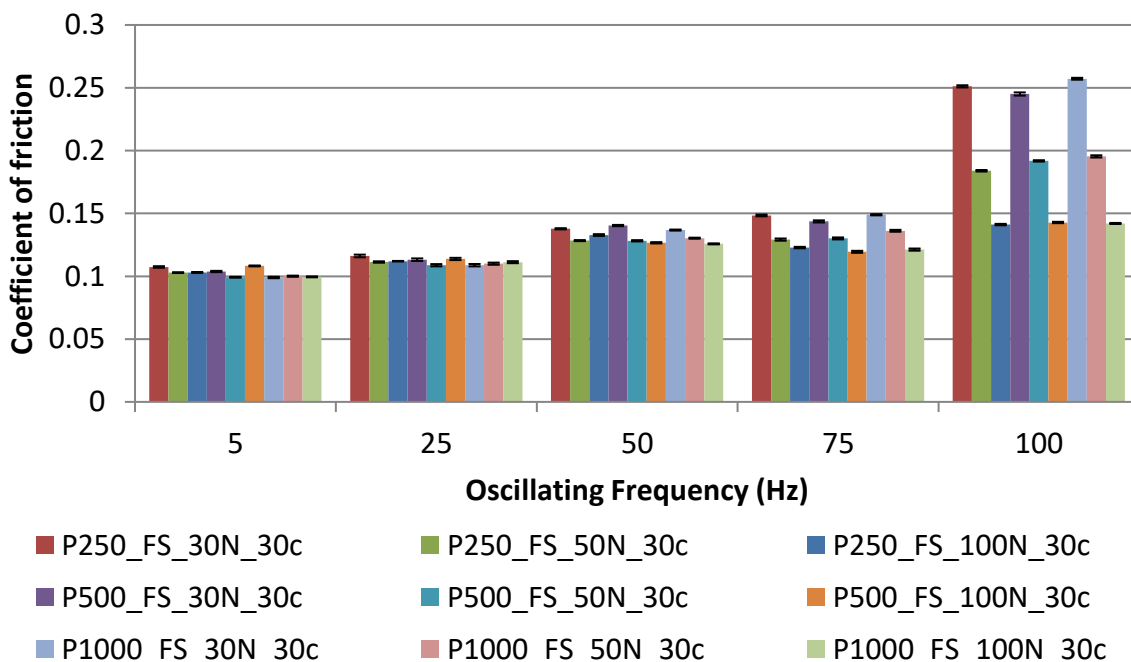
Figure 5-23: Statistical information for runs with palmitic acid (C-16) at 30 °C.
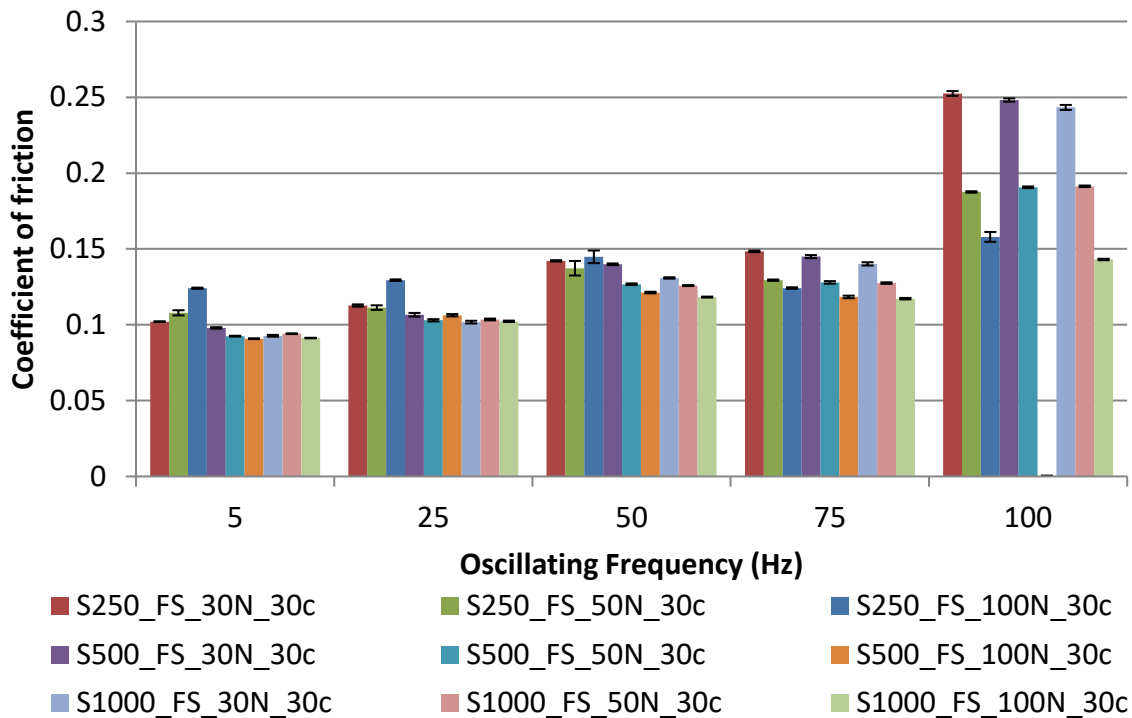
Figure 5-24: Statistical information for runs with stearic acid (C-18) at 30 °C.

To have a closer look at how an additive's chain length affects results at different oscillating frequencies the data was grouped based on additive concentration and applied load.

Concentration comparison

a) 250 ppm

Looking at Figure 5-25 we see the general trend of decreasing coefficient of friction as the load is increased. Some deviations are observed for stearic acid (C-18) and palmitic acid (C-16) at low frequencies. Palmitic acid (C-16) results for different loads are the same up to 50 Hz and follow the expected trend for higher frequencies. Stearic acid (C-18) showed a strange trend for 5 and 25 Hz. At these frequencies, the 100 N run had a higher coefficient of friction. At 50 Hz results are similar and differ as expected for 75 and 100 Hz. The longer chain length of the palmitic (C-16) and stearic acid (C-18) explains this behaviour. As the oscillating frequency is decreased less hydrostatic pressure is generated decreasing the distance between the two specimens. With longer chain length

additives, the two surface layers will start to interact at a larger separation distance compared to a shorter chain length additive.
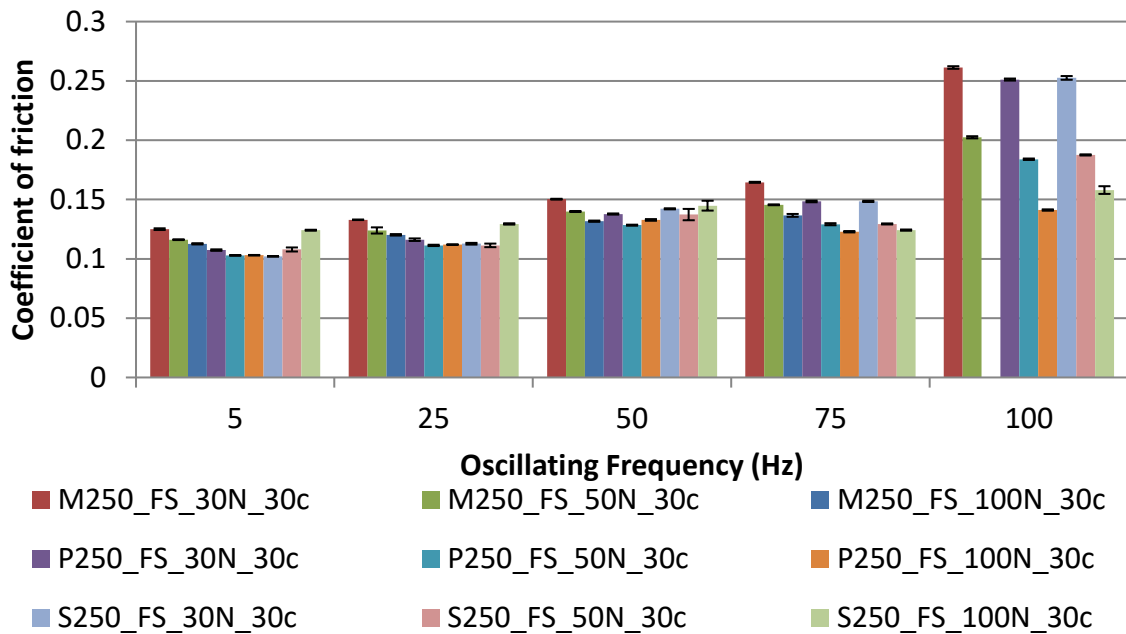
Figure 5-25: Average coefficient of friction for runs with 250 ppm additive concentrations at different oscillating frequencies steps.

The microscope wear measurements, Figure 5-26 – Figure 5-28, show more damage to the surfaces as the load is increased, shown by the increase in wear length and diameter. This shows a clear problem with just using the coefficient of friction as a performance parameter. According to the coefficient of friction, the lubricants are doing better under higher loads, but we know that by increasing the load we push the lubrication regime into boundary lubrication where the distance between surfaces becomes very small. The wear measurement shows this reduction in the thickness of the protective layers. The large jump in measurements at 100 N is due to the surfaces coming into contact with each other during the 100 N runs.
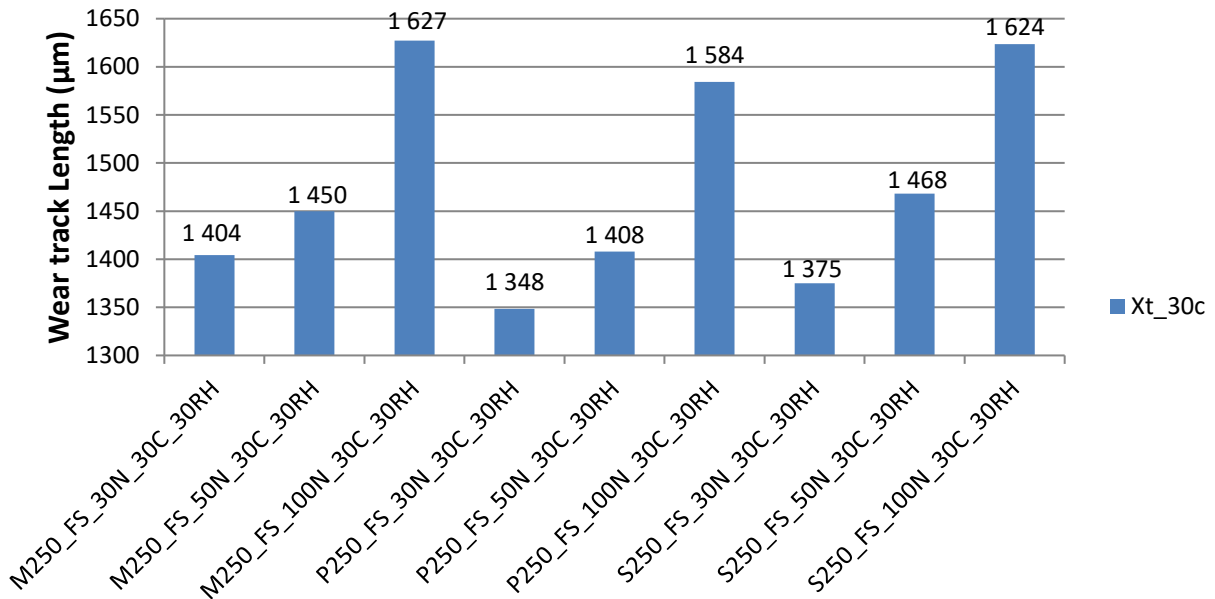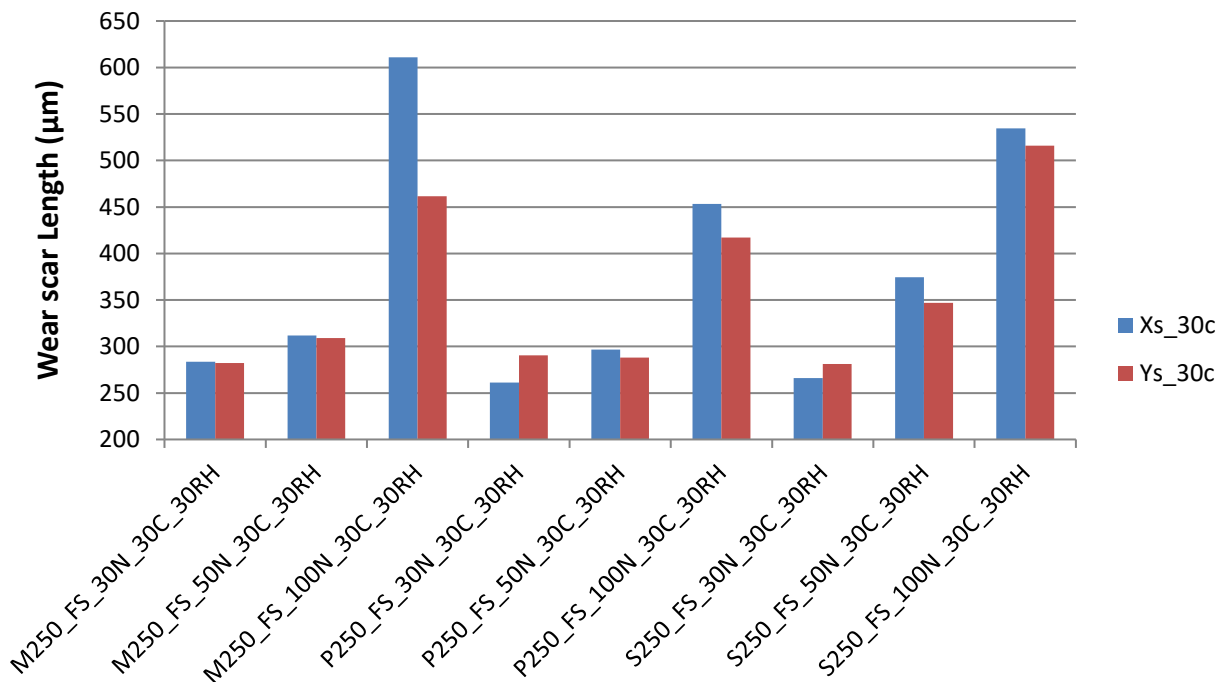
Figure 5-26: Average wear measurement of the wear track for runs with 250 ppm additive concentrations. Xt – x-direction (direction of movement) for the track.

From Figure 5-26 it seems that palmitic acid (C-16) offered the best protection for the disk across runs. Results for 100 N should be interpreted carefully with the breakthroughs in mind.

Based on the ball scar's average diameter in Figure 5-27 palmitic acid (C-16) also gave the best The same holds true at higher concentrations. This is likely due to chain matching described in Chapter 2.4.2.

The larger differences between the average diameter and the width of the wear track at higher loads indicate a deeper wear track. Generally, as the wear track deepens more of the ball's surface will be in contact with the disk. But this is dependent on the 3-dimensional space of the disk and ball (Litzow, Jess, Matzke, Caprotti, & Balfour, 2009). Very high wear on the ball results in a very flat ball surface and a similar-sized wear track. Lower ball wear rates result in a rounder wear scar and a deeper wear track. This wear scar sits inside the wear track growing as the wear track size increases but also as the track wear depth increases. The relative hardness of the two surfaces will also play a significant role.

102
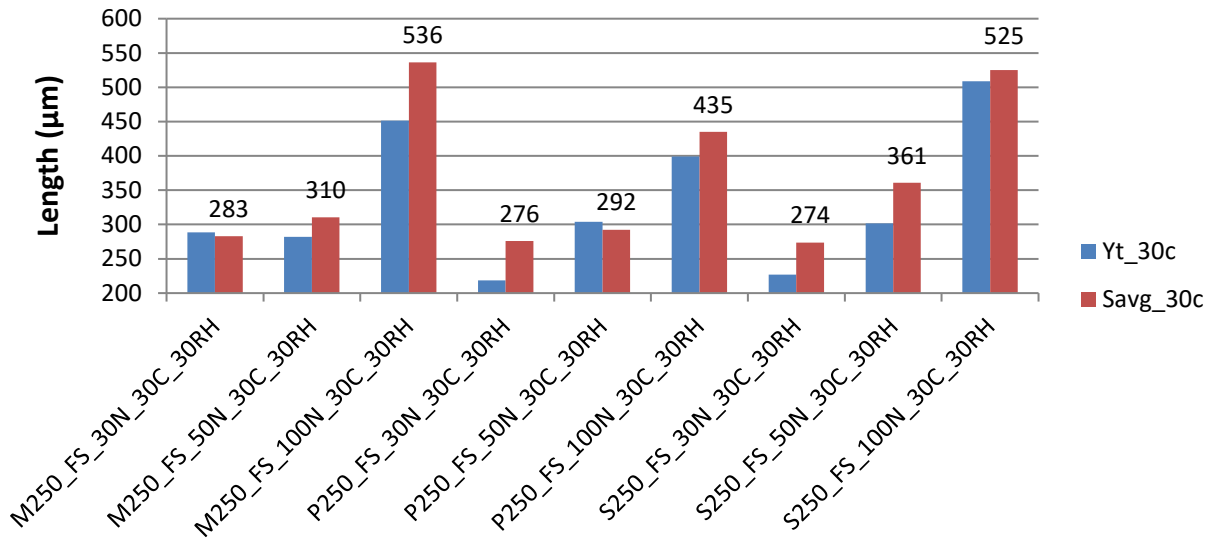
Figure 5-27: Average wear measurement of the wear track and WSD for runs with 250 ppm additive concentrations. Yt – Y-direction (parallel to the direction of movement) for the track, Savg – WSD.

Figure 5-28: Average wear measurement of the wear scar for runs with 250 ppm additive concentrations. Xs – x-direction (direction of movement) for the ball scar. Ys – y-direction for the scar.

Under higher loads, it is also common for the top specimen to slide further than the specified 1 mm stroke, called slipping. The effect this has can be seen in the ball wear scar and track images in Table 5-1 and Table 5-3. Some wear tracks had 2 measurements for the sliding direction length: One where the ball should have stopped and one corresponding to damage caused when slipping occurred. Different magnifications were used on the microscope for all 100 N runs due to an increase in the wear scar.

Table 5-1: Microscope images for M250.
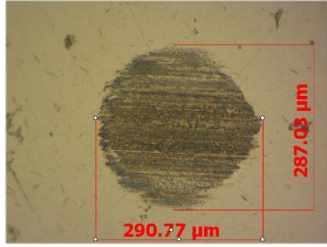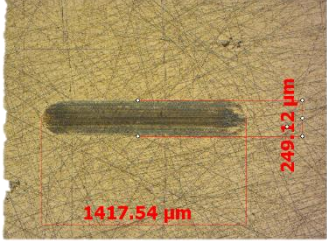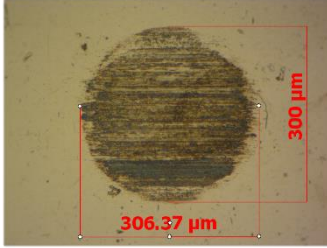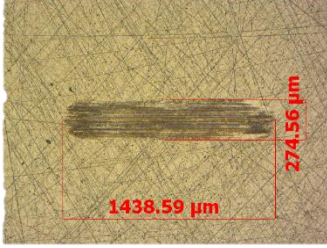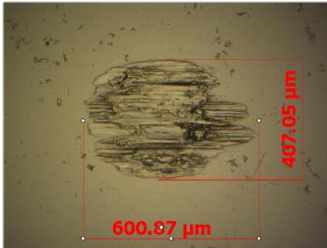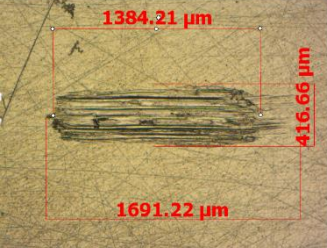
Test ID	Scar	Track
M250_30N 10x magnification on scar	287.03 µm 290.77 µm	249.12 µm 1417.54 µm
M250_50N 10x magnification on scar	300 µm 306.37 µm	274.56 µm 1438.59 µm
M250_100N 5x magnification on scar	407.05 µm 600.87 µm	1384.21 µm 416.66 µm 1691.22 µm

Table 5-2: Microscope images for P250.
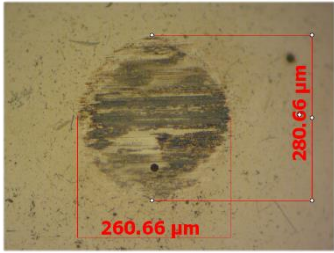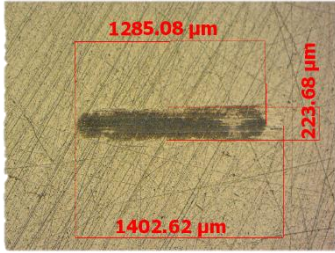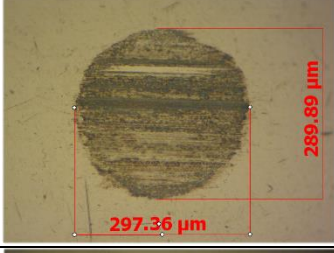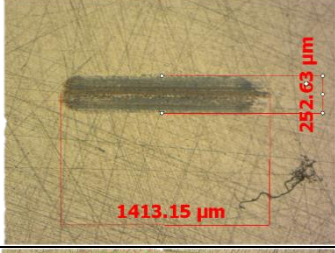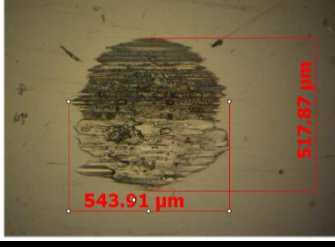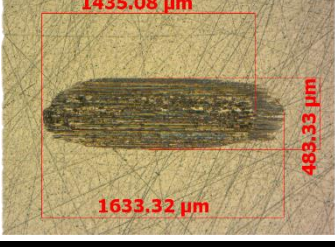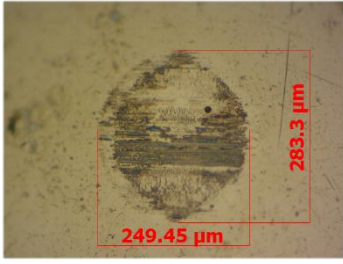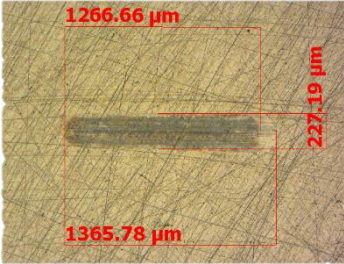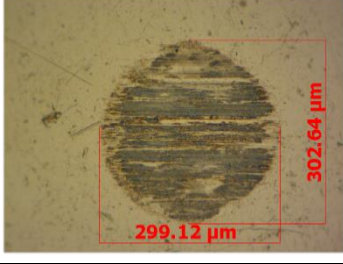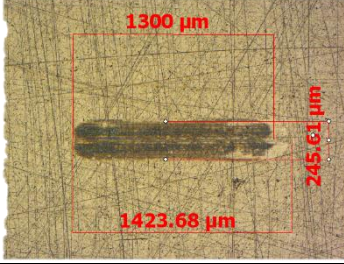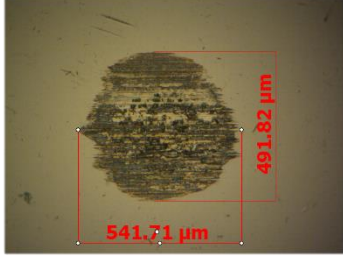
Test ID	Scar	Track
P250_30N 10x magnification on scar	 280.66 µm 260.66 µm	 1285.08 µm 223.68 µm 1402.62 µm
P250_50N 10x magnification on scar	 289.89 µm 297.36 µm	 252.63 µm 1413.15 µm
P250_100N 5x magnification on scar	 517.87 µm 543.91 µm	 1435.08 µm 483.33 µm 1633.32 µm

Table 5-3: Microscope images for S250.

Test ID	Scar	Track
S250_30N 10x magnification on scar	 283.3 µm 249.45 µm	 1266.66 µm 227.19 µm 1365.78 µm
S250_50N 10x magnification on scar	 302.64 µm 299.12 µm	 1300 µm 245.61 µm 1423.68 µm
S250_100N 5x magnification on scar	 491.82 µm 541.71 µm	 494.73 µm 1651.74 µm

It is important to notice the change in colour of the wear scar and track as the load is increased. This gives some indication of the depth of wear that occurred. The scratches on the disk also become out of focus at higher loads. Looking at the images for higher loads the scratches on the disk surface next to the scar are blurry compared to the clear image on the scratches at lower loads. This indicates a significant wear depth difference in the wear tracks, deeper than the focal depth of the microscope. Lighter areas at higher loads indicate where fusion between the surfaces occurred.

b) 500 ppm

For a concentration of 500 ppm, (Figure 5-29) only P500 showed a higher coefficient of friction for higher loads at low oscillating frequencies.
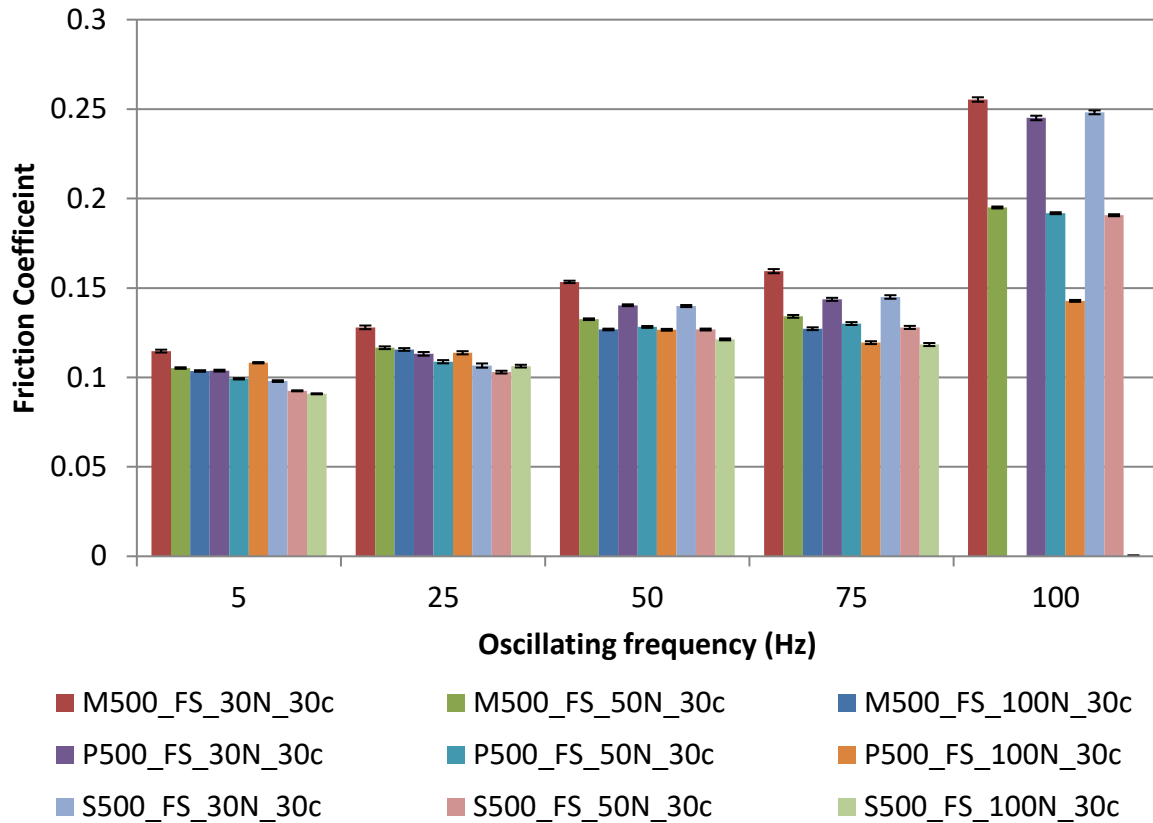
Figure 5-29: Average coefficient of friction for runs with 500 ppm additive concentrations at different oscillating frequency steps.

Measurements of the wear track on Figure 5-30 show how big the change in wear is when catastrophic breakthrough occurs.
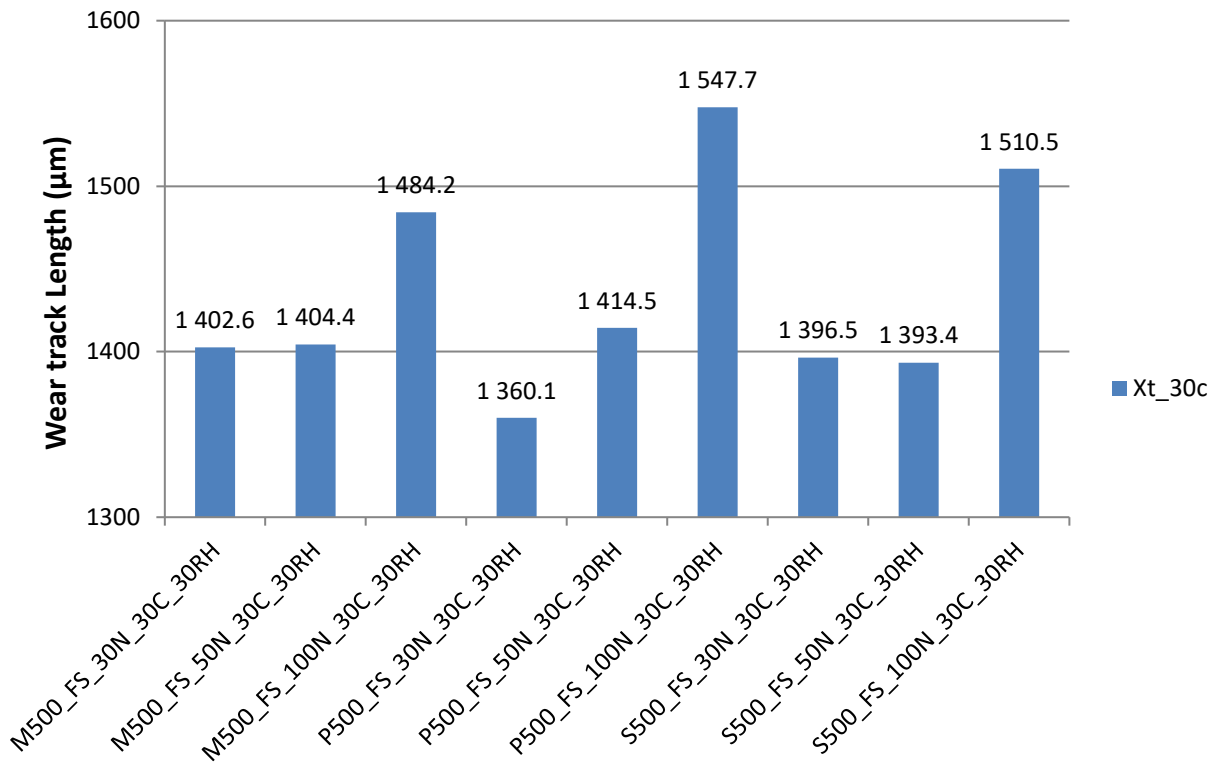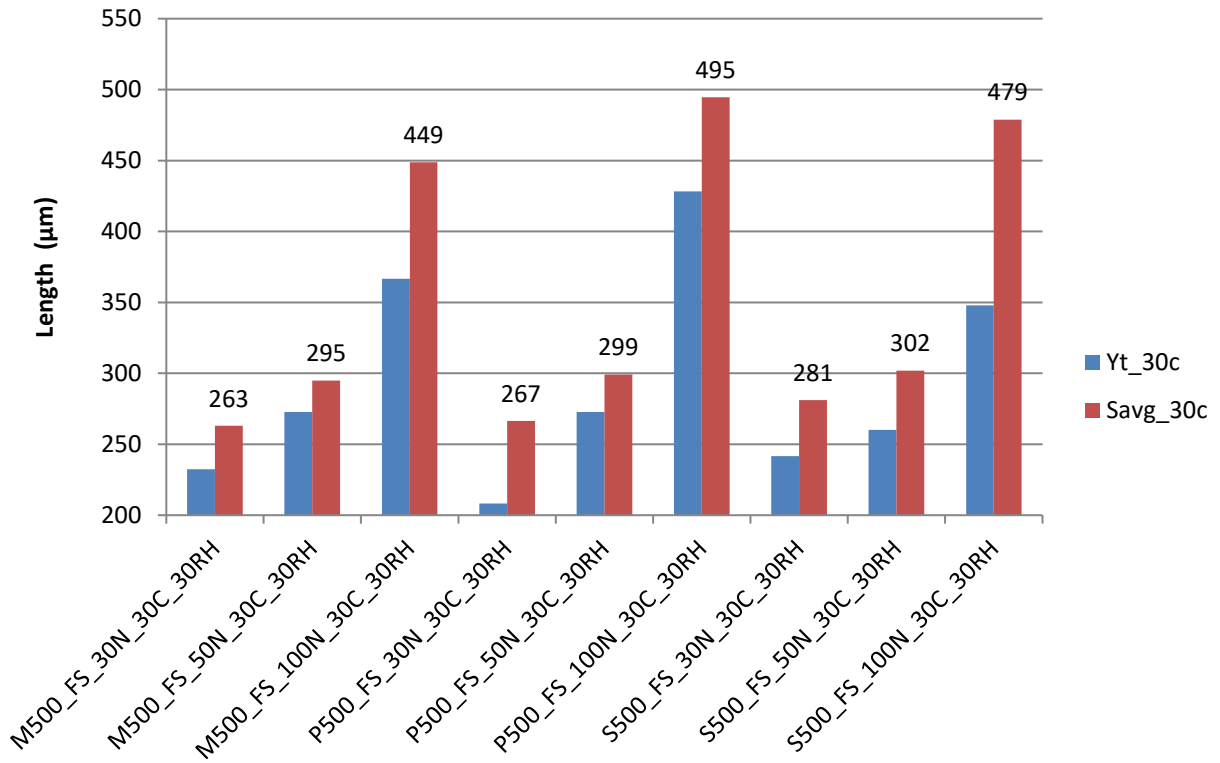
Figure 5-30: Average wear measurement of the wear track for runs with 500 ppm additive concentrations. Xt – x-direction (direction of movement) for the track.

With the increased additive concentration only a single test, S500 run 1 at 100 N showed slipping, shown in Table 5-4 – Table 5-6. The effect of 3-dimensional space on the wear track and scar sizes is even more pronounced with the 500 ppm runs. In Figure 5-31 every run gave a wear scar bigger than the wear track x-direction. As with 250 ppm runs the wear scar measurement in the direction of motions is bigger, Figure 5-32.

Figure 5-31: Average wear measurement of the wear track and WSD for runs with 500 ppm additive concentrations. Yt – Y-direction (parallel to the direction of movement) for the track, Savg – WSD.
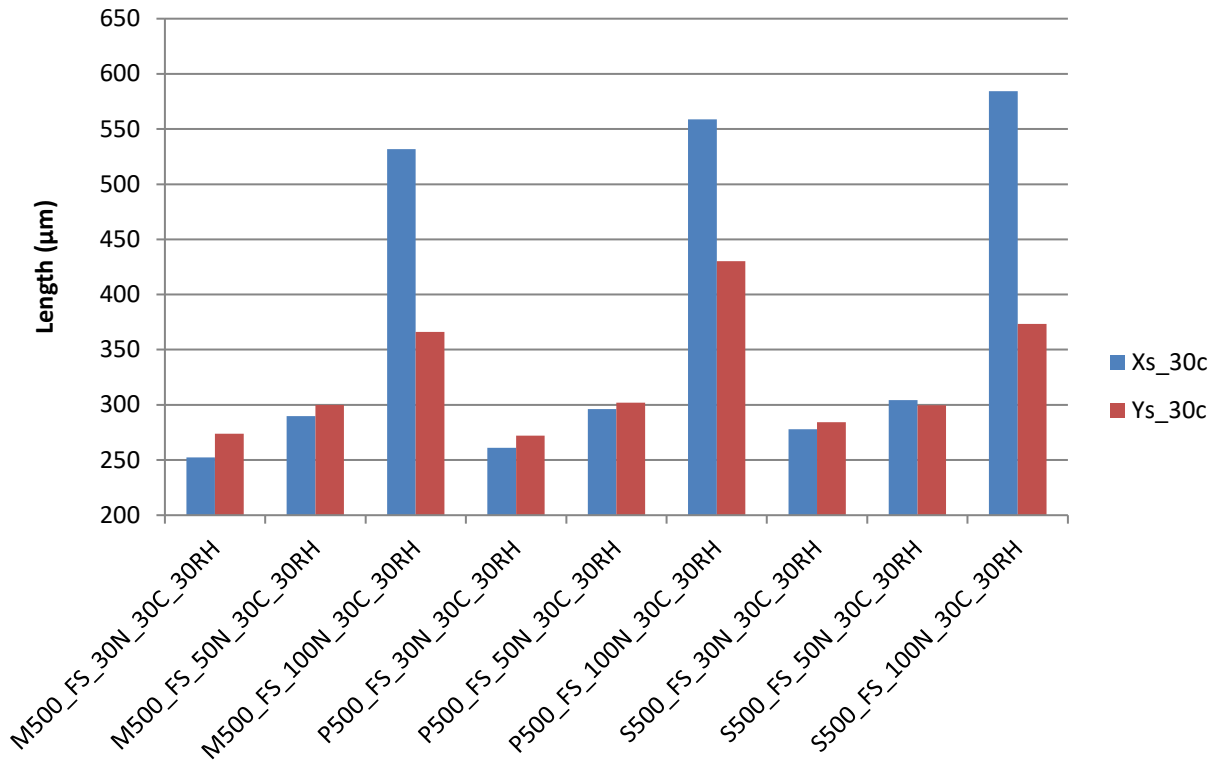
Figure 5-32: Average wear measurement of the wear track for runs with 500 ppm additive concentrations. Xs – x-direction (direction of movement) for the ball scar. Ys – Y-direction for the scar.

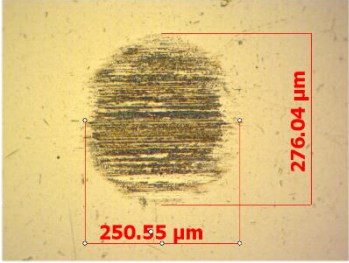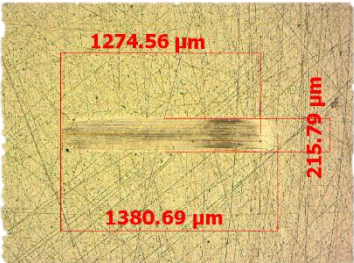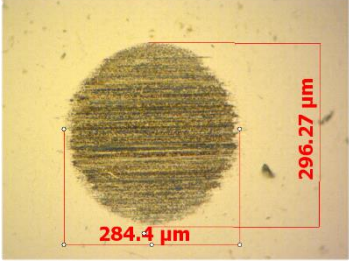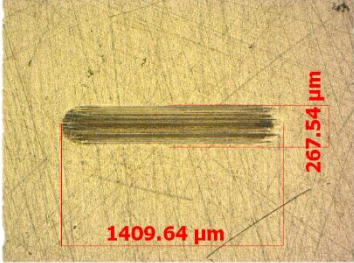Table 5-4: Microscope images for M500.
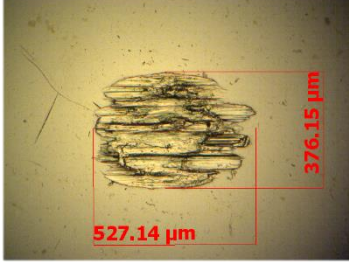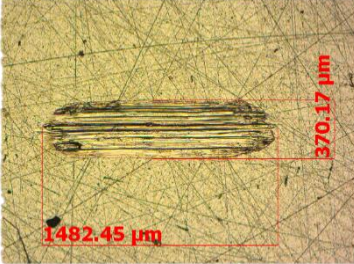
Test ID	Scar	Track
M500_30N 10x magnification on scar	276.04 µm, 250.55 µm	1274.56 µm, 215.79 µm, 1380.69 µm
M500_50N 10x magnification on scar	296.27 µm, 284.4 µm	267.54 µm, 1409.64 µm
M500_100N 5x magnification on scar	376.15 µm, 527.14 µm	370.17 µm, 1482.45 µm

Table 5-5: Microscope images for P500.
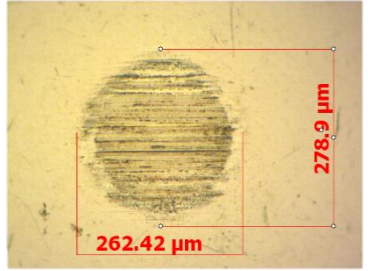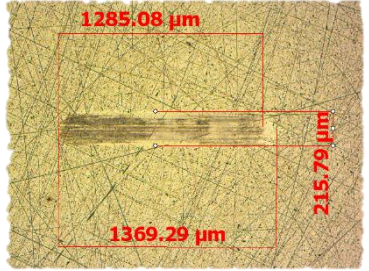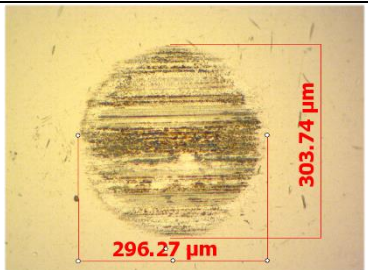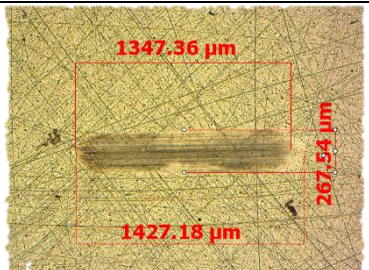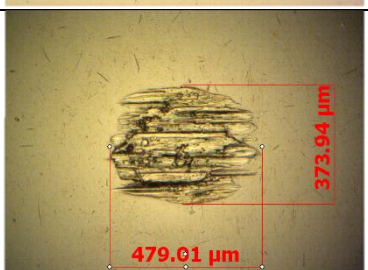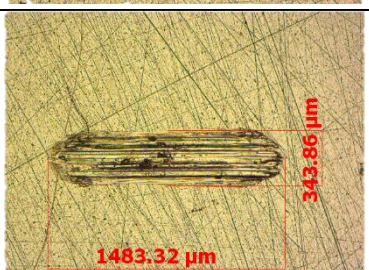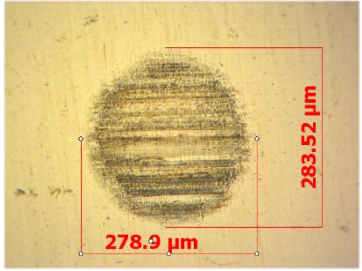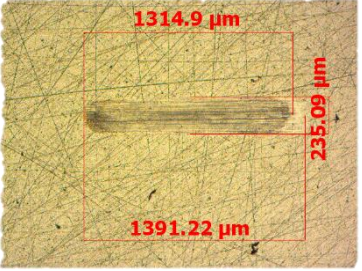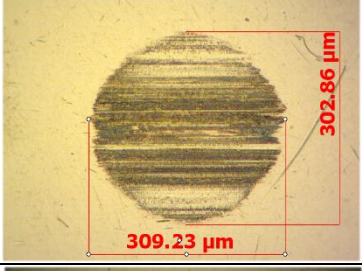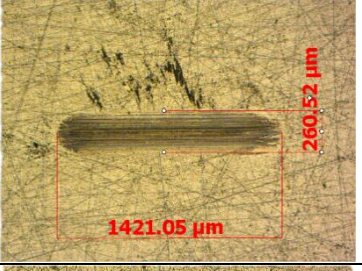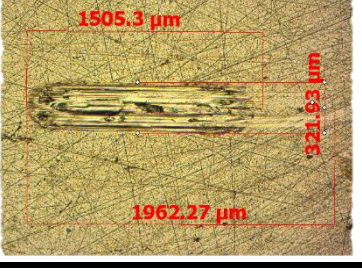
Test ID	Scar	Track
P500_30N 10x magnification on scar	 278.9 µm 262.42 µm	 1285.08 µm 215.79 µm 1369.29 µm
P500_50N 10x magnification on scar	 303.74 µm 296.27 µm	 1347.36 µm 267.54 µm 1427.18 µm
P500_100N 5x magnification on scar	 373.94 µm 479.01 µm	 343.86 µm 1483.32 µm

Table 5-6: Microscope images for S500.

Test ID	Scar	Track
S500_30N 10x magnification on scar	 283.52 µm 278.9 µm	 1314.9 µm 235.09 µm 1391.22 µm
S500_50N 10x magnification on scar	 302.86 µm 309.23 µm	 260.52 µm 1421.05 µm
S500_100N 5x magnification on scar	 357.61 µm 588.06 µm	 1505.3 µm 321.93 µm 1962.27 µm

c) 1000 ppm

Runs using concentrations of 1000 ppm, Figure 5-33, gave similar trends as other concentrations. Looking closely at the Stribeck curve, Figure 2-6, explains some of the behaviour seen at all concentrations. At the start of the boundary regime, the coefficient of friction curve evens out and then drastically increases up to adhesion as the Hersey number is decreased (higher load or lower linear velocity). This explains why so many of the results at lower frequencies are similar. Because of this area where the coefficient of friction does not change much with a change in the Hersey number, we find a situation where the low oscillating frequency gives boundary lubrication and changes in the applied load do not affect the coefficient of friction by much. What should also be kept in mind is the difference in the chain length of the additives. Because stearic acid (C-18)

has a longer carbon chain the boundary layers will interact at a larger separation distance compared to molecules with a shorter chain length. How the coefficient of friction will be affected will then depend on the different additive layers. Surface coverage and interaction zones explain why we see an increase in the coefficient of friction with stearic acid (C-18) at low concentrations but not with myristic acid (C-14). At high concentrations, we know that there will be good surface coverage of the wear surfaces. At 250 ppm the lower surface coverage can result in interaction zones between the additive layers drastically increasing the coefficient of friction. This implies that longer chain additives, that interact quicker, has its boundary regime shifted to the right on the Stribeck curve but the load-carrying capacity is also increased. The increase in the load-carrying capacity decreases the Somerfield number where the breakthrough will occur, compared to an additive with a shorter chain length. This increases in the range, in terms of the Hersey number at which the system will be in the boundary regime. Shorter chains reduce the size of the boundary regime by decreasing load-carrying capacity and decreasing the distance between two tribosystems before full boundary layer lubrication is achieved.
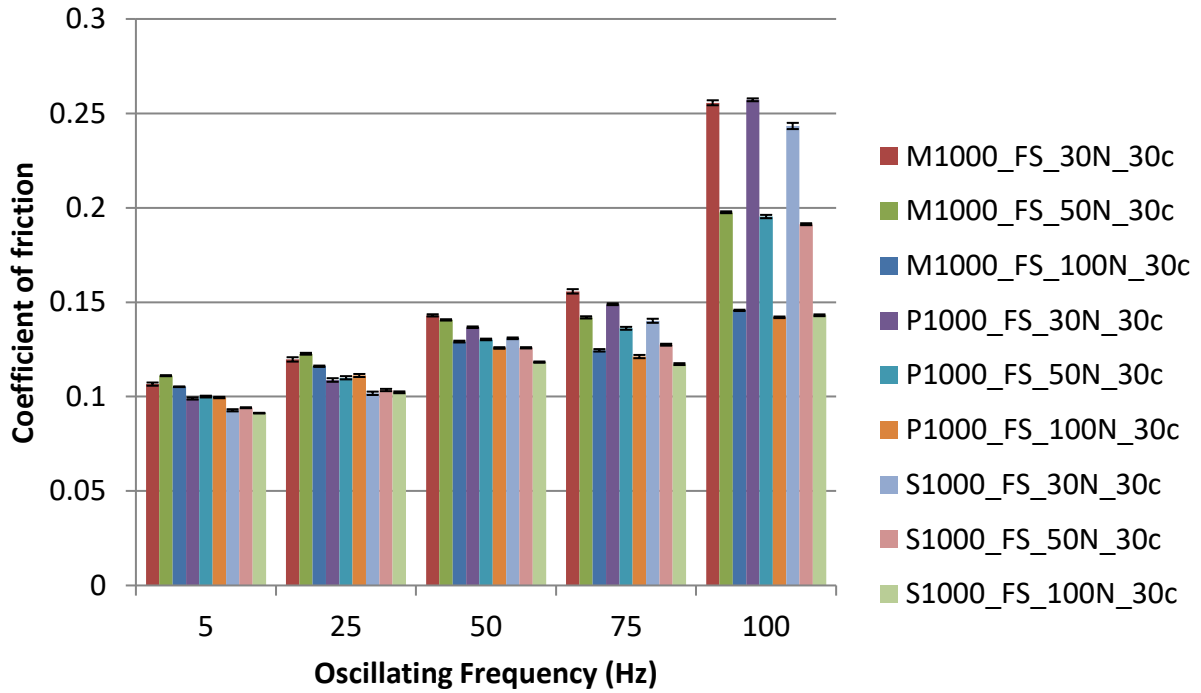
Figure 5-33: Average coefficient of friction for runs with 1000 ppm additive concentrations at different oscillating frequency steps.

The wear measurements measured on the microscope, Figure 5-34 to Figure 5-36, give very interesting results. The wear tracks results at 100 N were similar between additives, indicating that under some conditions different additives will give the same performance even if the coefficient of friction differs. At 50 N myristic acid (C-14) did poorly but at 30 N myristic acid gave the best protection.
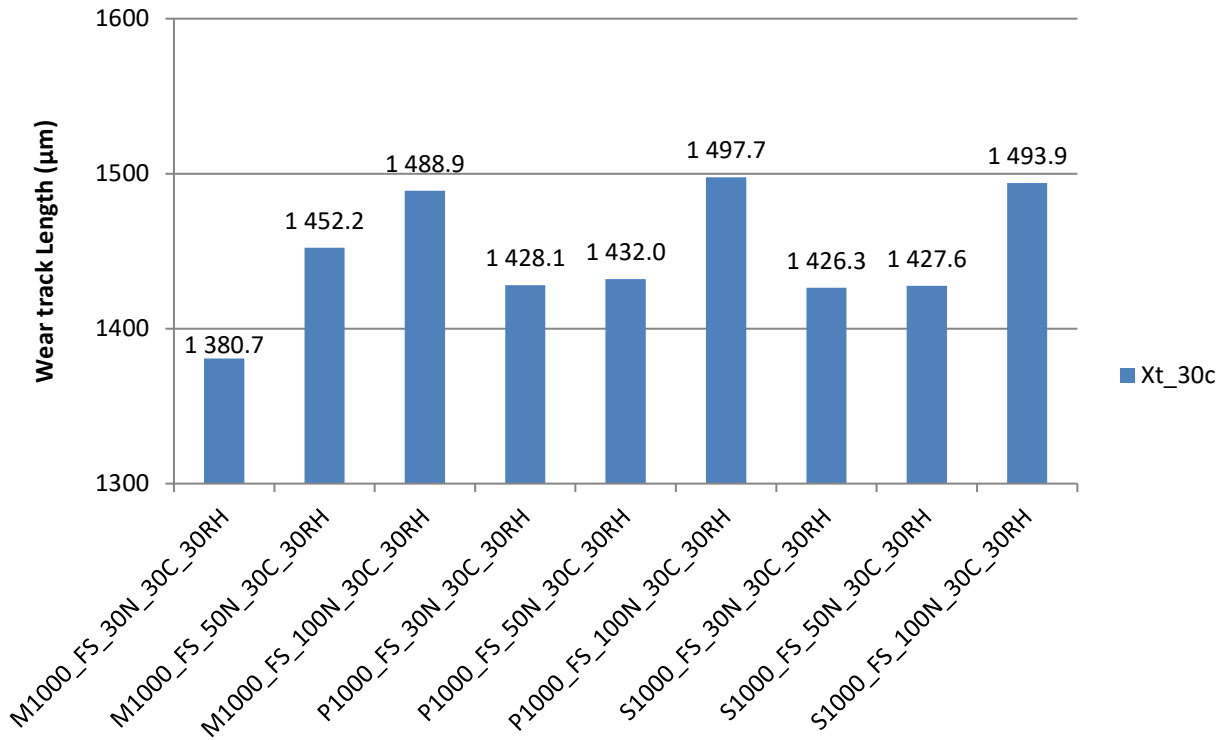
Figure 5-34: Average wear measurement of the wear track for runs with 1000 ppm additive concentrations.

What also becomes very clear is the difference in x and y-direction wear scar sizes. As the conditions become harsher the x-direction measurement becomes larger than the Y measurement. The wear scar size is also generally bigger than the wear track y-direction size.
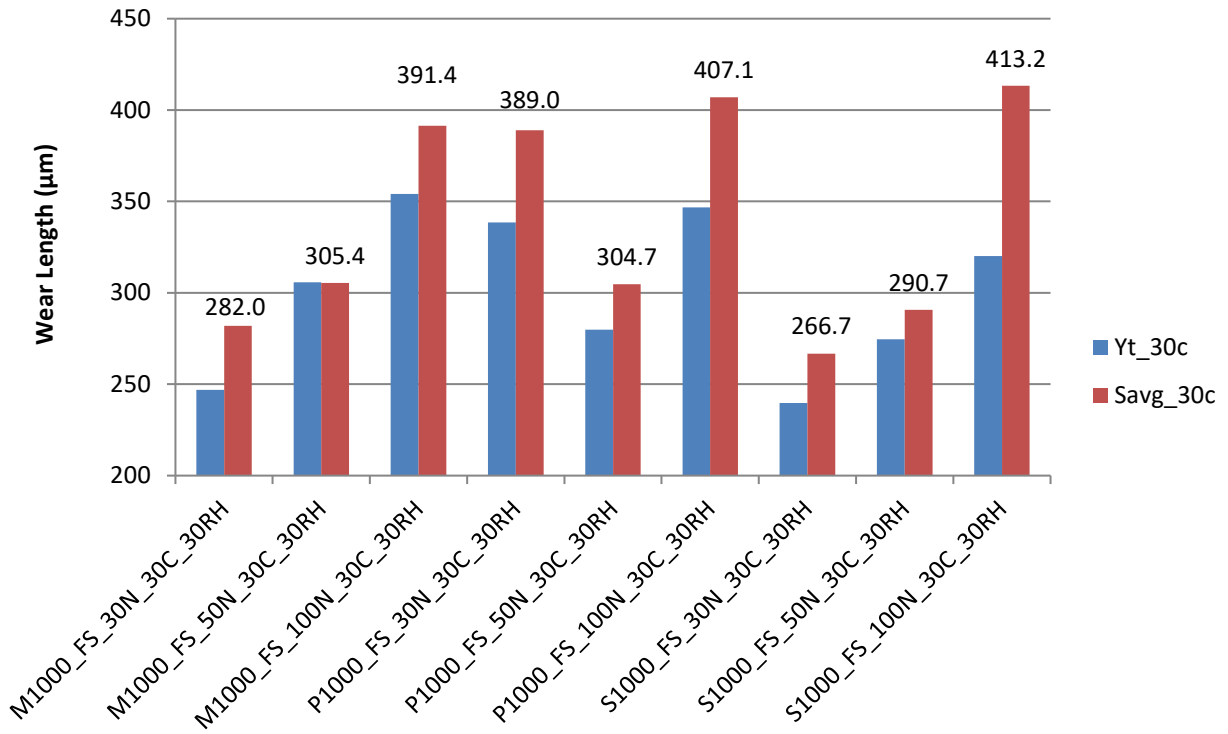
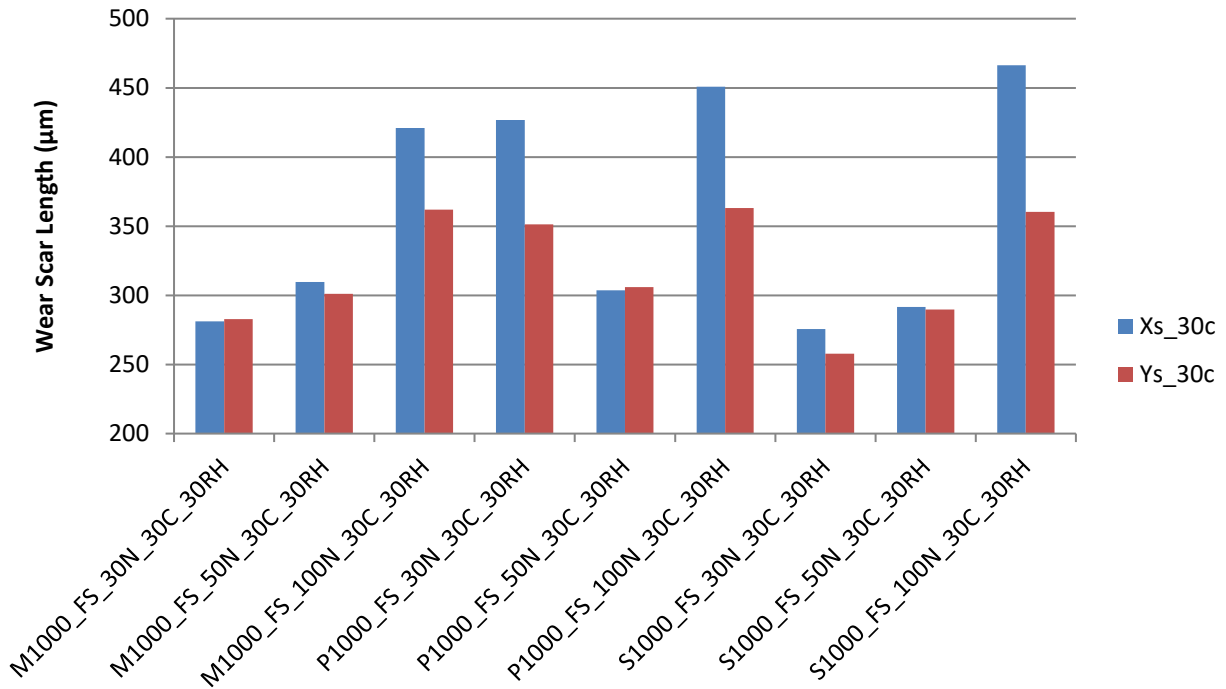Figure 5-35: Average wear measurement runs with 1000 ppm additive concentrations.

Figure 5-36: Average wear measurement of wear scars for runs with 1000 ppm additive concentrations

Table 5-7 and Table 5-9 shows how surface protection is increased with higher additive concentrations. The colour of the wear scars is lighter and there is no indication of slipping.

Table 5-7: Microscope images for M1000 and P1000.
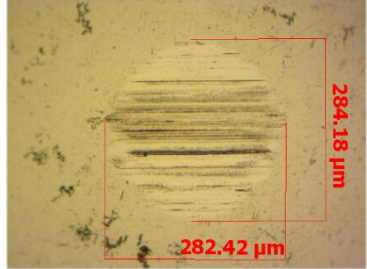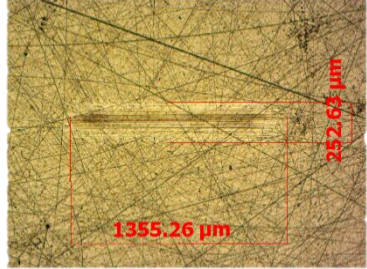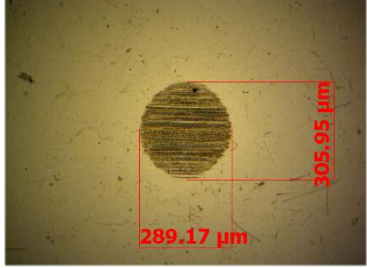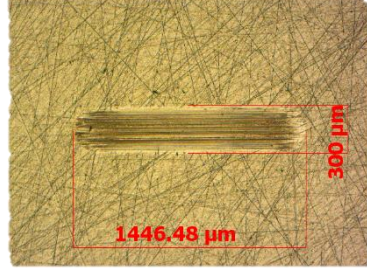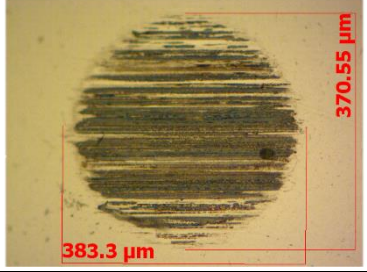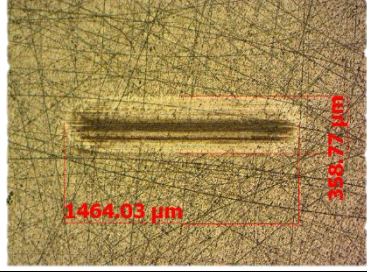
Test ID	Scar	Track
M1000_30N 10x magnification on scar	284.18 µm 282.42 µm	252.63 µm 1355.26 µm
M1000_50N 5x magnification on scar	305.95 µm 289.17 µm	300 µm 1446.48 µm
M1000_100N 10x magnification on scar	370.55 µm 383.3 µm	368.77 µm 1464.03 µm

Table 5-8: Microscope images for S1000.
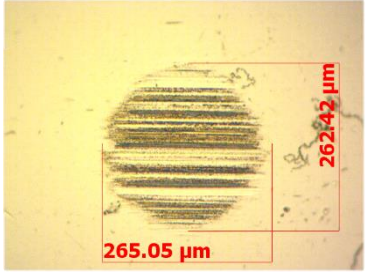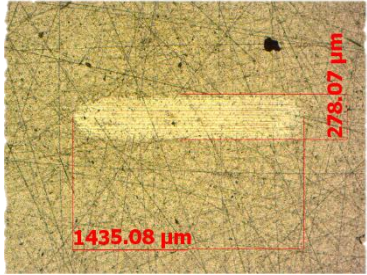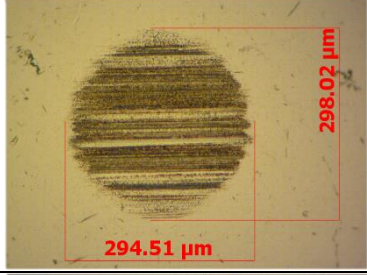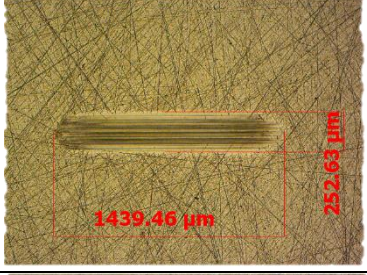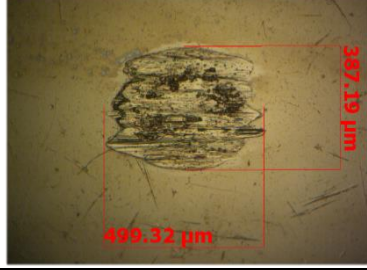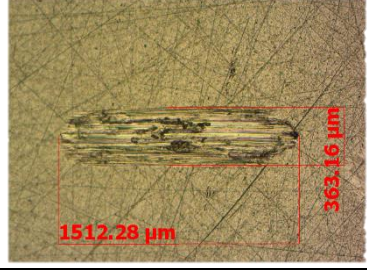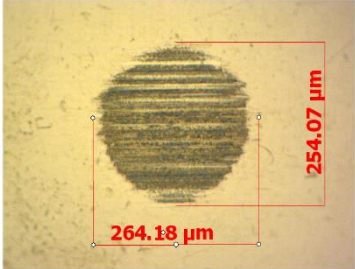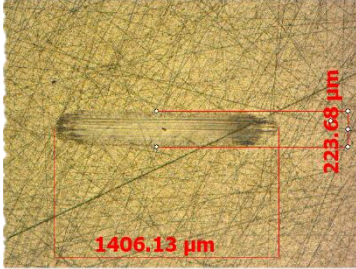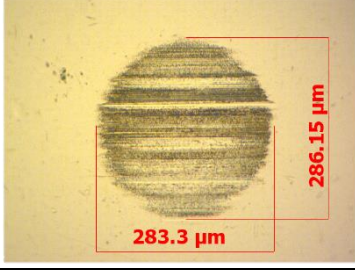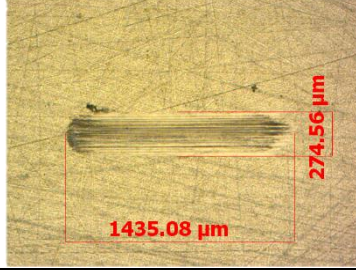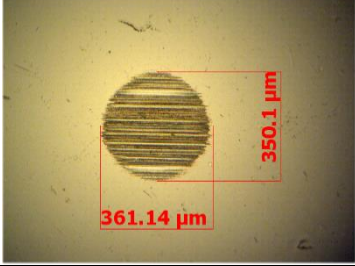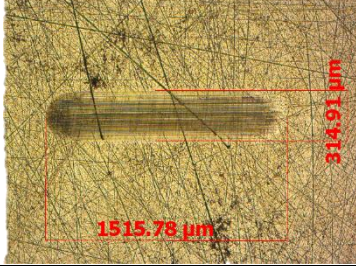
Test ID	Scar	Track
P1000_30N 10x magnification on scar	 262.42 µm 265.05 µm	 278.07 µm 1435.08 µm
P1000_50N 10x magnification on scar	 298.02 µm 294.51 µm	 252.63 µm 1439.46 µm
P1000_100N 5x magnification on scar	 387.19 µm 499.32 µm	 363.16 µm 1512.28 µm

Table 5-9: Microscope images for S1000.

Test ID	Scar	Track
S1000_30N 10x magnification on scar	254.07 µm 264.18 µm	223.68 µm 1406.13 µm
S1000_50N 10x magnification on scar	286.15 µm 283.3 µm	274.56 µm 1435.08 µm
S1000_100N 5x magnification on scar	350.1 µm 361.14 µm	314.91 µm 1515.78 µm

Load comparison

The disadvantage of comparing runs with the same additive concentrations is that all the runs showed were not completed under the same conditions. Comparing results based on the load has the advantage of ensuring that all the runs experienced similar wear conditions, making it easier to distinguish which additive showed the best performance.

a) 30 N

For runs at 30 N, Figure 5-37, S1000 gave the lowest coefficient of friction. For other concentrations, stearic acid (C-18) had the lowest or similar coefficient of friction compared to palmitic acid (C-16) with myristic acid (C-14) consistently achieving the highest coefficient of friction.
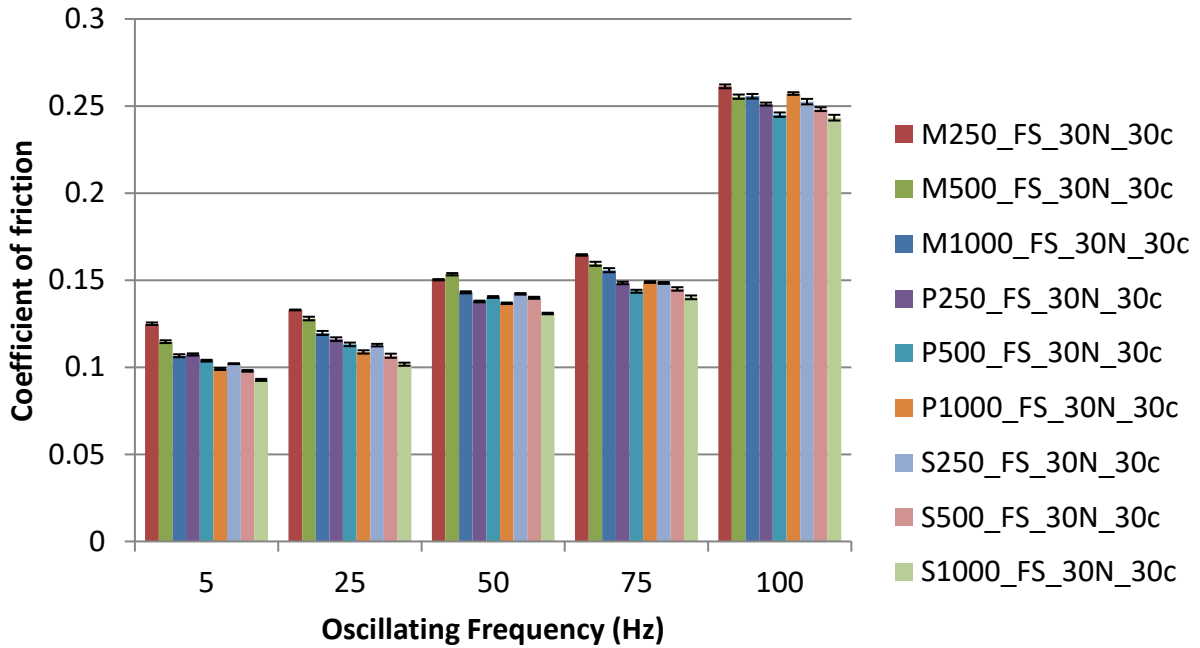
Figure 5-37: Average coefficient of friction for runs at 30 N.

Looking at the wear results obtained from an optical microscope, Figure 5-38 – Figure 5-39 give a completely different image to what additive performs best. For wear tracks, palmitic acid (C-16) gave the best protection at lower additive concentrations while myristic acid (C-14) gave the best performance for high additive concentration. This behaviour is likely due to chemical reactivity. On the ball specimens, there is practically no difference between most of the wear measurements, apart from P1000.

Figure 5-38: Wear results for runs at 30 N. Xt-track in direction of motion measurement.
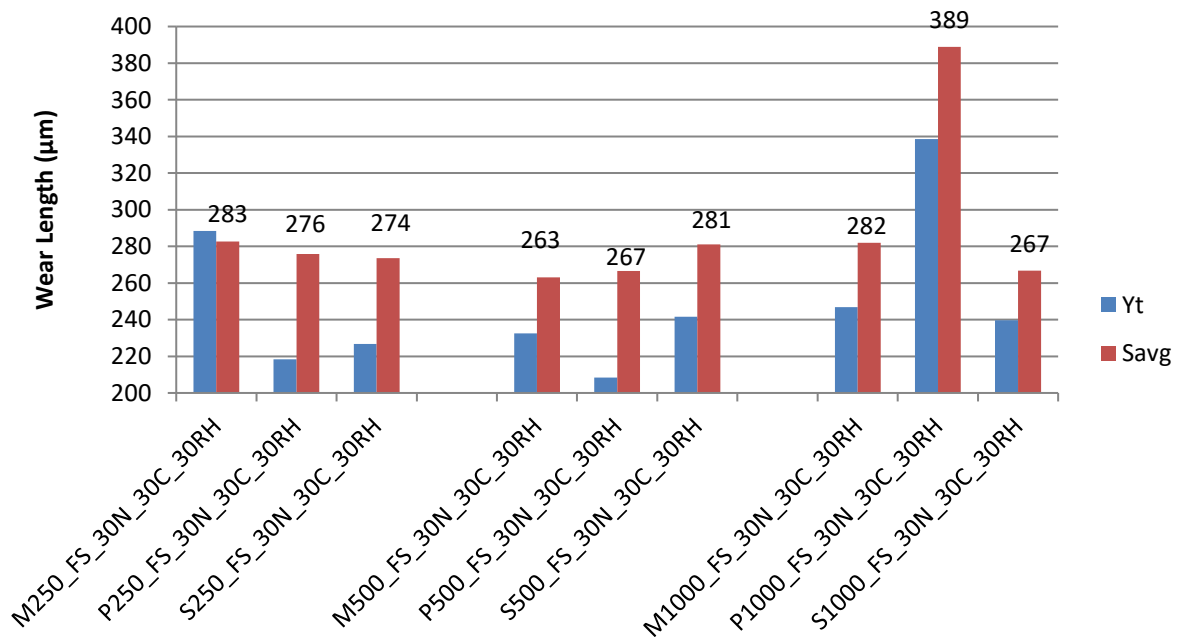
Figure 5-39: Wear results for runs at 30 N. Yt-track parallel to the direction of motion measurement, Savg- WSD.

b) 50 N

Increasing the load to 50 N, Figure 5-40, showed very similar behaviour to the 30 N run. Generally, myristic acid (C-14) had the highest coefficient of friction followed by palmitic and then stearic acid (C-18). Palmitic (C-16) and stearic acid (C-18) showed an increased coefficient of friction at higher oscillating frequency with increased load.
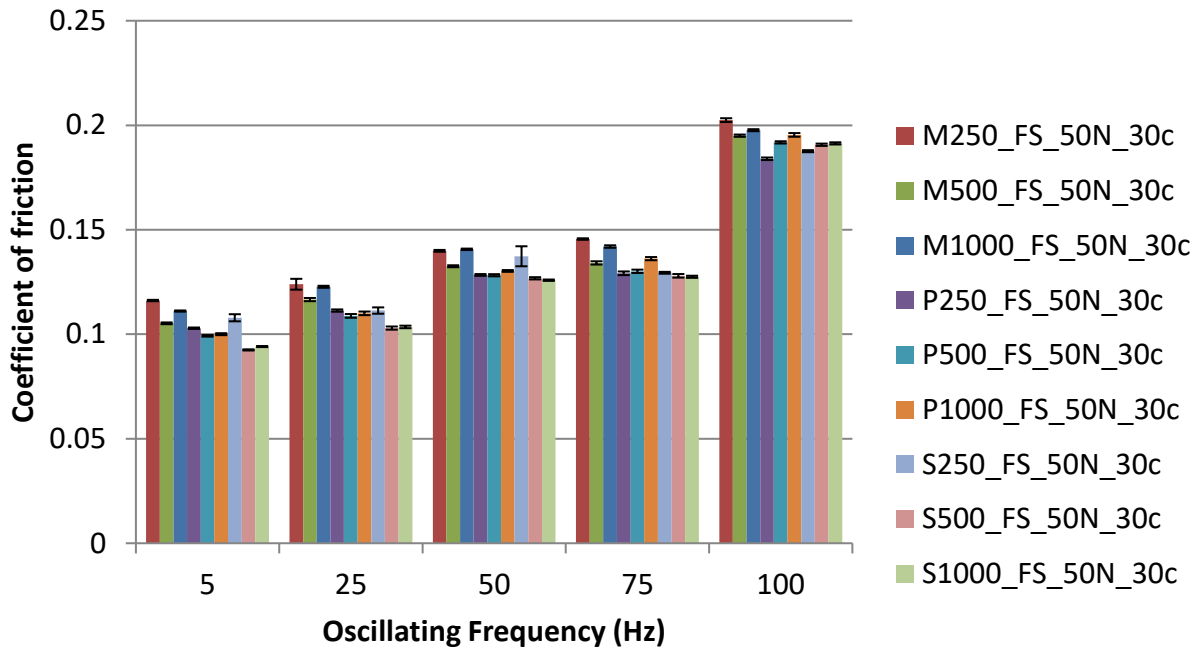
Figure 5-40: Average coefficient of friction for runs at 50 N.

Looking at the wear information on Figure 5-41 and Figure 5-42 the wear scars are of similar size again. The wear tracks show no clear trends.
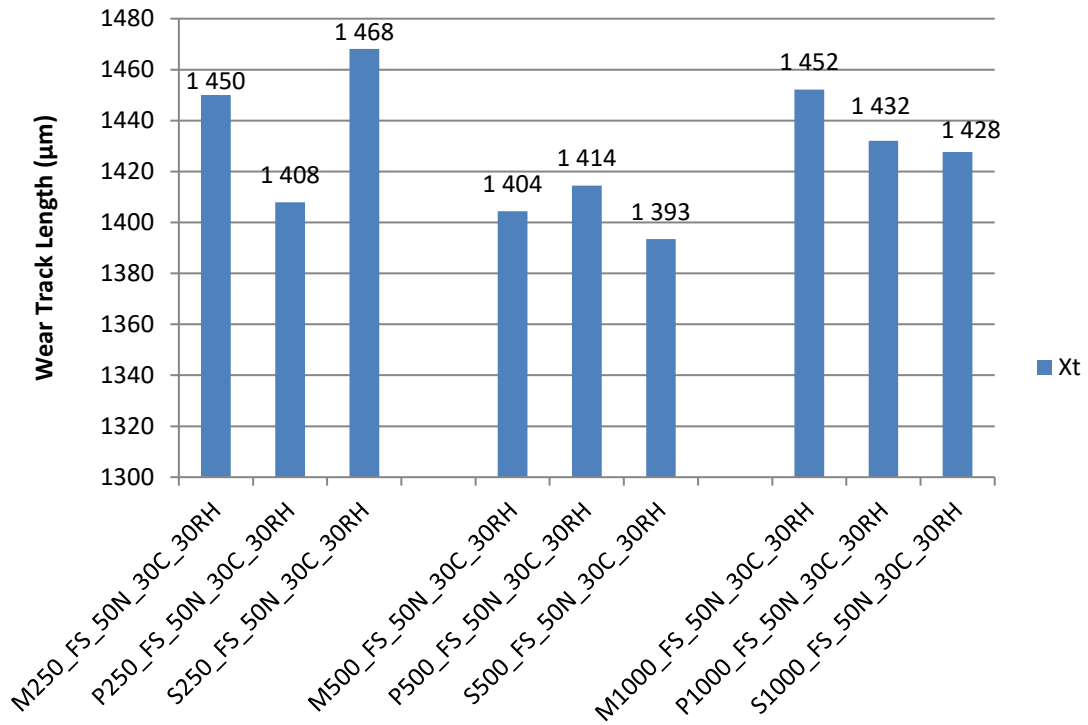
Figure 5-41: Microscope wear results for runs at 50 N. Xt-track in direction of motion measurement.
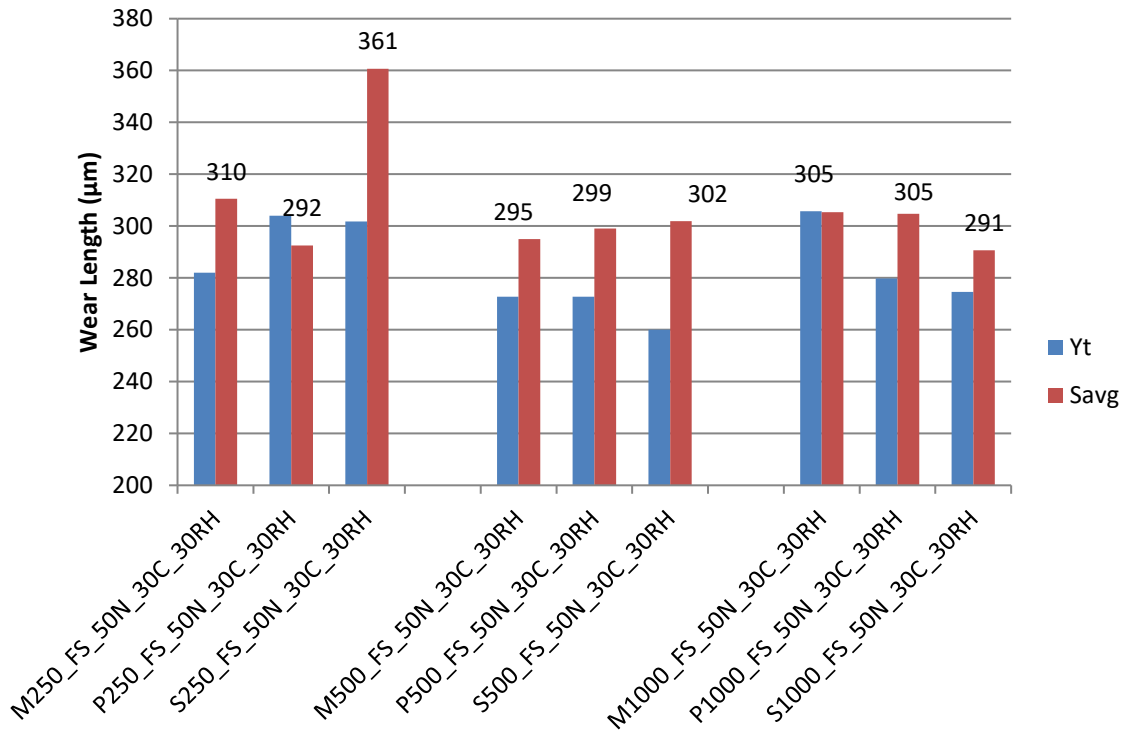
Figure 5-42: Microscope wear results for runs at 50 N. Yt-track parallel to the direction of motion measurement, Savg- WSD.

c) 100 N

For 100 N with low additive concentration stearic acid (C-18) performed poorly based on the coefficient of friction even after having a very high coefficient of friction during the run-in time. S250 did however complete the runs as mentioned previously in 5.1.7, likely due to the high coefficient of friction at the start of the test.

The wear results in Figure 5-44 and Figure 5-45 show that the protection given by the additives at high loads are very similar even if the coefficient of friction differ significantly during the tests.

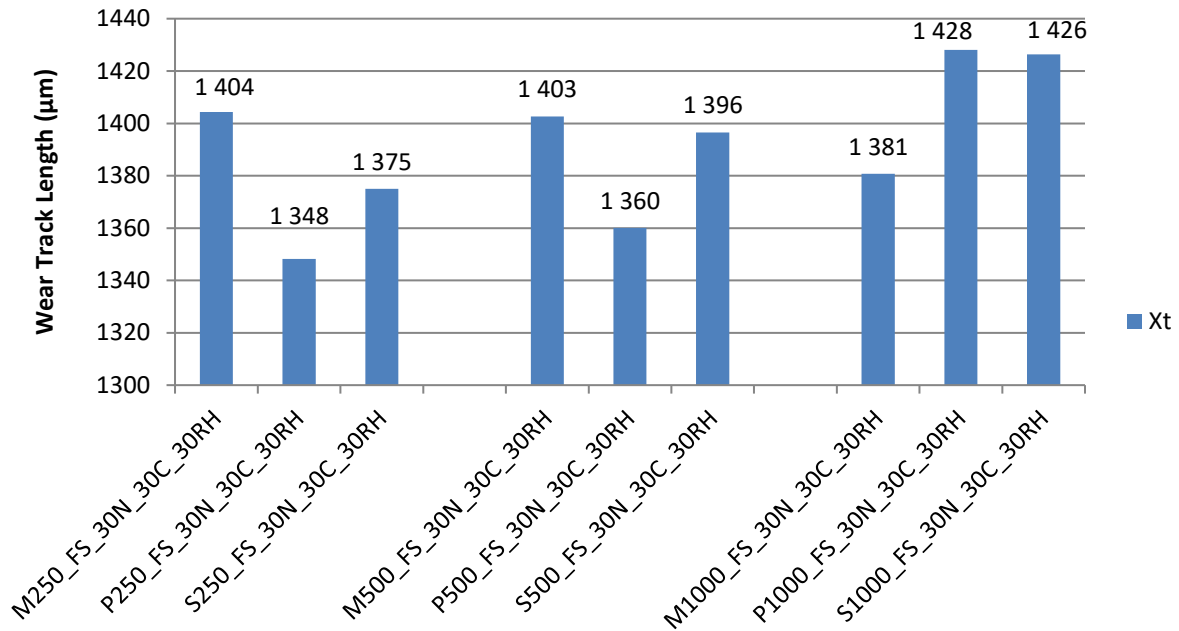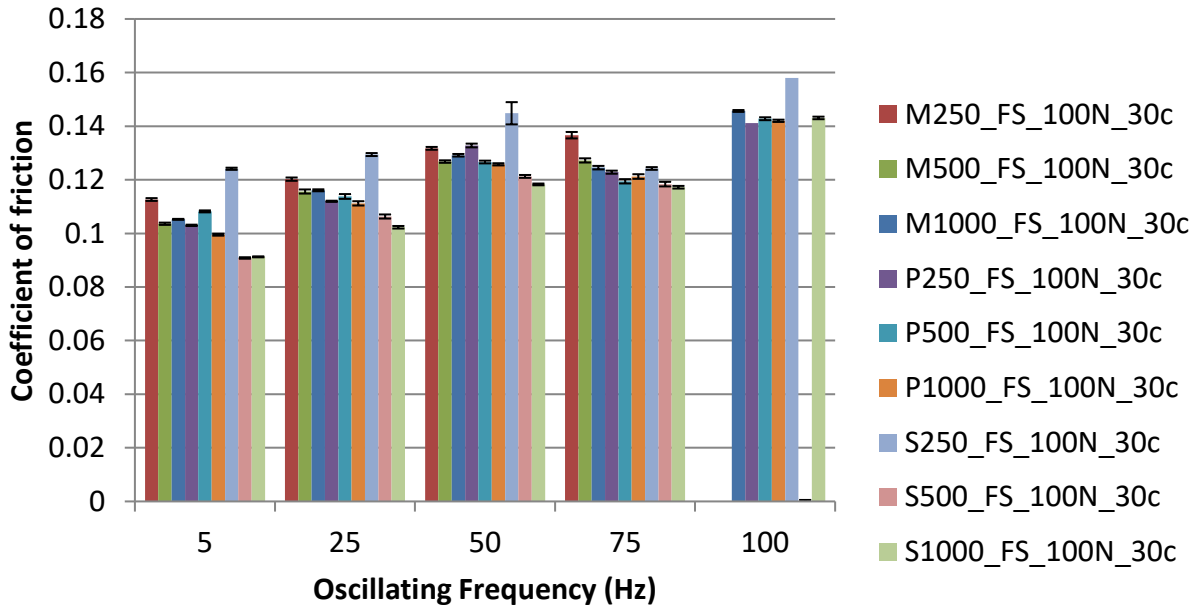Figure 5-43: Average coefficient of friction for runs at 100 N.
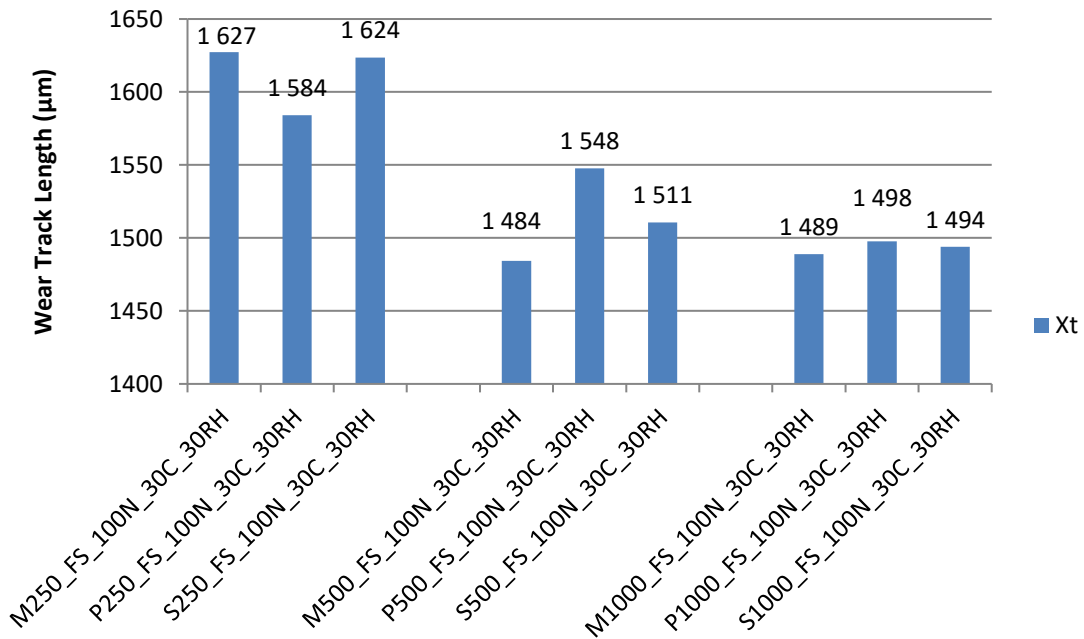
Figure 5-44: Wear results for runs at 100 N. Xt-track in direction of motion measurement.
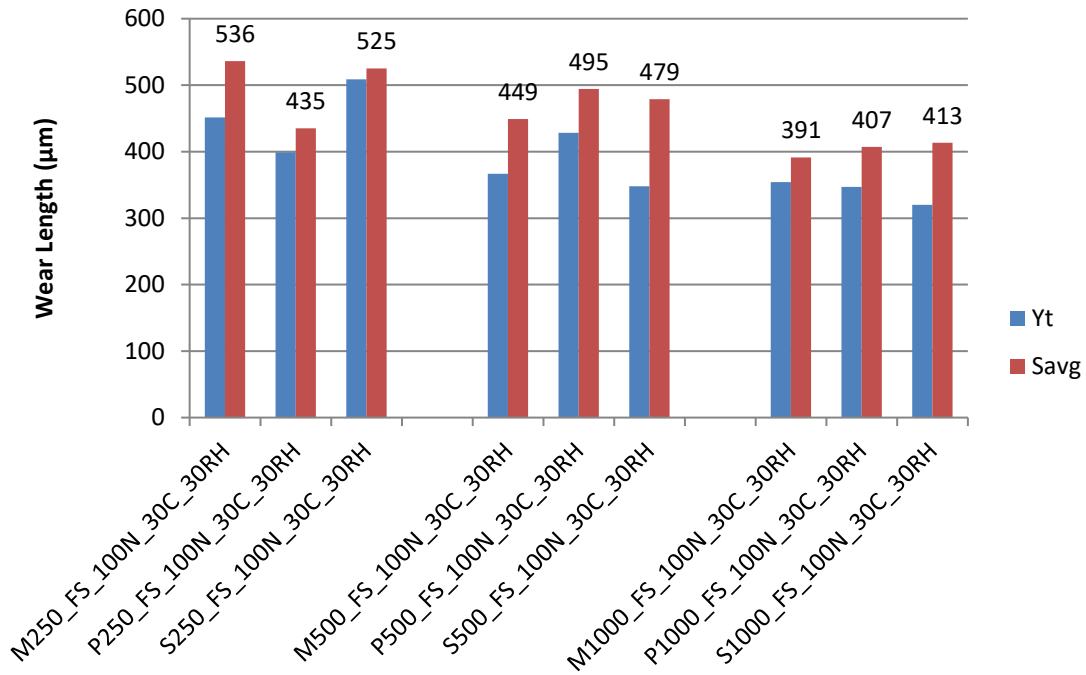
Figure 5-45: Wear results for runs at 100 N. Yt-track parallel to the direction of motion measurement, Savg- WSD.

5.1.11.   Wear profiles from the profilometer.

Wear on the disk

To further investigate the performance of the different additives the Nanovea profilometer data were combined to give Figure 5-46. As the load is increased the wear observed is increased as seen in the microscope results. The effect of adding more additive is also shown with the reduction in wear volume as more additive is added.
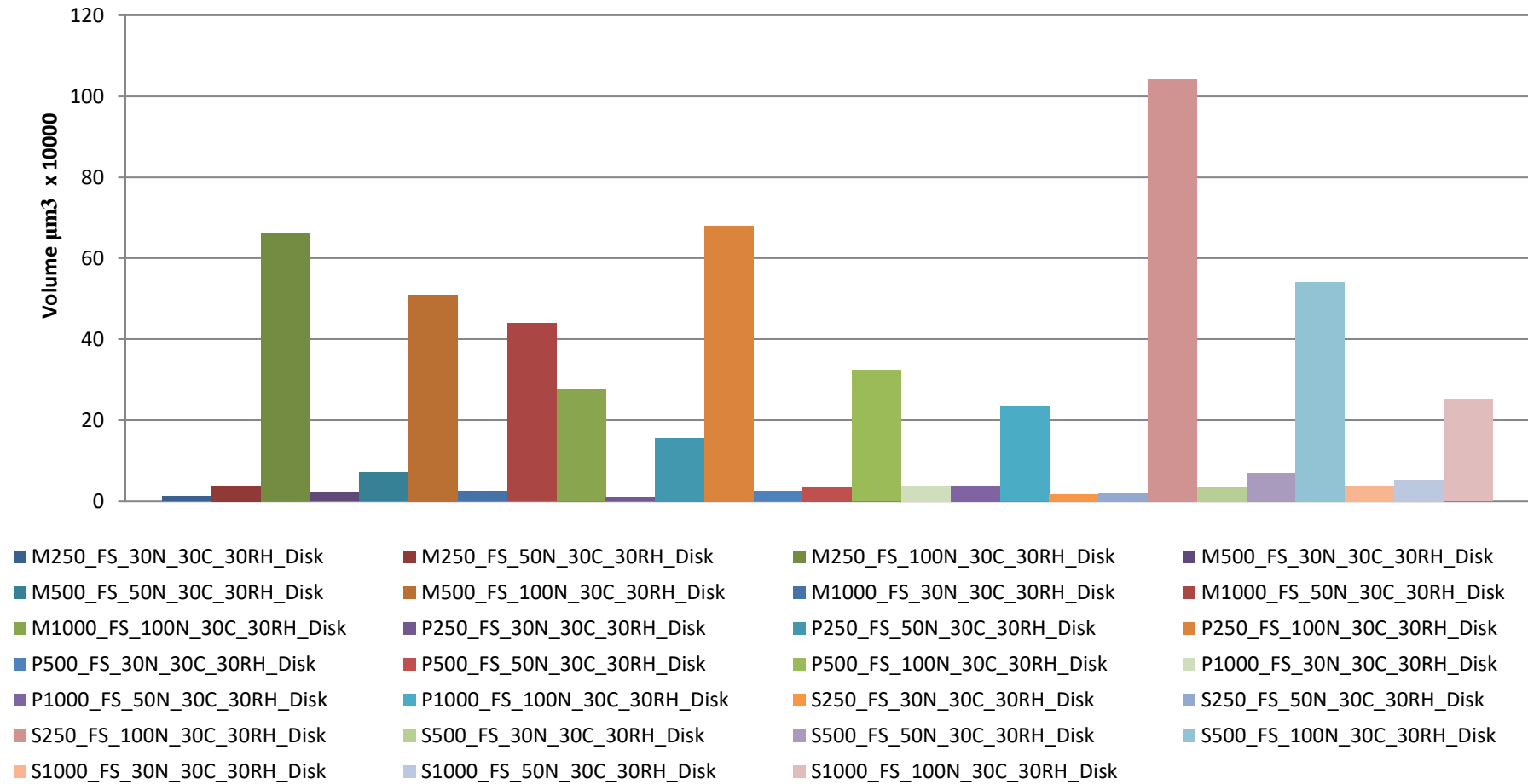
Figure 5-46: Profilometer wear data of disk scans for FS tests at 30 °C and 1 mm stroke.

Legend:
- M250_FS_30N_30C_30RH_Disk
- M250_FS_50N_30C_30RH_Disk
- M250_FS_100N_30C_30RH_Disk
- M500_FS_30N_30C_30RH_Disk
- M500_FS_50N_30C_30RH_Disk
- M500_FS_100N_30C_30RH_Disk
- M1000_FS_30N_30C_30RH_Disk
- M1000_FS_50N_30C_30RH_Disk
- M1000_FS_100N_30C_30RH_Disk
- P250_FS_30N_30C_30RH_Disk
- P250_FS_50N_30C_30RH_Disk
- P250_FS_100N_30C_30RH_Disk
- P500_FS_30N_30C_30RH_Disk
- P500_FS_50N_30C_30RH_Disk
- P500_FS_100N_30C_30RH_Disk
- P1000_FS_30N_30C_30RH_Disk
- P1000_FS_50N_30C_30RH_Disk
- P1000_FS_100N_30C_30RH_Disk
- S250_FS_30N_30C_30RH_Disk
- S250_FS_50N_30C_30RH_Disk
- S250_FS_100N_30C_30RH_Disk
- S500_FS_30N_30C_30RH_Disk
- S500_FS_50N_30C_30RH_Disk
- S500_FS_100N_30C_30RH_Disk
- S1000_FS_30N_30C_30RH_Disk
- S1000_FS_50N_30C_30RH_Disk
- S1000_FS_100N_30C_30RH_Disk

To see things more clearly, the data were separated based on the applied load to give Figure 5-47 to Figure 5-49. As the additive concentration is increased it is expected that the wear volume will decrease. At 30 N, Figure 33, the opposite is observed. An explanation for this is that at 30 N the test runs in the hydrodynamic lubrication regime where minimal or no wear is observed. The increase in wear as the concentration is increased can be attributed to chemical wear as adding more additive will make the lubricant more chemically active. As the concentration of additive is increased the higher activity of the lubricant increases the corrosive wear that takes place. Looking at the relative size of the wear that took place on Figure 5-46 shows that there is a difference in the wear volume that it is still very small compared to runs at higher loads where more severe wear was observed.

With an increase to 50 N, Figure 5-48, the advantages of adding more additive starts to show with palmitic and stearic acid (C-18) but, myristic acid (C-14) is still not showing the expected trend. With the increase in load to a 100 N, the expected trend is seen with increasing amounts of additive decreasing the wear observed, as shown in Figure 5-49.

Figure 5-47: Profilometer wear data of disk scans for FS tests at 30 N, 30 °C and 1 mm stroke.

Figure 5-48: Profilometer wear data of disk scans for FS tests at 50 N, 30 °C and 1 mm stroke.
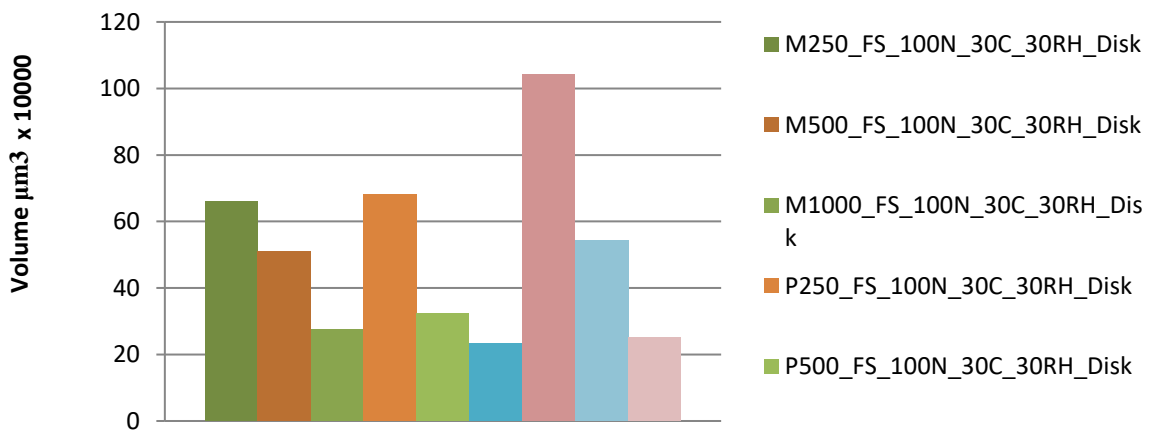
Figure 5-49: Profilometer wear data of disk scans for FS tests at 100 N, 30 °C and 1 mm stroke.

Figure 5-49 also shows that myristic acid (C-14) does have the ability to outperform stearic acid (C-18). While the coefficient of friction shows that stearic acid (C-18) had the best performance volumetric wear results shows that myristic acid (C-14) did better. As the additive concentrations are increased the difference between the volumetric wear becomes less.

Looking at Figure 5-50 to Figure 5-52 gives more perspective on the chemical wear seen at 30 N. The relative size of wear volume at 30 N is much smaller compared to the 100 N tests showing a clear change in lubrication regime toward boundary layer regime. From here the effect of adding more additive is also clear. More additive reduces the damage that takes place as long as conditions do not allow for the effect of chemical wear to become dominant.

Figure 5-50: Myristic acid (C-14) profilometer wear data of disk scans for FS tests at 30 °C and 1 mm stroke.

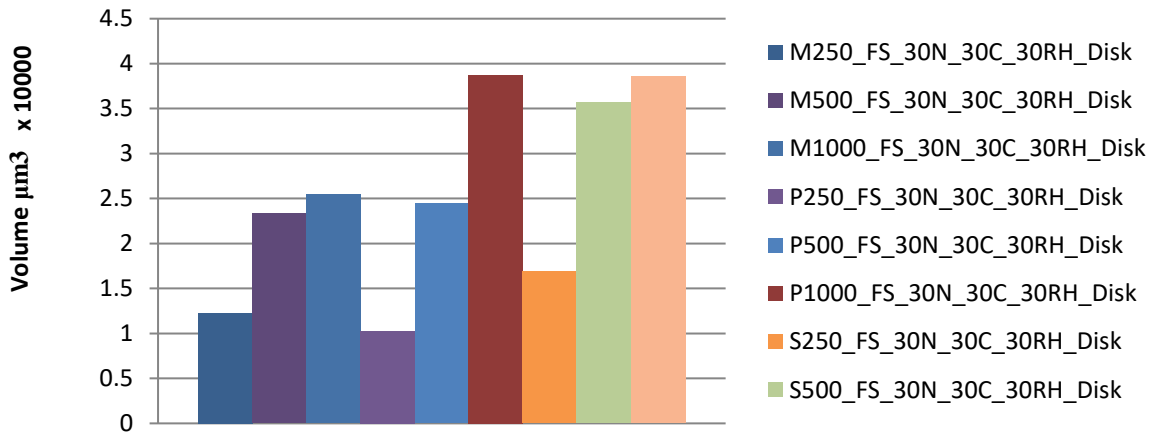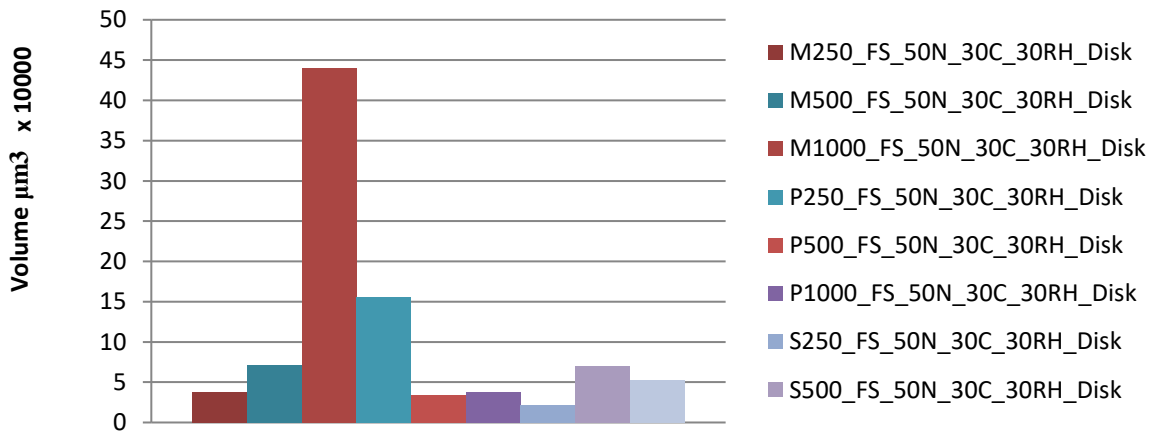Figure 5-51: Palmitic acid (C-16) Profilometer wear data of disk scans for FS tests at 30 °C and 1 mm stroke.

Figure 5-52: Stearic acid (C-18) Profilometer wear data of disk scans for FS tests at 30 °C and 1 mm stroke.

Wear on the ball

To calculate the actual wear volume on the ball from the original data, like the single line of data in Figure 5-53, a sphere, Figure 5-54, with the same radius as the ball specimen is mathematically subtracted from the data. This produced a flat surface and a valley making it easier to calculate the wear volume, Figure 5-55.
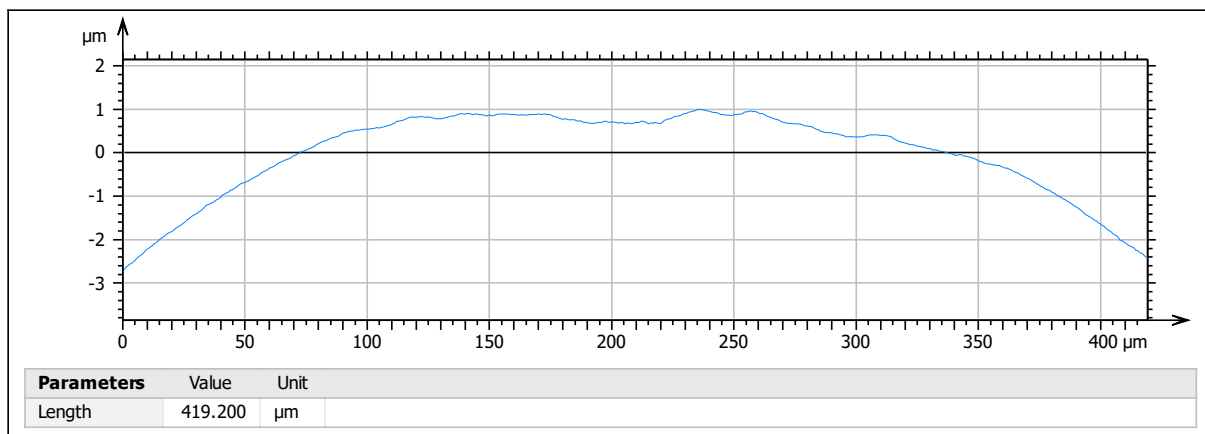
Figure 5-53: A single line of data of the ball profile scan of M1000 at 30 N.
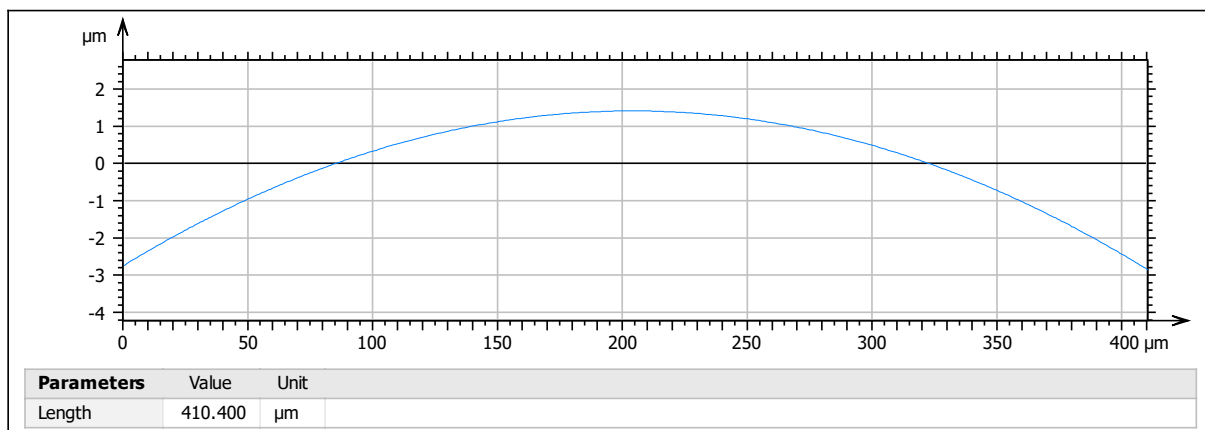
Figure 5-54: A single line of data for the mathematically modelled sphere

Parameters	Value	Unit
Length	392.800	µm
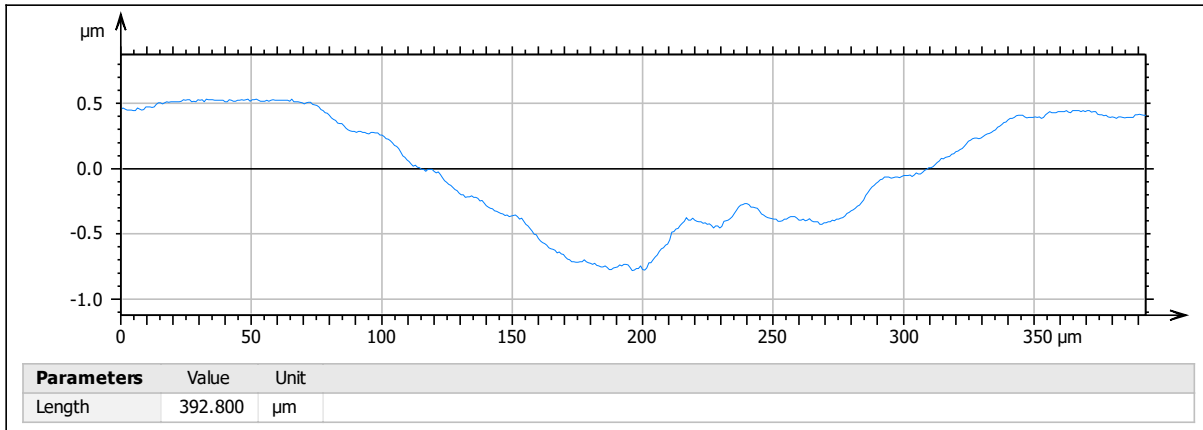
Figure 5-55: A single line of data for the resulting data when the sphere is subtracted from the original data.

All the wear scar data were then used to produce Figure 5-56.
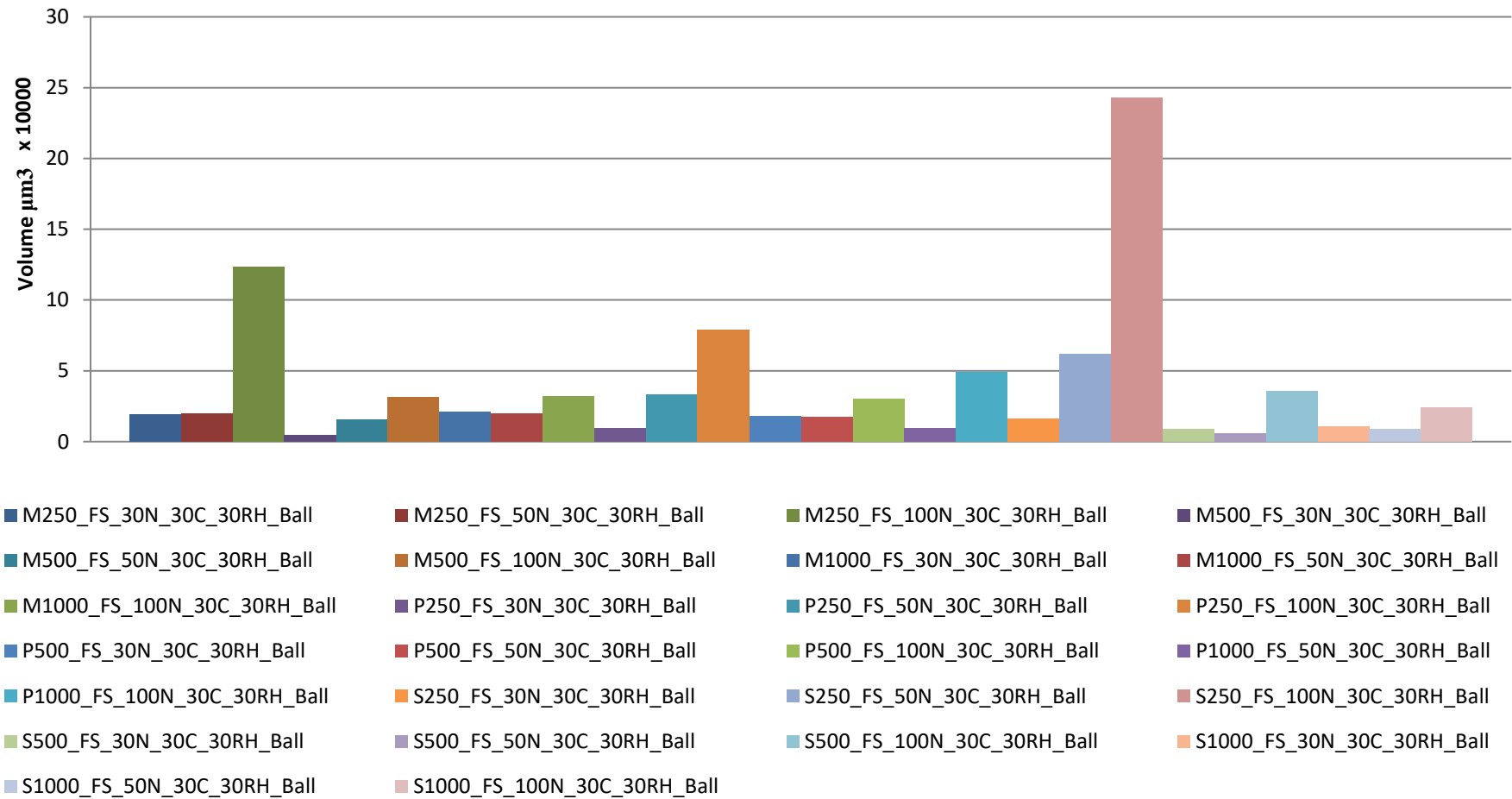
Figure 5-56: Profilometer wear data of ball specimen scans for FS tests at 30 °C and 1 mm stroke

As with the wear track volumes, the wear scar volume is drastically increased as the applied load is increased, shown in Figure 5-57 to Figure 5-59, while higher additive concentrations generally led to reduced wear volume.
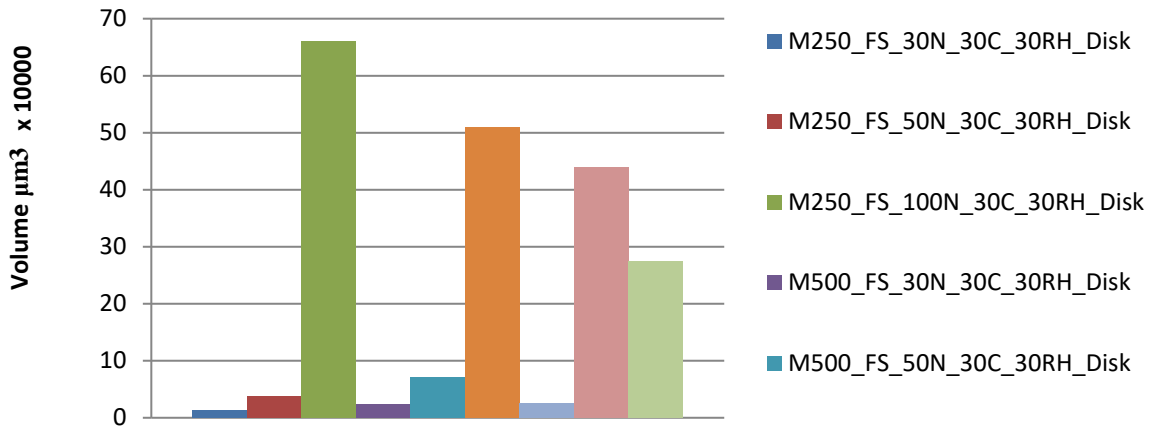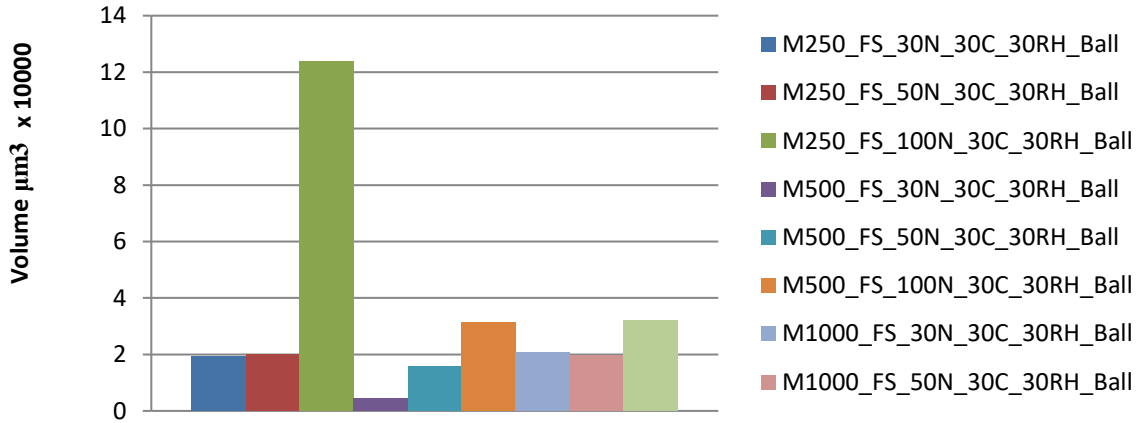
Figure 5-57: Myristic acid (C-14) profilometer wear data of ball specimen scans for FS tests at 30 °C and 1 mm stroke.
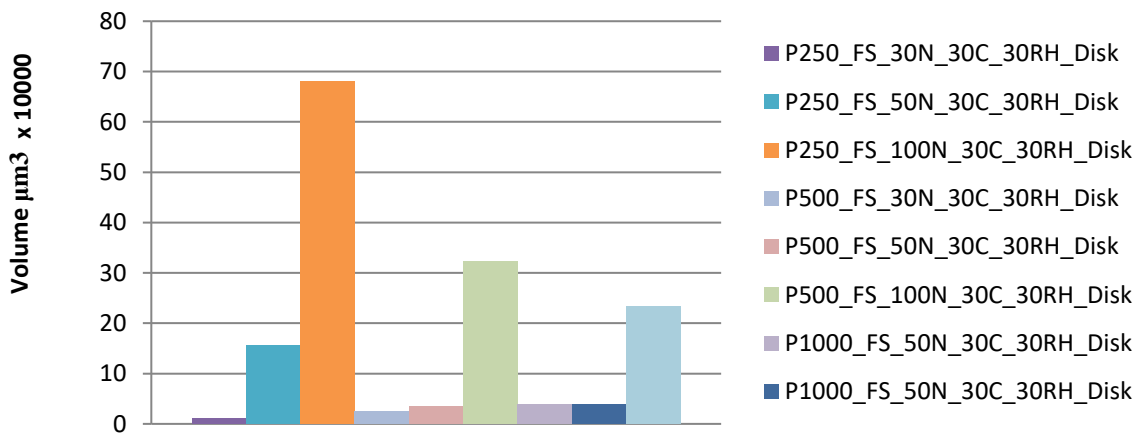

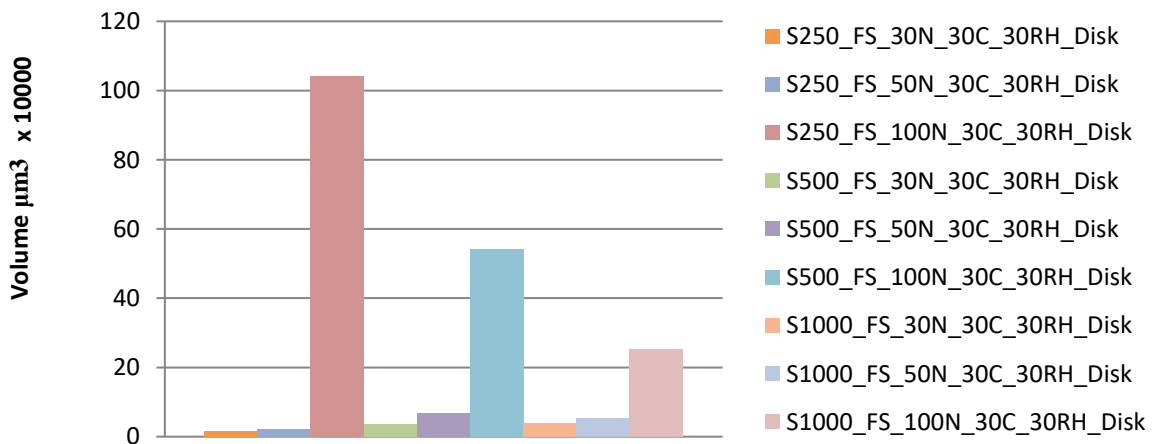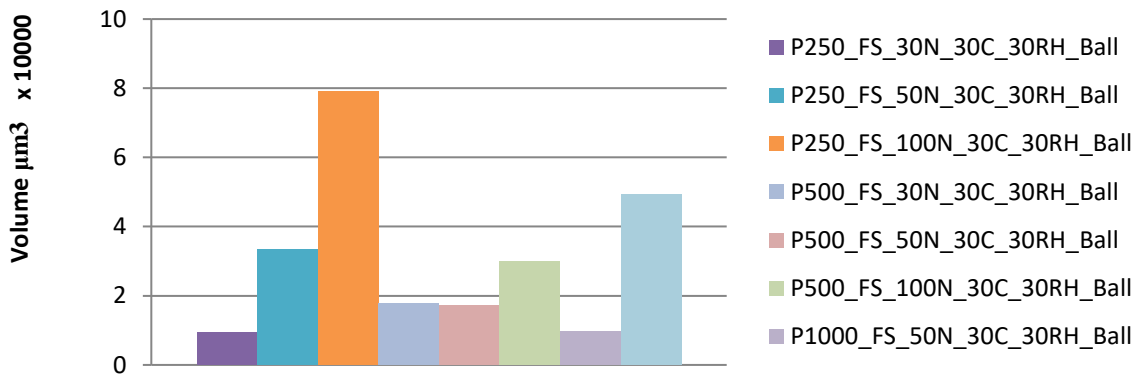Figure 5-58: Palmitic acid (C-16) profilometer wear data of ball specimen scans for FS tests at 30 °C and 1 mm stroke.
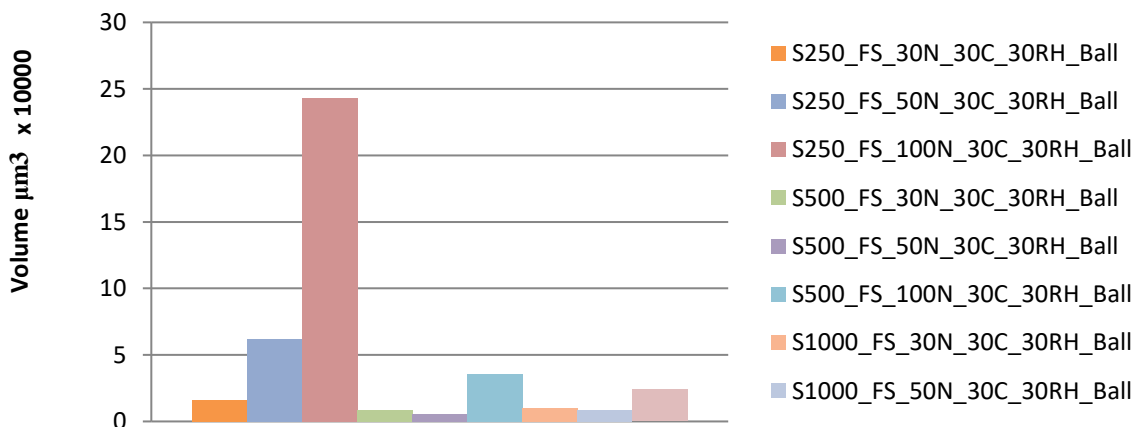
Figure 5-59: Stearic acid (C-18) profilometer wear data of ball specimen scans for FS tests at 30 °C and 1 mm stroke.

Comparing results for low additive concentrations, Figure 5-60, stearic acid (C-18) cannot protect the surface as well as the smaller palmitic C-16) and myristic acid (C-14). As the concentrations are increased stearic acid (C-18) becomes the best performer amongst the 3 additives. Looking at Figure 5-61 to Figure 5-62 we can see how the best performing additive shifts from myristic to stearic acid (C-18) as the concentration is increased.
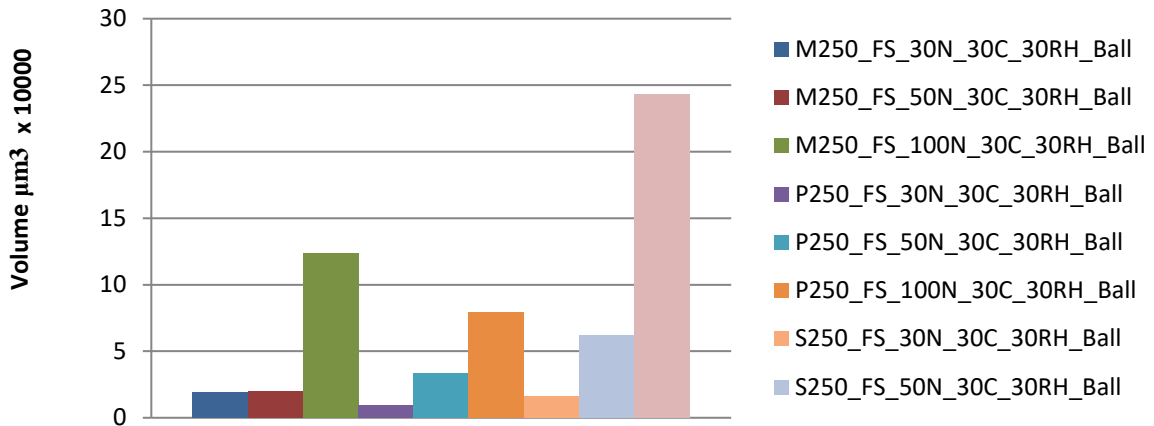
Figure 5-60: Comparing wear volumes for 250 ppm additive concentrations.
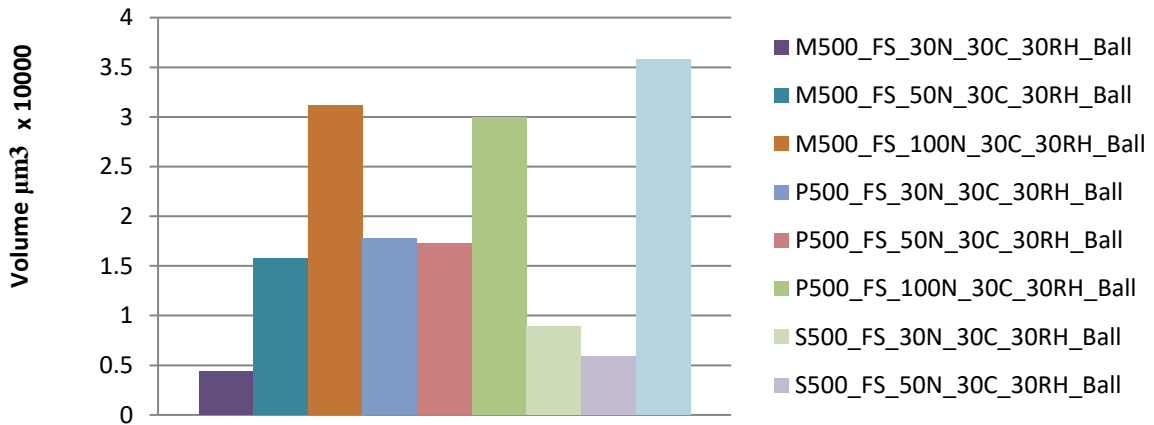
Figure 5-61: Comparing wear volumes for 500 ppm additive concentrations.
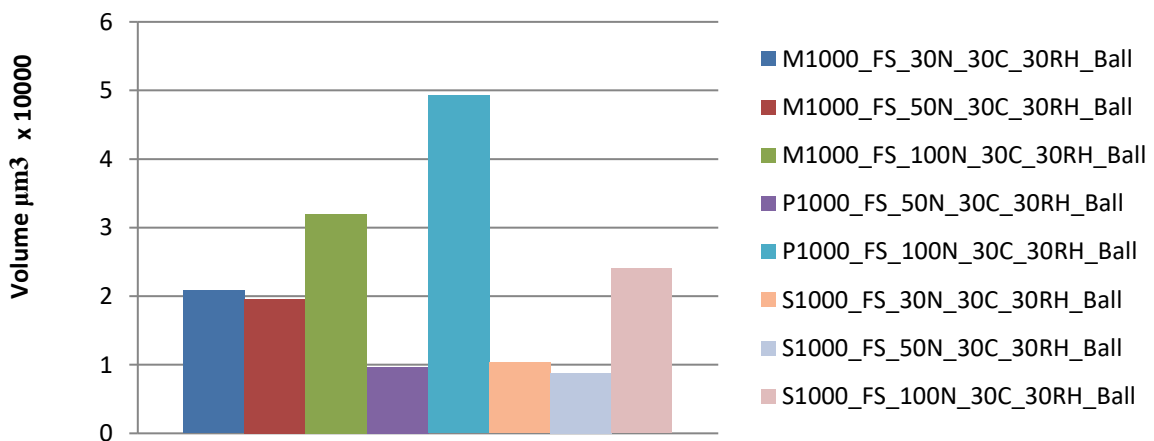
Figure 5-62: Comparing wear volumes for 1000 ppm additive concentrations.

5.2.   Frequency scan tests at 80 °C

To determine how temperature affects the situation the decision was made to do tests at 80 °C. Tests were conducted with 250 and 1000 ppm additive concentration. Looking at Figure 5-63 the coefficient of friction for 80 °C tests are slightly higher compared to runs at 30 °C. This trend persisted with the other additives, oscillating frequencies and loads, as shown in Figure 5-64 – Figure 5-65. Results are given in pairs of 2. The result at 30 °C first followed by the result at 80 °C under the same conditions.
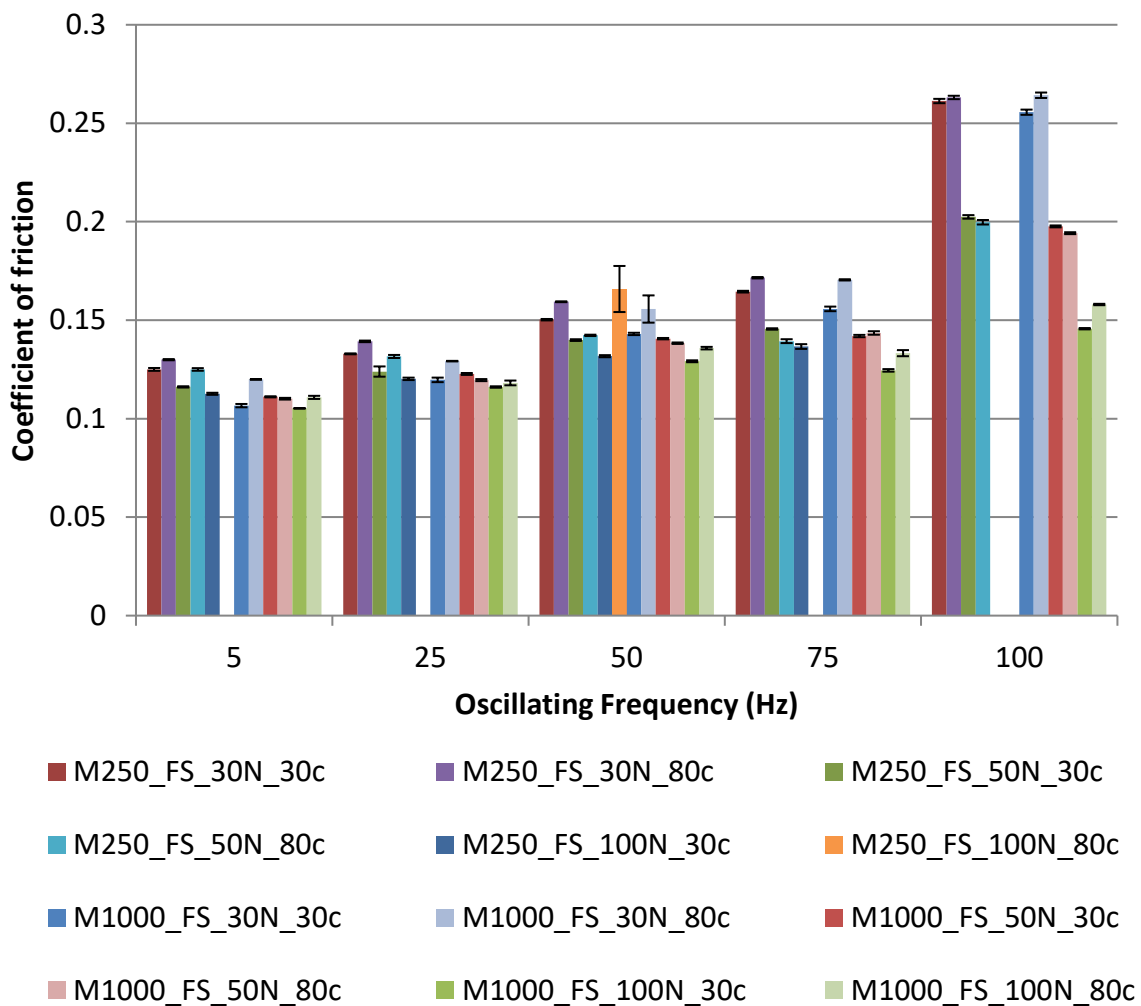
Figure 5-63: Average coefficient of friction results at different frequencies for runs with myristic acid (C-14) at 30 °C and 80 °C.
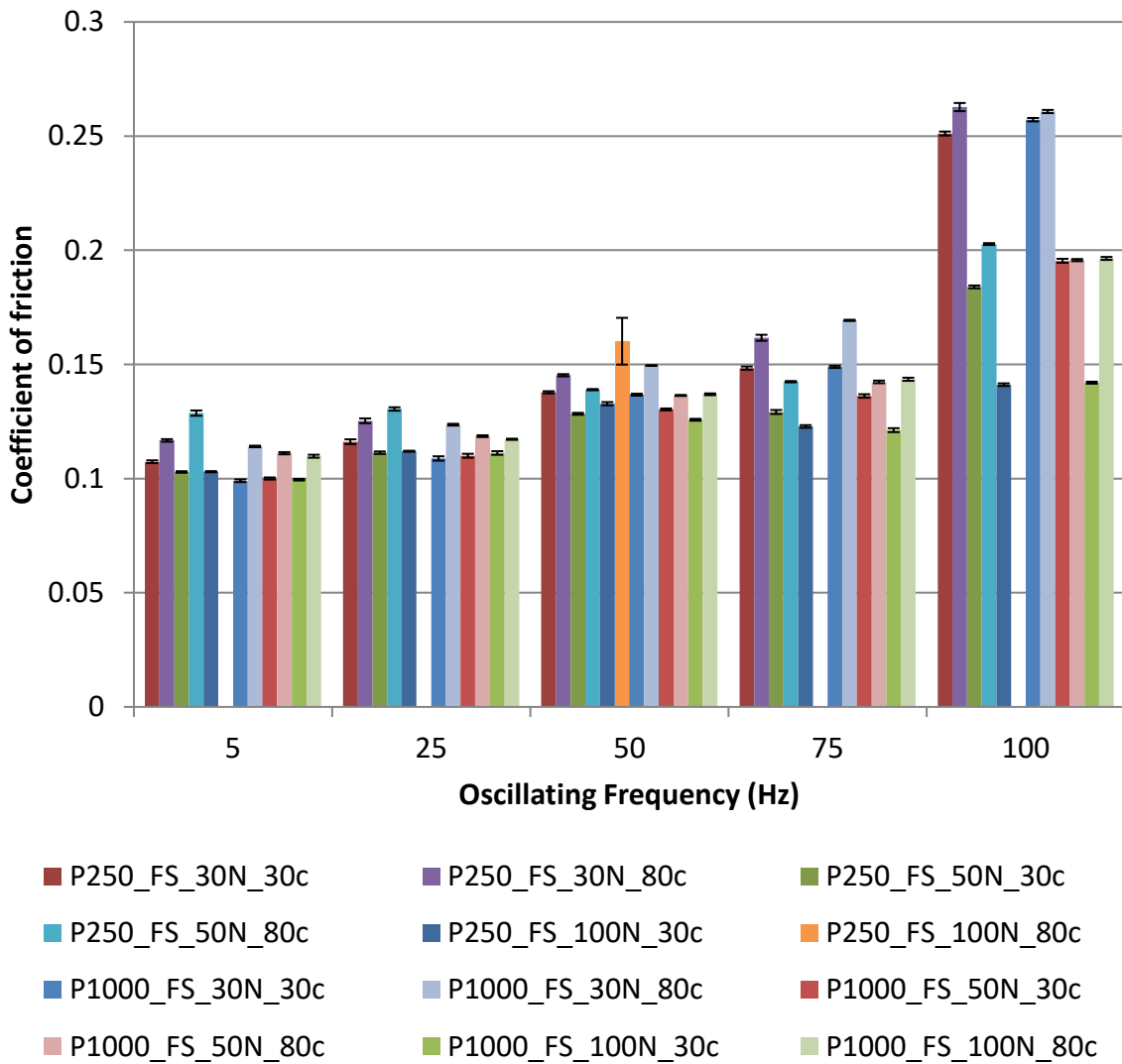
Figure 5-64: Average coefficient of friction results at different frequencies for runs with palmitic acid (C-16) at 30 °C and 80 °C.
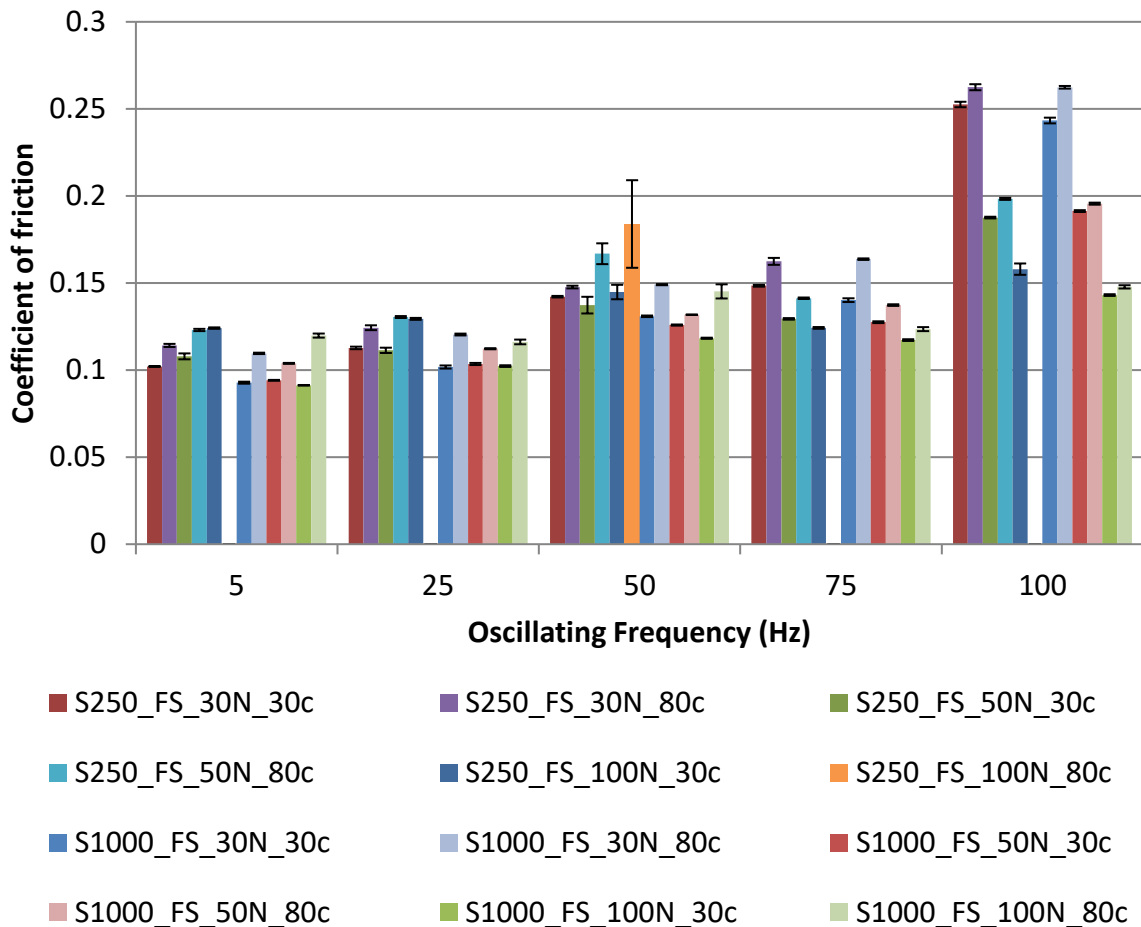
Figure 5-65: Average coefficient of friction results at frequencies frequency for runs with stearic acid (C-18) at 30 °C and 80 °C.

These results correspond with the work of other authors, (Lacey, Gunsel, DeLa Cruz, & Whalen, 2001), (Litzow, Jess, Matzke, Caprotti, & Balfour, 2009).

Temperature reduces viscosity, (Batchelor & Stachowiak, 2003), (Bhushan B. , 2002) implying that testing at higher temperatures causes viscosity to play less of a role in the coefficient of friction and wear. With a decrease in viscosity, there is less hydrodynamic pressure reducing the protective film size between the two surfaces. Machines operating under higher temperature will tend to operate in the boundary lubrication regime.

While the effect that temperature had on the coefficient of friction was relatively small, wear is affected drastically. For the wear scars, Figure 5-66 – Figure 5-68, results are difficult to interpret with the diversity of the wear results produced.
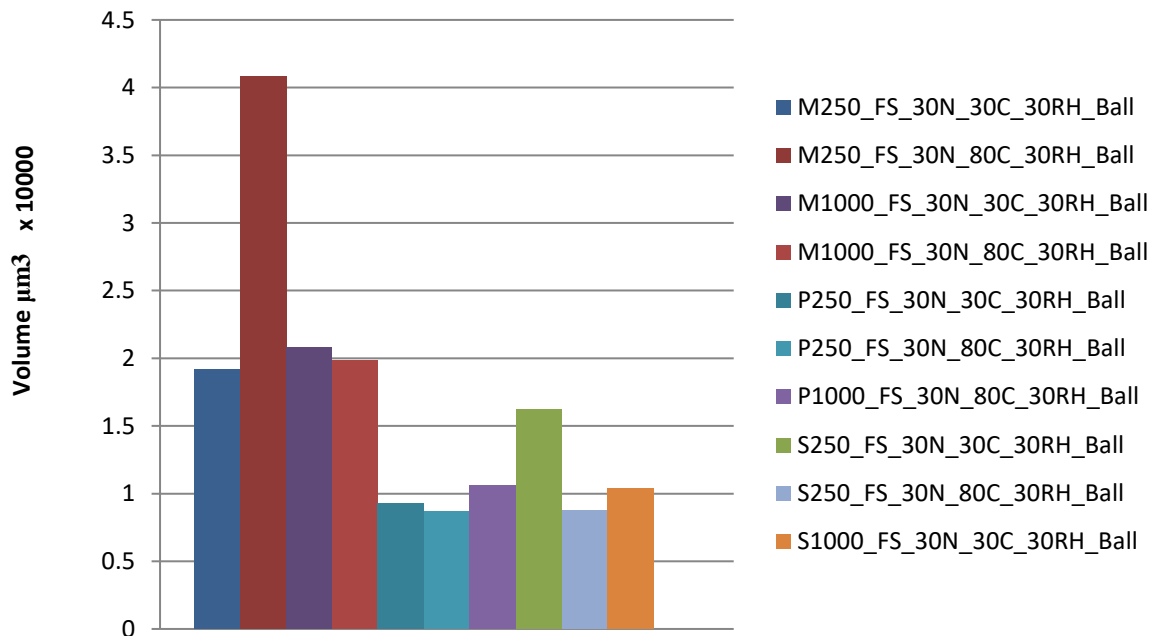
Figure 5-66: Profilometer wear data of ball specimen scans for FS tests at 30 °C and 80 °C tests with a 30 N load.

The runs at 50 N and 100 N, Figure 5-67 - Figure 5-68, all showed a clear trend. The increased temperature increased the volumetric wear that occurred especially at lower additive concentrations. Literature shows the same type of results where increased lubricity reduces the effect of other factors, (Litzow, Jess, Matzke, Caprotti, & Balfour, 2009).
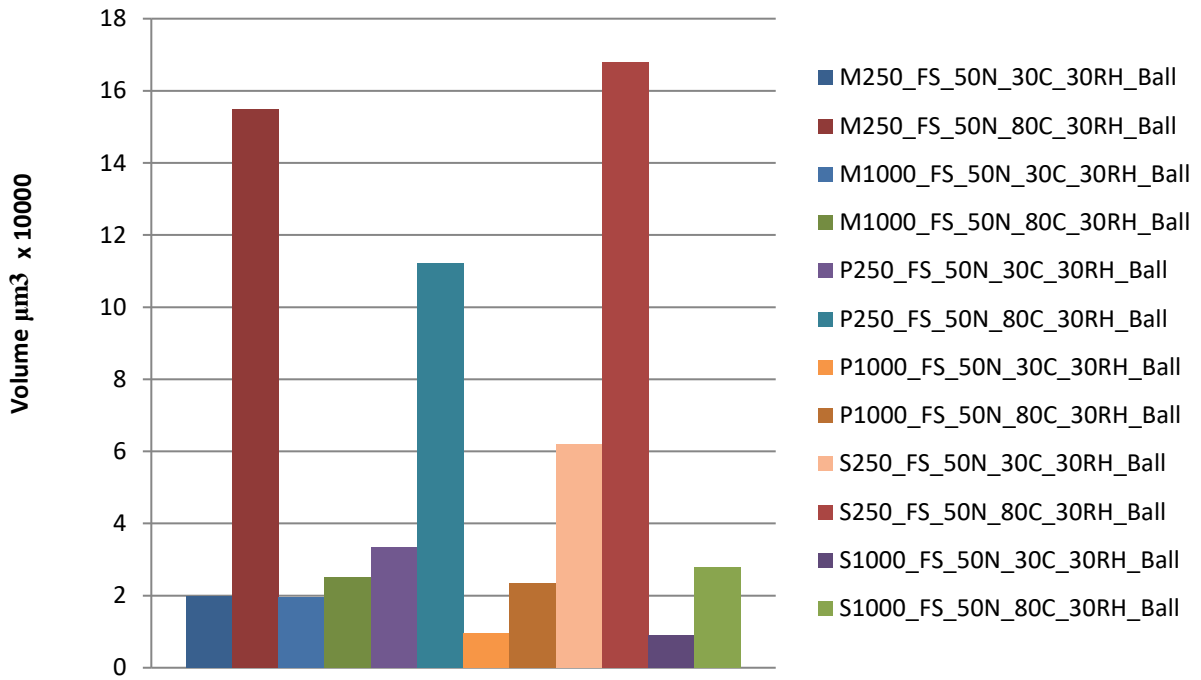
Figure 5-67: Profilometer wear data of ball specimen scans for FS tests at 30 °C
and 80 °C tests with a 50 N load.
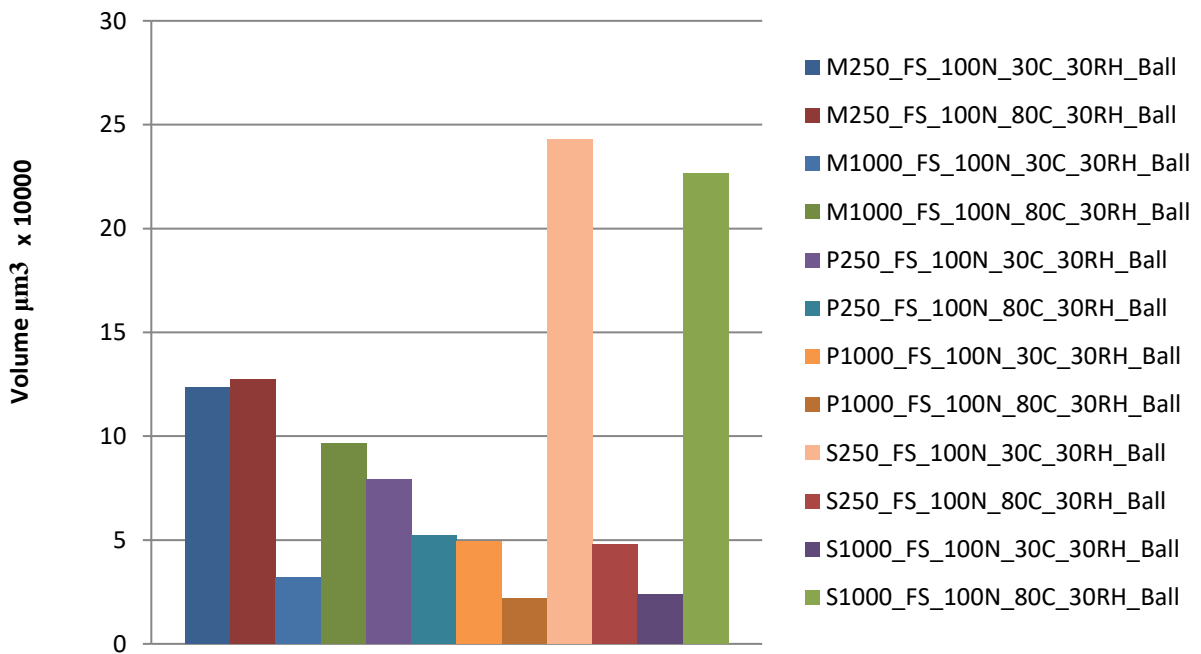
Figure 5-68: Profilometer wear data of ball specimen scans for FS tests at 30 °C
and 80 °C tests with a 100 N load.

Wear volumes where much easier to calculate on the disk surfaces due to the amount of wear and surface area over which the wear took place. Looking at the wear volumes of the disk gives a trend for wear volumes compared to temperature, additive size and additive concentration, Figure 5-69 – Figure 5-71. The temperature change affects the lubricating regime. At 30 N, Figure 5-63 a decrease in wear is observed with increasing additive concentration for 80 °C runs while the 30 °C runs showed the opposite trend.
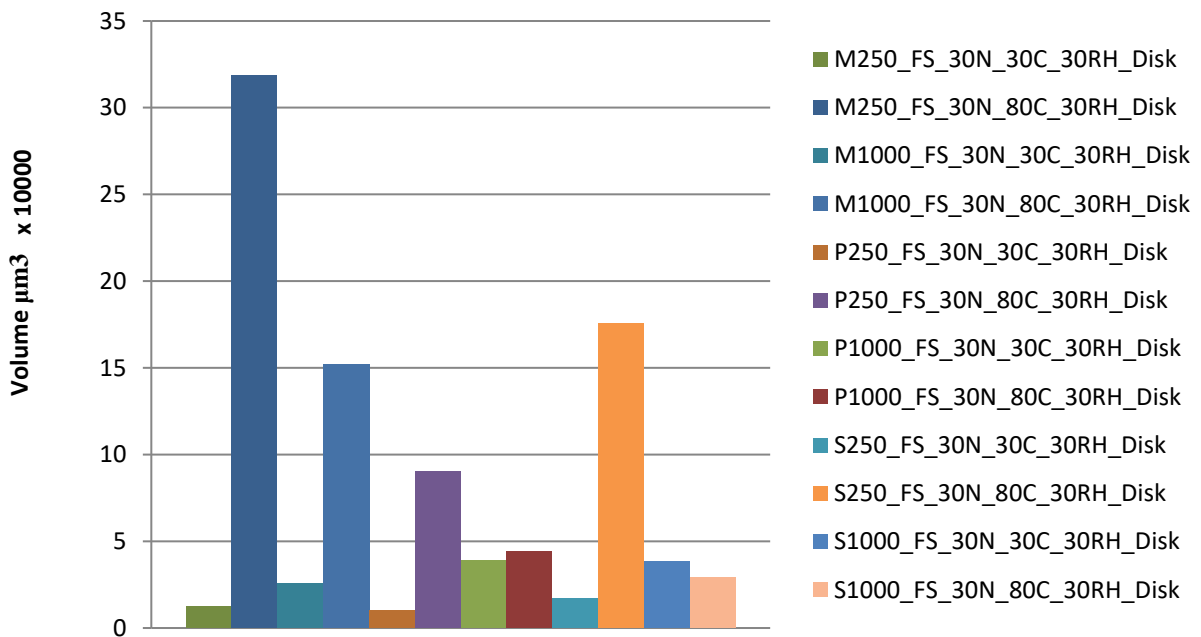
Figure 5-69: Profilometer wear data of disk scans for 30 °C and 80 °C tests with a 30 N load.
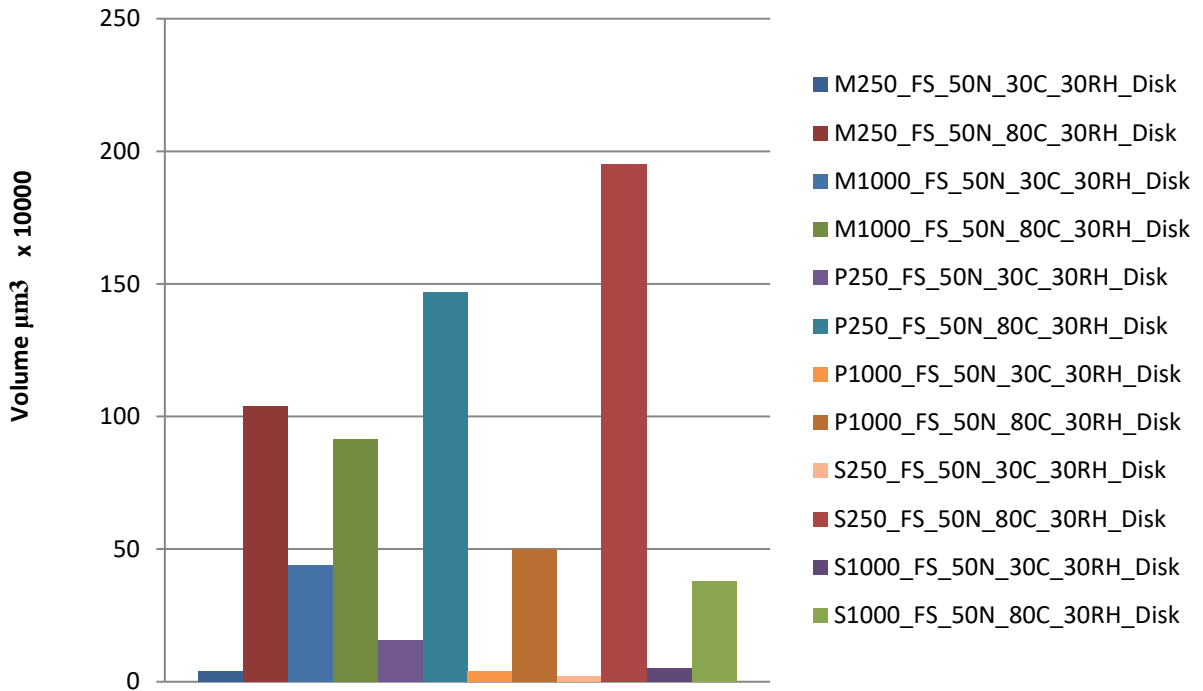
Figure 5-70: Profilometer wear data of disk scans for 30 °C and 80 °C tests with a 50 N load.
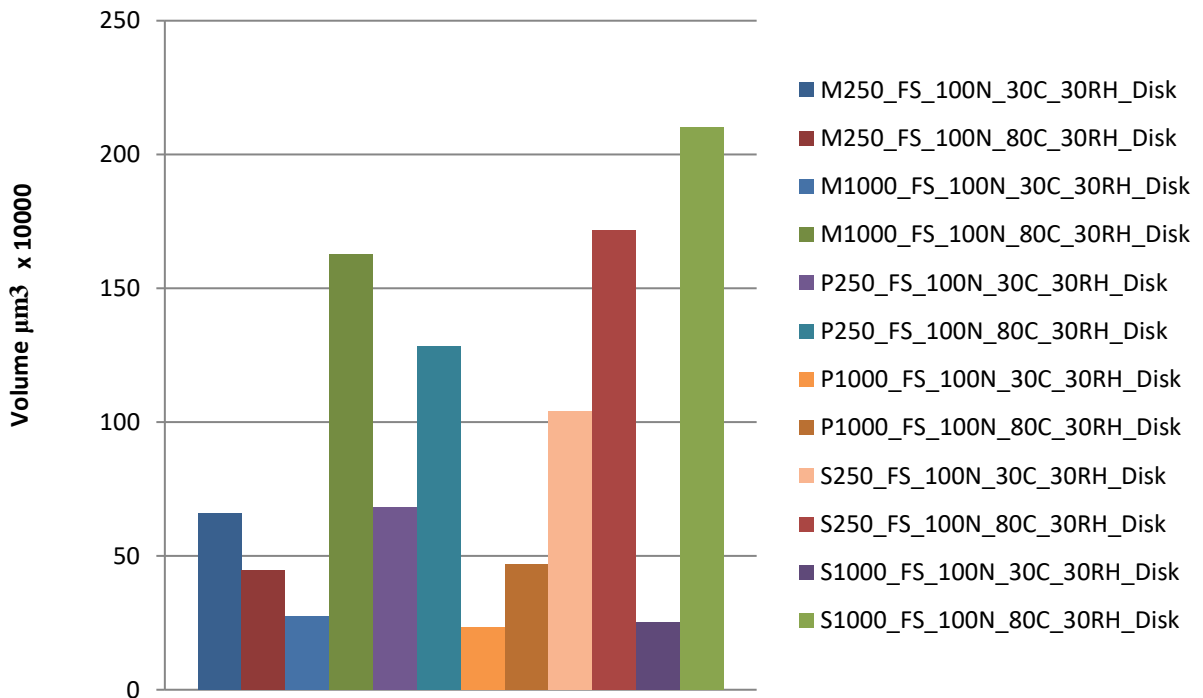
Figure 5-71: Profilometer wear data of disk scans for 30 °C and 80 °C tests with a 100 N load.

5.3. Comparing 2 mm and 1 mm stroke length

To try and reduce the effect that the endpoints have on results, the stroke length was changed to 2 mm reducing the relative amount of time that the top specimen is stationary in a stroke and increasing the time available for the additive layer to recover between strokes.

5.3.1. Comparing runs with 2 mm stroke to 1 mm stroke

To ensure that the average linear speed does not change, the oscillating frequency range was changed from 5 – 100 to 2 – 50 Hz. This ensures that the Hersey number for the oscillating frequency steps are similar. Comparing results between all of the tests done for M250, Figure 5-72 – Figure 5-74, gave a similar coefficient of friction for the same Hersey number with exceptions at a high oscillating frequency and in places where there is a shift in the vibrational tone of the SRV. At these points, there is a clear change in the sound made by the SRV.

It also seems as if the protective layer formed is more stable at 2 mm strokes compared to 1 mm. All the 2 mm runs are less jagged compared to the 1 mm runs, indicating a stronger and more stable protective layer. This change is highlighted in Figure 5-74. What is also important to note is that the 2 mm runs were done at 80 °C. Using 250 ppm myristic acid (C-14) at 1 mm was not enough to give the surface the protection it needed at 80 °C. At a 2 mm stroke, the test did not fail, even at higher Hersey number
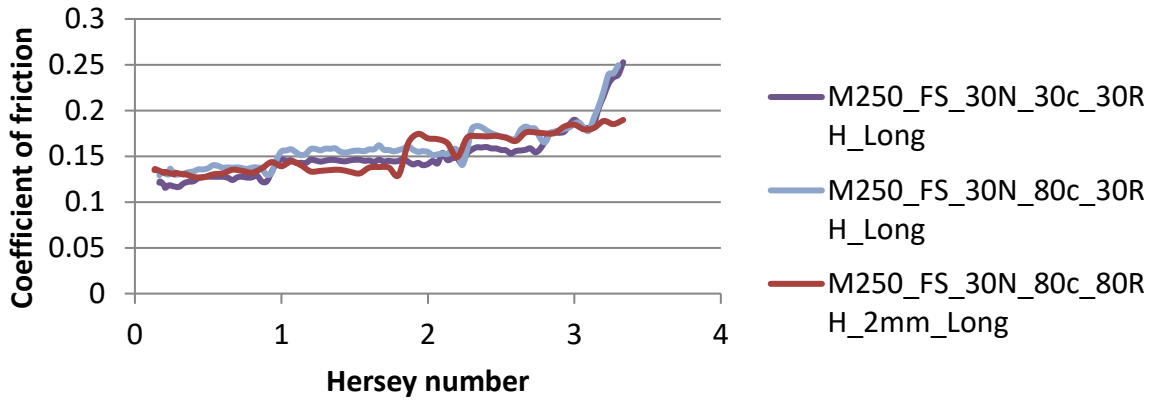
Figure 5-72: Average coefficient of friction data for all tests with M250 at 30 N load.
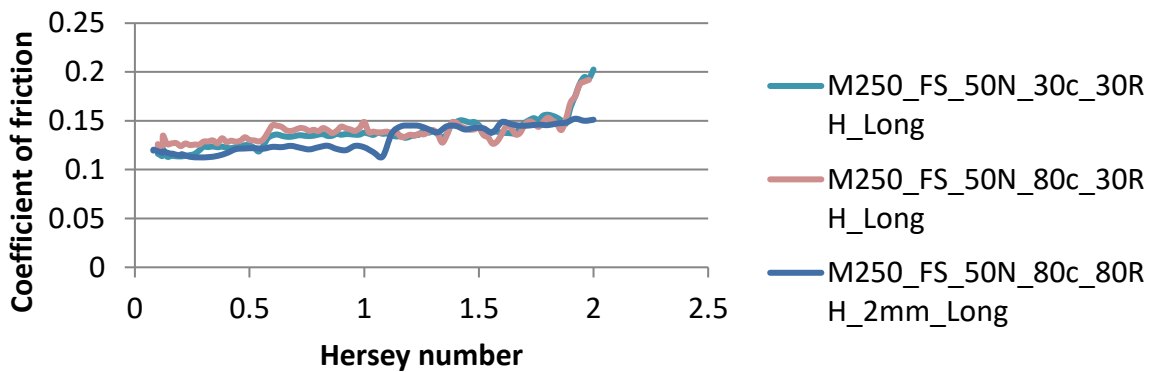
Figure 5-73: Average coefficient of friction data for all tests with M250 at 50 N load.
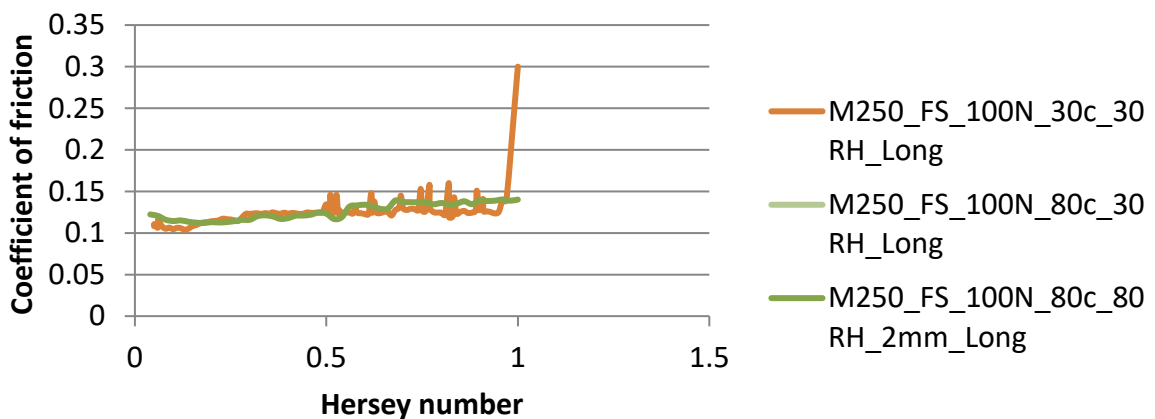
Figure 5-74: Average coefficient of friction data for all tests with M250 at 100 N load.

5.4.   Friction and wear tests using 2 mm stroke at 80 °C

The problem with the frequency scan setup is that surface history can affect the coefficient of friction as the test progresses over the range of oscillating frequency specified. The runs using the additised n-hexadecane so far varied test conditions over time. To better understand wear mechanism and to get a clear picture regarding wear volumes, steady-state conditions are required. From the experience gained so far, it is also important to allow for enough wear to take place to get good resolution on the wear data.

Tests were conducted at 6, 25 and 50 Hz with a 2 mm stroke at 80 °C and a load of 50 N. Using these conditions allow for good repeatability and lowers the influence of the endpoints on the wear track. To compare different runs the number of strokes in a test was kept constant by changing the run time for the test. A copper ring was also used on the bottom specimen to increase the maximum liquid volume on the disk to 1 mL. To ensure that there is good surface coverage as well runs were only conducted using 1000 ppm additised lubricants. As expected from other tests, data in Figure 5-75 shows an increase in the coefficient of friction as the frequency is increased. Comparing the average coefficient of friction for the F&W runs with the 2 mm FS runs gave Figure 5-76.
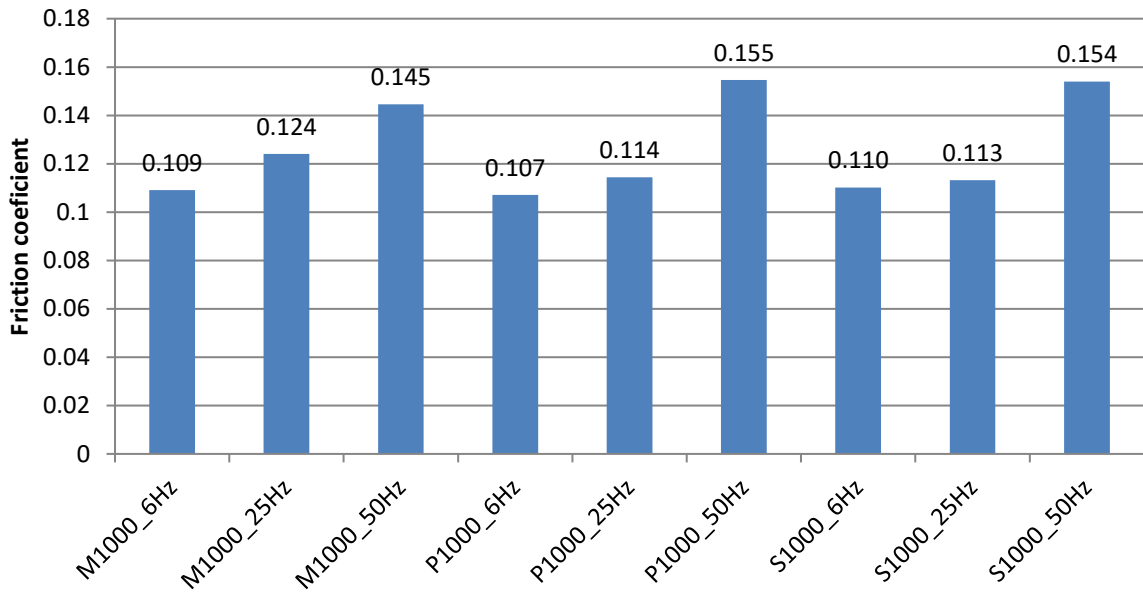
Figure 5-75: Coefficient of friction results for friction and wear tests at different frequencies.
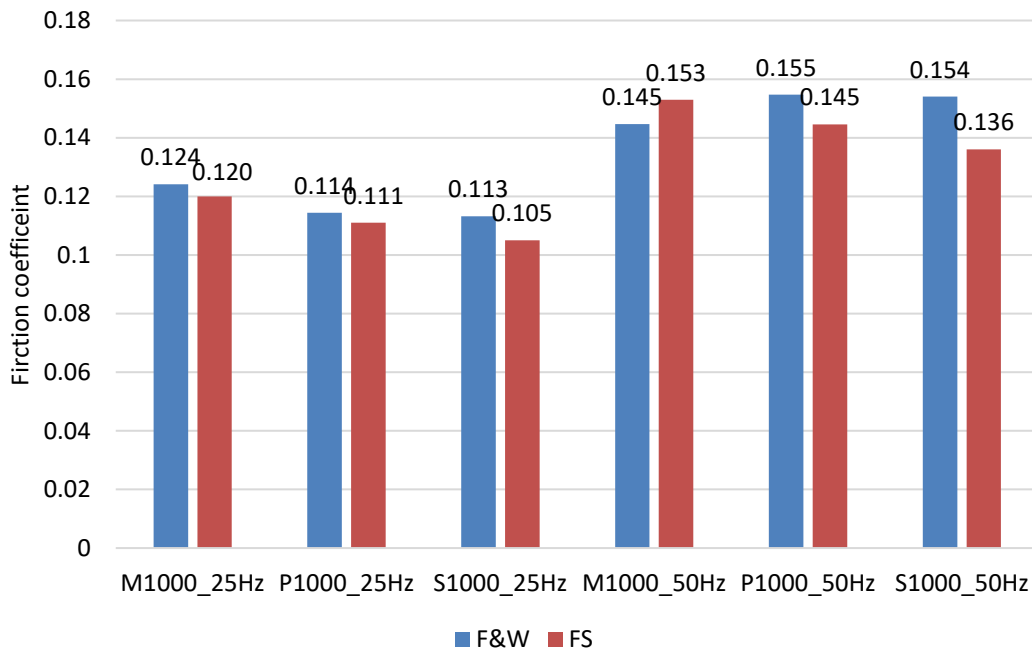
Figure 5-76: Average coefficient of friction at different frequencies for the F&W runs and FS runs at 2 mm.

Generally, the coefficient of friction for an FS run is lower compared to the F&W runs. This difference indicates that the surface history played a role in the coefficient of friction observed.

At low frequencies coefficient of friction for all the additives where similar corresponding well with results from FS tests, data reordered in Figure 5-77. At moderate frequencies palmitic and stearic acid (C-18) gave a lower coefficient of friction while myristic gave the lowest coefficient of friction at high oscillating frequency.
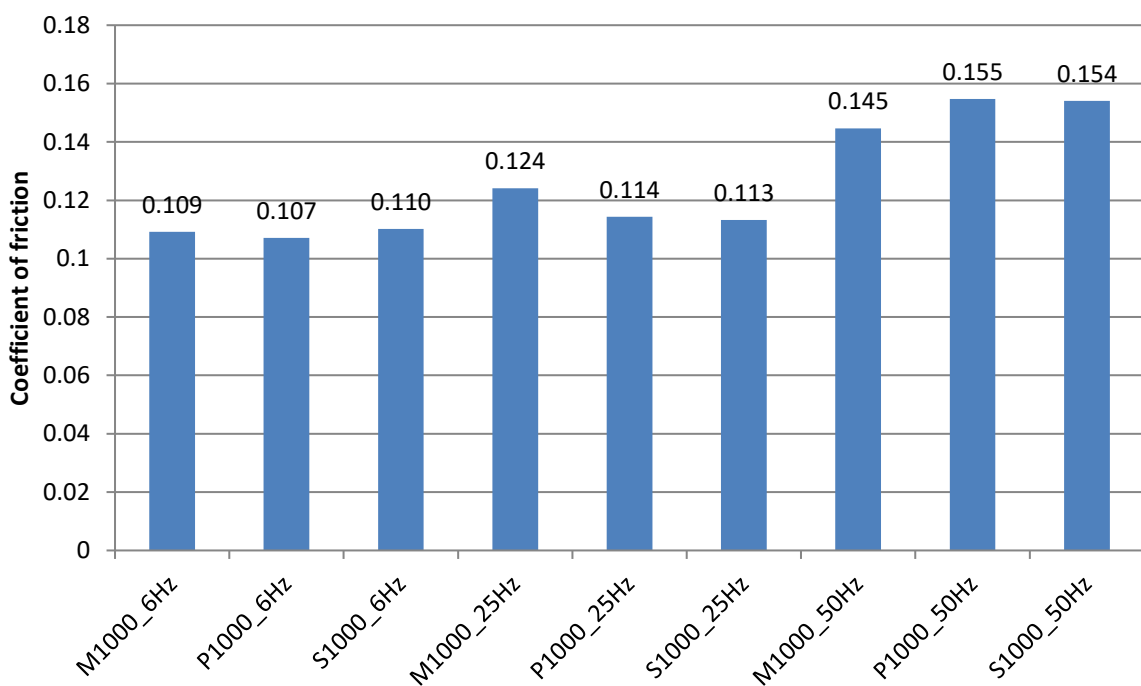
Figure 5-77: Friction and wear test results sorted based on oscillating frequency.

Looking at the wear scars and wear track Y-direction results in Figure 5-78 stearic acid (C-18) did not perform well under the circumstances with the highest wear measurements at 6 and 50 Hz. At 25 Hz stearic acid (C-18) gave similar results to palmitic acid (C-16) while myristic acid (C-14) gave the largest scars. The results for 25 Hz corresponding to the decreased coefficient of friction observed at 25 Hz for stearic acid (C-18).
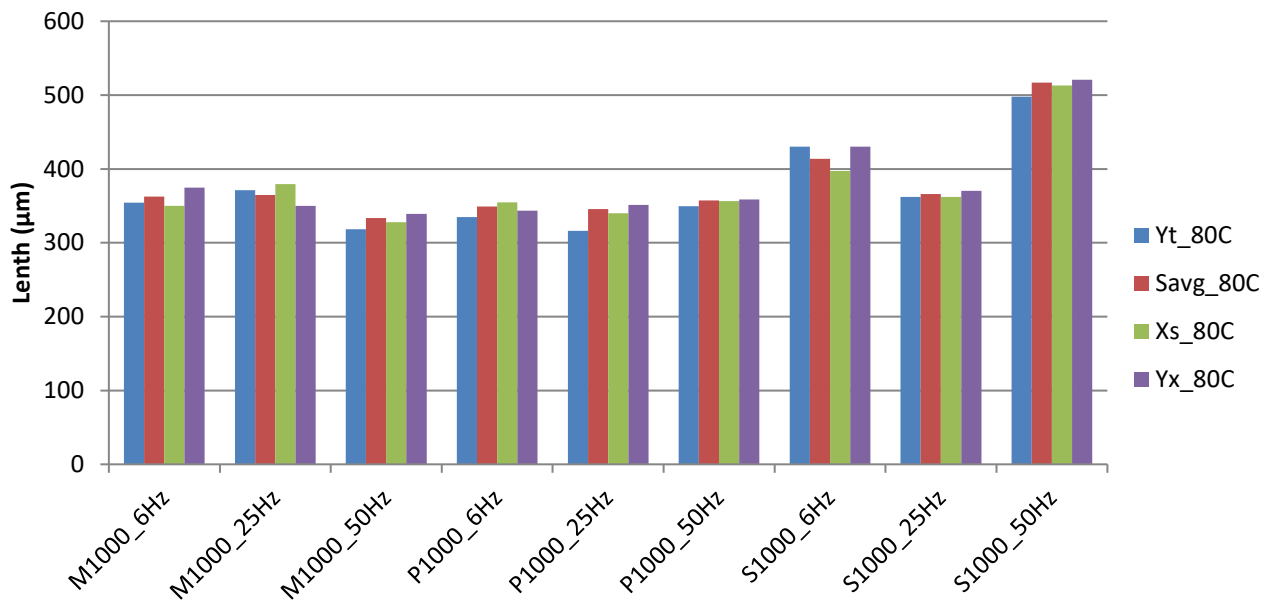
Figure 5-78: Wear track and scar measurements.

Knowing that the 3-dimensional space that the wear took place in is important the following 4 graphs were constructed from profile data of all the runs at constant frequencies, Figure 5-79 – Figure 5-82. The result from the wear volumes did not show any correspondence to the performance established by the coefficient of friction and wear measurements. Regarding the data in Figure 5-79 and Figure 5-80, under conditions that promoted full boundary lubrication stearic acid (C-18) gave the best wear protection for the ball but as the frequency was increased stearic acid (C-18) performance declined. Myristic acid (C-14) had poor performance under low oscillating frequencies but gave similar performance to palmitic acid (C-16) at high frequencies.
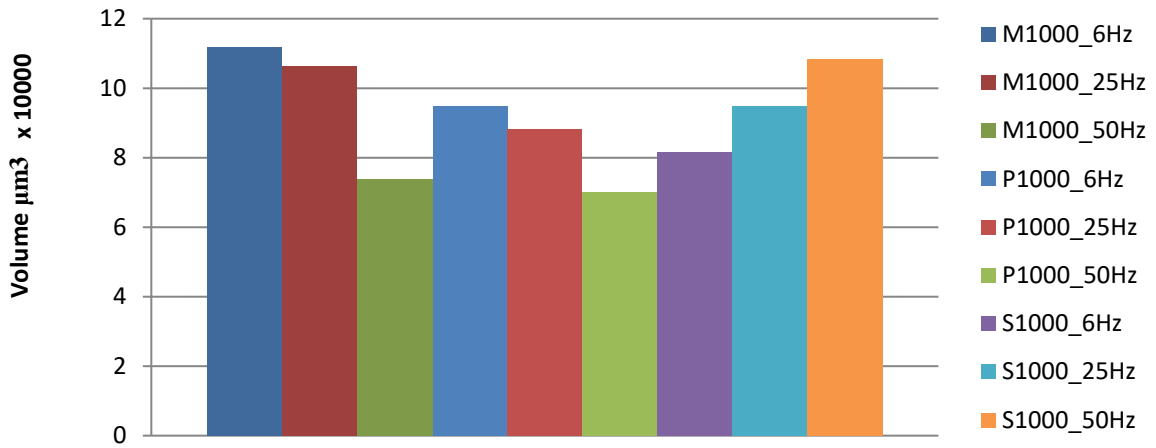
Figure 5-79: Ball specimen wear volumes.
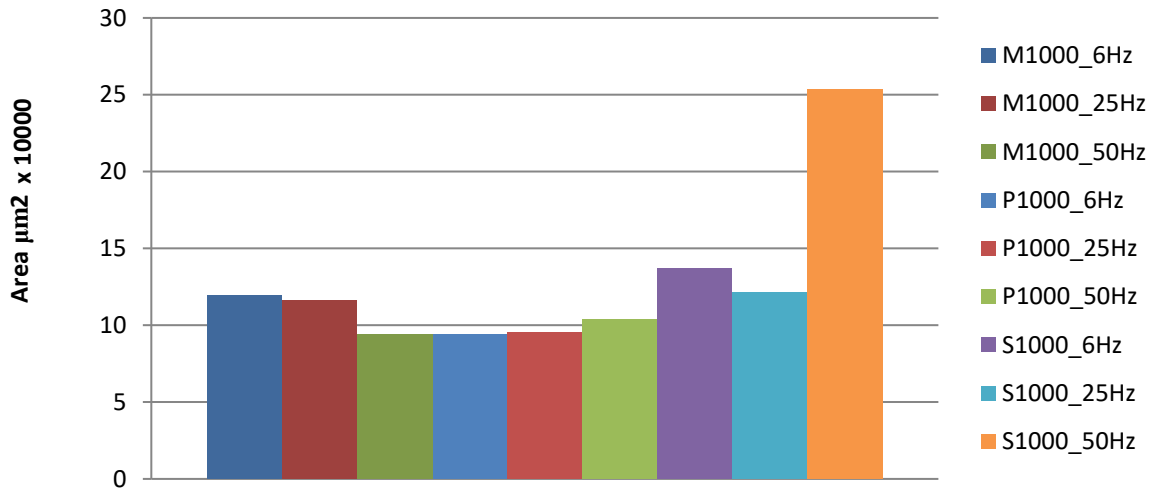
Figure 5-80: Ball specimen wear area.
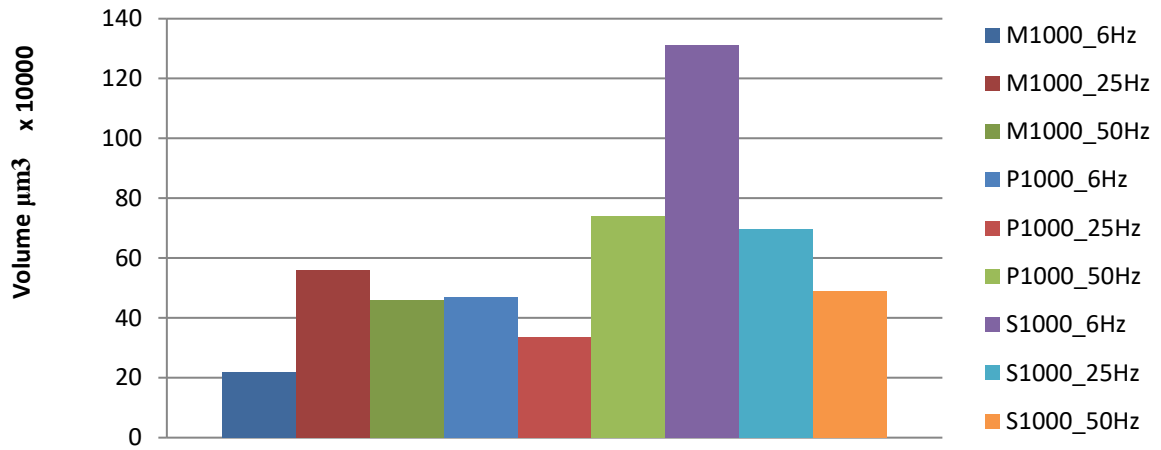
Figure 5-81: Disk specimen wear volume.
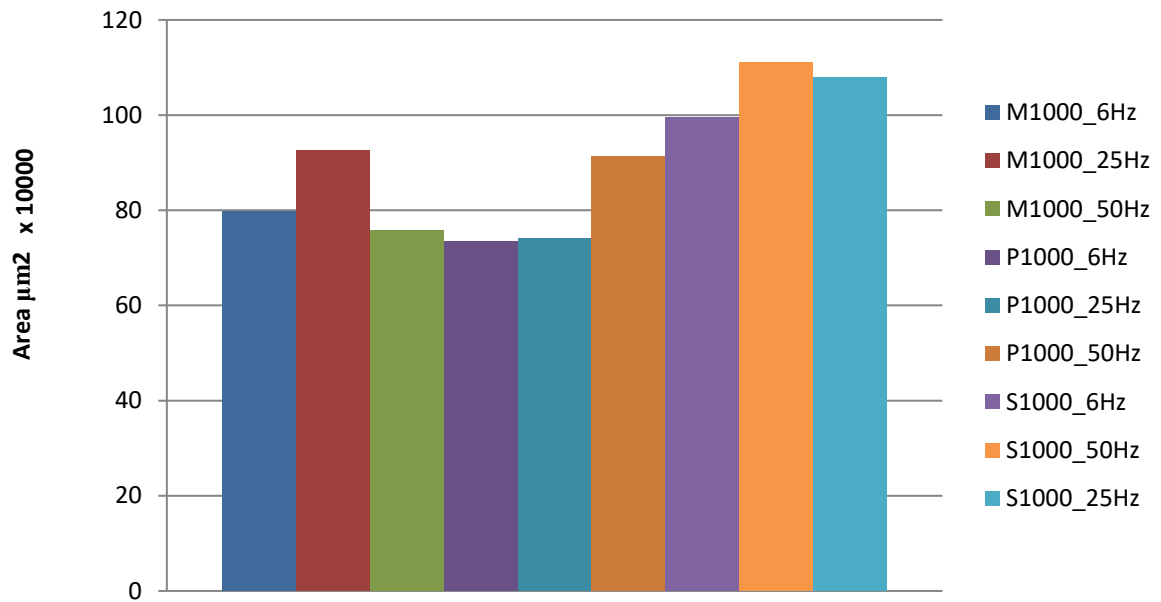
Figure 5-82: Disk specimen wear area.

6. Conclusions

6.1.   Initial test work

An odd behaviour was observed in initial experimentation in the frequency scan tests. In the initial experiments, the top specimen started to stick and slide at low oscillating frequencies when the load was increased, but the measured coefficient of friction never went above 0.3. This led to the discovery of several limitations on the SRV. When operating under lower oscillating frequencies the force used to move the top specimen is reduced. If the force is not enough the top specimen can stop without breakthrough occurring due to the applied load.

Testing showed that it is possible to generate a Stribeck curve on an SRV by changing the load or the oscillating frequency. Using load to generate a Stribeck curve gave more consistent results. Tests where the oscillating frequency was changed results deviated from what was expected at higher oscillating frequencies.

When comparing the results between generating a Stribeck curve by changing **load** or **oscillating frequency**, the coefficient of friction did not match up for some Hersey numbers. Investigations into the limits of the SRV also found that the coefficient of friction measurements at the endpoints are not taken.

6.2.   Frequency scan tests (FS)

During frequency scan testing, breakthrough occurred with increased oscillating frequency under a constant applied load. It makes no sense that a lubricant can sustain a load at low linear velocity but not at a high linear velocity. Increases in the velocity should increase the hydrodynamic pressure in the lubricant resulting in a higher load-carrying capacity. Imaging of the wear tracks suggests that the breakthroughs occurred at the endpoints of the stroke. Literature has shown that additive layers that do not chemically bond with a wear surface will not survive static friction (Johnston, Wayte, & Spikes, 1991). The erratic nature of the

156

coefficient of friction at higher loads and variations in the stroke length suggests that the top specimen started to stick to the lower specimen as the oscillating frequency was increased, indicating that some adhesion occurred between asperities. At higher additive concentration coefficient of friction at high oscillating frequencies where less erratic compared to the coefficient of friction of tests with low additive concentrations. This indicates that an SRV operates over a Stribeck curve range as the linear velocity changes to oscillate the ball specimen. Increased temperatures increased the coefficient of friction and wear. The problem that a test would fail under constant load at higher oscillating frequencies persisted.

Another limit to consider when using the SRV was also found. Coefficient of friction results at oscillating frequencies of 27 to 30 Hz and 68 to 70 Hz do not appear to be accurate. In these two ranges, the coefficient of friction drops suddenly and the SRV makes a different noise. Changing the stroke length, temperature or additive used did not change the frequencies where this happened. Whether the inherent weakness is due to the motor or natural oscillating frequencies within the materials of the SRV could not be determined.

Several test runs showed a high coefficient of friction during the run-in time. All these tests completed the test run where the other repeats that did not have the high coefficient of friction at the start could not get to the 100 Hz mark. It is very important to remember that a wear surface has a history and results heavily depend on the running-in duration and what happened during the run-in. To generate repeatable results the running-in period for all tests needs to be the same.

Changing the stroke to 2 mm while maintaining the same linear velocity gave more stable results. Imaging of the wear surfaces for the 2 mm runs did not show evidence of failure at the endpoints. Runs that previously failed at higher frequencies were able to complete the run with a 2 mm stroke using the same linear velocity.

Testing suggests that it is possible to generate a Stribeck curve by changing the oscillating frequency on an SRV. As discussed in chapter 5, the endpoints play a significant role in when the breakthrough will occur in an oscillating contact. To generate a Stribeck curve on an SRV increasing the stroke length will reduce the effect endpoints have on results and give a Stribeck curve that is similar to a curve generated by changing the applied load.

The following is a list of all the trends observed for frequency scan tests.

- Load increases:
    - Decreased the observed coefficient of friction up to the breakthrough point where the coefficient of friction suddenly increases, and the test fails.
    - Increased the wear observed on both ball and disk specimens, volume and the apparent wear area.
    - Decreased coefficient of friction does not correlate with a decrease in wear.
- Increases in additive concentration:
    - At low loads increases in additive, concentration resulted in higher wear. Suggests increased chemical wear. At higher loads, a reduction in wear is observed with increased additive concentration.
    - Generally, decreases the coefficient of friction.
- Oscillating frequency
    - At low oscillating frequencies, the coefficient of friction increase slightly corresponding to a change to the boundary from mixed lubrication regimes. No breakthroughs observed.
    - Generally, the coefficient of friction increases as the oscillating frequency is increased following the path from mixed into electrohydrodynamic lubrication.
    - Breakthrough can occur at increased oscillating frequencies due to the bidirectional motion. Coefficient of friction at endpoints are not measured and unless specified only one average measurement

158

over a second is given as data. The constant start-stop at the endpoints removes the additive layer and if there is not enough time for the layer to recover seizure occurs at the endpoint.

  – At low oscillating frequencies, the chain length of the additive starts to play a role. Longer chain additives show an increase in the coefficient of friction as the frequency is lower while for shorter chain additives coefficient of friction continued to drop.

- Effect of chain length

  – As the chain length is increased the range of Hersey number that will result in boundary lubrication is increased. Higher load-carrying capacities with increased chain lengths move the breakthrough point to the left and the interaction between additive layers moves the boundary regime to the right into the mixed regime.

6.3.   Friction and wear tests (FW)

- Under steady-state conditions, all the trends observed during the FS tests where maintained.

- Higher frequencies resulted in a higher coefficient of friction for all the additives.

- At low frequencies, all the additives gave a similar coefficient of friction. Stearic and palmitic acid (C-16) showed a lower coefficient of friction at moderate frequencies and myristic acid (C-14) showed the lowest coefficient of friction at high frequencies. This corresponds with the idea that myristic acid (C-14) diffuses faster and can give better protection under certain conditions.

7. Recommendations

From the study several factors where identified that deserve to be researched separately.

The liquid volume and differences between continuous and batch samples should be investigated further. Special attention should be placed on lubricants with surface-active additives. Different atmospheres and oxidation of the lubricant or contacting surfaces will also play a role. This study showed that it is possible to increase the load-carrying capacity of a lubricant by changing the amount of lubricant.

The effect of oscillating frequency on the **Volumetric wear** could not be established in the current study. More detailed work on how volumetric wear is affected by different additive sizes under different oscillating frequencies will give a better understanding of how additives protect a wear surface.

3-D wear profiles. There seems to be a relation between the depth of the wear track and the difference in the width of the wear track and wear scar. If the wear track and wear scar y-dimensions (parallel to the direction of movement) are the same sizes, we can expect to find a very flat wear scar and track. More research on this could lead to an advance in wear analysis using 2-D surfaces with a model when it is not possible to do 3-D wear profiles.

Bibliography

Anastopoulos, G., E, L., Karonis, F., Zannikos, F., & Kalligeros, S. (2001). A Preliminary Evaluation of Esters of Monocarboxylic Fatty Acid on he Lubrication Properties of Diesel Fuel. *Ind. Eng. Chem., 40*, 452 - 456.

Anastopoulos, G., E, L., Zannikos, F., Kalligeros, S., & Teas, C. (2001). Influence of aceto acetic esters and di-carboxylic acid esters on diesel fuel lubricity. *Tribology International, 34*, 749 - 755.

Anastopoulos, G., Lois, E., Zannikos, F., Kalligeros, C., & Teas, C. (2002). HFRR lubricity response of an additized aviation kerosene for use in CI engines. *Tribology International, 35*, 599 - 604.

Anastopoulos, G., Lois, E., Zannikos, S., Kalligeros, C., & Teas, C. (2002). The Tribological Behavior of Alkyl Ethers and Alcohols in Low Sulfur Automotive Diesel. *Fuel, 81*, 1017 - 1024.

Anghel, V., Bovington, C., & Spikes, H. A. (1999). Thick Film Formation by Friction Modifier Additives. *Lubrication Science, 11*, 313 - 335.

Appeldoorn, J. K., & Dukek, W. G. (1966). *Lubricity of Jet Fuels.* Society of Automotive Engineers. Warrendale, PA: Society of Automotive Engineers.

Batchelor, A. W., & Stachowiak, G. W. (2003). *Engineering Tribology* (2nd ed.). Butterworth Heinemann.

Bhushan, B. (2001). *Modern Tribology Handbook.* New York: CRC Press LLC.

Bhushan, B. (2002). *Introduction to Tribology.* New York: John Wiley & Sons.

Cann, P. M. (1996). Starvation and reflow in a grease-lubricated elastohydrodynamic contact. *Tribology Transcipts*, 698-704 .

Gohar, R., & Rahnejat, H. (2012). *Fundametals of Tribology.* United Kingdom: Imperial College Press.

Hamrock, B. J., Jacobson, B. O., & Schmid, A. R. (2005). *Fundamentals of Fluid Film Lubrication.* New York: Marcel Dekker.

Hutchings, I. M. (1992). *Tribology friction and wear of engineering materials .* London: Elsevier: Butterworth Heinemann Ltd.

Jacobson, B. (2003). The Stribeck memorial lecture. *Tribology International*, 781 - 789.

Johnston, G. J., Wayte, R., & Spikes, H. A. (1991). The Measurement and Study of very Thin Lubricating Films in Concentrated Contacts. *Tribology Transactions, 34*, 187 - 94.

Kaline, M. (2004). Influence of flash temperatures on the tribological behaviour in low-speed sliding: a review. *Materials Science and Engineering*, 390–397.

Lacey, P., Gunsel, S., DeLa Cruz, J., & Whalen, M. (2001). Effects of High Temperature and Pressure on Fuel Lubricated Wear. *SAE, 3523*, 1 - 10.

Langenhoven, J. (2012). *Fundametals of Tribology the effect of laboratory Test Conditions on lubricity Testing. A litrature review.* University of Pretoria. Pretoria: Department of Chemical engineering.

Langenhoven, J. (2014). *The effects of humidity and soluble water content on the lubricity testing of a n-hexadecane and palmitic acid tests fluid. Dissertation for completion of masters.* Department of Chemical Engineering. University of Pretoria.

Litzow, U., Jess, A., Matzke, M., Caprotti, R., & Balfour, G. (2009). Diesel Lubricity Requirements of Future Fuel Injection Equipment. *Society of Automotive Engineers*.

Loehle, S. (2014). *Understanding of adsorption mechanism and tribological behaviors of C18 fatty acids on iron-based surfaces : a molecular simulation approach.* Lyon: Université de Lyon.

Marais, G. (2009). *A Fundamental Modelling Approach to Relate Laboratory-based Lubricity Testing to Practical Application. A dissertation for completion of master.* Department of Chemical Engineering. Pretoria: University of Pretoria.

Mo"ller, V. P. (2012). *Exploring Fundamental Differences Between Wear and Seizure Load Testing. A dissertaion for completion of masters.* University of Pretoria. Pretoria: Department of Chemical Engineering.

Papay, A. G. (1983). Oil Soluble Friction Reducers- Theory & Application. *American Society of Lubrication Engineers, 39*(7), 419 - 426 .

PCS Instruments. (2005). *HFRR Installation & PreparationManual, Hardware version 1.* PCS Instruments.

Petty, M. C. (1996). *Languir-Blodgett films: an Introduction.* Cambridge: Cambridge univercity press.

Ratoi, M., Angel, V., Bovington, C., & Spikes, H. A. (2000). Mechanism of oiliness additives. *Tribology International, 33*, 241 - 247 .

Rengstorff, G. W., Miyoshi, K., & Buckley, D. H. (1986). Interaction of Sulfuric Acid Corrosion and Mechanical Wear of Iron. *ASLW Transactions, 29*, 43 - 51.

Roberts, W. (1990). Lubrication - looking forward to the nineties. *The South African Mechanical Engineer*, 225 - 239.

Stribeck, R. (1902). Die wesentlichen Eigenschaften der Gleit- und Rollenlager (Characteristics of Plain and Roller Bearings). *Zeitschrift des Vereines deutcher Ingenieure.*